

**Elucidating the Impact of Low Dissolved  
Oxygen Wastewater Treatment on  
Pharmaceutical Fate**

by

**Lauren B. Stadler**

A dissertation submitted in partial fulfillment  
of the requirements for the degree of  
Doctor of Philosophy  
(Environmental Engineering)  
in The University of Michigan  
2016

**Doctoral Committee:**

Professor Nancy G. Love, Chair  
Professor Diana S. Aga, University at Buffalo  
Charles B. Bott, Hampton Roads Sanitation District  
Professor Lutgarde M. Raskin  
Professor Thomas M. Schmidt

© Lauren B. Stadler 2016

## **Acknowledgments**

This dissertation was supported by numerous funding sources including: the Water Environment Research Foundation (Project U1R09), the U.S. National Science Foundation Graduate Research Fellowship, the University of Michigan Dow Doctoral Fellowship, the University of Michigan Rackham Merit Fellowship, and the University of Michigan Predoctoral Fellowship.

This dissertation represents many years of my life filled with exploration, discovery, and joy from learning about a field that I hope to continue to study throughout my career. There are many people that need to be acknowledged for their help and support throughout this process. First, I would like to express deep thanks to my advisor, Dr. Nancy Love, for her incredible mentorship, encouragement, guidance, and patience. I have learned a great deal from her, as a scientist, a leader, and an advocate. I would like to thank my committee members, Dr. Lutgarde Raskin, Dr. Diana Aga, Dr. Charles Bott, and Dr. Thomas Schmidt for their thoughtful input and guidance. I would also like to thank Dr. Steven Skerlos for the opportunity to work with him on research outside of my dissertation, and for his guidance and support over the past several years.

I would like to thank the Love Research group (past and present), and in particular Jeseth Delgado Vela. It has been a joy to collaborate with a such an intelligent and thoughtful friend. I would also like to thank Dr. Adam Smith and Dr. Tara Clancy, for their positivity, enduring support, and friendship. I have learned a tremendous amount and enjoyed working alongside

members of the entire Environmental Biotechnology lab. I would like to thank Nadine Kotlarz, Dr. Kelly Martin, Dr. Sarah Haig, Dr. Rebecca Lahr, Heather Goetsch, Andrea McFarland, and Chia-Chen Wu for many conversations. I would like to thank Sara Rimer for her support and friendship, and for keeping me accountable over the last five years. I would also like to thank my fellow Dow Doctoral Fellows, who both inspired me and pushed me to think outside of my comfort zone. I would also like to acknowledge Sunit Jain and Dr. Greg Dick for their input to Chapter 6.

I am grateful for the hard work of numerous undergraduates and master's students who contributed to the research in this dissertation. It was a pleasure to work with Luke Stevens, Anton Dapcic, Diana Bach, and David Glubzinski. I would like to thank the staff in the Department of Civil and Environmental Engineering, and in particular, Tom Yavaraski for his patience and help with learning new instruments, and Rick Burch help building the lab reactors. I am also thankful to the administrative team for their assistance, including Nancy Osugi, Kimberly Simmons, Sherry Brueger, Stephanie Ford, and Tabitha Rohn.

I have never felt anything but unconditional support from my parents and siblings. They taught me to push myself and set high standards. My competitive spirit, cultivated since birth, is thanks to my family and has made me the person that I am today. For that, and their constant encouragement, I am extremely thankful.

Finally, and most importantly, I would like to thank my husband, Jonathan. His absolute support, humor, and excellent cooking skills have made graduate school some of the best years of my life. He has been an anchor, and without him this dissertation would not have been possible.

## Table of Contents

Acknowledgments.....	ii
List of Figures.....	vi
List of Tables.....	ix
List of Appendices.....	xi
Abstract.....	xii
Chapter 1. Introduction.....	1
1.1 Background.....	1
1.2 Overview of dissertation.....	6
1.3 Literature cited.....	8
Chapter 2. Background.....	11
2.1 Low dissolved oxygen wastewater treatment.....	11
2.2 Pharmaceutical fate in wastewater treatment.....	16
2.3 Literature cited.....	25
Chapter 3. Effect of Redox Conditions on Pharmaceutical Loss during Biological Wastewater Treatment using Sequencing Batch Reactors.....	32
3.1 Introduction.....	32
3.2 Methods.....	35
3.3 Results and discussion.....	41
3.4 Summary and conclusions.....	53
3.5 Literature cited.....	54
Chapter 4. Impact of microbial physiology and microbial community structure on pharmaceutical fate driven by dissolved oxygen concentration in nitrifying bioreactors.....	60
4.1 Introduction.....	60
4.2 Materials and methods.....	63
4.3 Results and discussion.....	69

4.4 Summary and potential applications .....	82
4.5 Literature cited .....	84
Chapter 5. Impact of dissolved oxygen on pharmaceutical biotransformation rates and microbial activity in wastewater treatment .....	90
5.1 Introduction .....	90
5.2 Materials and methods .....	92
5.3 Results .....	99
5.4 Discussion .....	110
5.5 Literature cited .....	115
Chapter 6. Elucidating the impact of microbial community diversity on pharmaceutical biotransformation during wastewater treatment .....	119
6.1 Introduction .....	119
6.2 Materials and methods .....	122
6.3 Results .....	129
6.4 Discussion .....	141
6.5 Literature cited .....	145
Chapter 7. Conclusions and Engineering Significance .....	150
7.1 Overview .....	150
7.2 Main findings and significance .....	151
7.3 Future research .....	155
7.4 Literature cited .....	157
Appendices .....	159

## List of Figures

<b>Figure 1-1.</b> Direct and indirect impacts of DO on pharmaceutical biotransformation during wastewater treatment. ....	4
<b>Figure 3-1.</b> Representative cross-cycle profile of nitrogen species in each reactor. ....	43
<b>Figure 3-2.</b> Overall percent losses of pharmaceuticals in each reactor. ....	46
<b>Figure 3-3.</b> Deconjugation and conjugation reactions between sulfamethoxazole and its transformation products, acetyl-sulfamethoxazole and sulfamethoxazole-glucuronide. ....	51
<b>Figure 4-1.</b> Volatile suspended solids (VSS) concentration and <i>amoA</i> copies per milliliter in the low and high DO parent reactors. ....	71
<b>Figure 4-2.</b> Ammonia oxidation rates in the batch experiments with biomass from each parent reactor. ....	73
<b>Figure 4-3.</b> Percent loss of ibuprofen, sulfamethoxazole, 17 $\alpha$ -ethinylestradiol (EE2), acetaminophen, and atenolol in the low and high DO parent communities. ....	75
<b>Figure 5-1.</b> Specific biotransformation rates observed for each compound in the 0.5 mg-DO/L batch experiment. ....	100
<b>Figure 5-2.</b> Pharmaceutical biotransformation rates plotted as a function of DO concentration for each compound. ....	103
<b>Figure 5-3.</b> Oxygen half-saturation constants ( $K_{O_2}$ ) for each pharmaceutical compound and heterotrophs and nitrifiers. ....	104
<b>Figure 5-4.</b> Non-metric multidimensional scaling biplot showing the active microbial community structures ( $\theta_{yc}$ ) from each of the batch experiments, shown in different colors (A). DO concentration and individual pharmaceutical biotransformation rates that significantly correlated with either of the two axis are shown as arrows (B). ....	106
<b>Figure 5-5.</b> Rank abundance curve of phylotypes that had significant and positive associations with individual compounds' biotransformation rates (Spearman, $p < 0.01$ ). ....	108
<b>Figure 5-6.</b> Specific growth rate versus DO concentration of <i>r</i> - versus <i>K</i> -strategists according to Monod kinetics. ....	113

<b>Figure 6-1.</b> Rarefaction plots for the dilution cultures based on 16S rRNA gene and 16S rRNA sequencing (taxonomic) and whole genome and metagenome sequencing (functional).....	132
<b>Figure 6-2.</b> Observed functional richness versus taxonomic richness.....	133
<b>Figure 6-3.</b> Average pharmaceutical loss (disappearance of the parent compound) normalized to volatile suspended solids concentration for each dilution condition (black: $10^{-2}$ ; blue: $10^{-4}$ ; green: $10^{-7}$ ).....	135
<b>Figure 6-4.</b> Spearman correlation p-values for associations between richness and pharmaceutical biotransformation rates.....	137
<b>Figure 6-5.</b> The relationship between the mean expression across all of the samples, and the log change in expression between the $10^{-2}$ and $10^{-7}$ cultures.....	138
<b>Figure 6-6.</b> Relative expression of significantly differentially expressed genes (likelihood ratio, $p_{\text{adj}} < 0.05$ ) that were also significantly associated with EE2 biotransformation (Spearman, $p < 0.05$ ).....	139
<b>Figure A1.</b> Cross-cycle concentrations of atenolol in the anoxic/aerobic SBR (reactor A) collected on three separate dates.....	163
<b>Figure A2.</b> Cross-cycle concentrations of sulfamethoxazole (SMX), acetyl-sulfamethoxazole (acetyl-SMX), and sulfamethoxazole-glucuronide (SMX-gluc) in select samples from the anoxic/aerobic SBR and the microaerobic SBR.....	164
<b>Figure B1.</b> Concentration profiles of ammonia-, nitrite-, and nitrate-N in batch reactors supplemented with 10 mg/L ATU using biomass from the low DO and high DO parent reactors.....	169
<b>Figure B2.</b> Concentration profiles of EE2 (a), acetaminophen (b), atenolol (c), and sulfamethoxazole (d) in abiotic batch experiments performed with media and sodium azide....	171
<b>Figure B3.</b> Concentration profiles of ibuprofen (a), sulfamethoxazole (b), EE2 (c), acetaminophen (d), and atenolol (e) in batch experiments performed with low DO parent biomass.....	174
<b>Figure B4.</b> Concentration profiles of ibuprofen (a), sulfamethoxazole (b), EE2 (c), acetaminophen (d), and atenolol (e) in batch experiments performed with high DO parent biomass.....	177
<b>Figure C1.</b> Initial and final concentrations of ammonia-N in batch reactors from preliminary batch experiment.....	182
<b>Figure C2.</b> Initial and final concentrations of ammonia-N (a) and nitrate-N (b) from the 2.0 mg-DO/L batch experiment.....	183
<b>Figure C3.</b> Sodium azide concentration used in respirometry versus maximum oxygen uptake rate.....	184



<b>Figure C4.</b> Relative activity of significant and positively associated (Spearman, $p < 0.01$ ) phylotypes for each compound. ....	209
<b>Figure D1.</b> Dissolved organic carbon profiles for each batch reactor over the first 2 days of the experiment.....	216
<b>Figure D2.</b> RNA-based functional richness versus scaled, normalized biotransformation rates for each compound: atenolol (a), EE2 (b), trimethoprim (c), venlafaxine (d), carbamazepine (e), glyburide (f), erythromycin (g), and collective (h).....	222
<b>Figure D3.</b> Spearman correlation p-values for associations between pharmaceutical biotransformation rates and functional richness based on expressed metabolism genes and all expressed genes.....	223
<b>Figure D4.</b> Relative expression of significantly differentially expressed genes (likelihood ratio, $p_{adj} < 0.05$ ) that were also significantly associated with atenolol biotransformation (Spearman, $p < 0.05$ ).....	224
<b>Figure D5.</b> Relative expression of significantly differentially expressed genes (likelihood ratio, $p_{adj} < 0.05$ ) that were also significantly associated with trimethoprim biotransformation (Spearman, $p < 0.05$ ).....	225
<b>Figure D6.</b> Relative expression of significantly differentially expressed genes (likelihood ratio, $p_{adj} < 0.05$ ) that were also significantly associated with venlafaxine biotransformation (Spearman, $p < 0.05$ ).....	226
<b>Figure D7.</b> Relative expression of significantly differentially expressed genes (likelihood ratio, $p_{adj} < 0.05$ ) that were also significantly associated with the collective biotransformation of atenolol, EE2, trimethoprim, venlafaxine and carbamazepine (Spearman, $p < 0.05$ ) .....	227
<b>Figure D8.</b> Relative expression of significantly differentially expressed genes (likelihood ratio, $p_{adj} < 0.05$ ) that were also significantly associated with erythromycin biotransformation (Spearman, $p < 0.05$ ).....	228

## List of Tables

<b>Table 3-1.</b> Target pharmaceuticals and transformation products under Investigation: Structure, Properties, and Wastewater Concentration.....	38
<b>Table 3-2.</b> Losses in aerobic, anoxic/aerobic, and microaerobic treatment determined in this study alongside reported literature values .....	49
<b>Table 4-1.</b> Compounds selected for investigation.....	65
<b>Table 4-2.</b> Richness and diversity indices of the low and high DO parent reactor communities ..	73
<b>Table 4-3.</b> Observed specific kinetic biotransformation constants (normalized by VSS concentration) for ibuprofen, EE2, sulfamethoxazole, acetaminophen, and atenolol. ....	75
<b>Table 5-1.</b> Shared phylotypes that associated with biotransformation rates of pairs of compounds and whether the UM-PPS predicted a shared biotransformation pathway .....	109
<b>Table 6-1.</b> Biodiversity indices based on 16S rRNA gene, 16S rRNA, metagenomic, and metatranscriptomic sequencing of biomass from the dilution cultures. ....	131
<b>Table A1.</b> Micronutrient solution used to supplement influent feed.....	160
<b>Table A2.</b> Multiple reaction monitoring (MRM) parameters with retention times for each target compound.....	161
<b>Table A3.</b> Method detection limit using 100 mL for solid phase extraction .....	162
<b>Table A4.</b> Percent loss across reaction cycle for atenolol and sulfamethoxazole.....	163
<b>Table A5.</b> Average system removal (%) of venlafaxine-family compounds.....	165
<b>Table B1.</b> Parent reactor influent media.....	166
<b>Table B2.</b> Target compounds with accurate mass and retention times used for quantification..	168
<b>Table B3.</b> Observed kinetic biotransformation rate constants for ibuprofen, EE2, sulfamethoxazole, acetaminophen, and atenolol .....	177
<b>Table B4.</b> Ammonia oxidizing bacterial (AOB) and nitrite oxidizing bacteria (NOB) identified in the low and high DO parent reactors. ....	178

<b>Table C1.</b> Target compounds with accurate mass and retention times used for quantification..	181
<b>Table C2.</b> Pharmaceutical concentrations in biotransformation batch experiments performed at different DO concentrations (6.0, 2.0, 0.5, 0.25, 0.15, and 0.05 mg/L).....	185
<b>Table C3.</b> Kinetic parameters from curve fitting Monod or Andrews equations to experimental data using non-linear least squares regression analysis. ....	198
<b>Table C4.</b> Phylotypes with significant associations (Spearman, $p < 0.01$ ) with DO concentration.....	203
<b>Table C5.</b> Phylotypes with significant associations (Spearman, $p < 0.01$ ) with biotransformation rates for each compound. ....	205
<b>Table D1.</b> Final concentrations of micronutrients in semi-synthetic sewage media.....	212
<b>Table D2.</b> Predicted biotransformation pathways for selected compounds.....	213
<b>Table D3.</b> Target compounds with accurate mass and retention times used for quantification. ....	215
<b>Table D4.</b> Initial and final pharmaceutical concentrations in each batch reactor, biotransformation rates, and rates normalized by volatile suspended solids (VSS) concentration. ....	217
<b>Table D5.</b> Candidate gene lists for each compound.....	229

## **List of Appendices**

Appendix A. Supplementary Information for Chapter 3 .....	160
Appendix B. Supplementary Information for Chapter 4 .....	166
Appendix C. Supplementary Information for Chapter 5 .....	179
Appendix D. Supplementary Information for Chapter 6 .....	211

## **Abstract**

More than half of the energy in conventional wastewater treatment is consumed by aeration. To achieve substantial energy savings and comply with increasingly stringent effluent nutrient regulations, wastewater utilities are beginning to control and minimize aeration, thereby operating at a lower dissolved oxygen (DO) concentration. As utilities implement low DO processes, the impact of DO on non-regulated pollutants, such as pharmaceuticals, warrants attention to understand the impact of these technologies on pharmaceutical loads to the environment. This dissertation focuses on the impact of DO on pharmaceutical biotransformation during treatment. Low DO treatment could impact pharmaceutical biotransformation directly by acting as a limiting substrate and slowing the activity of microorganisms involved in biotransformation, and indirectly by selecting for a community that is more (or less) effective at biotransformation. The objective of this work was to evaluate and characterize both direct and indirect impacts of low DO conditions in wastewater treatment bioprocesses on pharmaceutical biotransformation.

To characterize how DO concentration directly impacts pharmaceutical biotransformation rates, oxygen half-saturation constants ( $K_{O_2}$ ) were determined for a suite of compounds that describe the impact of DO on a compound's biotransformation rate. Indirect impacts of DO concentration on pharmaceutical biotransformation rates were demonstrated using bench-scale nitrifying bioreactors operated for over a year under low ( $\sim 0.3$  mg-DO/L) and high ( $>4$  mg-DO/L)

DO conditions. Results showed that long-term low DO conditions resulted in a greater biomass concentration in the low DO reactor compared to high DO reactor. The greater biomass concentration in the low DO reactor resulted in a community with lower specific pharmaceutical biotransformation rates but greater net biotransformation rates under non-limiting DO conditions. In addition, the low DO reactor supported the growth of a more diverse microbial community. To follow up on this finding, a direct test of how microbial diversity affects pharmaceutical biotransformation was performed using a dilution-to-extinction approach. The results showed a strong positive association between biodiversity and collective pharmaceutical biotransformation rates. Taken together, these studies demonstrate that that substantial energy savings can be achieved by operating at lower bulk liquid DO concentrations (0.5 - 1 mg/L) without compromising net pharmaceutical biotransformation rates.

## **Chapter 1.**

### **Introduction**

#### **1.1 Background**

Wastewater collection emerged in the 1800's in response to outbreaks of disease, and the first biological treatment was introduced in the late 19<sup>th</sup> century when cities became aware of the deleterious impact of discharging raw sewage into local water bodies (Riffat, 2012). Over a century after activated sludge was first introduced by Ardern and Lockett (Ardern and Lockett, 1914), substantial advances in wastewater treatment technology are being driven by current needs. Today, the water industry grapples with the stressors of climate change (Zouboulis and Tolkou, 2015), rapid population growth and urbanization (e.g. Semadeni-Davies et al., 2008), ageing water and wastewater infrastructure (ASCE, 2009), increasingly stringent effluent regulations (e.g. EPA, 2008), and the adverse impacts of a society that practices “better living through chemistry” (Crane et al., 2006). In an effort to increase sustainability and achieve cost savings, wastewater utilities are beginning to prioritize improvements in energy efficiency. Concurrently, mounting evidence shows that trace chemical contaminants present in wastewater, such as pharmaceuticals, personal care products, and pesticides, pose a threat to environmental health (Santos et al., 2010). The intent of this research was to elucidate a complex relationship between two environmental sustainability goals relevant to wastewater treatment: enhancing energy efficiency and reducing pharmaceutical contamination.

One of the original and primary goals of wastewater treatment is carbon removal. After it became clear that nutrients were also responsible for eutrophication in receiving water bodies, advanced treatment systems were developed to remove nitrogen and phosphorus (U.S. EPA, 2008). Today, we are still discovering pollutants in wastewater, such as trace organic chemicals, that threaten environmental health (e.g. Brodin et al., 2013; Kidd et al., 2007). Humans excrete thousands of chemicals used in medicines as the active pharmaceutical ingredient (API) and in metabolized forms; both are conveyed through collected sewage to wastewater treatment plants (WWTPs). If a particular pharmaceutical or its metabolite is not removed by wastewater treatment processes through one of several mechanisms before entering our waterways (Deblonde et al., 2011), then it becomes trace contaminant pollution in the receiving stream. In this way, WWTPs represent a primary entry point for the proliferation of pharmaceuticals in the environment (Kolpin et al., 2002), but they are also a last line of defense against this form of chemical pollution. Pharmaceuticals have been widely detected in surface and groundwater (Focazio et al., 2008), and have detrimental impacts on aquatic life at extremely low concentrations (Jobling et al., 1998; Kidd et al., 2007; Painter et al., 2009). As reusing wastewater for drinking water and irrigation becomes more commonplace as a sustainable solution to ensure water access in water-scarce regions and to improve water security in urban areas, the cycling of pharmaceuticals could pose a more serious and direct threat to human health.

Our limited understanding of pharmaceutical degradation and transformation pathways prevents us from aligning the design and operation of WWTPs to reduce pharmaceutical exposure and associated risks in receiving environments (Stadler et al., 2012). In addition, as wastewater utilities move toward implementing lower energy technologies in the name of sustainability, they must recognize the consequences these systems have on other treatment objectives, such as



pharmaceutical removal. One strategy for implementing sustainable wastewater management practices involves a reduction in the energy consumption used in conventional activated sludge wastewater treatment by moving towards treatment that minimizes aeration (Leu et al., 2009), as conventional treatment is an extremely energy intensive process. Aeration is the most energy intensive operation in activated sludge wastewater treatment, accounting for approximately 3% of the US electrical energy demand (U.S. EPA, 2006) and making up 45–75% of a typical WWTP's total energy costs (Rosso et al., 2008). Conventional activated sludge WWTPs typically operate with bulk liquid dissolved oxygen (DO) concentrations of greater than 2 mg/L to ensure complete nitrification and stable nitrifying populations (WEF, 2008). There is mounting evidence that stable carbon removal and nitrification can occur at low DO concentrations (<0.7 mg/L) (Schuyler et al., 2009; Jimenez et al., 2011), suggesting that substantial energy and cost savings are possible by reducing DO concentrations. Despite this benefit, we still lack an understanding of how reducing operational DO concentration will impact pharmaceutical fate in WWTPs.

It is necessary to understand the ecology and physiology of microorganisms that are central to wastewater treatment and the impact of low DO on their abundance and activity to understand the impact of DO on pharmaceutical biotransformation. Many studies have measured pharmaceutical biotransformation rates in wastewater systems (e.g. Abegglen et al., 2009; Urase and Kikuta, 2005) and proposed to classify the relative biodegradability of individual compounds based on their transformation rate (Joss et al., 2006; Salgado et al., 2012). Despite these efforts, few studies have reported measured rates in different redox environments and even fewer have linked microbial community characteristics with pharmaceutical biotransformation patterns. The objective of this dissertation was to elucidate how low DO impacts the activity and structure of wastewater microbial communities, and thus affects pharmaceutical biotransformation rates. Low

DO treatment could impact pharmaceutical biotransformation directly by slowing the activity of microorganisms involved in biotransformation by acting as a limiting substrate, and indirectly by selecting for a community that is more (or less) effective at biotransformation (Figure 1-1).

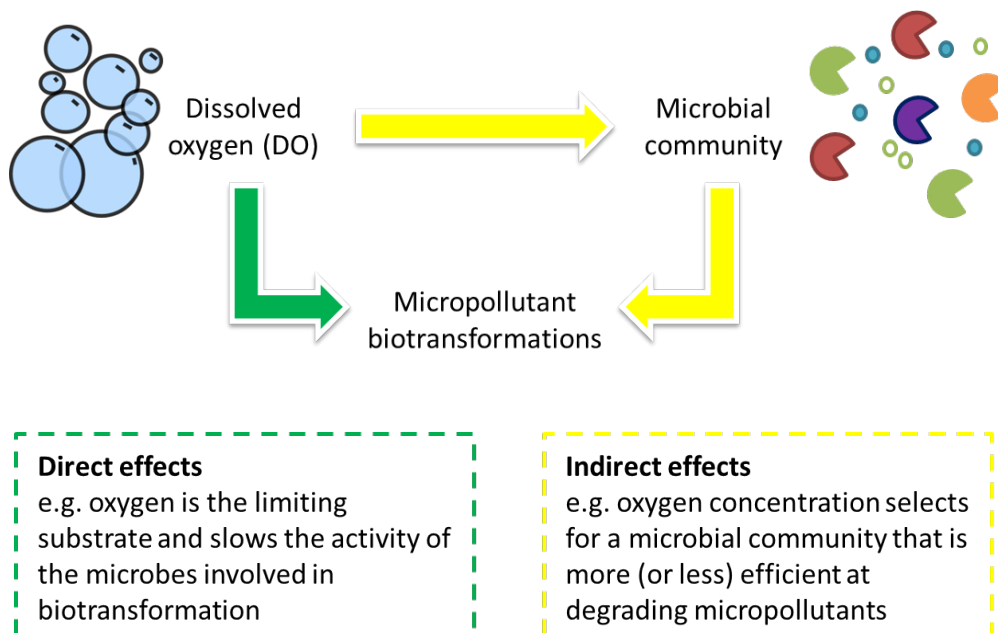


**Figure 1-1.** Direct and indirect impacts of DO on pharmaceutical biotransformation during wastewater treatment.

Monod-type equations are typically used to describe the direct impact of varying concentrations of a growth rate-limiting substrate on process rates. However, no studies to date have determined oxygen half-saturation constants to characterize the impact of DO concentration on pharmaceutical biotransformation rates. Kinetic parameters that describe pharmaceutical biotransformation, such as  $K_{O_2}$  values, are necessary to model the transformation of pharmaceuticals in existing wastewater treatment plant models (Plósz et al., 2012). Researchers, consultants, and utilities have regularly used wastewater models to inform the design of new WWTPs and improve treatment performance. Model-based approaches allow for systematic

evaluations that would not be feasible experimentally. Models, however, are only as good as the parameters that they employ. To advance pharmaceutical fate models, there is a clear need for experimentally-determined kinetic parameters, such as oxygen half saturation constants, that describe the impact of DO on biotransformation rates. Eventually, with the establishment of calibrated kinetic parameters, models can be used to predict the fate of pharmaceuticals in emerging and advanced treatment processes and reduce time- and resource-intensive monitoring. Integrated treatment performance and ecotoxicity models can be used to advance a technology-based regulatory framework favoring technologies that reduce pharmaceutical impacts on the environment, instead of setting regulations for concentrations of individual compounds (Clouzot et al., 2013).

In addition to direct impacts of DO limitation on pharmaceutical biotransformation rates, long-term low DO treatment could indirectly impact pharmaceutical biotransformation by shaping the wastewater microbial community or by selecting for microorganisms with greater oxygen affinities (Park and Noguera, 2004; Liu and Wang, 2015), and/or modified maximum biotransformation rates. WWTPs, which harbor complex assemblages of microorganisms, have been used as model systems to study microbial ecology. Ecological theory predicts that limiting resources drive competition that, in turn, drives diversification in microbial communities (Huston, 1994). Mounting evidence, from both macro and microbial ecology suggests a strong positive association between biodiversity and ecosystem function (Duffy, 2008; Cardinale et al., 2012). The degree to which DO concentration influences biodiversity in WWTPs is not known. A better fundamental understanding of how DO shapes wastewater microbial communities and the microorganisms involved in pharmaceutical biotransformation will improve our ability to design WWTPs that both reduce energy demands and transform pharmaceuticals.

## 1.2 Overview of dissertation

This dissertation seeks to advance our understanding of both direct and indirect impacts of DO concentration on pharmaceutical biotransformation during wastewater treatment. Chapter 2 provides background on where and why low DO wastewater treatment is emerging, and how it might impact microbial physiology and community structure. It also lays the foundation for how we understand both the fate of pharmaceuticals during wastewater treatment, and factors that are thought to impact overall pharmaceutical removal, such as nitrification and microbial biodiversity.

To determine if low DO wastewater treatment causes differences in the extent of pharmaceutical removal, an investigation into the fate of six pharmaceuticals in sequencing batch reactors operated under different redox conditions was performed (Chapter 3). The results of this initial investigation suggest that redox environment is an important variable that defines pharmaceutical fate, and motivated subsequent studies focused on identifying mechanisms that explain observed differences in pharmaceutical loss under different redox conditions. To tease apart direct and indirect impacts of DO concentration on pharmaceutical removal, parent nitrifying enrichment bioreactors were operated under low and high DO conditions for over a year. Batch experiments were performed using biomass from each parent reactor under low and high DO conditions to measure pharmaceutical biotransformation rates (Chapter 4). By characterizing the microbial communities in the parent enrichment bioreactors and performing short-term batch kinetic experiments, we were able to discern between direct and indirect impacts of DO on biotransformation rates and begin to link microbial community characteristics with enhanced biotransformation. Further characterization of the direct impact of DO concentration on pharmaceutical biotransformation was performed using biomass from a full-scale wastewater treatment plant (Chapter 5). Oxygen half-saturation constants that can be used to model the impact

of DO concentration on pharmaceutical biotransformation rates were determined for eight pharmaceuticals. In addition, correlations between active phylogenetic groups (based on 16S rRNA) and pharmaceutical biotransformation rates were developed and indicated phylotypes that might mediate these transformations. The role of nitrifiers, whose activity has been implicated (but not proven) to explain enhanced pharmaceutical removal in nitrifier enrichment cultures that include heterotrophs (e.g. Tran et al., 2013), and who have been shown to degrade the synthetic estrogen 17 $\alpha$ -ethinylestradiol more rapidly than heterotrophs (Khunjar et al., 2011), was assessed using inhibitors (Chapters 4 and 5). Chapter 6 followed up on the findings from Chapter 4 and directly tested the impact of microbial biodiversity on pharmaceutical biotransformation using a dilution to extinction approach. Biotransformation batch experiments combined with sequencing of the 16S rRNA gene, 16S rRNA, metagenome, and metatranscriptome were performed to assess diversity-function relationships and identify taxa and genes associated with pharmaceutical biotransformation. Drawing on these findings, I discuss the impact of this research on the wastewater treatment field (Chapter 7).

### 1.3 Literature cited

Abegglen, C.; Joss, A.; McArdell, C. S.; Fink, G.; Schlüsener, M. P.; Ternes, T. a; Siegrist, H. The Fate of Selected Micropollutants in a Single-House MBR. *Water Res.* **2009**, *43* (7), 2036–2046.

Ardern, E.; Lockett, W. T. Experiments on the Oxidation of Sewage without the Aid of Filters. *J. Soc. Chem. Ind.* **1914**, *33* (10), 523–539.

ASCE. *Report Card for American Infrastructure.* **2009**. Retrieved from ASCE: [www.infrastructurereportcard.org](http://www.infrastructurereportcard.org) on November 15, 2015.

Brodin, T.; Fick, J.; Jonsson, M.; Klaminder, J. Dilute Concentrations of a Psychiatric Drug Alter Behavior of Fish from Natural Populations. *Science* **2013**, *339* (6121), 814–815.

Cardinale, B. J.; Duffy, J. E.; Gonzalez, A.; Hooper, D. U.; Perrings, C.; Venail, P.; Narwani, A.; Mace, G. M.; Tilman, D.; Wardle, D. A. Biodiversity Loss and Its Impact on Humanity. *Nature* **2012**, *486* (7401), 59–67.

Clouzot, L.; Choubert, J.-M.; Cloutier, F.; Goel, R.; Love, N. G.; Melcer, H.; Ort, C.; Patureau, D.; Plósz, B. G.; Pomiès, M. Perspectives on Modelling Micropollutants in Wastewater Treatment Plants. *Water Sci. Technol.* **2013**, *68* (2), 448–461.

Crane, M.; Watts, C.; Boucard, T. Chronic Aquatic Environmental Risks from Exposure to Human Pharmaceuticals. *Sci. Total Environ.* **2006**, *367* (1), 23–41.

Deblonde, T.; Cossu-Leguille, C.; Hartemann, P. Emerging Pollutants in Wastewater: A Review of the Literature. *Int. J. Hyg. Environ. Health* **2011**, *214* (6), 442–448.

Duffy, J. E. Why Biodiversity Is Important to the Functioning of Real-World Ecosystems. *Front. Ecol. Environ.* **2008**, *7* (8), 437–444.

Focazio, M. J.; Kolpin, D. W.; Barnes, K. K.; Furlong, E. T.; Meyer, M. T.; Zaugg, S. D.; Barber, L. B.; Thurman, M. E. A National Reconnaissance for Pharmaceuticals and Other Organic Wastewater Contaminants in the United States—II) Untreated Drinking Water Sources. *Sci. Total Environ.* **2008**, *402* (2), 201–216.

Huston, M. A. *Biological Diversity: The Coexistence of Species*; Cambridge University Press, **1994**.

Jimenez, J.; Dold, P.; La Motta, E.; Houweling, D.; Bratby, J.; Parker, D. Simultaneous Biological Nutrient Removal in a Single-Stage, Low Oxygen Aerobic Reactor. *Proc. Water Environ. Fed.* **2011**, No. 1, 31–48.

Jobling, S.; Nolan, M.; Tyler, C. R.; Brighty, G.; Sumpter, J. P. Widespread Sexual Disruption in Wild Fish. *Environ. Sci. Technol.* **1998**, *32* (17), 2498–2506.

- Joss, A.; Zabczynski, S.; Göbel, A.; Hoffmann, B.; Löffler, D.; McArdell, C. S.; Ternes, T. A.; Thomsen, A.; Siegrist, H. Biological Degradation of Pharmaceuticals in Municipal Wastewater Treatment: Proposing a Classification Scheme. *Water Res.* **2006**, *40* (8), 1686–1696.
- Khunjar, W. O.; Mackintosh, S. A.; Skotnicka-Pitak, J.; Baik, S.; Aga, D. S.; Yi, T.; Jr., W. F. H.; Love, N. G. Elucidating the Relative Roles of Ammonia Oxidizing and Heterotrophic Bacteria during the Biotransformation of 17 $\alpha$ -Ethinylestradiol and Trimethoprim. *Environ. Sci. Technol.* **2011**, *45* (8), 3605–3612.
- Kidd, K. A.; Blanchfield, P. J.; Mills, K. H.; Palace, V. P.; Evans, R. E.; Lazorchak, J. M.; Flick, R. W. Collapse of a Fish Population after Exposure to a Synthetic Estrogen. *Proc. Natl. Acad. Sci.* **2007**, *104* (21), 8897–8901.
- Kolpin, D. W.; Furlong, E. T.; Meyer, M. T.; Thurman, E. M.; Zaugg, S. D.; Barber, L. B.; Buxton, H. T. Pharmaceuticals, Hormones, and Other Organic Wastewater Contaminants in U.S. Streams, 1999–2000: A National Reconnaissance. *Environ. Sci. Technol.* **2002**, *36* (6), 1202–1211.
- Leu, S.-Y.; Rosso, D.; Larson, L. E.; Stenstrom, M. K. Real-Time Aeration Efficiency Monitoring in the Activated Sludge Process and Methods to Reduce Energy Consumption and Operating Costs. *Water Environ. Res.* **2009**, *81* (12), 2471–2481.
- Liu, G.; Wang, J. Quantifying the Chronic Effect of Low DO on the Nitrification Process. *Chemosphere* **2015**, *141*, 19–25.
- Painter, M. M.; Buerkley, M. A.; Julius, M. L.; Vajda, A. M.; Norris, D. O.; Barber, L. B.; Furlong, E. T.; Schultz, M. M.; Schoenfuss, H. L. Antidepressants at Environmentally Relevant Concentrations Affect Predator Avoidance Behavior of Larval Fathead Minnows (*Pimephales Promelas*). *Environ. Toxicol. Chem.* **2009**, *28* (12), 2677–2684.
- Park, H.-D.; Noguera, D. R. Evaluating the Effect of Dissolved Oxygen on Ammonia-Oxidizing Bacterial Communities in Activated Sludge. *Water Res.* **2004**, *38* (14–15), 3275–3286.
- Plósz, B. G.; Langford, K. H.; Thomas, K. V. An Activated Sludge Modeling Framework for Xenobiotic Trace Chemicals (ASM-X): Assessment of Diclofenac and Carbamazepine. *Biotechnol. Bioeng.* **2012**, *109* (11), 2757–2769.
- Riffat, R. *Fundamentals of Wastewater Treatment and Engineering*; CRC Press, **2012**.
- Rosso, D.; Stenstrom, M. K.; Larson, L. E. Aeration of Large-Scale Municipal Wastewater Treatment Plants: State of the Art. *Water Sci. Technol.* **2008**, *57* (7), 973–978.
- Salgado, R.; Marques, R.; Noronha, J. P.; Carvalho, G.; Oehmen, A.; Reis, M. A. M. Assessing the Removal of Pharmaceuticals and Personal Care Products in a Full-Scale Activated Sludge Plant. *Environ. Sci. Pollut. Res.* **2012**, *19* (5), 1818–1827.
- Santos, L. H. M. L. M.; Araújo, A. N.; Fachini, A.; Pena, A.; Delerue-Matos, C.; Montenegro, M.

- C. B. S. M. Ecotoxicological Aspects Related to the Presence of Pharmaceuticals in the Aquatic Environment. *J. Hazard. Mater.* **2010**, *175* (1–3), 45–95.
- Schuyler, R. G.; Tamburini, J. R.; Hogg, S.; Staggs, R. How Low Is Too Low: Several Years of Low Dissolved Oxygen Operations Improve Effluent Quality. *Water Env. Technol.* **2009**, *21*, 32–39.
- Semadeni-Davies, A.; Hernebring, C.; Svensson, G.; Gustafsson, L.-G. The Impacts of Climate Change and Urbanisation on Drainage in Helsingborg, Sweden: Combined Sewer System. *J. Hydrol.* **2008**, *350* (1–2), 100–113.
- Stadler, L. B.; Ernstoff, A. S.; Aga, D. S.; Love, N. G. Micropollutant Fate in Wastewater Treatment: Redefining “Removal.” *Environ. Sci. Technol.* **2012**, *46* (19), 10485–10486.
- Tran, N. H.; Urase, T.; Ngo, H. H.; Hu, J.; Ong, S. L. Insight into Metabolic and Cometabolic Activities of Autotrophic and Heterotrophic Microorganisms in the Biodegradation of Emerging Trace Organic Contaminants. *Bioresour. Technol.* **2013**, *146*, 721–731.
- U.S. EPA. Despite Progress, EPA Needs to Improve Oversight of Wastewater Upgrades in the Chesapeake Bay Watershed. *EPA 08-P-0049*, **2008**.
- U.S. EPA. Wastewater Management Fact Sheet, Energy Conservation. *EPA 832-F-06-024*. U.S. Environmental Protection Agency: EPA Office of Water. **2006**.
- U.S. EPA. Municipal Nutrient Removal Technologies Reference Document. *EPA 832-R-08-006*; **2008**.
- Urase, T.; Kikuta, T. Separate Estimation of Adsorption and Degradation of Pharmaceutical Substances and Estrogens in the Activated Sludge Process. *Water Res.* **2005**, *39* (7), 1289–1300.
- WEF. Activated Sludge. In *Operation of Municipal Wastewater Treatment Plants: MoP No. 11, Sixth Edition*; McGraw Hill Professional, Access Engineering: Water Environment Federation, **2008**.
- Zouboulis, A.; Tolkou, A. Effect of Climate Change in Wastewater Treatment Plants: Reviewing the Problems and Solutions. In *Managing Water Resources under Climate Uncertainty*; Springer, **2015**, 197–220.



## **Chapter 2.**

### **Background**

#### **2.1 Low dissolved oxygen wastewater treatment**

Wastewater treatment plants (WWTPs) in the US consumed over 30 terawatt hours of electricity in 2011, and aeration accounted for over half of the electricity use (Pabi et al., 2013). Conventionally, wastewater treatment plants were designed to operate at dissolved oxygen (DO) concentrations of 2 mg/L or greater because nitrification performance was thought to be highly sensitive to DO limitation. However, mounting evidence has demonstrated that complete and stable nitrification can occur at DO concentrations of 0.5 mg/L or less (Hanaki et al., 1990; Park and Noguera, 2004; Bellucci et al., 2011), and instabilities in low DO nitrification performance can be countered by increasing the solids retention time (SRT) of a system (Liu and Wang, 2015).

The amount of aeration required in a WWTP is a function of oxygen demand, oxygen transfer efficiency, and mixing requirements. Oxygen demand depends on the amount of substrates (pollutants and decay products) oxidized. Thus, the amount of biomass produced and decay rate can have a major impact on the oxygen demand of a system. A few studies have demonstrated reduced biomass decay rates under low DO conditions ( $< 0.5$  mg-DO/L) as compared to fully aerobic conditions ( $> 2$  mg-DO/L) (Habermacher et al., 2015; Liu and Wang, 2015). The impact of DO concentration on decay rates of heterotrophs and nitrifiers has only been evaluated by a few studies and is typically not accounted for in activated sludge models. The endogenous decay

coefficient, used to model decay in wastewater treatment models, accounts for loss in cell mass due to oxidation of internal storage products for energy required for cell maintenance and death, as well as predation by other organisms (Lawrence and McCarty, 1970). Liu and Wang (2013, 2015) found that long-term low DO treatment selects for nitrifiers with higher oxygen affinities and a substantially lower decay rate, and concluded that only a 10% increase in SRT is necessary to maintain effluent quality when DO is reduced from 2.0 mg/L to 0.5 mg/L. Previous studies have shown that low DO inhibits select protozoan predators, which may also impact the observed decay rate and biomass concentration (Madoni, 1993). The oxygen transfer efficiency of a system depends on factors such as diffuser design and placement, operational DO concentration, temperature, and suspended solids concentration (Tchobanoglous et al., 2003). Reducing the operational bulk liquid DO concentration from 2.0 to 0.5 mg-DO/L would result in an increase in oxygen transfer efficiency by at least 15% (Tchobanoglous et al., 2003). Thus, reducing operational DO concentrations could reduce aeration energy by both reducing oxygen demands by selecting for biomass with higher oxygen affinities and reducing decay, and increasing oxygen transfer efficiency. However, aeration also provides mixing in activated sludge systems. In the winter, the aeration may be driven by mixing requirements as opposed to oxygen demands. Thus, additional mixing mechanisms may be necessary if aeration is reduced, which would negate the energy benefits of reduced aeration to some degree.

### ***2.1.1 Applications of low DO wastewater treatment***

Operating under low DO conditions can achieve nitrogen removal in some instances by supporting the growth of both nitrifiers and denitrifiers, a process referred to as simultaneous nitrification-denitrification (SND) (Daigger and Littleton, 2000; Baek and Pagilla, 2008; Jimenez et al., 2011). Many full scale SND systems have demonstrated effective nitrogen removal from

domestic wastewater (80 – 90% TN removal) by operating at constant low DO levels (Jimenez et al., 2013). Nitrite-shunt processes that stop nitrification at nitrite and prevent the oxidation of nitrite to nitrate can also employ low DO environments (Jimenez et al., 2014).

Wastewater treatment plants increasingly are installing more advanced aeration control systems to realize energy savings and meet more stringent effluent nutrient requirements (Jimenez et al., 2013; Uprety et al., 2015). Aeration control strategies, such as DO set point based aeration control and ammonia based aeration control (ABAC) are two strategies that have been implemented in full-scale treatment plants that have resulted in reduced bulk liquid DO concentrations and significant treatment plant energy savings (Vrecko et al., 2006; Rieger et al., 2014). With DO set point control, airflow is controlled via feedback from online DO sensors to prevent over-aeration and maintain a set point DO concentration, typically around 2 mg/L. ABAC uses both DO and ammonia concentrations as feedback variables to control airflow. In this strategy, aeration is controlled around a DO set point that is calculated based on the ammonia concentration that is determined in real time using ammonia probes located at the end of the aeration tanks. This strategy can enable partial nitrification, in which only a portion of the influent ammonia is oxidized, and simultaneous nitrification and denitrification by maintaining the aerobic zones at low DO concentrations (typically between 0.5 and 0.8 mg-DO/L (Uprety et al., 2015). Full-scale demonstrations of ABAC have reported not only substantial energy savings, but also substantial reductions in supplemental carbon usage to achieve effluent TN requirements (Uprety et al., 2015).

### ***2.1.2 Impact of low DO on microbial physiology and community structure***

DO concentration impacts both microbial physiology and community structure, and consequently affects process rates and effluent quality. If acting as a limiting substrate, DO will

influence microbial physiology and directly impact the activity of aerobic microorganisms, and thus the kinetics of substrate utilization. Monod-type equations are typically used to describe the impact of DO concentration on process rates. DO concentration can also shape a WWTP's microbial community structure by selecting for organisms that outcompete in an oxygen-limiting environment. For example, long-term low DO operation may select for microorganisms with high oxygen affinities over fast growth rates because oxygen scavenging ability dictates their survival in a low DO environment (Gudelj et al., 2007). Low DO can also result in oxygen-free niches, such as within flocs or granules, and support the growth of anaerobic microorganisms and/or increase the activity of anaerobic metabolisms (Hocaoglu et al., 2011).

The impact of aeration on enhanced biological phosphorus removal (EBPR), and specifically on the competition between polyphosphate accumulating organisms (PAOs) and glycogen accumulating organisms (GAOs), has also been studied to understand how energy saving strategies affect EBPR performance. A recent study found that low DO treatment could be beneficial for EBPR performance because *Accumulibacter* PAOs have a competitive advantage over *Competibacter* GAOs at low DO levels due to the PAO's higher oxygen affinity (Carvalho et al., 2014). Carvalho et al. (2014) also found that aerobic HRT affected PAO-GAO competition, with longer aerobic HRTs resulting in reduced P release and uptake by PAOs, and favoring the growth of GAOs. Thus reducing aeration and controlling the aerobic HRT are promising strategies that could result in both reduced aeration energy and improvements in EBPR performance.

In addition to phosphorus removal, a substantial amount of research on low DO wastewater treatment has focused on nitrification, as nitrifiers have lower oxygen affinities than heterotrophs and are thus more sensitive to oxygen limitation. One proposed hypothesis for the impact of

oxygen limitation on nitrifying communities is that the community undergoes a physiological, as opposed to structural, adaptation to low DO conditions. Arnaldos et al. (2013) observed an enhanced expression of a particular heme protein and increased specific oxygen uptake rates in a nitrifying enrichment culture adapted to low DO conditions (0.1 mg-DO/L) as compared to a high DO enrichment that was operated near saturation. This suggests that microorganisms may ramp up oxygen delivery machinery, such as heme proteins that transport oxygen, in response to oxygen limitation.

Other studies have hypothesized that low DO environments select for nitrifier lineages that have high oxygen affinities (Gieseke et al., 2001; Park and Noguera, 2004; Bellucci et al., 2011). The results, however, have been conflicting in terms of the specific lineages of AOBs enriched for under low DO conditions. Park and Noguera (2004) reported that the dominant AOBs present under low DO conditions (< 0.24 mg/L) were members of *Nitrosomonas europaea*, whereas members of the *Nitrosomonas oligotropha* lineage were present in the high DO system. Bellucci et al. (2011) also found that the dominant AOB in both their low (0.5 mg/L) and high DO enrichments belonged to the *Nitrosomonas oligotropha* lineage. Liu and Wang (2013) found that long-term low DO conditions enriched for *Nitrosomonas europaea/eutropha* as the dominant AOB.

It is not clear whether oxygen affinity is the sole trait necessary for thriving in low DO environments. Park and Noguera (2007) characterized two AOB isolated from low DO reactors and found that the *Nitrosomonas europaea* strain had a high affinity for oxygen and low affinity for ammonia, while the *Nitrosomonas oligotropha* strain had a low affinity for oxygen and a high affinity for ammonia. This suggests that there may be other mechanisms, such as ammonia affinity, that allow AOB to persist in low DO environments. In general, *Nitrosomonas*-type AOB and

*Nitrobacter*-type NOB are thought to be “r” strategists with high specific growth rates and low substrate affinities that thrive in low SRT, high substrate conditions (Dytczak et al., 2008). Whereas *Nitrosopsira*-type AOB and *Nitrospira*-type NOB are thought to be “K” strategists with low specific growth rates and high substrate affinities that thrive in low substrate, long SRT systems (Schramm et al., 1999; Kim and Kim, 2006; Dytczak et al., 2008). At present, not enough is known about the relationship between electron donor and acceptor substrate affinities, or their relative importance, to predict how low DO environments select for specific lineages of AOB and NOB.

## **2.2 Pharmaceutical fate in wastewater treatment**

Pharmaceuticals are of increasing environmental and public health concern because of their widespread detection in the aquatic environment (Hirsch et al., 1999; Zuccato et al., 2000; Kolpin et al., 2002) and drinking water sources (Benotti et al., 2008; Focazio et al., 2008), and their threat to ecological health (Arnold et al., 2014). Pharmaceuticals are present in influent wastewater because we take medications, but only a fraction of what we consume enters our bloodstream. The remainder of the ingested chemicals pass through our bodies and are excreted either in intact or metabolized forms, primarily in urine (Daughton, 2010). These chemicals then reach wastewater treatment plants (WWTPs), where they may be completely mineralized, partially metabolized, or pass through unchanged and are released into the environment (Onesios et al., 2009). The microbes that we harness to treat wastewater and remove conventional pollutants such as carbon, nitrogen, and phosphorus are also capable of transforming many pharmaceuticals during treatment. Thus, WWTPs represent an important barrier of entry for pharmaceuticals in the environment. The factors that impact the degree that microbes degrade pharmaceuticals are numerous, complex, and

interconnected, making it challenging to align the design and operation of WWTPs to maximize pharmaceutical transformations.

The removal of an individual pharmaceutical compound depends on factors such as its molecular properties, influent wastewater composition, and treatment configuration (Khan and Ongerth, 2002; Blair et al., 2013). Monitoring of full-scale WWTPs and bench-scale reactor studies have generated a substantial body of data describing the fate of a wide range of pharmaceuticals in wastewater; however, as new pharmaceuticals are constantly entering the market, only a small fraction of all pharmaceuticals have been investigated. Volatilization, sorption, and biodegradation are three major pathways that describe the fate of chemicals during treatment. Volatilization is expected to be negligible for most pharmaceuticals (Jones et al., 2002), and thus sorption to biomass and biodegradation constitute the two primary removal mechanisms during treatment. There is a growing body of research focused on predicting removal by sorption and biodegradation based on a chemical's structure, such as via quantitative structure–activity relationship (QSAR) models (Khan and Ongerth, 2004). While these models have been experimentally validated for some compounds, there are many other environmental factors such as redox environment (Ericson, 2007; Stadler et al., 2015), active microbial groups (Tran et al., 2009), and physical factors such as reactor configuration (Clara et al., 2005a) and solids retention time (Clara et al., 2005b), that have been shown to impact removal.

Where biologically-mediated transformation is the primary loss mechanism for a compound, most studies have simply quantified overall removal efficiencies by comparing a WWTP's liquid phase influent and effluent concentrations. It is increasingly apparent that for many pharmaceuticals, transformation products (TPs) (conjugated or metabolized forms of the parent compound) exist and may even exceed the parent form in both concentration and toxicity

in WWTP effluents. For example, oxidation of the antiviral drug acyclovir and its biodegradation product carboxy-acyclovir, produces a TP more acutely toxic than its parent form (Prasse et al., 2012). TPs complicate our understanding of how treatment conditions affect pharmaceutical fate and are a contributing factor for large reported differences in removal of pharmaceuticals across WWTPs. In a Viewpoint that was published in *Environmental Science & Technology* (Stadler et al., 2012), we argued that misleading conclusions might arise by describing pharmaceutical fate in wastewater treatment in terms of compound "removal." To more accurately interpret environmental data, focus should shift from "removal" as currently used to a comprehensive understanding of pharmaceutical fate that incorporates the mechanisms and kinetics of TP formation and disappearance. While research on TPs is increasing (e.g. Escher and Fenner, 2011, Pérez et al., 2006) and analytical capabilities for detecting and screening for "unknown" TPs are improving (Gómez et al., 2010; de Jongh et al., 2012), the research presented in this dissertation focuses primarily on the loss of parent compounds. The research would be strengthened by an understanding of the formation and further conversion of TPs and thus this represents an area with great potential for future research.

### ***2.2.1 Impact of redox environment on pharmaceutical biotransformation***

Environmental conditions such as redox state influence the biodegradation pathways employed by microorganisms. Oxygen availability impacts the terminal enzymes of the electron transport train and the synthesis of enzymes involved in biodegradation (Çinar et al., 2003). Some pharmaceuticals can be transformed in aerobic, anoxic, and anaerobic environments; however, transformation rates may vary and biotransformation pathways and products will differ based on redox environment. The strategy often employed by microorganisms to degrade pharmaceuticals in aerobic environments depends on the availability of oxygen as a reactant. Microbial aerobic



degradation pathways for substituted and unsubstituted aromatic rings, a structure common to many pharmaceuticals, have been studied extensively (e.g. Dagley, 1971; Harayama et al., 1992; Hayaishi, 1994). In oxic environments, oxygenase enzymes transform aromatic compounds by incorporating one or two oxygen molecules into them, which also enhances their biodegradability by other enzymes. Dihydroxylation, a prerequisite of ring cleavage, can occur by either monooxygenase enzymes that add one oxygen atom at a time, or dioxygenase enzymes that add two oxygen atoms simultaneously. The resulting catechol can be cleaved by dioxygenase enzymes, thereby making the target compound more amenable to further biodegradation via central metabolism. In anaerobic environments, aromatic compounds undergo reduction prior to ring cleavage. Central intermediates (e.g. benzoyl-CoA) in anaerobic degradation pathways have substituents with an electron-withdrawing effect that enables the transfer of electrons to the ring (Fuchs et al., 2011). In low redox environments, hydroxylation of adjoining carbon atoms is the primary mechanism for ring cleavage and degradation of aromatic compounds (Pitter and Chudoba, 1990). However, the nature and location of substituents on aromatic rings can either promote or suppress hydroxylation, and therefore a compound's biodegradability. While some substituents, such as carboxyl and hydroxyl groups, promote ring cleavage, others occupy sites on the ring preventing direct hydroxylation or spatially interfere with enzymes that might degrade it (Wackett and Ellis, 1999).

As more monitoring studies of pharmaceuticals in WWTPs are performed, there is an emerging body of research on the impact of redox environments relevant to WWTPs on pharmaceutical fate. Most monitoring studies of WWTPs normally only consider influent and effluent concentrations of pharmaceuticals, making it difficult to understand the impact of anoxic versus aerobic treatment. Exceptions include Andersen et al. (2003), in which they individually

sampled the denitrification and nitrification tanks at a WWTP. Joss et al. (2004) and Suarez et al. (2010) also performed experiments to compare the fate of pharmaceuticals in aerobic and anoxic environments. In general, the studies observed that while some compounds were recalcitrant in both aerobic and anoxic environments, the remainder of compounds were transformed at a faster rate in aerobic than anoxic environments. This may be explained by faster growth rates of aerobic microorganisms due to greater energy gained from using oxygen as an electron acceptor and because many of the compounds may be more amenable to aerobic biodegradation pathways.

Most studies on aerobic environments in WWTPs have examined oxygen saturated or DO > 4 mg/L in the system of interest. As low DO environments become more commonplace to reduce energy demands associated with aeration and reduce effluent nutrient concentrations, there is a need to understand the impact of DO on pharmaceutical transformation rates. Prior studies have shown that slowly biodegradable aromatic compounds, such as benzene, toluene, o-, m-, and p-xylene (BTX compounds), are biotransformed equally if not more efficiently in low DO conditions in the presence of nitrite or nitrate as compared to oxygen saturated conditions (Ma and Love, 2001). These results motivate a desire for a deeper understanding of why biotransformation rates are faster under low DO environments, whether those impacts are true for all or only a subset of compounds, and why. Further, the impact of DO on pharmaceutical transformation by different microbial populations (e.g. heterotrophs and nitrifiers) is not well understood. It is possible that certain groups of microorganism are more equipped to adapt to low DO conditions, and therefore their ability to biotransform pharmaceuticals is less affected by low DO operation.

### ***2.2.2 Links between nitrification and pharmaceutical biotransformation***

Ammonia oxidizers, which perform the first step of nitrification and use the enzyme ammonia monooxygenase (AMO) for catabolism, may play a major role in pharmaceutical

biotransformation and contribute to greater observed overall losses of pharmaceuticals at long SRTs. AMO is a fairly nonspecific enzyme and can catalyze the oxidation of a relatively wide range of substrates (Arp et al., 2002). Several studies have shown that pharmaceutical transformation is enhanced in nitrifying activated sludge systems (e.g. Tran et al., 2009), and have implicated the involvement of AMO. Pure culture work has shown the ability of AMO to biotransform several pharmaceuticals (Shi et al., 2004; Khunjar et al., 2011; Sun et al., 2012). For example, previous research revealed that AOBs biotransformed 17 $\alpha$ -ethinylestradiol (EE2) five times faster than heterotrophs (Khunjar et al., 2011). This study and others (Shi et al., 2004; Yi and Harper, 2007) suggest that AMO, the enzyme that oxidizes ammonia to hydroxylamine on its way to nitrite, is involved in the biotransformation of certain pharmaceuticals, such as EE2.

For pharmaceuticals that are transformed by AMO cometabolically, both ammonia and oxygen are necessary substrates to activate AMO. Previous research showed that AMO is regulated by ammonia (NH<sub>3</sub>) at the transcriptional (Sayavedra-Soto et al., 1996), translational (Hyman and Arp, 1995; Stein et al., 1997), and post-translational levels (Stein et al., 1997). Stein et al. (1997) hypothesized that there are two different types of AMO activity in *Nitrosomonas europaea*: the first type is a base level of activity that is insensitive to changes in available ammonia concentration and the second type of activity is increased in response to increases in ammonia concentration. These types of activity appear to be regulated differently and allow *N. europaea* to respond to fluctuations in ammonia concentrations. Other substrates, such as methane which is a competitive inhibitor of ammonia oxidation by AMO (Hyman and Wood, 1983), have been shown to preserve AMO activity when ammonium is limiting (Stein and Arp, 1998). The impact of pharmaceuticals on the regulation and activity of AMO is not well understood. Pharmaceuticals could serve as substrates or competitive inhibitors of AMO. High concentrations

of ammonium have been found to repress co-metabolic transformations of pharmaceuticals by AOB (Fernandez-Fontaina et al., 2012). Teasing out the importance of ammonia and oxygen availability on pharmaceutical transformation rates by AMO is clearly needed to understand how the design and operation of WWTPs may dictate the fate of certain pharmaceuticals.

While AMO has been linked to the transformation of natural and synthetic estrogens and bisphenol A in pure culture experiments (Khunjar et al., 2011; Shi et al., 2004; Sun et al., 2012) and of antibiotics, antidepressants, synthetic estrogens, and other pharmaceutical compounds in wastewater communities through the use of AMO-inhibitors (Helbling et al., 2012; Khunjar et al., 2011; Shi et al., 2004; Tran et al., 2009; Yi et al., 2007), other enzymes may be involved and may be the primary catalysts of oxidation reactions. In a study by Helbling et al. (2012), biotransformation rates of isoproturon (a herbicide), ranitidine (an antacid), and venlafaxine (an antidepressant) were found to positively associate with archaeal *amoA* expression. However, in experiments where AMO was inhibited, inhibition of pharmaceutical biotransformation was not observed for any compounds with the exception of one (isoproturon). This suggests that while greater AMO activity may be indicative of environments capable of enhanced biotransformation, other microbial processes are responsible or are major contributors to catalyzing transformations. In wastewater microbial communities both heterotrophs and nitrifiers may contribute to biotransformation reactions, as has been demonstrated for 17 $\alpha$ -ethinylestradiol (Khunjar et al., 2011) and tetrabromobisphenol A (a flame retardant, Li et al., 2015), thus their removal may be enhanced in a nitrifying system.

### ***2.2.3 Links between biodiversity and pharmaceutical biotransformation***

The microbial communities present in WWTPs are a complex assemblage of bacteria, archaea, eukaryote (protozoa and fungi), and viruses. The biomass is primarily comprised of

bacteria, which are extremely diverse and play an important role in the removal of traditional pollutants such as carbon, nitrogen, and phosphorus, as well as emerging contaminants such as pharmaceuticals and personal care products. Advances in sequencing technologies and analytical tools has propelled our knowledge of the microbial groups and vast diversity of the microorganisms present in WWTPs. In a survey of 10 full-scale WWTPs, taxonomic richness was found to differ by 4- to 6-fold among the treatment systems (Johnson et al., 2014). Solids retention time (SRT) has been shown to have a strong correlation with the capacity of a WWTPs to remove micropollutants (Clara et al., 2005b). This observation may be explained by the fact that longer SRTs support the growth of slower growing organisms, resulting in more diverse microbial communities. Differences in microbial community biodiversity is one factor that may explain wide ranges of observed pharmaceutical removal efficiencies across WWTPs.

The relationship between microbial biodiversity and ecosystem function is an area of considerable research and debate in ecology. Microbial model systems have been commonly used to study this phenomenon (Cook et al., 2006; Franklin and Mills, 2006; Peter et al., 2010; Levine et al., 2011). Many decades of research in ecology has demonstrated a positive relationship between biodiversity and ecosystem functioning (Cardinale et al., 2012). If many different taxa present in the community perform the same function but occupy different niches, resulting in complementary effects, this would result in a positive relationship between richness and process rates. A positive relationship between diversity (or richness) and process rates would also emerge if facilitative interactions between different species occurred; for example, if the presence of one taxa enhances the activity of another taxa (e.g. via detoxification or producing limiting-nutrients). Levine et al. (2011) studied soil microbial communities and found that for narrow processes, i.e. processes performed by few species, (e.g., methanotrophy), increased diversity resulted in

increased functionality (process rate). Conversely, for broad processes such as denitrification, increased diversity did not positively associate with process rates because many functionally redundant populations coexist to perform denitrification.

In wastewater treatment systems, there are thousands of different pharmaceutical compounds and a vast number of mechanisms for their biodegradation. Substantial research has advanced our knowledge of pharmaceutical biotransformation pathways (Ellis et al., 2006), but few studies have linked chemical transformation data with microbial ecology to develop predictive relationships between the characteristics of the microbial community and pharmaceutical biotransformation pathways and rates. In a previous study of 10 full-scale WWTPs, a positive association between biodiversity and some, but not all, micropollutants was observed (Johnson et al., 2015). The relationship between biodiversity and an individual compound's biotransformation rate is a function of whether its biotransformation is a narrow or broad process. We lack an understanding of which pharmaceutical biotransformations are broad processes catalyzed by highly redundant populations, and which are narrow processes performed by rare taxa. By advancing our knowledge of the specific taxa and enzymes that catalyze pharmaceutical biotransformation and the environmental factors that influence their abundance and activity, we will be able to exploit opportunities for enhancing biotransformation during wastewater treatment.

## 2.3 Literature cited

Andersen, H.; Siegrist, H.; Halling-Sorensen, B.; Ternes, T. A. Fate of Estrogens in a Municipal Sewage Treatment Plant. *Environ. Sci. Technol.* **2003**, *37* (18), 4021–4026.

Arnaldos, M.; Kunkel, S.; Stark, B.; Pagilla, K. Enhanced Heme Protein Expression by Ammonia-Oxidizing Communities Acclimated to Low Dissolved Oxygen Conditions. *Appl. Microbiol. Biotechnol.* **2013**, *97* (23), 10211–10221.

Arnold, K. E.; Brown, A. R.; Ankley, G. T.; Sumpter, J. P. Medicating the Environment: Assessing Risks of Pharmaceuticals to Wildlife and Ecosystems. *Philos. Trans. R. Soc. London B Biol. Sci.* **2014**, *369* (1656), 20130569.

Arp, D.; Sayavedra-Soto, L.; Hommes, N. Molecular Biology and Biochemistry of Ammonia Oxidation by *Nitrosomonas europaea*. *Arch. Microbiol.* **2002**, *178* (4), 250–255.

Baek, S. H.; Pagilla, K. R. Simultaneous Nitrification and Denitrification of Municipal Wastewater in Aerobic Membrane Bioreactors. *Water Environ. Res.* **2008**, *80* (2), 109–117.

Bellucci, M.; Ofițeru, I. D.; Graham, D. W.; Head, I. M.; Curtis, T. P. Low-Dissolved-Oxygen Nitrifying Systems Exploit Ammonia-Oxidizing Bacteria with Unusually High Yields. *Appl. Env. Microbiol.* **2011**, *77* (21), 7787–7796.

Benotti, M. J.; Trenholm, R. A.; Vanderford, B. J.; Holady, J. C.; Stanford, B. D.; Snyder, S. A. Pharmaceuticals and Endocrine Disrupting Compounds in U.S. Drinking Water. *Env. Sci. Technol.* **2008**, *43* (3), 597–603.

Blair, B. D.; Crago, J. P.; Hedman, C. J.; Treguer, R. J. F.; Magruder, C.; Royer, L. S.; Klaper, R. D. Evaluation of a Model for the Removal of Pharmaceuticals, Personal Care Products, and Hormones from Wastewater. *Sci. Total Environ.* **2013**, *444*, 515–521.

Cardinale, B. J.; Duffy, J. E.; Gonzalez, A.; Hooper, D. U.; Perrings, C.; Venail, P.; Narwani, A.; Mace, G. M.; Tilman, D.; Wardle, D. A. Biodiversity Loss and Its Impact on Humanity. *Nature* **2012**, *486* (7401), 59–67.

Carvalho, M.; Oehmen, A.; Carvalho, G.; Eusébio, M.; Reis, M. A. The Impact of Aeration on the Competition Between Polyphosphate Accumulating Organisms and Glycogen Accumulating Organisms. *Water Res.* **2014**, *66*, 296–307.

Çinar, Ö.; Deniz, T.; Grady, C. P. L. Jr. Effects of Oxygen on Anoxic Biodegradation of Benzoate during Continuous Culture. *Water Environ. Res.* **2003**, *75* (5), 434–443.

Clara, M.; Strenn, B.; Gans, O.; Martinez, E.; Kreuzinger, N.; Kroiss, H. Removal of Selected Pharmaceuticals, Fragrances and Endocrine Disrupting Compounds in a Membrane Bioreactor and Conventional Wastewater Treatment Plants. *Water Res.* **2005a**, *39* (19), 4797–4807.

- Clara, M.; Kreuzinger, N.; Strenn, B.; Gans, O.; Kroiss, H. The Solids Retention Time—a Suitable Design Parameter to Evaluate the Capacity of Wastewater Treatment Plants to Remove Micropollutants. *Water Res.* **2005b**, *39* (1), 97–106.
- Cook, K. L.; Garland, J. L.; Layton, A. C.; Dionisi, H. M.; Levine, L. H.; Sayler, G. S. Effect of Microbial Species Richness on Community Stability and Community Function in a Model Plant-Based Wastewater Processing System. *Microb. Ecol.* **2006**, *52* (4), 725–737.
- Dagley, S. Catabolism of Aromatic Compounds by Microorganisms. In *Advances in Microbial Physiology*. **1971**, 1–76.
- Daigger, G. T.; Littleton, H. X. Characterization of Simultaneous Nutrient Removal in Staged, Closed-Loop Bioreactors. *Water Environ. Res.* **2000**, *72* (3), 330–339.
- Daughton, C. G. *Drugs and the Environment: Stewardship & Sustainability*; U.S. Environmental Protection Agency, Office of Research and Development, National Exposure Research Laboratory, **2010**.
- Dytczak, M. A.; Londry, K. L.; Oleszkiewicz, J. A. Activated Sludge Operational Regime Has Significant Impact on the Type of Nitrifying Community and Its Nitrification Rates. *Water Res.* **2008**, *42* (8), 2320–2328.
- Ellis, L. B. M.; Roe, D.; Wackett, L. P. The University of Minnesota Biocatalysis/biodegradation Database: The First Decade. *Nucleic Acids Res.* **2006**, *34* (suppl 1), D517–D521.
- Ericson, J. F. An Evaluation of the OECD 308 Water/sediment Systems for Investigating the Biodegradation of Pharmaceuticals. *Environ. Sci. Technol.* **2007**, *41* (16), 5803–5811.
- Escher, B. I.; Fenner, K. Recent Advances in Environmental Risk Assessment of Transformation Products. *Environ. Sci. Technol.* **2011**, *45* (9), 3835–3847.
- Fernandez-Fontaina, E.; Omil, F.; Lema, J. M.; Carballa, M. Influence of Nitrifying Conditions on the Biodegradation and Sorption of Emerging Micropollutants. *Water Res.* **2012**, *46* (16), 5434–5444.
- Focazio, M. J.; Kolpin, D. W.; Barnes, K. K.; Furlong, E. T.; Meyer, M. T.; Zaugg, S. D.; Barber, L. B.; Thurman, M. E. A National Reconnaissance for Pharmaceuticals and Other Organic Wastewater Contaminants in the United States—II) Untreated Drinking Water Sources. *Sci. Total Environ.* **2008**, *402* (2), 201–216.
- Franklin, R. B.; Mills, A. L. Structural and Functional Responses of a Sewage Microbial Community to Dilution-Induced Reductions in Diversity. *Microb. Ecol.* **2006**, *52* (2), 280–288.
- Fuchs, G.; Boll, M.; Heider, J. Microbial Degradation of Aromatic Compounds - From One Strategy to Four. *Nat. Rev. Microbiol.* **2011**, *9* (11), 803–816.



- Gieseke, A.; Purkhold, U.; Wagner, M.; Amann, R.; Schramm, A. Community Structure and Activity Dynamics of Nitrifying Bacteria in a Phosphate-Removing Biofilm. *Appl. Env. Microbiol.* **2001**, *67* (3), 1351–1362.
- Gómez, M. J.; Gómez-Ramos, M. M.; Malato, O.; Mezcuca, M.; Fernández-Alba, A. R. Rapid Automated Screening, Identification and Quantification of Organic Micro-Contaminants and Their Main Transformation Products in Wastewater and River Waters Using Liquid Chromatography–Quadrupole-Time-of-Flight Mass Spectrometry with an Accurate-Mass. *J. Chromatogr. A* **2010**, *1217* (45), 7038–7054.
- Gudelj, I.; Beardmore, R. E.; Arkin, S. S.; MacLean, R. C. Constraints on Microbial Metabolism Drive Evolutionary Diversification in Homogeneous Environments. *J. Evol. Biol.* **2007**, *20* (5), 1882–1889.
- Habermacher, J.; Benetti, A. D.; Derlon, N.; Morgenroth, E. The Effect of Different Aeration Conditions in Activated Sludge–Side-Stream System on Sludge Production, Sludge Degradation Rates, Active Biomass and Extracellular Polymeric Substances. *Water Res.* **2015**, *85*, 46–56.
- Hanaki, K.; Wantawin, C.; Ohgaki, S. Nitrification at Low Levels of Dissolved Oxygen with and without Organic Loading in a Suspended-Growth Reactor. *Water Res.* **1990**, *24* (3), 297–302.
- Harayama, S.; Kok, M.; Neidle, E. L. Functional and Evolutionary Relationships among Diverse Oxygenases. *Annu. Rev. Microbiol.* **1992**, *46* (1), 565–601.
- Hayaishi, O. Tryptophan, Oxygen, and Sleep. *Annu. Rev. Biochem.* **1994**, *63* (1), 1–25.
- Helbling, D. E.; Johnson, D. R.; Honti, M.; Fenner, K. Micropollutant Biotransformation Kinetics Associate with WWTP Process Parameters and Microbial Community Characteristics. *Environ. Sci. Technol.* **2012**, *46* (19), 10579–10588.
- Hirsch, R.; Ternes, T.; Haberer, K.; Kratz, K. L. Occurrence of Antibiotics in the Aquatic Environment. *Sci. Total Environ.* **1999**, *225* (1-2), 109–118.
- Hocaoglu, S. M.; Insel, G.; Cokgor, E. U.; Orhon, D. Effect of Low Dissolved Oxygen on Simultaneous Nitrification and Denitrification in a Membrane Bioreactor Treating Black Water. *Bioresour. Technol.* **2011**, *102* (6), 4333–4340.
- Hyman, M. R.; Wood, P. M. Methane Oxidation by *Nitrosomonas europaea*. *Biochem. J.* **1983**, *212* (1), 31–37.
- Hyman, M. R.; Arp, D. J. Effects of Ammonia on the de Novo Synthesis of Polypeptides in Cells of *Nitrosomonas europaea* Denied Ammonia as an Energy Source. *J. Bacteriol.* **1995**, *177* (17), 4974–4979.
- Jimenez, J.; Dold, P.; La Motta, E.; Houweling, D.; Bratby, J.; Parker, D. Simultaneous Biological Nutrient Removal in a Single-Stage, Low Oxygen Aerobic Reactor. *Proc. Water Environ. Fed.*

**2011**, 31–48.

Jimenez, J.; Bott, C.; Regmi, P.; Rieger, L. Process Control Strategies for Simultaneous Nitrogen Removal Systems. *Proc. Water Environ. Fed. Nutrient*. **2013**, 492–505.

Jimenez, J.; Wise, G.; Burger, G.; Du, W.; Dold, P. Mainstream Nitrite-Shunt with Biological Phosphorus Removal at the City of St. Petersburg Southwest WRF. *Proc. Water Environ. Fed.* **2014**, 696–711.

Johnson, D. R.; Helbling, D. E.; Lee, T. K.; Park, J.; Fenner, K.; Kohler, H. P. E.; Ackermann, M. Association of Biodiversity with the Rates of Micropollutant Biotransformations among Full-Scale Wastewater Treatment Plant Communities. *Appl. Env. Microbiol.* **2015**, *81* (2), 666–675.

Johnson, D. R.; Lee, T. K.; Park, J.; Fenner, K.; Helbling, D. E. The Functional and Taxonomic Richness of Wastewater Treatment Plant Microbial Communities Are Associated with Each Other and with Ambient Nitrogen and Carbon Availability. *Environ. Microbiol.* **2014**, *17* (12), 4851–4860.

Jones, O. A. H.; Voulvoulis, N.; Lester, J. N. Aquatic Environmental Assessment of the Top 25 English Prescription Pharmaceuticals. *Water Res.* **2002**, *36* (20), 5013–5022.

de Jongh, C. M.; Kooij, P. J. F.; de Voogt, P.; ter Laak, T. L. Screening and Human Health Risk Assessment of Pharmaceuticals and Their Transformation Products in Dutch Surface Waters and Drinking Water. *Sci. Total Environ.* **2012**, *427*, 70–77.

Joss, A.; Andersen, H.; Ternes, T.; Richle, P. R.; Siegrist, H. Removal of Estrogens in Municipal Wastewater Treatment under Aerobic and Anaerobic Conditions: Consequences for Plant Optimization. *Environ. Sci. Technol.* **2004**, *38* (11), 3047–3055.

Khan, S. J.; Ongerth, J. E. Estimation of Pharmaceutical Residues in Primary and Secondary Sewage Sludge Based on Quantities of Use and Fugacity Modelling. *Water Sci. Technol.* **2002**, *46* (3), 105–113.

Khan, S. J.; Ongerth, J. E. Modelling of Pharmaceutical Residues in Australian Sewage by Quantities of Use and Fugacity Calculations. *Chemosphere* **2004**, *54* (3), 355–367.

Khunjar, W. O.; Mackintosh, S. A.; Skotnicka-Pitak, J.; Baik, S.; Aga, D. S.; Yi, T.; Jr., W. F. H.; Love, N. G. Elucidating the Relative Roles of Ammonia Oxidizing and Heterotrophic Bacteria during the Biotransformation of 17 $\alpha$ -Ethinylestradiol and Trimethoprim. *Environ. Sci. Technol.* **2011**, *45* (8), 3605–3612.

Kim, D. J.; Kim, S. H. Effect of Nitrite Concentration on the Distribution and Competition of Nitrite-Oxidizing Bacteria in Nitrification Reactor Systems and Their Kinetic Characteristics. *Water Res.* **2006**, *40* (5), 887–894.

Kolpin, D. W.; Furlong, E. T.; Meyer, M. T.; Thurman, E. M.; Zaugg, S. D.; Barber, L. B.; Buxton,

H. T. Pharmaceuticals, Hormones, and Other Organic Wastewater Contaminants in U.S. Streams, 1999–2000: A National Reconnaissance. *Environ. Sci. Technol.* **2002**, *36* (6), 1202–1211.

Lawrence, A. W.; McCarty P. L. Unified Basis for Biological Treatment Design and Operation. *J. San. Eng. Div.* **1970**, *96* (3), 757-778.

Levine, U. Y.; Teal, T. K.; Robertson, G. P.; Schmidt, T. M. Agriculture's Impact on Microbial Diversity and Associated Fluxes of Carbon Dioxide and Methane. *ISME J.* **2011**, *5* (10), 1683–1691.

Liu, G.; Wang, J. Long-Term Low DO Enriches and Shifts Nitrifier Community in Activated Sludge. *Environ. Sci. Technol.* **2013**, *47* (10), 5109–5117.

Liu, G.; Wang, J. Quantifying the Chronic Effect of Low DO on the Nitrification Process. *Chemosphere* **2015**, *141*, 19–25.

Ma, G.; Love, N. G. BTX Biodegradation in Activated Sludge under Multiple Redox Conditions. *J. Environ. Eng.* **2001**, *127* (6), 509.

Madoni, P. A Sludge Biotic Index (SBI) for the Evaluation of the Biological Performance of Activated Sludge Plants Based on the Microfauna Analysis. *Water Res.* **1994**, *28* (1), 67-75.

Onesios, K. M.; Yu, J. T.; Bower, E. J. Biodegradation and Removal of Pharmaceuticals and Personal Care Products in Treatment Systems: A Review. *Biodegradation* **2009**, *20* (4), 441–466.

Pabi, S.; Amarnath, A.; Goldstein, R.; Reekie, L. Electricity Use and Management in the Municipal Water Supply and Wastewater Industries. Final Report from Electric Power Research Institute: Palo Alto, CA, **2013**.

Park, H. D.; Noguera, D. R. Characterization of Two Ammonia-Oxidizing Bacteria Isolated from Reactors Operated with Low Dissolved Oxygen Concentrations. *J. Appl. Microbiol.* **2007**, *102* (5), 1401–1417.

Park, H. D.; Noguera, D. R. Evaluating the Effect of Dissolved Oxygen on Ammonia-Oxidizing Bacterial Communities in Activated Sludge. *Water Res.* **2004**, *38* (14–15), 3275–3286.

Pérez, S.; Eichhorn, P.; Celiz, M. D.; Aga, D. S. Structural Characterization of Metabolites of the X-ray Contrast Agent Iopromide in Activated Sludge using Ion Trap Mass Spectrometry. *Anal. Chem.* **2006**, *78* (6), 1866-1874.

Peter, H.; Beier, S.; Bertilsson, S.; Lindström, E. S.; Langenheder, S.; Tranvik, L. J. Function-Specific Response to Depletion of Microbial Diversity. *ISME J.* **2010**, *5* (2), 351–361.

Pitter, P.; Chudoba, J. *Biodegradability of Organic Substances in the Aquatic Environment*; CRC Press, Inc.: Boca Raton, FL, **1990**.

Prasse, C.; Wagner, M.; Schulz, R.; Ternes, T. A. Oxidation of the Antiviral Drug Acyclovir and

- Its Biodegradation Product Carboxy-Acyclovir with Ozone: Kinetics and Identification of Oxidation Products. *Environ. Sci. Technol.* **2012**, *46* (4), 2169–2178.
- Rieger, L.; Jones, R. M.; Dold, P. L.; Bott, C. B. Ammonia-Based Feedforward and Feedback Aeration Control in Activated Sludge Processes. *Water Environ. Res.* **2014**, *86* (1), 63–73.
- Sayavedra-Soto, L. A.; Hommes, N. G.; Russell, S. A.; Arp, D. J. Induction of Ammonia Monooxygenase and Hydroxylamine Oxidoreductase mRNAs by Ammonium in *Nitrosomonas europaea*. *Mol. Microbiol.* **1996**, *20* (3), 541–548.
- Schramm, A.; de Beer, D.; van den Heuvel, J. C.; Ottengraf, S.; Amann, R. Microscale Distribution of Populations and Activities of *Nitrosospira* and *Nitrospira* Spp. along a Macroscale Gradient in a Nitrifying Bioreactor: Quantification by In Situ Hybridization and the Use of Microsensors. *Appl. Environ. Microbiol.* **1999**, *65* (8), 3690–3696.
- Shi, J.; Fujisawa, S.; Nakai, S.; Hosomi, M. Biodegradation of Natural and Synthetic Estrogens by Nitrifying Activated Sludge and Ammonia-Oxidizing Bacterium *Nitrosomonas europaea*. *Water Res.* **2004**, *38* (9), 2323–2330.
- Stadler, L. B.; Ernstoff, A. S.; Aga, D. S.; Love, N. G. Micropollutant Fate in Wastewater Treatment: Redefining “Removal.” *Environ. Sci. Technol.* **2012**, *46* (19), 10485–10486.
- Stadler, L. B.; Su, L.; Moline, C. J.; Ernstoff, A. S.; Aga, D. S.; Love, N. G. Effect of Redox Conditions on Pharmaceutical Loss during Biological Wastewater Treatment Using Sequencing Batch Reactors. *J. Hazard. Mater.* **2015**, *282* (23), 106–115.
- Stein, L. Y.; Arp, D. J. Ammonium Limitation Results in the Loss of Ammonia-Oxidizing Activity in *Nitrosomonas europaea*. *Appl. Env. Microbiol.* **1998**, *64* (4), 1514–1521.
- Stein, L. Y.; Arp, D. J.; Hyman, M. R. Regulation of the Synthesis and Activity of Ammonia Monooxygenase in *Nitrosomonas europaea* by Altering pH To Affect NH<sub>3</sub> Availability. *Appl. Env. Microbiol.* **1997**, *63* (11), 4588–4592.
- Suarez, S.; Lema, J. M.; Omil, F. Removal of Pharmaceutical and Personal Care Products (PPCPs) under Nitrifying and Denitrifying Conditions. *Water Res.* **2010**, *44* (10), 3214–3224.
- Sun, Q.; Li, Y.; Chou, P.-H.; Peng, P.-Y.; Yu, C.-P. Transformation of Bisphenol A and Alkylphenols by Ammonia-Oxidizing Bacteria through Nitration. *Environ. Sci. Technol.* **2012**, *46* (8), 4442–4448.
- Tchobanoglous, G.; Burton, F. L.; Stensel, H. D. Wastewater Engineering: Treatment and Reuse, 4th Ed. McGraw-Hill: New York, NY, **2003**.
- Tran, N. H.; Urase, T.; Kusakabe, O. The Characteristics of Enriched Nitrifier Culture in the Degradation of Selected Pharmaceutically Active Compounds. *J. Hazard. Mater.* **2009**, *171* (1–3), 1051–1057.

Uprety, K.; Balzer, W.; Baurner, R.; Duke, R.; Bott, C. Implementing Ammonia-Based Aeration Control at Biological Nutrient Removing Wastewater Treatment Plants. *Proc. Water Environ. Fed.* **2015**.

Vrecko, D.; Hvala, N.; Stare, A.; Burica, O.; Strazar, M.; Levstek, M.; Cerar, P.; Podbevsek, S. Improvement of Ammonia Removal in Activated Sludge Process with Feedforward-Feedback Aeration Controllers. *Water Sci. Technol.* **2006**, *53* (4-5), 125-132.

Wackett, L. P.; Ellis, L. B. M. Predicting Biodegradation. *Environ. Microbiol.* **1999**, *1*, 119–124.

Yi, T.; Harper, W. F. The Link between Nitrification and Biotransformation of 17 $\alpha$ -Ethinylestradiol. *Environ. Sci. Technol.* **2007**, *41* (12), 4311–4316.

Zuccato, E.; Calamari, D.; Natangelo, M.; Fanelli, R. Presence of Therapeutic Drugs in the Environment. *Lancet* **2000**, *355*, 1789–1790.

## Chapter 3.

### Effect of redox conditions on pharmaceutical loss during biological wastewater treatment using sequencing batch reactors

Reprinted with permission from (Lauren B. Stadler, Lijuan Su, Christopher J. Moline, Alexi S. Ernstoff, Diana S. Aga, and Nancy G. Love, Effect of redox conditions on pharmaceutical loss during biological wastewater treatment using sequencing batch reactors, *Journal of Hazardous Materials*, **2015**, 282, 106 – 115), Copyright (2015) American Chemical Society.

#### 3.1 Introduction

Concerns are rising due to the widespread detection of pharmaceuticals in the aquatic environment (Heberer, 2002; Kolpin et al., 2002; Vieno et al., 2005; Metcalfe et al., 2010). There is evidence that very low concentrations of pharmaceuticals, similar to those found in wastewater treatment plant (WWTP) effluents, disrupt fish behavior and may collapse entire ecosystems (Kidd et al., 2007; Brodin et al., 2013). Biologically active pharmaceuticals enter water bodies by way of WWTPs that are not designed or regulated to remove such compounds. During wastewater treatment, pharmaceuticals have various fates; they may be involved in abiotic or biotic reactions to form transformation products (TPs) or be mineralized completely to carbon dioxide, sorb to biosolids, or pass through unaltered. While WWTPs represent an entry point for the environmental proliferation of pharmaceuticals (Golet et al., 2002; Kolpin et al., 2002; Giger et al., 2003; Metcalfe et al., 2003; Ternes et al., 2004; Vieno et al., 2006), they are also a last line of defense against environmental release. There is a clear need to understand the effect of WWTP process parameters

on pharmaceutical fate in order to mitigate the proliferation of these compounds in the environment.

Reported pharmaceutical removal efficiencies in WWTPs vary widely in the literature. For a given pharmaceutical, there is a large suite of potential TPs formed in the human body, sewer system, or during treatment that often is not considered and consequently complicate removal efficiency metrics. For this reason, the disappearance of a parent compound herein is referred to as “loss” as opposed to “removal”. TP concentrations can exceed that of the parent compound in WWTP influent and/or effluent, and result in the reformation of the parent compound during treatment (Plósz et al., 2010; Griffith et al., 2014). Accounting for TPs is imperative to improving our understanding of pharmaceutical fate during wastewater treatment and developing technologies that enable mineralization or conversion to stable and benign TPs (Stadler et al., 2012).

In order to harness WWTPs to mitigate the loading of pharmaceuticals on the aquatic environment, a better understanding of how WWTP process design and operation impact parent compound and TP loss is needed. To date, studies have investigated the impact of hydraulic residence time (HRT), solids residence time (SRT), and temperature on pharmaceutical loss (reviewed by Cirja et al. (2008)), but few studies have directly investigated the impact of redox environment. As energy conservation strategies and more stringent regulations on effluent nutrient concentrations are enacted, it is likely WWTPs will increasingly employ a range of redox environments beyond conventional aerobic processes. Energy consumption can be reduced by adopting controls to minimize aeration and dissolved oxygen (DO) set points (Flores-Alsina et al., 2011). Low DO treatment strategies ( $DO < 1 \text{ mg/L}$ ; hereafter referred to as microaerobic) may offer other advantages such as nitrogen removal (Collivignarelli and Bertanza, 1999; Daigger and

Littleton, 2000; Baek and Pagilla, 2008; Jimenez et al., 2011). In general, faster degradation rates have been observed for pharmaceuticals and other trace organic compounds transformed under aerobic conditions than anoxic or anaerobic conditions (Joss et al., 2004; Suarez et al., 2010) with a few notable exceptions such as certain refractory compounds (Hai et al., 2011). A better understanding of how redox conditions impact biodegradation pathways and rates is needed to predict pharmaceutical fate during wastewater treatment.

The objective of this work was to determine the extent of pharmaceutical transformation under various redox environments common to wastewater treatment processes. Sequencing batch reactors (SBRs) were operated in the lab to treat local domestic wastewater under different redox conditions: fully aerobic, anoxic/aerobic, and microaerobic conditions. Carbon and nitrogen removal was characterized in each SBR because understanding reactor performance is important to understanding pharmaceutical fate as the physiological and metabolic state of the microbial community can influence the degree and types of biotransformations that occur. Six environmentally relevant pharmaceuticals and several TPs were monitored in the influent, across the reaction cycle, and in the effluent of each SBR to characterize their transformation during treatment. As real time aeration control is implemented and microaerobic treatment strategies become more commonplace for saving energy and achieving nutrient removal (Åmand et al., 2013), the impact of DO concentration on pharmaceutical biotransformation must be considered, particularly if tradeoffs exist between energy efficiency gains and pharmaceutical loss.



## 3.2 Methods

### 3.2.1 Sequencing batch reactors (SBRs)

Four SBRs were operated in the laboratory for 351 days to examine the impact of redox environment on pharmaceutical fate during wastewater treatment. Each SBR had a working volume of 1.8 L and was inoculated with activated sludge collected from the aeration basin of a local domestic WWTP that operates an anoxic/aerobic process without recirculation and at an average SRT of 8 days. Each reactor had an SRT of 10 days and HRT of 24 hours. SRT was controlled by manually wasting mixed liquor, with consideration given to reactor effluent total suspended solids (TSS). The reactors were operated with an 8-hour cycle where one third of the reactor liquid volume was decanted after solids settling at the end of each cycle. The cycle consisted of four periods: 6 minute fill; 7 hour-24 minute reaction; 25 minute settle; and 5 minute decant. The influent to the reactors was primary effluent collected weekly from the WWTP. Primary effluent was frozen at -18 °C and thawed prior to use. Due to weekly variation and relatively dilute primary effluent (averaged approximately 150 mg-COD/L), it was supplemented with additional substrate in the form of acetate, glycerol, and yeast extract (equal parts as COD) and additional nutrients in the form of ammonia chloride and a trace elements solution (Table A1, Appendix A). Upon collection, primary effluent was analyzed for organic carbon and ammonium in order to determine the nutrient additions required to reach final concentrations of 250 mg-COD/L and 25 mg-NH<sub>4</sub>-N/L. The concentrations of carbon, nitrogen, and pharmaceuticals in the reactors at the beginning of the reaction period were calculated based on their concentration in the effluent at the end of the previous cycle (which made up 1/3 of the reactor volume) and the concentrations in the influent (making up the remaining 2/3 of the reactor volume). pH was controlled at  $7.5 \pm 0.1$  in each reactor via automated base addition (30 mg/L sodium bicarbonate).

Aeration was controlled to achieve the desired redox conditions in each reactor. The anoxic/aerobic reactor (reactor A) was aerated only during the second half of the reaction period, to a DO concentration greater than 2 mg/L. The fully aerobic reactor (reactor B) was constantly aerated to maintain a DO concentration greater than 2 mg/L. The microaerobic reactors (reactors C and D) were operated and controlled to maintain an average DO concentration of approximately 0.30 mg/L. This was achieved via real-time feedback from optical DO probes (Orion RDO<sup>®</sup> Pro, In-Situ Inc.) that controlled the aerators. Reactors C and D were controlled slightly differently: microaerobic reactor C was operated so that DO fluctuated  $\pm 0.10$  mg/L around 0.30 mg/L, and microaerobic reactor D was operated so that the DO averaged 0.3 mg/L but fluctuated between 0.01 and 0.60 mg/L. The redox condition in the reactors was also monitored using an oxidation reduction potential (ORP) probe (Van London-Pheonix Co.).

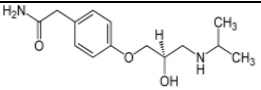
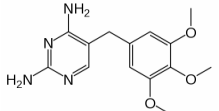
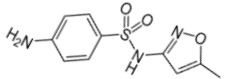
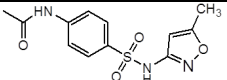
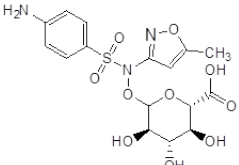
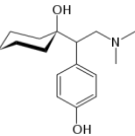
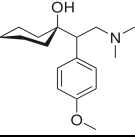
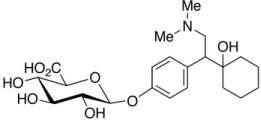
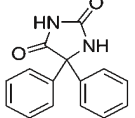
### ***3.2.2 Water quality analyses***

Standard water quality parameters were used to characterize reactor influent and effluent and overall reactor performance. Reactor total and volatile suspended solids (TSS and VSS) were determined weekly according to Standard Methods (2005). Twice weekly effluent samples were analyzed for soluble and total chemical oxygen demand (sCOD and COD), dissolved organic carbon and non-purgeable dissolved organic carbon (DOC and NPOC), ammonium, nitrite, nitrate, and total nitrogen. Samples were filtered through 0.45  $\mu\text{m}$  nitrocellulose filters prior to analysis of soluble chemicals. Reactor performance results are based on samples collected over the last 140 days of operation, which corresponds to when samples were collected for pharmaceutical analysis. In addition to influent and effluent samples, samples were collected across the reaction cycle in each reactor to characterize if and when during the reaction period carbon oxidation, nitrification, and denitrification occurred.

### ***3.2.3 Selection of pharmaceuticals***

The following compounds were selected for evaluation in this study: atenolol (a beta-blocker), venlafaxine and desvenlafaxine (antidepressants), phenytoin (an anticonvulsant), trimethoprim (an antibiotic), and sulfamethoxazole (an antibiotic). These compounds were selected based on their prevalence in WWTP effluents, potential for environmental impact, structural characteristics, and reported low sorption to biomass (e.g., biotransformation is the primary loss mechanism) (Table 3-1). Preliminary experiments were performed to verify low sorption to biomass (Love et al., 2012), and results were consistent with reported literature findings. Compounds were not artificially supplemented in experiments; rather, all experiments were performed using local domestic wastewater and compounds were present at endogenous concentrations. Therefore, the pharmaceutical selection was in part based on what compounds could be detected at endogenous concentrations in local primary effluent, which served as influent to the reactors. In addition to the compounds listed above, TPs of sulfamethoxazole and desvenlafaxine were also screened for. Specifically, acetyl-sulfamethoxazole and sulfamethoxazole-glucuronide, conjugated forms of sulfamethoxazole, and desvenlafaxine-glucuronide, a conjugated form of desvenlafaxine, were quantified in select influent, effluent, and reactor samples.

**Table 3-1.** Target pharmaceuticals and transformation products under Investigation: Structure, Properties, and Wastewater Concentration ( $K_{ow}$  – octanol-water partition coefficient;  $K_d$  – solid-liquid partition coefficient;  $pK_a$  – acid dissociation constant; TP – transformation product; NF – not found).

Chemical	Structure	Use	$\log K_{ow}$	$\log K_d$	$pK_a$	WWTP Primary Effluent Incidence Concentration [ng/L]
Atenolol		Beta-blocker	0.16 <sup>a</sup>	0.5 <sup>b</sup>	9.6 <sup>a</sup>	1,630 ± 560 (n=9)
Trimethoprim		Antibiotic	0.91 <sup>a</sup>	2.2-2.6 <sup>c, d</sup>	7.1 <sup>a</sup>	500 ± 120 (n=9)
Sulfamethoxazole		Antibiotic	0.89 <sup>a</sup>	<2.17 <sup>e</sup>	6.0 <sup>a</sup>	1,430 ± 290 (n=9)
Acetyl-sulfamethoxazole		Antibiotic TP	NF	NF	NF	1,680 ± 100 (n=3)
Sulfamethoxazole-glucuronide		Antibiotic TP	NF	NF	NF	140 ± 40 (n=3)
Desvenlafaxine		Antidepressant (drug & TP)	0.74 <sup>f</sup>	1.8-2.26 <sup>h</sup>	9.7 <sup>f</sup>	890 ± 250 (n=9)
Venlafaxine		Antidepressant	0.43- 0.87 <sup>f, g</sup>	2.30-3.17 <sup>h</sup>	9.4 <sup>i</sup>	370 ± 120 (n=7)
Desvenlafaxine-glucuronide		Antidepressant TP	N.F.	N.F.	N.F.	190 ± 90 (n=7)
Phenytoin		Antiepileptic	2.47 <sup>j</sup>	1.51-1.91 <sup>c</sup>	8.33 <sup>j</sup>	70 ± 10 (n=7)

<sup>a</sup>Gros et al., 2006; <sup>b</sup>Scheurer et al. 2010; <sup>c</sup>Stevens-Garmon et al., 2011; <sup>d</sup>Radjenović et al., 2009; <sup>e</sup>Carballa et al., 2008; <sup>f</sup>Shaver et al., 2011; <sup>g</sup>Rosal et al., 2010; <sup>h</sup>Lajeunesse et al., 2012; <sup>i</sup>Balasubramaniam et al., 2008; <sup>j</sup>Ni et al., 2002

### ***3.2.4 Sampling campaigns***

Seven distinct sampling campaigns were performed on separate days over a four month period. These sampling events involved quantifying concentrations of the monitored compounds in the influent and effluent of each SBR to calculate each compound's overall percent loss, defined as  $(\text{influent concentration} - \text{effluent concentration}) / (\text{influent concentration}) * 100\%$ . A Student's *t*-test was used to determine whether the percent loss of each compound based on the seven sampling campaigns was significantly different between reactors. Probability (*p*) values less than 0.05 were considered significant. In addition to influent and effluent sampling, four cross-cycle sampling events were performed in which samples were collected at different time points during the reactors' cycles. These were performed to understand patterns of transformation during the 8-hour reaction cycle.

### ***3.2.5 Sample preparation and LC/MS/MS analysis***

Samples were concentrated prior to pharmaceutical concentration quantification using solid phase extraction (SPE) in order to detect endogenous concentrations present in wastewater samples. Extraction volumes were optimized using the matrix of the samples being analyzed. Prior to SPE, samples were filtered through a 0.45  $\mu\text{m}$  nitrocellulose filter. Oasis® HLB cartridges (500 mg, 6 mL, Waters Corp., Milford, MA) were used for SPE. Cartridges were pre-conditioned with 6 mL LC/MS-grade acetonitrile (Sigma-Aldrich, St. Louis, MO), followed by 6 mL water. Samples were loaded on the SPE cartridges and drawn through by vacuum pressure at approximately 4 mL/min. After loading, the cartridges were rinsed with 6 mL of 5% HPLC-grade methanol (Honeywell B & J, Muskegon, MI) in water and allowed to dry on a vacuum manifold (Supelco Visiprep TM, Sigma-Aldrich, St. Louis, MO) for 30 min. Cartridges were stored at -20

°C prior to elution. To unload the target analytes, the cartridges were eluted with 8 mL LC-MS grade acetonitrile. Each eluent was collected in a pre-cleaned, baked 10 mL graduated tube, and was evaporated to 0.1 mL under a stream of nitrogen gas at 35°C. Then, 100 µL of methanol was added and vortexed to recover the very lipophilic compounds. Samples were reconstituted in water to a final sample volume of 1 mL.

Isotope dilution was used to correct for any losses that may have occurred during SPE and quantify the compounds while accounting for matrix effects inherent to wastewater samples. Specifically, nitrocellulose membrane-filtered samples were supplemented with 50 µL of a surrogate standard mixture containing 1 mg/L of deuterated analogs of the target compounds (Table A2, Appendix A) prior to SPE. After LC/MS/MS analysis, target compounds were quantified by using the ratio of the signal of the deuterated surrogate and the signal of the target analyte to calculate the concentration of the analyte in the sample. Acetyl-sulfamethoxazole and sulfamethoxazole-glucuronide were quantified using an external calibration curve using standards of acetyl-sulfamethoxazole and sulfamethoxazole-glucuronide (Toronto Research Chemicals, Inc.), as no deuterated surrogates of these compounds were added to the samples prior to SPE. This method likely underestimates the concentrations of the compounds in samples as there is no correction for losses during SPE. d6-Desvelanfaxine was used to quantify desvenlafaxine-glucuronide using isotope dilution.

Analysis of pharmaceutical compounds was performed on an Agilent 1100 HPLC coupled with Agilent triple quadrupole Mass Spectrometry, MSD 6410 (Palo Alto, CA). Separation was achieved on a Thermo Scientific BetaBasic-18 C18 2.1 × 100 mm, 3-µm particle size column and a guard column with the same material (Fullerton, CA). A 10 µL sample was injected at the beginning and a gradient of water with 0.3% formic acid and acetonitrile was used to elute all

compounds with minimal overlap (gradient details provided in the SI). The total run time for one sample was 21 min at a flow rate of 0.2 mL/min.

Ionization was achieved by positive electron spray ionization (ESI), using a spray voltage of 4 kV situated at a 90° angle to the entrance. Drying gas temperature was set as 350 °C, nebulizer pressure (N<sub>2</sub>) as 22 psi and drying gas flow rate as 11 L/min to achieve the highest sensitivity. All compounds were monitored at positive ESI mode by using two product ions in multiple reaction monitoring. The fragmentor and collision energy were tuned for each specific analyte to achieve the optimum signal-to-noise ratio (Table A2, Appendix A). All data were collected and processed using the Agilent Technologies MassHunter Software Version B (Palo Alto, CA).

### **3.3 Results and discussion**

#### ***3.3.1 Reactors achieved stable carbon removal and nitrification***

All reactors achieved stable carbon oxidation and there were no significant differences in carbon removal performance ( $p > 0.2$  in all comparisons), which averaged  $93 \pm 2\%$  sCOD removal. Cross-cycle sampling indicated that NPOC was consumed rapidly in the first 30 minutes in all reactors (data not shown). Mixed liquor suspended solids concentrations were similar in all reactors and averaged  $1,125 \pm 93$  (anoxic/aerobic),  $951 \pm 176$  (aerobic),  $1,038 \pm 188$  (microaerobic C), and  $1,053 \pm 200$  (microaerobic D) mg/L. While low DO operation has been associated with poor settleability and high effluent solids (Wilén and Balmér, 1999; Martins et al., 2003), we did not observe any detrimental impacts on settleability in the microaerobic SBRs resulting from the presence of filamentous bacteria. In fact, lower effluent solids were observed in the microaerobic SBRs (reactor C and D effluent TSS averaged  $8 \pm 4$  and  $5 \pm 2$  mg/L, respectively), as compared to the aerobic reactor ( $13 \pm 6$  mg/L) and the anoxic/aerobic reactor ( $11 \pm 4$  mg/L). The microaerobic reactors also had the highest average sludge volume index ( $111 \pm 23$  and  $99 \pm 21$  ml/g, respectively

for C and D), although the values were still within a range considered typical of good settleability (Tchobanoglous et al., 2003). The reactors were operated as SBRs, and therefore achieved a concentration gradient across the reaction cycle which allowed for floc formers to sequester most of the organic carbon and prevent the proliferation of filamentous organisms, similar to how a selector functions (Chudoba et al., 1973). A study on full-scale and lab-scale systems that used low DO treatment found that limited filamentous bulking resulted in lower effluent suspended solids than conditions with no bulking (Guo et al., 2010). These results suggest that DO control and appropriate management of filamentous bacterial growth, substantial energy savings are possible by reducing DO levels while still achieving water quality goals typical for secondary effluents.

Complete and stable nitrification was also achieved in all SBRs. Cross-cycle sampling showed that nitrification (based on ammonia removal) was complete within 4 hours in the aerobic and microaerobic reactors (Figure 3-1). Denitrification was discerned through total nitrogen loss and occurred in the anoxic/aerobic and microaerobic reactors, which had average effluent total nitrogen concentrations of  $10.0 \pm 0.9$  mg-N/L and  $18.8 \pm 3.6$  mg-N/L primarily as nitrate, respectively. These levels were considerably less than the average effluent total nitrogen concentration in the aerobic-only reactor, which averaged  $25.7 \pm 2.3$  mg/L as N, primarily as nitrate. For the first 30 minutes after the influent feed was added, both microaerobic reactors (C & D) experienced an initial phase where the DO concentration was below detection ( $< 0.01$  mg/L) despite aeration throughout the period, during which carbon was being consumed. After the initial phase, the microaerobic reactors were maintained in low DO conditions, averaging 0.30 mg/L. Cross-cycle sampling of the microaerobic reactors demonstrated that denitrification occurred during that initial phase, as opposed to throughout the cycle (Figure 3-1). Overall total nitrogen



removal averaged  $74 \pm 3\%$ ,  $26 \pm 1\%$ ,  $45 \pm 8\%$  and  $44 \pm 7\%$  in the anoxic/aerobic A, aerobic B, microaerobic C and microaerobic D reactors, respectively. No significant difference in nitrogen removal was observed between the microaerobic C and D reactors despite the larger DO fluctuations in reactor D.

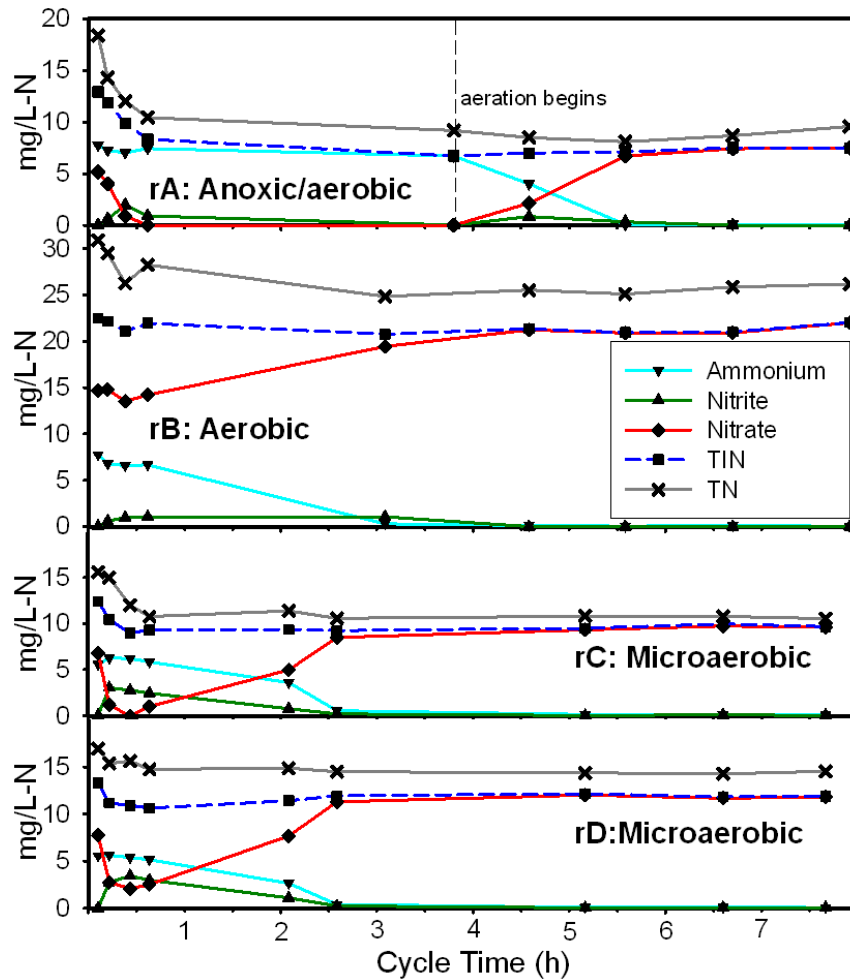


**Figure 3-1.** Representative cross-cycle profile of nitrogen species in each reactor (r). rA – anoxic/aerobic SBR; rB – aerobic SBR; rC and rD – microaerobic SBRs. TIN – total inorganic nitrogen; TN – total nitrogen.

Conventional nitrifying activated sludge WWTPs typically operate at bulk DO concentrations of greater than 2 mg/L to ensure complete nitrification and stable nitrifying populations (WEF, 2008). This study, as well as several others (Park and Noguera, 2004; Bellucci

et al., 2011; Arnaldos et al., 2013; Liu and Wang, 2013), demonstrates that stable nitrification is possible at substantially lower DO concentrations than are typically found in nitrifying WWTPs. WWTPs can achieve low DO concentrations at high oxygen transfer efficiencies by operating at reduced air flow rates (Tchobanoglous et al., 2003), offering the potential for considerable aeration energy savings. Advances in blower technologies, aeration control programs, and online sensors has enabled many WWTP to implement aeration control and achieve energy savings (e.g. Åmand and Carlsson, 2013; Flores et al., 2013, reviewed by Åmand et al. (2013)) and can further support stable, low DO operation. While low DO treatment may save energy during aeration, it can also increase nitrous oxide ( $N_2O$ ) emissions from both nitrifier denitrification and heterotrophic denitrification (Chandran et al., 2011). Therefore, low DO operating conditions offer tradeoffs between reduced energy demand for aeration and the potential for reasonable pharmaceutical transformation versus greenhouse gas emissions.

Low DO treatment has an added benefit of achieving greater nitrogen removal as compared to fully-aerobic conventional activated sludge processes that only achieve nitrification. Many full scale simultaneous nitrification-denitrification (SND) systems have demonstrated effective nitrogen removal from domestic wastewater (80-90% TN removal) by operating at constant low DO levels between 0.25-0.5 mg/L (Jimenez et al., 2013). SND activity and nitrogen removal performance depends on a number of factors, such as the influent carbon to nitrogen (C:N) ratio, bulk DO concentration, bioreactor configuration and mixing (macro environment), and floc size (micro environment) (Pochana and Keller, 1999; Daigger and Littleton, 2000; Littleton et al., 2003; Ju et al., 2007; Jimenez et al., 2010). It is likely that the aeration or feeding process could have been optimized to encourage floc formation and improve overall nitrogen removal in the microaerobic SBRs.

### ***3.3.2 Atenolol loss was highest with aerobic treatment***

The greatest degree of loss was observed for atenolol in all treatment conditions as compared to the other compounds studied (Figure 3-2). The greatest loss of atenolol was observed in the aerobic ( $89 \pm 13\%$ ), followed by the microaerobic ( $73 \pm 10\%$ , average of both reactors), and then the anoxic/aerobic SBR ( $63 \pm 20\%$ ). Atenolol losses were significantly different between the aerobic and anoxic/aerobic SBR ( $p = 0.019$ ) and between the aerobic and microaerobic SBRs ( $p = 0.043$ ). However, losses of atenolol in the anoxic/aerobic and microaerobic SBRs were not significantly different from each other ( $p = 0.25$ ). Based on cross-cycle monitoring, atenolol loss occurred during both anoxic and aerobic periods of the cycle to a similar extent (no significant differences based on three cross-cycle sampling campaigns, Figure A1, Appendix A).

Reported losses of atenolol across treatment plants vary widely in the literature. Miège et al. (2009) reported an average loss of approximately  $10 \pm 5\%$  for atenolol based on the results of 29 different studies. While this average is significantly lower than our findings, a number of other studies not included in the Miège et al. study have also reported considerably greater losses. Radjenovic et al. (2009) examined a full-scale conventional activated sludge treatment plant and a pilot-scale membrane bioreactor system and reported losses of 61% and 73%, respectively. Similarly, Kasprzyk-Hordern et al. (2008) also reported losses in the range of 70 to 80% for atenolol for systems with trickling filters and activated sludge. Two studies also observed atenolol loss in anoxic environments, such as in a constructed wetland treating wastewater effluent (Park et al., 2009) and laboratory-scale SBRs treating municipal wastewater (Carucci et al., 2006). We observed the highest loss of atenolol in the aerobic SBR, and also observed substantial losses in the microaerobic SBRs and anoxic/aerobic SBR. While significant loss was observed in all

reactors (averaged  $75 \pm 11\%$  in all SBRs), our results suggest that aerobic conditions are more favorable for atenolol transformation than anoxic or microaerobic conditions.

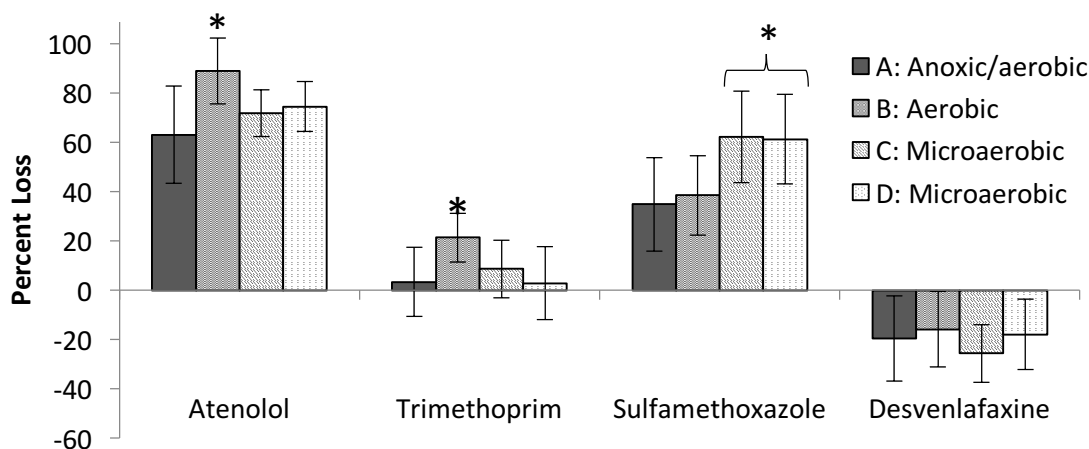


**Figure 3-2.** Overall percent losses of pharmaceuticals in each reactor ( $n=7$ ), where negative percent loss refers to higher concentrations observed in effluent than influent (\*statistically different from other reactors ( $p$ -value  $< 0.05$ ))

### 3.3.3 Limited trimethoprim loss was observed under all conditions

Trimethoprim was not significantly removed in any SBR, with percent losses of  $< 10\%$  in all reactors except the aerobic reactor, which had an average loss of  $19.9 \pm 10\%$ . Pairwise t-test comparisons between different redox environments indicated that loss of trimethoprim was significantly different between the aerobic and anoxic/aerobic SBR ( $p = 0.019$ ) and significantly different between the aerobic and microaerobic SBRs ( $p = 0.027$ ). Loss of trimethoprim in the anoxic/aerobic and microaerobic SBRs were not significantly different from each other ( $p = 0.74$ ).

There are large variations in reported losses for lab, pilot, and full-scale treatment systems. Laboratory batch studies showed minimal to no significant loss in aerobic environments and concluded that trimethoprim is not readily aerobically biodegradable (Alexy et al., 2004; Carucci

et al., 2006). Conversely, several other studies reported significantly greater losses (40 to 85%) in full-scale aerobic WWTPs (Karthikeyan and Meyer, 2006; Batt et al., 2007; Watkinson et al., 2007; Radjenović et al., 2009). Another set of studies observed negative loss across full-scale treatment processes, with losses between -60% and -4%, likely due to deconjugation reactions that resulted in the reformation of the parent compound (Lindberg et al., 2006; Gulkowska et al., 2008; Plósz et al., 2010). The link between nitrification and trimethoprim is still unclear; Batt et al. (2006) observed enhanced biodegradation of trimethoprim in nitrifying activated sludge but did not clarify the role of nitrifiers versus heterotrophic bacteria; however, in a later study, limited to no transformation of trimethoprim by pure cultures of *Nitrosomonas europaea* was observed (Khunjar et al., 2011). In the present study, complete nitrification occurred in all SBRs, further indicating no explicit link between nitrification and trimethoprim biodegradation. The highest observed loss, albeit low, was in the fully aerobic SBR, suggesting aerobic environments are most favorable for trimethoprim transformation, but not necessarily due to nitrifier activity.

#### ***3.3.4 Sulfamethoxazole loss was highest in microaerobic treatment and TPs resulted in reformation of sulfamethoxazole***

Sulfamethoxazole, an antimicrobial commonly detected in wastewater effluents and surface water (Hirsch et al., 1999; Kolpin et al., 2002; Batt and Aga, 2005), was the only compound for which we observed significantly higher loss in the microaerobic SBRs than the fully aerobic ( $p = 0.019$ ) and anoxic/aerobic SBRs ( $p = 0.044$ ). Differences in sulfamethoxazole loss were not significantly different between the aerobic and anoxic/aerobic SBRs ( $p = 0.51$ ). Reported WWTP losses for sulfamethoxazole range greatly from -138% to 96% (Carballa et al., 2004; Lindberg et al., 2005; Karthikeyan and Meyer, 2006; Batt et al., 2007; Watkinson et al., 2007; Radjenović et al., 2009; Plósz et al., 2010), but only a fraction of the studies explicitly state the redox

environments used in the treatment processes studied (Table 3-2). Regarding the effect of redox conditions, a previous study by Hai et al. (2011) investigated the fate of sulfamethoxazole in microaerobic (DO = 0.5 mg/L) and fully aerobic (DO > 2 mg/L) membrane bioreactors and found comparable biodegradation irrespective of DO concentration. A limited number of studies have also observed biodegradation of sulfamethoxazole in anoxic environments (Park et al., 2009; Plósz et al., 2009). Plósz et al. (2009) found comparable biodegradation rates of sulfamethoxazole in aerobic and anoxic batch experiments using primary effluent and activated sludge. Our results suggest that microaerobic treatment may be advantageous over fully aerobic treatment for the biodegradation of sulfamethoxazole. Enhanced loss of sulfamethoxazole under microaerobic conditions may occur because the conditions support both aerobic and anoxic metabolisms, potentially allowing for multiple transformation pathways and rendering the compound more biodegradable. Further research is needed to understand likely biodegradation pathways and the redox conditions that enable them.

**Table 3-2.** Losses in aerobic, anoxic/aerobic, and microaerobic treatment determined in this study alongside reported literature values (MLE = Modified Ludzack-Ettinger; BNR = biological nutrient removal; CAS – conventional activated sludge; NF = not found).

	Experimental Results Loss (%)			Literature Results Loss (%)		
	Anox/aer (A)	Aerobic (B)	Microaerobic (avg. of C & D)	Anox/aer (i.e. MLE or other BNR)	Aerobic (i.e. CAS)	Microaerobic
<b>Atenolol</b>	63 ± 20	89 ± 13	73 ± 10	36-76 <sup>a,b</sup>	<10-81 <sup>b,c,d,e,f,g</sup>	NF
<b>Trimethoprim</b>	3.4 ± 14	21 ± 10	5.8 ± 13	-20-60 <sup>h</sup>	-42-97 <sup>a,i,j,k,l,m,n</sup>	NF
<b>Sulfamethoxazole</b>	35 ± 19	38 ± 17	62 ± 18	-138-60 <sup>h</sup>	-24-96 <sup>a,j,l,m,n,o,p</sup>	65 <sup>q</sup>
<b>Venlafaxine-family</b>	-5.3 ± 16	0.1 ± 12	-4.7 ± 12	-91-80 <sup>r</sup>	-142-56 <sup>s,t,u,v,w</sup>	NF
<b>Phenytoin</b>	-5.6 ± 20	-3.1 ± 10	-14 ± 32	44 <sup>x</sup>	~0 <sup>y</sup>	NF

<sup>a</sup>Maurer et al., 2007; <sup>b</sup>Carucci et al., 2006; <sup>c</sup>Radjenović et al., 2009; <sup>d</sup>Castiglioni et al., 2006; <sup>e</sup>Kasprzyk-Hordern et al., 2009; <sup>f</sup>Behera et al. 2011; <sup>g</sup>Paxeus et al., 2004; <sup>h</sup>Plósz et al., 2010; <sup>i</sup>Gulkowska et al., 2008; <sup>j</sup>Lindberg et al., 2005; <sup>k</sup>Lindberg et al., 2006; <sup>l</sup>Batt et al., 2007; <sup>m</sup>Karthikeyan et al., 2006; <sup>n</sup>Göbel et al., 2007; <sup>o</sup>Carballa et al., 2004; <sup>p</sup>Watkinson et al., 2007; <sup>q</sup>Hai et al., 2011; <sup>r</sup>Gasser et al., 2012; <sup>s</sup>Metcalf et al., 2010; <sup>t</sup>Gracia-Lor et al., 2012; <sup>u</sup>Rua-Gomez et al., 2012; <sup>v</sup>Lajeunesse et al., 2012; <sup>w</sup>Kasprzyk-Hordern et al., 2010; <sup>x</sup>Yu et al., 2006; <sup>y</sup>Gerrity et al., 2011

Reported negative losses in published studies are likely due to deconjugation of conjugated sulfamethoxazole compounds commonly detected in urine and raw wastewater. Cross-cycle sampling revealed that sulfamethoxazole formation occurred during treatment (Figure A2, Appendix A). This observation is likely explained by the presence of TPs of sulfamethoxazole in the reactor influent that deconjugated to reform sulfamethoxazole during the reaction cycle. After ingestion, sulfamethoxazole is excreted by humans in both its parent form as well as the conjugated forms acetyl-sulfamethoxazole and sulfamethoxazole-glucuronide, which can comprise 45% and 9 to 15% of the total excreted dose of sulfamethoxazole, respectively (van der Ven et al., 1994, 1995). Acetyl-sulfamethoxazole has been detected in wastewater influents (Hilton and Thomas, 2003; Göbel et al., 2005), and it readily deconjugates to reform sulfamethoxazole (Radke et al., 2009; Hai et al., 2011).

To investigate the presence of acetyl-sulfamethoxazole and sulfamethoxazole-glucuronide in reactor influent and cross-cycle samples, several samples from three different dates were selected for quantification of the compounds. Influent and cross-cycle samples were selected based on when significant increases in sulfamethoxazole were observed. Acetyl-sulfamethoxazole and sulfamethoxazole-glucuronide were detected in the influent in all samples analyzed (n=3), and their average concentrations were  $1,680 \pm 100$  and  $140 \pm 40$  ng/L, respectively. Increases in sulfamethoxazole concentrations in cross-cycle samples corresponded with decreases in acetyl-sulfamethoxazole and sulfamethoxazole-glucuronide concentrations. These results strongly suggest that acetyl-sulfamethoxazole and sulfamethoxazole-glucuronide deconjugate rapidly in both redox environments, and deconjugation is faster than sulfamethoxazole degradation (Figure 3-3). This is a likely explanation for reported “negative removal” values in the literature for sulfamethoxazole across wastewater treatment plants. Overall losses of acetyl-sulfamethoxazole



in the anoxic/aerobic and microaerobic (C) reactors were 84 and 90%, respectively. Sulfamethoxazole-glucuronide loss was also significant, with >90% loss in both reactors. These results indicate that attention must be paid to the metabolites and conjugated forms of pharmaceuticals and their fate in WWTPs and the environment to avoid promoting systems with excellent “removal” that may simply result in the discharge of compounds that could retransform back into their active parent form in the environment.

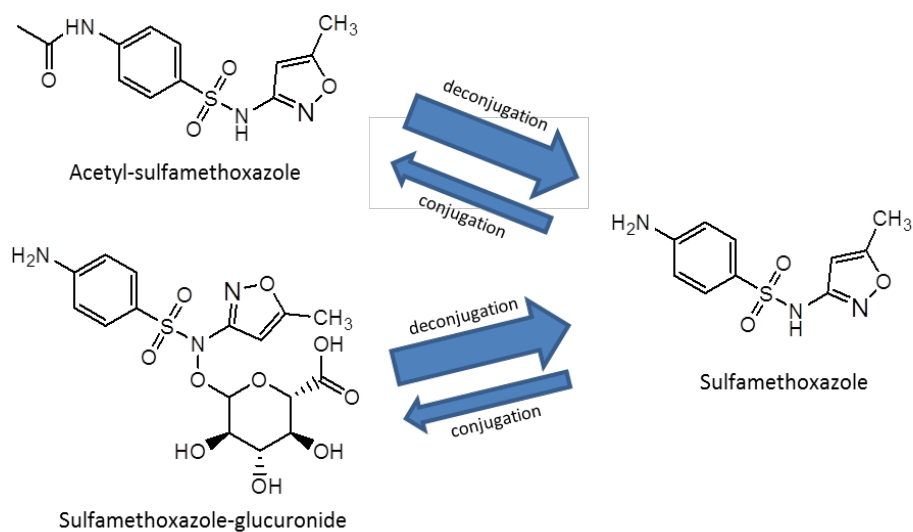


**Figure 3-3.** Deconjugation and conjugation reactions between sulfamethoxazole and its transformation products, acetyl-sulfamethoxazole and sulfamethoxazole-glucuronide. Size of arrows implies relative rates observed during wastewater treatment.

### 3.3.5 Desvenlafaxine TPs resulted in desvenlafaxine formation

Desvenlafaxine was observed at higher concentrations in the effluent than the influent of the reactors (Figure 3-2). Upon further investigation, TPs were found in the influent that deconjugated to reform desvenlafaxine during treatment, as previously observed (Gasser et al., 2012). Desvenlafaxine is a biologically active metabolite of venlafaxine. Both desvenlafaxine and venlafaxine are serotonin/norepinephrine reuptake inhibitors prescribed to treat depression. In humans, desvenlafaxine may pass through unaltered or undergo conjugation. Approximately 19%

of administered dose is excreted as desvenlafaxine-glucuronide (*Withdrawal Assessment Report*, 2009). Other metabolites, such as N,O-di-desmethyl can also be formed, but typically comprise less than 5% percent of the administered dose. By accounting for venlafaxine and desvenlafaxine-glucuronide in addition to desvenlafaxine in the influent and effluent of the reactors, we observed limited loss of the desvenlafaxine-family of compounds in all SBRs (<10%; Table A5, Appendix A). The increase in desvenlafaxine can be explained by the deconjugation of desvenlafaxine-glucuronide, which was detected in the influent at  $189 \pm 83$  ng/L ( $n = 7$ ) and was removed (>99%) in all SBRs.

Previous studies on full-scale municipal wastewater treatment systems report moderate losses for venlafaxine and its metabolites: Metcalfe et al. (2010b) observed 40% loss of venlafaxine and its demethylation products, and Rúa-Gómez and Püttmann (2012) also reported partial losses (25 – 50%) of venlafaxine and desvenlafaxine in four German WWTPs. Lajeunesse et al. (2012) observed less than 10% loss of venlafaxine in both a secondary biological WWTP and chemically enhanced primary treatment. It is unclear from these survey studies how WWTP configuration and operation impact the fate of desvenlafaxine and venlafaxine. Helbling et al. (2012) found an association between venlafaxine biotransformation and the abundance of archaeal ammonia monooxygenase transcripts in batch experiments using activated sludge samples from 10 different WWTPs. This suggests that ammonia oxidizers may play a role in the oxidation of venlafaxine. In our systems, complete nitrification occurred in all SBRs and the presence of ammonia oxidizing archaea was not known. Further research is needed to investigate the relationship between nitrification and venlafaxine and desvenlafaxine biotransformations and the relative contributions of different ammonia oxidizers. Our results highlight the importance of considering major metabolites and conjugated forms when tracking the fate of compounds across

a treatment process as “in” versus “out” concentrations may be misleading when compounds are being formed during treatment due to deconjugation processes.

### **3.4 Summary and conclusions**

In this study, four SBRs operated under different redox conditions achieved different levels of nitrogen removal and pharmaceutical loss. Stable COD removal and nitrification were achieved at a DO concentration of 0.3 mg/L with good settleability, highlighting the potential for energy savings by reducing aeration during treatment. Nitrogen removal occurred to a greater extent in microaerobic than fully aerobic conditions, while sequential anoxic/aerobic conditions achieved the most nitrogen removal. Redox environment influenced the overall loss of atenolol, trimethoprim, and sulfamethoxazole. The greatest overall loss of atenolol and trimethoprim was observed in the aerobic SBR, whereas the greatest loss of sulfamethoxazole was found in the microaerobic SBRs. Conjugated forms of sulfamethoxazole and desvenlafaxine were detected in the influent (local primary effluent) and contributed to the observed increases in sulfamethoxazole and desvenlafaxine across the reaction cycles. The results of this study imply that redox environment is an important factor that can influence the biodegradability of certain persistent micropollutants. Attention must be given to TPs to accurately account for pharmaceutical fate during wastewater treatment and estimate pharmaceutical loading on receiving waters. Further research should focus on elucidating the biotransformation pathways and microbes responsible for the degradation of these pharmaceuticals and their TPs in each redox environment in order to prevent their introduction into the aquatic environment.

### 3.5 Literature cited

Alexy, R.; Kämpel, T.; Kümmerer, K. Assessment of Degradation of 18 Antibiotics in the Closed Bottle Test. *Chemosphere* **2004**, *57* (6), 505–512.

Åmand, L.; Carlsson, B. The Optimal Dissolved Oxygen Profile in a Nitrifying Activated Sludge Process-Comparisons with Ammonium Feedback Control. *Water Sci. Technol.* **2013**, *68* (3), 641–649.

Åmand, L.; Olsson, G.; Carlsson, B. Aeration Control – A Review. *Water Sci. Technol.* **2013**, *67* (11), 2374–2398.

APHA; AWWA; WEF, Standard Methods for the Examination of Water and Wastewater. 21st Ed. Washington, D.C., **2005**.

Arnaldos, M.; Kunkel, S.; Stark, B.; Pagilla, K. Enhanced Heme Protein Expression by Ammonia-Oxidizing Communities Acclimated to Low Dissolved Oxygen Conditions. *Appl. Microbiol. Biotechnol.* **2013**, *97* (23), 10211–10221.

Baek, S. H.; Pagilla, K. R. Simultaneous Nitrification and Denitrification of Municipal Wastewater in Aerobic Membrane Bioreactors. *Water Environ. Res.* **2008**, *80* (2), 109–117.

Batt, A. L.; Aga, D. S. Simultaneous Analysis of Multiple Classes of Antibiotics by Ion Trap LC/MS/MS for Assessing Surface Water and Groundwater Contamination. *Anal. Chem.* **2005**, *77* (9), 2940–2947.

Batt, A. L.; Kim, S.; Aga, D. S. Enhanced Biodegradation of Iopromide and Trimethoprim in Nitrifying Activated Sludge. *Environ. Sci. Technol.* **2006**, *40* (23), 7367–7373.

Batt, A. L.; Kim, S.; Aga, D. S. Comparison of the Occurrence of Antibiotics in Four Full-Scale Wastewater Treatment Plants with Varying Designs and Operations. *Chemosphere* **2007**, *68* (3), 428–435.

Bellucci, M.; Ofițeru, I. D.; Graham, D. W.; Head, I. M.; Curtis, T. P. Low-Dissolved-Oxygen Nitrifying Systems Exploit Ammonia-Oxidizing Bacteria with Unusually High Yields. *Appl. Env. Microbiol.* **2011**, *77* (21), 7787–7796.

Brodin, T.; Fick, J.; Jonsson, M.; Klaminder, J. Dilute Concentrations of a Psychiatric Drug Alter Behavior of Fish from Natural Populations. *Science* **2013**, *339* (6121), 814–815.

Carballa, M.; Omil, F.; Lema, J. M.; Llombart, M.; García-Jares, C.; Rodríguez, I.; Gomez, M.; Ternes, T. Behavior of Pharmaceuticals, Cosmetics and Hormones in a Sewage Treatment Plant. *Water Res.* **2004**, *38* (12), 2918–2926.

Carucci, A.; Cappai, G.; Piredda, M. Biodegradability and Toxicity of Pharmaceuticals in

- Biological Wastewater Treatment Plants. *J. Environ. Sci. Heal. Part A* **2006**, *41* (9), 1831–1842.
- Chandran, K.; Stein, L. Y.; Klotz, M. G.; van Loosdrecht, M. C. M. Nitrous Oxide Production by Lithotrophic Ammonia-Oxidizing Bacteria and Implications for Engineered Nitrogen-Removal Systems. *Biochem. Soc. Trans.* **2011**, *39* (6), 1832.
- Chudoba, J.; Grau, P.; Ottová, V. Control of Activated-Sludge Filamentous Bulking–II. Selection of Microorganisms by Means of a Selector. *Water Res.* **1973**, *7* (10), 1389–1406.
- Cirja, M.; Ivashechkin, P.; Schäffer, A.; Corvini, P. F. X. Factors Affecting the Removal of Organic Micropollutants from Wastewater in Conventional Treatment Plants (CTP) and Membrane Bioreactors (MBR). *Rev. Environ. Sci. Biotechnol.* **2008**, *7* (1), 61–78.
- Collivignarelli, C.; Bertanza, G. Simultaneous Nitrification-Denitrification Processes in Activated Sludge Plants: Performance and Applicability. *Water Sci. Technol.* **1999**, *40* (4–5), 187–194.
- Daigger, G. T.; Littleton, H. X. Characterization of Simultaneous Nutrient Removal in Staged, Closed-Loop Bioreactors. *Water Environ. Res.* **2000**, *72* (3), 330–339.
- Flores, V. R.; Sanchez, E. N.; Béteau, J.-F.; Hernandez, S. C. Dissolved Oxygen Regulation by Logarithmic/antilogarithmic Control to Improve a Wastewater Treatment Process. *Environ. Technol.* **2013**, *34* (23), 3103–3116.
- Flores-Alsina, X.; Corominas, L.; Snip, L.; Vanrolleghem, P. A. Including Greenhouse Gas Emissions during Benchmarking of Wastewater Treatment Plant Control Strategies. *Water Res.* **2011**, *45* (16), 4700–4710.
- Gasser, G.; Pankratov, I.; Elhanany, S.; Werner, P.; Gun, J.; Gelman, F.; Lev, O. Field and Laboratory Studies of the Fate and Enantiomeric Enrichment of Venlafaxine and O-Desmethylvenlafaxine under Aerobic and Anaerobic Conditions. *Chemosphere* **2012**, *88* (1), 98–105.
- Giger, W.; Alder, A. C.; Golet, E. M.; Kohler, H.-P. E.; McArdell, C. S.; Molnar, E.; Siegrist, H.; Suter, M. J. F. Occurrence and Fate of Antibiotics as Trace Contaminants in Wastewaters, Sewage Sludges, and Surface Waters. *Chim. Int. J. Chem.* **2003**, *57* (9), 485–491.
- Göbel, A.; Thomsen, A.; McArdell, C. S.; Joss, A.; Giger, W. Occurrence and Sorption Behavior of Sulfonamides, Macrolides, and Trimethoprim in Activated Sludge Treatment. *Environ. Sci. Technol.* **2005**, *39* (11), 3981–3989.
- Golet, E. M.; Alder, A. C.; Giger, W. Environmental Exposure and Risk Assessment of Fluoroquinolone Antibacterial Agents in Wastewater and River Water of the Glatt Valley Watershed, Switzerland. *Environ. Sci. Technol.* **2002**, *36* (17), 3645–3651.
- Griffith, D. R.; Kido Soule, M. C.; Matsufuji, H.; Eglinton, T. I.; Kujawinski, E. B.; Gschwend, P. M. Measuring Free, Conjugated, and Halogenated Estrogens in Secondary Treated Wastewater

Effluent. *Environ. Sci. Technol.* **2014**, *48* (5), 2569–2578.

Gulkowska, A.; Leung, H. W.; So, M. K.; Taniyasu, S.; Yamashita, N.; Yeung, L. W. Y.; Richardson, B. J.; Lei, A. P.; Giesy, J. P.; Lam, P. K. S. Removal of Antibiotics from Wastewater by Sewage Treatment Facilities in Hong Kong and Shenzhen, China. *Water Res.* **2008**, *42* (1), 395–403.

Guo, J. H.; Peng, Y. Z.; Peng, C. Y.; Wang, S. Y.; Chen, Y.; Huang, H. J.; Sun, Z. R. Energy Saving Achieved by Limited Filamentous Bulking Sludge under Low Dissolved Oxygen. *Bioresour. Technol.* **2010**, *101* (4), 1120–1126.

Hai, F. I.; Li, X.; Price, W. E.; Nghiem, L. D. Removal of Carbamazepine and Sulfamethoxazole by MBR under Anoxic and Aerobic Conditions. *Bioresour. Technol.* **2011**, *102* (22), 10386–10390.

Heberer, T. Occurrence, Fate, and Removal of Pharmaceutical Residues in the Aquatic Environment: A Review of Recent Research Data. *Toxicol. Lett.* **2002**, *131* (1), 5–17.

Helbling, D. E.; Johnson, D. R.; Honti, M.; Fenner, K. Micropollutant Biotransformation Kinetics Associate with WWTP Process Parameters and Microbial Community Characteristics. *Environ. Sci. Technol.* **2012**, *46* (19), 10579–10588.

Hilton, M. J.; Thomas, K. V. Determination of Selected Human Pharmaceutical Compounds in Effluent and Surface Water Samples by High-Performance Liquid Chromatography–electrospray Tandem Mass Spectrometry. *J. Chromatogr. A* **2003**, *1015* (1), 129–141.

Hirsch, R.; Ternes, T.; Haberer, K.; Kratz, K.-L. Occurrence of Antibiotics in the Aquatic Environment. *Sci. Total Environ.* **1999**, *225* (1–2), 109–118.

Jimenez, J.; Dursun, D.; Dold, P.; Bratby, J.; Keller, J.; Parker, D. Simultaneous Nitrification-Denitrification to Meet Low Effluent Nitrogen Limits: Modeling, Performance and Reliability. *Proc. Water Environ. Fed.* **2010**, 2404–2421.

Jimenez, J.; Dold, P.; La Motta, E.; Houweling, D.; Bratby, J.; Parker, D. Simultaneous Biological Nutrient Removal in a Single-Stage, Low Oxygen Aerobic Reactor. *Proc. Water Environ. Fed.* **2011**, 31–48.

Jimenez, J.; Bott, C.; Regmi, P.; Rieger, L. Process Control Strategies for Simultaneous Nitrogen Removal Systems. *Proc. Water Environ. Fed. Nutrient*. **2013**, 492–505.

Joss, A.; Andersen, H.; Ternes, T.; Richle, P. R.; Siegrist, H. Removal of Estrogens in Municipal Wastewater Treatment under Aerobic and Anaerobic Conditions: Consequences for Plant Optimization. *Environ. Sci. Technol.* **2004**, *38* (11), 3047–3055.

Ju, L. K.; Huang, L.; Trivedi, H. Simultaneous Nitrification, Denitrification, and Phosphorus Removal in Single-Tank Low-Dissolved-Oxygen Systems under Cyclic Aeration. *Water Environ.*

*Res.* **2007**, *79* (8), 912–920.

Karthikeyan, K. G.; Meyer, M. T. Occurrence of Antibiotics in Wastewater Treatment Facilities in Wisconsin, USA. *Sci. Total Environ.* **2006**, *361* (1), 196–207.

Kasprzyk-Hordern, B.; Dinsdale, R.; Guwy, A. Multiresidue Methods for the Analysis of Pharmaceuticals, Personal Care Products and Illicit Drugs in Surface Water and Wastewater by Solid-Phase Extraction and Ultra Performance Liquid Chromatography–electrospray Tandem Mass Spectrometry. *Anal. Bioanal. Chem.* **2008**, *391* (4), 1293–1308.

Khunjar, W. O.; Mackintosh, S. A.; Skotnicka-Pitak, J.; Baik, S.; Aga, D. S.; Yi, T.; Jr., W. F. H.; Love, N. G. Elucidating the Relative Roles of Ammonia Oxidizing and Heterotrophic Bacteria during the Biotransformation of 17 $\alpha$ -Ethinylestradiol and Trimethoprim. *Environ. Sci. Technol.* **2011**, *45* (8), 3605–3612.

Kidd, K. A.; Blanchfield, P. J.; Mills, K. H.; Palace, V. P.; Evans, R. E.; Lazorchak, J. M.; Flick, R. W. Collapse of a Fish Population after Exposure to a Synthetic Estrogen. *Proc. Natl. Acad. Sci.* **2007**, *104* (21), 8897–8901.

Kolpin, D. W.; Furlong, E. T.; Meyer, M. T.; Thurman, E. M.; Zaugg, S. D.; Barber, L. B.; Buxton, H. T. Pharmaceuticals, Hormones, and Other Organic Wastewater Contaminants in U.S. Streams, 1999–2000: A National Reconnaissance. *Environ. Sci. Technol.* **2002**, *36* (6), 1202–1211.

Lajeunesse, A.; Smyth, S. A.; Barclay, K.; Sauvé, S.; Gagnon, C. Distribution of Antidepressant Residues in Wastewater and Biosolids Following Different Treatment Processes by Municipal Wastewater Treatment Plants in Canada. *Water Res.* **2012**, *46* (17), 5600–5612.

Lindberg, R. H.; Wennberg, P.; Johansson, M. I.; Tysklind, M.; Andersson, B. a V. Screening of Human Antibiotic Substances and Determination of Weekly Mass Flows in Five Sewage Treatment Plants in Sweden. *Environ. Sci. Technol.* **2005**, *39* (10), 3421–3429.

Lindberg, R. H.; Olofsson, U.; Rendahl, P.; Johansson, M. I.; Tysklind, M.; Andersson, B. A. V. Behavior of Fluoroquinolones and Trimethoprim during Mechanical, Chemical, and Active Sludge Treatment of Sewage Water and Digestion of Sludge. *Environ. Sci. Technol.* **2006**, *40* (3), 1042–1048.

Littleton, H. X.; Daigger, G. T.; Strom, P. F. Summary Paper: Mechanisms of Simultaneous Biological Nutrient Removal in Closed Loop Bioreactors. *Proc. Water Environ. Fed.* **2003**, 641–658.

Liu, G.; Wang, J. Long-Term Low DO Enriches and Shifts Nitrifier Community in Activated Sludge. *Environ. Sci. Technol.* **2013**, *47* (10), 5109–5117.

Love, N. G.; Moline, C.; Ernstoff, A. S.; Stadler, L. B.; Aga, D. S.; Su, L. Pharmaceutical Fate Under Varying Redox Biological Treatment Environments; Water Environment Research

Foundation, **2012**.

Martins, A. M. P.; Heijnen, J. J.; Van Loosdrecht, M. C. M. Effect of Dissolved Oxygen Concentration on Sludge Settleability. *Appl. Microbiol. Biotechnol.* **2003**, *62* (5-6), 586–593.

Metcalf, C. D.; Koenig, B. G.; Bennie, D. T.; Servos, M.; Ternes, T. A.; Hirsch, R. Occurrence of Neutral and Acidic Drugs in the Effluents of Canadian Sewage Treatment Plants. *Environ. Toxicol. Chem.* **2003**, *22* (12), 2872–2880.

Metcalf, C. D.; Chu, S.; Judt, C.; Li, H.; Oakes, K. D.; Servos, M. R.; Andrews, D. M. Antidepressants and Their Metabolites in Municipal Wastewater, and Downstream Exposure in an Urban Watershed. *Environ. Toxicol. Chem.* **2010**, *29* (1), 79–89.

Miège, C.; Choubert, J. M.; Ribeiro, L.; Eusèbe, M.; Coquery, M. Fate of Pharmaceuticals and Personal Care Products in Wastewater Treatment Plants – Conception of a Database and First Results. *Environ. Pollut.* **2009**, *157* (5), 1721–1726.

Park, H. D.; Noguera, D. R. Evaluating the Effect of Dissolved Oxygen on Ammonia-Oxidizing Bacterial Communities in Activated Sludge. *Water Res.* **2004**, *38* (14-15), 3275–3286.

Park, N.; Vanderford, B. J.; Snyder, S. A.; Sarp, S.; Kim, S. D.; Cho, J. Effective Controls of Micropollutants Included in Wastewater Effluent Using Constructed Wetlands under Anoxic Condition. *Ecol. Eng.* **2009**, *35* (3), 418–423.

Plósz, B. G.; Leknes, H.; Thomas, K. V. Impacts of Competitive Inhibition, Parent Compound Formation and Partitioning Behavior on the Removal of Antibiotics in Municipal Wastewater Treatment. *Environ. Sci. Technol.* **2009**, *44* (2), 734–742.

Plósz, B. G.; Leknes, H.; Liltved, H.; Thomas, K. V. Diurnal Variations in the Occurrence and the Fate of Hormones and Antibiotics in Activated Sludge Wastewater Treatment in Oslo, Norway. *Sci. Total Environ.* **2010**, *408* (8), 1915–1924.

Pochana, K.; Keller, J. Study of Factors Affecting Simultaneous Nitrification and Denitrification (SND). *Water Sci. Technol.* **1999**, *39* (6), 61–68.

Radjenović, J.; Petrović, M.; Barceló, D. Fate and Distribution of Pharmaceuticals in Wastewater and Sewage Sludge of the Conventional Activated Sludge (CAS) and Advanced Membrane Bioreactor (MBR) Treatment. *Water Res.* **2009**, *43* (3), 831–841.

Radke, M.; Lauwigi, C.; Heinkele, G.; Mürdter, T. E.; Letzel, M. Fate of the Antibiotic Sulfamethoxazole and Its Two Major Human Metabolites in a Water Sediment Test. *Environ. Sci. Technol.* **2009**, *43* (9), 3135–3141.

Rúa-Gómez, P.; Püttmann, W. Occurrence and Removal of Lidocaine, Tramadol, Venlafaxine, and Their Metabolites in German Wastewater Treatment Plants. *Environ. Sci. Pollut. Res.* **2012**, *19* (3), 689–699.



Stadler, L. B.; Ernstoff, A. S.; Aga, D. S.; Love, N. G. Micropollutant Fate in Wastewater Treatment: Redefining “Removal.” *Environ. Sci. Technol.* **2012**, *46* (19), 10485–10486.

Suarez, S.; Lema, J. M.; Omil, F. Removal of Pharmaceutical and Personal Care Products (PPCPs) under Nitrifying and Denitrifying Conditions. *Water Res.* **2010**, *44* (10), 3214–3224.

Tchobanoglous, G.; Burton, F. L.; Stensel, H. D. Wastewater Engineering: Treatment and Reuse, 4th Ed. McGraw-Hill: New York, NY, **2003**.

Ternes, T. A.; Joss, A.; Siegrist, H. Peer Reviewed: Scrutinizing Pharmaceuticals and Personal Care Products in Wastewater Treatment. *Environ. Sci. Technol.* **2004**, *38* (20), 392A – 399A.

van der Ven, A. J.; Mantel, M. A.; Vree, T. B.; Koopmans, P. P.; van der Meer, J. W. Formation and Elimination of Sulphamethoxazole Hydroxylamine after Oral Administration of Sulphamethoxazole. *Br. J. Clin. Pharmacol.* **1994**, *38* (2), 147–150.

van der Ven, A. J.; Vree, T. B.; van Ewijk-Beneken Kolmer, E. W.; Koopmans, P. P.; van der Meer, J. W. Urinary Recovery and Kinetics of Sulphamethoxazole and Its Metabolites in HIV-Seropositive Patients and Healthy Volunteers after a Single Oral Dose of Sulphamethoxazole. *Br. J. Clin. Pharmacol.* **1995**, *39* (6), 621–625.

Vieno, N. M.; Tuhkanen, T.; Kronberg, L. Seasonal Variation in the Occurrence of Pharmaceuticals in Effluents from a Sewage Treatment Plant and in the Recipient Water. *Environ. Sci. Technol.* **2005**, *39* (21), 8220–8226.

Vieno, N. M.; Tuhkanen, T.; Kronberg, L. Analysis of Neutral and Basic Pharmaceuticals in Sewage Treatment Plants and in Recipient Rivers Using Solid Phase Extraction and Liquid Chromatography–Tandem Mass Spectrometry Detection. *J. Chromatogr. A* **2006**, *1134* (1–2), 101–111.

Watkinson, A. J.; Murby, E. J.; Costanzo, S. D. Removal of Antibiotics in Conventional and Advanced Wastewater Treatment: Implications for Environmental Discharge and Wastewater Recycling. *Water Res.* **2007**, *41* (18), 4164–4176.

WEF. Activated Sludge. In *Operation of Municipal Wastewater Treatment Plants: MoP No. 11, Sixth Edition*; McGraw Hill Professional, Access Engineering: Water Environment Federation, **2008**.

Wilén, B. M.; Balmér, P. The Effect of Dissolved Oxygen Concentration on the Structure, Size and Size Distribution of Activated Sludge Flocs. *Water Res.* **1999**, *33* (2), 391–400.

Withdrawal Assessment Report for Ellefore (International Nonproprietary Name: Desvenlafaxine). European Medicines Agency Report, **2009**.

## **Chapter 4.**

### **Impact of microbial physiology and microbial community structure on pharmaceutical fate driven by dissolved oxygen concentration in nitrifying bioreactors**

Lauren B. Stadler<sup>1</sup> and Nancy G. Love<sup>1</sup>

<sup>1</sup>Department of Civil and Environmental Engineering, University of Michigan

#### **4.1 Introduction**

Energy conservation is an increasingly desirable goal in wastewater treatment given rising concerns over fossil fuel energy resources and climate change. The most energy intensive process in activated sludge wastewater treatment is aeration, which makes up 45- 75% of a conventional wastewater treatment plant's (WWTP's) total energy costs (Rosso et al., 2008). Therefore, one strategy for implementing more sustainable wastewater treatment involves a reduction in energy consumption by moving towards treatment that minimizes aeration (Rosso et al., 2008; Leu et al., 2009; Flores-Alsina et al., 2011). Conventional nitrifying activated sludge WWTPs typically operate with bulk liquid dissolved oxygen (DO) concentrations of greater than 2 mg/L to ensure complete nitrification and stable nitrifying populations (WEF, 2008), which results in a substantial energy demand for aeration. There is mounting evidence that stable carbon removal and nitrification can occur at low DO concentrations (<1 mg/L) (Schuyler et al., 2009; Jimenez et al., 2011), suggesting that substantial energy and cost savings are possible by reducing DO levels.

Advances in sensor technology and aeration control strategies in recent years have demonstrated that strategies such as ammonia-based aeration control can result in operation at DO concentrations between 1 and 0.5 mg/L (Rieger et al., 2014; Uprety et al., 2015). Low DO treatment also can also enable simultaneous nitrification and denitrification, resulting in supplemental carbon savings in addition to aeration energy savings (Daigger and Littleton, 2000; Jimenez et al., 2011).

Fundamental research on low DO wastewater treatment has focused mostly on nitrification; nitrifiers grow relatively slowly as compared to heterotrophs due to their chemolithoautotrophic metabolism and inferior oxygen scavenging ability. Selecting for nitrifiers that are adapted to low DO environments and taking advantage of improvements in mass transfer efficiencies during low DO operation can result in at least 20% less energy for aeration (Arnaldos and Pagilla, 2014). As we move toward low DO treatment processes, there is a need to better understand how low DO environments affect the function and structure of nitrifying wastewater communities to ensure stable performance without compromising treatment outcomes.

Ammonia oxidizers, which perform the first step of nitrification using the enzyme ammonia monooxygenase (AMO), may also play a major role in pharmaceutical biotransformation during wastewater treatment. AMO can catalyze the oxidation of a relatively wide range of substrates (Arp et al., 2002). Several studies have shown that pharmaceutical loss is enhanced in nitrifying activated sludge systems (e.g. Tran et al., 2009), and have implicated the involvement of AMO. Further, pure culture work has shown the ability of AMO to biotransform compounds such as natural and synthetic estrogens, as well as bisphenol A (Shi et al., 2004; Khunjar et al., 2011; Sun et al., 2012). While AMO has been linked to the transformation of some pharmaceuticals, other enzymes may be involved as primary and/or secondary catalysts of oxidation reactions. WWTPs with long solids retention times (SRTs) that support the growth of

nitrifiers also support the growth of other slow growing heterotrophs that can biotransform pharmaceuticals. Thus, while greater nitrifying activity may be indicative of environments capable of enhanced biotransformation, other microbial processes may be responsible for those biotransformations, many of which are poorly understood and not well-characterized.

Low DO treatment can impact the rate and extent of pharmaceutical biotransformation by 1) slowing the activity of the microorganisms involved in biotransformation because DO acts as a limiting substrate in respiration or catabolic reactions; and/or 2) selecting for a community that is more (or less) efficient at biotransformation. The objective of this work was to determine the impact of low DO treatment on pharmaceutical biotransformations by nitrifying communities, and specifically to discern between effects of DO concentration on microbial physiology (activity) and on microbial community structure (selection). Parent chemostat reactors were used to grow nitrifying enrichment cultures under low ( $\sim 0.3$  mg/L) and high ( $> 4$  mg/L) DO concentrations to understand how DO growth conditions impact microbial community structure. Short-term batch experiments using the biomass from the parent reactors were performed under low and high DO conditions to understand how DO concentration impacts microbial physiology. This experimental design allowed us to distinguish between long-term (microbial community structure) and short-term (physiologic) effects of DO on pharmaceutical biotransformations. Allylthiourea-inhibited batch experiments were also conducted to assess the link between nitrification and pharmaceutical biotransformations. This research will contribute to improvements in the design and operation of WWTPs using low DO-adapted metabolisms in wastewater treatment and a better understanding of the impact that energy efficient treatment strategies on pharmaceutical removal.

## 4.2 Materials and methods

### 4.2.1 Parent reactors and water quality analyses

Two parent chemostat reactors, a high DO and a low DO reactor, were operated for over a year. Each reactor consisted of a 19 L plastic bucket with a liquid volume of 12 L. The residence time in each reactor was 20 days, and this was achieved by intermittently feeding 25 mL of influent and wasting 25 mL every hour. The influent to the reactors was a synthetic medium containing 195 mg-N/L as ammonia-N plus trace nutrients (influent details provided in Table B1, Appendix B). pH was controlled via base addition (30 g/L sodium bicarbonate) to maintain the pH at approximately 7.5. The high DO parent reactor was aerated constantly to maintain a DO concentration above 4 mg/L. The DO concentration in the low DO parent reactor was controlled using real-time feedback from an optical DO probe (Orion RDO® Pro, In Situ Inc.). The DO probe triggered the aerator to turn on when the DO dropped below the setpoint of 0.2 mg/L, which resulted in a DO concentration that fluctuated between 0.2 and 0.4 mg/L. The reactors were operated at room temperature (typically between 21 and 24 °C). Both reactors were seeded with sludge from the Ann Arbor, MI WWTP, which uses an anaerobic-aerobic process to achieve biological phosphorus removal and nitrification. The Ann Arbor WWTP has an SRT of approximately 9 days and operates at a DO concentration of 2-3 mg/L in the aerobic basins. Samples were collected from the parent reactors one or two times per week and analyzed for soluble nitrogen species concentrations (ammonia-N, nitrite-N, and nitrate-N) according to Standard Methods (methods 4500F-NH<sub>3</sub>, 4500B-NO<sub>2</sub><sup>-</sup>, and 4110; 2005). Samples were filtered through 0.45 µm nitrocellulose filters and stored at 4°C until analysis (within one week of sampling).

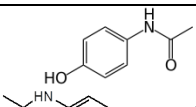
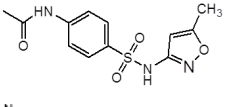
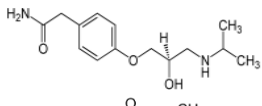
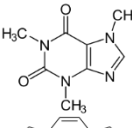
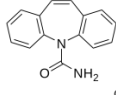
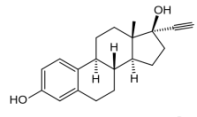
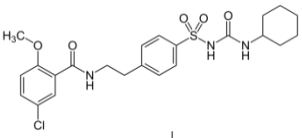
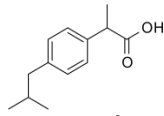
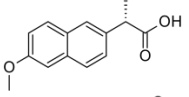
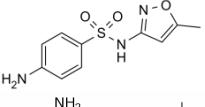
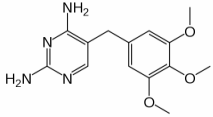
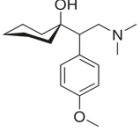
#### ***4.2.2 Pharmaceutical selection***

The pharmaceuticals selected for investigation included: atenolol, 17 $\alpha$ -ethinylestradiol (EE2), ibuprofen, sulfamethoxazole, trimethoprim, venlafaxine, acetaminophen, acetyl-sulfamethoxazole, caffeine, carbamazepine, glyburide, naproxen, sucralose, and erythromycin (Table 4-1). These compounds were selected based on their prevalence in WWTP influents and effluents, structural characteristics, and reported low sorption to biomass such that biotransformation is likely the primary mechanism responsible for loss during treatment.

#### ***4.2.3 Pharmaceutical biotransformation batch experiments***

Batch experiments were performed using the biomass taken from the low and high DO parent reactors (after over a year of operation) to determine the extent and rate of pharmaceutical biotransformation by each parent community. Batch experiments were performed for each parent biomass at two different DO concentrations: high DO (constantly aerated) and low DO (DO maintained between 0.2 and 0.4 mg/L). DO control in the low DO batch reactors during the batch experiments was performed by sparging with a mixture of nitrogen gas and air. Optical DO probes (WTW, Weilheim, Germany) were used to monitor the DO concentration throughout each batch experiment. Biomass from the parent reactors was concentrated and washed prior to initiating the batch experiments. For each batch experiment, 500 mL of the mixed liquor from a parent reactor was centrifuged (5 min at 5,500 rpm, 20 °C) to pellet, and then washed three times with N-free media. The pelleted and washed biomass was then re-suspended in N-free media to make a final volume of 200 mL.

**Table 4-1.** Compounds selected for investigation

Chemical	Structure	Chemical Formula and Molecular Weight	Use
Acetaminophen		C <sub>8</sub> H <sub>9</sub> NO <sub>2</sub> 151.16 g/mol	Analgesic and antipyretic
Acetyl-sulfamethoxazole		C <sub>12</sub> H <sub>13</sub> N <sub>3</sub> O <sub>4</sub> S 295.31 g/mol	Antibiotic TP
Atenolol		C <sub>14</sub> H <sub>22</sub> N <sub>2</sub> O <sub>3</sub> 266.34 g/mol	Beta-blocker
Caffeine		C <sub>8</sub> H <sub>10</sub> N <sub>4</sub> O <sub>2</sub> 194.19 g/mol	Stimulant
Carbamazepine		C <sub>15</sub> H <sub>12</sub> N <sub>2</sub> O 236.27 g/mol	Anticonvulsant
17 $\alpha$ -Ethinylestradiol		C <sub>20</sub> H <sub>24</sub> O <sub>2</sub> 296.40 g/mol	Synthetic hormone
Glyburide		C <sub>23</sub> H <sub>28</sub> ClN <sub>3</sub> O <sub>5</sub> S 494.00 g/mol	Antidiabetic
Ibuprofen		C <sub>13</sub> H <sub>18</sub> O <sub>2</sub> 206.29 g/mol	Nonsteroidal anti-inflammatory drug
Naproxen		C <sub>14</sub> H <sub>14</sub> O <sub>3</sub> 230.26 g/mol	Nonsteroidal anti-inflammatory drug
Sulfamethoxazole		C <sub>10</sub> H <sub>11</sub> N <sub>3</sub> O <sub>3</sub> S 253.28 g/mol	Antibiotic
Trimethoprim		C <sub>14</sub> H <sub>18</sub> N <sub>4</sub> O <sub>3</sub> 290.32 g/mol	Antibiotic
Venlafaxine		C <sub>17</sub> H <sub>27</sub> NO <sub>2</sub> 277.40 g/mol	Antidepressant

A mixture of the pharmaceuticals dissolved in methanol was added to 500 mL glass flasks (250  $\mu$ L of a 1 mg/L mixture) and allowed to evaporate until dry in a fume hood. After evaporation was complete, 50 mL of a phosphate buffered media containing 150 mg-N/L as ammonia-N was

added to each flask such that after the 200 mL of washed biomass was added to the flask the initial concentration of each compound, ammonia, and phosphate buffer were 1 µg/L, 30 mg-N/L, and 0.05 M, respectively. The flask with 50 mL of buffered nitrogen media was placed on a stir plate for 1 hour to allow the dried compounds to re-dissolve in the media prior to adding the washed biomass and initiating the biotransformation experiment. Two batch reactors were aerated constantly (high DO batch conditions), two reactors were maintained at low DO concentrations (as described above), two reactors were supplemented with 10 mg/L of allylthiourea (ATU) (Khunjar et al., 2011), an ammonia oxidation inhibitor, to understand the role of nitrifiers in pharmaceutical biotransformation, and a final batch reactor consisted of biomass inactivated with sodium azide (0.1% w/v; Batt et al., 2007). Complete ammonia oxidation inhibition using ATU was confirmed by measuring the concentration of ammonia-N across the batch experiments (Figure B1, Appendix B).

#### ***4.2.4 Samples collection and analysis from biotransformation experiments***

Samples were collected from each batch reactor at approximately  $t = 2$  min, 2.5 h, 5 h, 8.5 h, 12 h, 1 d, 2 d, and 3 d. To sample, 10 mL was collected from each flask using a graduated glass pipette, the sample was spiked with 100 µL of 50 µg/L stock containing a mixture of deuterated pharmaceutical analogs (Toronto Research Chemicals, Toronto, ON, Canada), filtered through a 0.3 glass fiber filter (Sterlitech Inc., Kent, Washington), and stored at 4°C until analysis. Ammonia-N, nitrite-N, and nitrate-N concentrations were determined in all samples as described above. Pharmaceutical concentrations were determined in samples corresponding to time points of 2 min, 5 h, 12 h, 1 d, 2 d, and 3 d via on-line solid phase extraction, liquid chromatography, and mass spectrometry (described below).



Biomass samples for microbial community analysis were collected from the parent reactors on the day that biomass was taken from them for the biotransformation batch experiments. Briefly, 50 mL samples of mixed liquor were collected from each parent reactor, biomass was pelleted via centrifugation at 6,200 x g for 5 minutes at 4°C and the supernatant was discarded. The biomass pellet was transferred to a 2 mL microcentrifuge tube, re-pelleted, decanted, and the biomass was stored at -80°C until DNA was extracted. Total and volatile suspended solids (TSS/VSS) concentrations of the parent reactors were also determined according to Standard Methods (method 2540; 2005) on the day of the batch experiments.

#### ***4.2.5 Pharmaceutical quantification***

Pharmaceuticals were quantified via on-line pre-concentration followed by high performance liquid chromatography (HPLC) and high resolution mass spectrometry (HRMS). Matrix-matched external calibration curves containing a mixture of the target compounds and deuterated analogs were used for quantification. On-line pre-concentration of the compounds of interest was performed using the Equan™ system (Thermo Fisher Scientific, Grand Island, New York) (system details are provided in Fayad et al., 2013). The on-line pre-concentration was performed using a Hypersil Gold aQ trapping column (20 x 2.1 mm, 12 µM particle size; Thermo Fisher Scientific) and chromatographic separation was done with an Accucore aQ column (50 x 2.1 mm, 2.6 µm particle size; Thermo Fisher Scientific). A 500 µL sample was injected onto the trapping column. A mobile phase containing water with 0.1% formic acid and methanol with 0.1% formic acid was applied via gradient flow to elute all compounds with minimal overlap. Total run time for one sample was 16 minutes at a flow rate of 1 mL/min on the trapping column and 0.175-0.250 mL/min on the analytical column. Complete method details including gradient flow rates are provided in Appendix B.

Ionization of the compounds was achieved by positive electron spray ionization (ESI) for: atenolol, 17 $\alpha$ -ethinylestradiol (EE2), sulfamethoxazole, trimethoprim, venlafaxine, acetyl-sulfamethoxazole, caffeine, carbamazepine, acetaminophen, glyburide, and erythromycin; negative ESI was used for: ibuprofen, naproxen, triclosan, and sucralose. The following source parameters were used: capillary temperature of 250 °C, auxiliary gas heater temperature of 275 °C, a spray voltage of 3.5 kV, sheath gas flow rate of 30 arbitrary units, auxiliary gas flow rate of 20 arbitrary units, and sweep gas flow rate of 1 arbitrary unit. In both positive and negative mode a full scan ranging from 150 to 750 m/z was performed at a resolution of 70,000 and target automatic gain control (AGC) of  $1 \times 10^{-6}$ . All data were collected and processed using the Thermo TraceFinder Software Version 3.2 (Thermo Fisher Scientific).

#### ***4.2.6 Molecular analyses***

DNA was extracted from the frozen biomass samples collected from the parent reactor on the day of the biotransformation batch experiments, as described above. DNA extraction involved three bead beating steps (Mini-Beadbeater-96, BioSpec Products, Bartlesville, OK) with 0.1 mm diameter zirconium beads in lysis buffer, followed by proteinase K digestion, and automated extraction using the Maxwell 16 Blood LEV kit according to the manufacturer's instructions (Promega, Madison, WI). Extracted DNA quality was verified using a NanoDrop spectrophotometer (Thermo Fisher Scientific, Waltham, MA) and DNA quantity was determined using the QuantiFluor dsDNA kit (Promega, Madison, WI). DNA extracts were stored at -20 °C until they were submitted for sequencing or analyzed by quantitative polymerase chain reaction (qPCR).

Polymerase chain reaction (PCR), multiplexing, and sequencing was performed by the Center for Microbial Systems (University of Michigan, Ann Arbor, MI) using the Illumina MiSeq

platform (San Diego, CA) targeting the V4 region of the 16S rRNA gene (Caporaso et al., 2011). The resulting sequences were processed and analyzed using Mothur (version 1.33.3) (Schloss et al., 2009) following the MiSeq standard operating procedure. Sequence classification was performed using the Ribosomal Database Project (Cole et al., 2009) and the Basic Local Alignment Search Tool (BLAST; NCBI, Bethesda, MD).

The abundance of ammonia oxidizers was quantified in the parent reactor biomass samples via qPCR. Primers targeting the bacterial ammonia monooxygenase gene (*amoA*) were used (*amoA*-1F (5'-GGGGTTTCTACTGGTGGT-3') and *amoA*-2R (5'-CCCCTCKGSAAAGCCTTCTTC-3'); Rotthauwe et al., 1997). qPCR standards were prepared using PCR-amplified *amoA* products from pooled DNA extracts from the parent reactors (detailed in Appendix B) (He and McMahon, 2011; Sonthiphand et al., 2013). qPCR was performed on a Mastercycler Realplex ep (Eppendorf, Hamburg, Germany). 20  $\mu$ L qPCR reaction volumes consisted of 10  $\mu$ L of 2x EvaGreen Fast Plus qPCR Master Mix (Biotium, Hayward, CA), 0.2  $\mu$ L each of 50  $\mu$ M forward and reverse primer (final concentration of 50  $\mu$ M), 8.6  $\mu$ L of nuclease free water, and 1  $\mu$ L of DNA template. All samples were run in triplicate at three different dilutions: 5x, 50x, and 500x and each plate contained no template controls.

## 4.3 Results and discussion

### 4.3.1 Reactor performance and microbial community characteristics of parent reactors

Complete and stable nitrification was achieved in both parent reactors. The low and high DO parent reactors achieved ammonia removal efficiencies of  $99.0 \pm 2.3\%$  and  $99.9 \pm 0.1\%$ , respectively, over the 6 months prior to when the batch experiments were performed. Further, no buildup of nitrite was observed in either reactor, demonstrating complete nitrification. Effluent

total inorganic nitrogen (sum of ammonia, nitrite, and nitrate-N) concentrations were slightly lower in the low DO than the high DO parent reactor, with average total inorganic nitrogen (TIN) removal efficiencies of 11% and 2%, respectively, indicating slightly more denitrification occurred in the low DO parent reactor.

While the low and high DO parent reactors achieved similar effluent quality and performance with respect to nitrification efficiency, there were observable differences in biomass concentration between the reactors. The suspended solids concentration in the low DO parent reactor was significantly higher than the high DO parent reactor (Figure 4-1), despite being loaded with the same amount of electron donor (195 mg ammonia-N/L/day). qPCR indicated that the low DO parent reactor had significantly more ammonia oxidizers than the high DO parent reactor (Figure 4-1). Further, the ratio of ammonia oxidizers to total biomass concentration (as VSS) was more than two times greater in the low than the high DO parent reactor. Therefore, low DO growth conditions not only resulted in greater biomass concentrations and a greater abundance of ammonia oxidizers, but also an enriched ammonia oxidizer population. Previous studies have found that nitrifiers grown under low DO conditions had greater observed yields than nitrifiers grown under high DO conditions (Bellucci et al., 2011; Liu and Wang, 2013). The observed yield coefficient is determined by the true growth yield, endogenous decay rate, and the sludge age (Grady et al., 2011). The endogenous decay coefficient is a lumped parameter that accounts for loss in cell mass due to oxidation of internal storage products for energy required for cell maintenance and death and predation by other organisms (Lawrence and McCarty, 1970). A reduced endogenous decay rate in low DO environments is consistent with the greater observed yield in the low versus high DO parent reactor. It is also consistent with previous research that showed increased observed yields and reduced specific sludge degradation rates under low DO conditions compared to fully

aerobic conditions (Habermacher et al., 2015). One explanation for why this happens is that low DO inhibits select protozoan predators (Madoni, 1993), which reduces decay rate and increases biomass concentration.

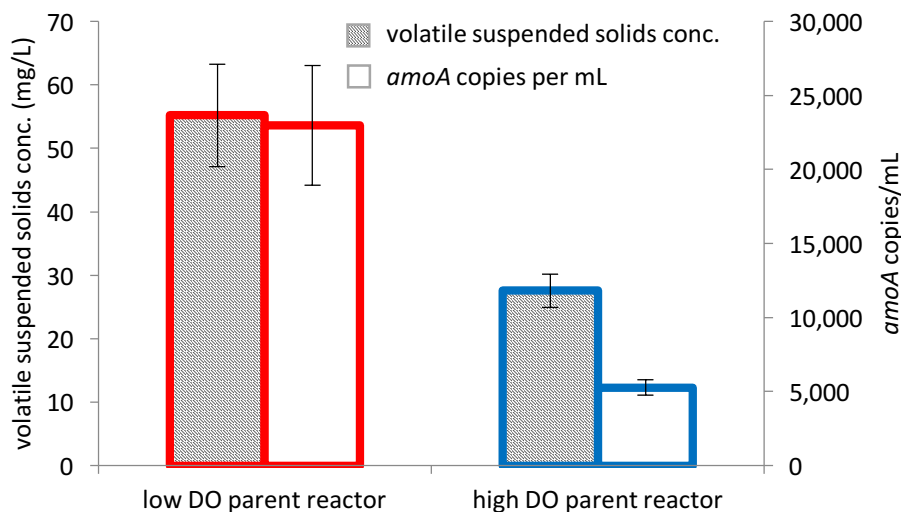


**Figure 4-1.** Volatile suspended solids (VSS) concentration (striped bar) and *amoA* copies per milliliter (open bars) in the low and high DO parent reactors. Error bars represent the standard deviation from the mean of technical triplicates.

The batch experiments were performed by taking the same volume of mixed liquor from each of the reactors, and this resulted in the batch experiments with the low DO parent reactor biomass having greater total biomass concentrations and a greater abundance of ammonia oxidizers than those performed using the high DO parent reactor biomass. Ammonia oxidation rates in the batch experiments were significantly different under low and high DO batch conditions, and between the low and high DO parent reactors (Figure 4-2). Faster ammonia oxidation rates were observed in the high DO batch conditions, regardless of parent reactor biomass, illustrating the direct impact of DO as a limiting substrate. Under low DO batch conditions, the low DO parent biomass performed ammonia oxidation slightly faster than the high DO parent biomass. However, when normalized to *amoA* copy concentration, the rates were not significantly different between

the batch experiments (unpaired t-test,  $p = 0.65$ ). Under high DO batch conditions, the ammonia oxidation rates normalized to *amoA* copy concentration for the low DO parent biomass were significantly slower than the high DO parent biomass (unpaired t-test,  $p = 0.025$ ). Thus, while the low DO parent reactor harbored a more abundant population of ammonia oxidizers, they were slower at performing ammonia oxidation under high DO conditions. Furthermore, this demonstrated that the low DO parent reactor biomass was not able to adapt well to high DO conditions over the three day batch experiments. Trade-offs between substrate affinity and maximum substrate utilization rates have been demonstrated in pure cultures (Wirtz, 2002; Elbing et al., 2004) and this biochemical trade-off is theorized to be a driver of microbial diversification (Gudelj et al., 2007). Our results indicate that low DO growth conditions may select for ammonia and nitrite oxidizers with high oxygen affinities, i.e. “K” strategists, with high substrate affinities and low maximum activity, as opposed to “r” strategists. Even though the normalized rates were different between the low and high DO parent reactor biomasses, the raw rates were not significantly different (unpaired t-test,  $p = 0.30$ ). The increased abundance of ammonia oxidizers due to low DO growth conditions compensated for the slower per organism rates of ammonia oxidation.

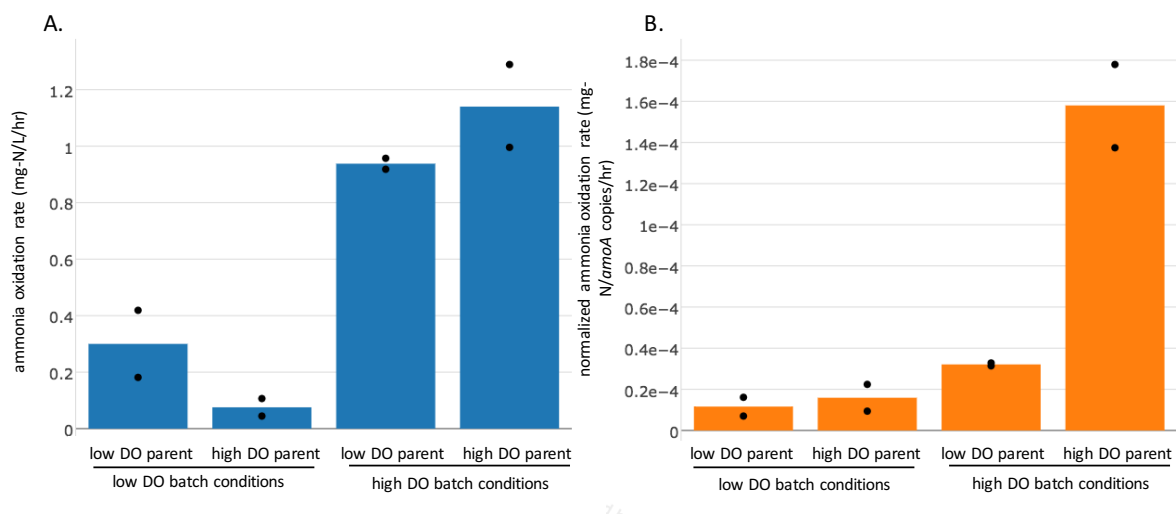


**Figure 4-2.** Ammonia oxidation rates in the batch experiments with biomass from each parent reactor. Non-normalized ammonia oxidation rates are shown in blue bars (A) and ammonia oxidation rates normalized to *amoA* copies per mL are shown in orange bars (B). Bars represent the average of duplicates and the dots represent the individual measurements.

In addition to characterizing the impact of DO concentration on the abundance of microorganisms and ammonia oxidizers, amplicon sequencing of the 16S rRNA gene was performed to understand community composition differences between the low and high DO parent reactors. At equal sequencing depths, three diversity indices that vary in their weighting of abundance all show that the low DO parent reactor supported the growth of a much more diverse community (larger value for all indices) than the high DO reactor (Table 4-2). While the microbial community as a whole was more diverse in the low DO reactor, the dominant AOB and NOB in the reactors were similar (AOB: *Nitrosomonas*-type; NOB: *Nitrospira*-type) based on OTU groupings with a 97% similarity threshold (Table B4, Appendix B).

**Table 4-2.** Richness and diversity indices of the low and high DO parent reactor communities

	Operational taxonomic unit (OTU) richness	Inverse Simpson diversity	Shannon diversity
Low DO	1,140	59	5.2
High DO	350	21	3.8

#### ***4.3.2 Direct impact of DO concentration on pharmaceutical transformations***

Only a subset of the compounds biotransformed during the batch experiments. No significant biotransformation of trimethoprim, venlafaxine, acetyl-sulfamethoxazole, caffeine, carbamazepine, glyburide, sucralose, and erythromycin was observed by either the low or high DO parent communities. For the compounds for which we observed significant biotransformation (ibuprofen, sulfamethoxazole, 17 $\alpha$ -ethinylestradiol, acetaminophen, and atenolol), both DO concentration during the batch experiment and the DO concentration of the parent reactor impacted the degree of biotransformation.

For ibuprofen, sulfamethoxazole, 17 $\alpha$ -ethinylestradiol, and acetaminophen, greater loss of the parent compound was observed in high versus low DO batch conditions (Figure 4-3). Atenolol was the one exception – greater loss was observed under low DO than high DO batch conditions (Figure 4-3). The first-order rate constant describing the biotransformation rate of each of the compounds varied significantly between compounds (Table 4-3). Ibuprofen biotransformation occurred most rapidly, with a half-life of 2-6 hours in high DO batch conditions. Conversely, complete loss of the other compounds was not observed over the 3-day batch experiments, and the biotransformation rate constants were significantly lower (Table 4-3). These results are consistent with previous studies that report the relative biodegradability of these compounds in wastewater systems (Joss et al., 2006; Yu et al., 2006).



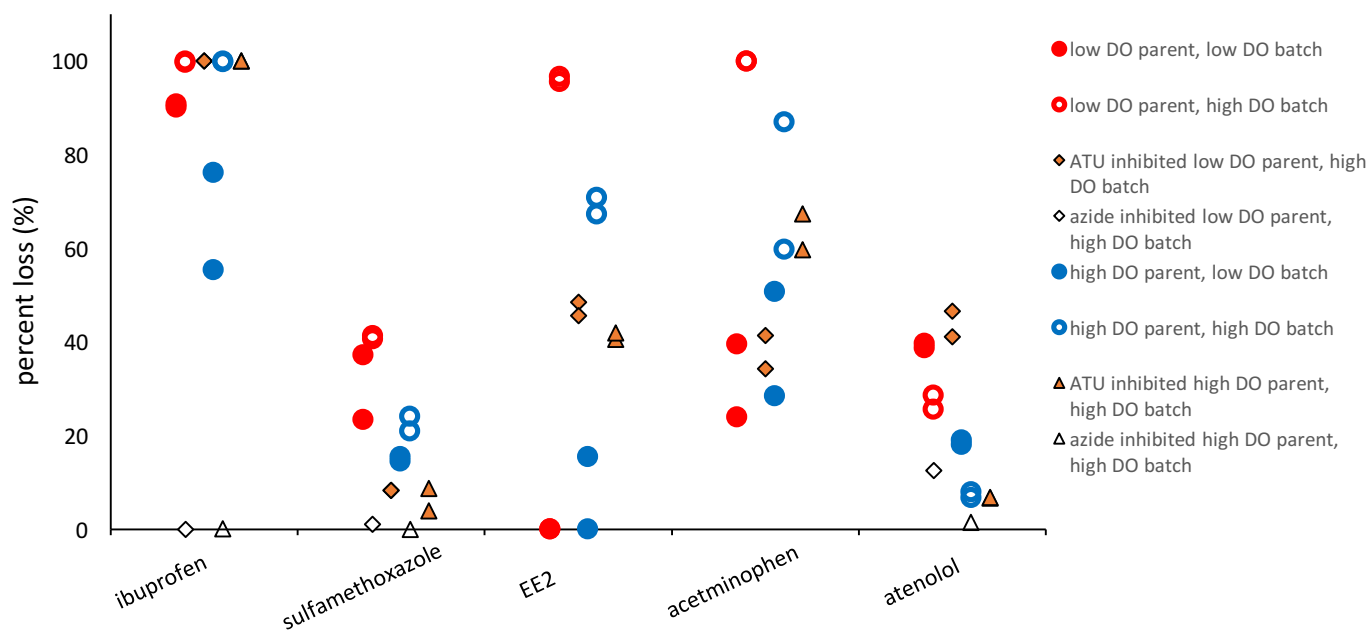


**Figure 4-3.** Percent loss of ibuprofen, sulfamethoxazole, 17 $\alpha$ -ethinylestradiol (EE2), acetaminophen, and atenolol in the low (red) and high (blue) DO parent communities. The solid markers represent low DO batch conditions (0.2-0.3 mg/L), and the open markers represent high DO batch conditions (constantly aerated, DO > 4 mg/L). Black outlined markers represent inhibited batch conditions. Azide-inhibited controls are not shown for EE2 and acetaminophen because of abiotic reactions with azide contributed to losses of these compounds (details in Appendix B).

**Table 4-3.** Observed specific kinetic biotransformation constants (normalized by VSS concentration) for ibuprofen, EE2, sulfamethoxazole, acetaminophen, and atenolol. No biotransformation rate is reported for EE2 for low DO batch conditions because no significant biotransformation occurred.

	$k_{obs}$ [L mg <sup>-1</sup> day <sup>-1</sup> ]				
	Ibuprofen	EE2	Sulfamethoxazole	Acetaminophen	Atenolol
Low DO parent & low DO batch	2.4E-02 $\pm$ 1.3E-03	N.A.	2.8E-03 $\pm$ 1.2E-03	2.9E-03 $\pm$ 1.6E-03	3.8E-03 $\pm$ 2.4E-04
Low DO parent & high DO batch	1.1 E-01 $\pm$ 6.4E-03	2.1E-02 $\pm$ 2.2E-03	3.3E-03 $\pm$ 2.1E-04	2.4E-02 $\pm$ 7.7E-03	1.9E-03 $\pm$ 2.0E-04
High DO parent & low DO batch	1.4E-02 $\pm$ 6.0E-03	N.A.	2.2E-03 $\pm$ 8.1E-05	7.0E-03 $\pm$ 3.8E-03	2.9E-03 $\pm$ 3.7E-04
High DO parent & high DO batch	1.0E-01 $\pm$ 3.0E-02	1.3E-02 $\pm$ 4.1E-03	3.1E-03 $\pm$ 9.5E-04	2.1E-02 $\pm$ 6.2E-03	8.3E-04 $\pm$ 2.8E-04

While complete and stable nitrification is possible at considerably lower bulk liquid DO concentrations than typically used in conventional activated sludge treatment systems, these results (and other previous studies, e.g. Jimenez et al., 2011) indicate that low DO slows the rate of ammonia oxidation. Our results show that this also reduces the rate of trace chemical transformations. If DO is a limiting substrate, it will slow the activity of aerobic microorganisms and impact their kinetics, resulting in reduced rates of biotransformation of primary and cometabolic substrates. These results suggest that DO concentration will impact the degree of transformation of these compounds during treatment and that the oxygen half-saturation constant ( $K_{O_2}$ ) of the microbial groups involved in biotransformation is an important parameter to predict the impact of DO concentration on the rate of pharmaceutical biotransformation. More research is needed to determine oxygen half-saturation constants ( $K_{O_2}$ ) for pharmaceuticals in order to accurately model their fate in wastewater treatment and determine appropriate operational targets for DO concentration that do not negatively impact pharmaceutical removal, and this topic is further investigated in Chapter 5.

Atenolol was the only compound for which we observed a faster biotransformation rate under low than high DO batch conditions. Other studies have reported that atenolol undergoes an initial amide-hydrolysis and is converted to atenolol-acid in wastewater treatment systems (Kern et al., 2010; Barbieri et al., 2012a). Hydrolysis reactions, unlike hydroxylation reactions, do not use oxygen as a substrate in catalysis. Faster hydrolysis rates in low DO conditions indicate that oxygen is not a limiting substrate in this reaction and might be enhanced as low DO environments can enable the growth of both aerobic and anoxic organisms. Previous studies have observed atenolol loss in anoxic environments during wastewater treatment (Carucci et al., 2006; Park et al., 2009; Stadler et al., 2015). Our previous study on sequencing batch reactors treating real municipal

wastewater observed greater loss of atenolol in high than low DO conditions (Stadler et al., 2015). Another study of atenolol fate in different redox conditions in aquifer material found that removal occurred fastest in the most reducing conditions considered (sulfate reducing conditions; Barbieri et al., 2011). The collective results suggest that we do not fully understand the factors that control atenolol transformation and there may be a complex relationship between redox condition and transformation rate.

#### ***4.3.3 Links between nitrification and pharmaceutical biotransformation***

Batch experiments were performed using allylthiourea, a specific inhibitor of ammonia oxidation, to understand the relationship between nitrification and pharmaceutical biotransformation. Allylthiourea inhibits ammonia oxidation and acts by binding to the copper center of ammonia monooxygenase (Bédard and Knowles, 1989). As expected, no ammonia loss was observed in batch experiments with allylthiourea (Figure B1, Appendix B). Batch experiment results showed that the biotransformation of certain compounds (sulfamethoxazole, 17 $\alpha$ -ethinylestradiol, and acetaminophen) was linked to nitrification, as the extent and rate of transformation of these compounds were reduced in the presence of allylthiourea (Figure 4-3). Allylthiourea did not cease the transformation of these compounds, which indicates that both heterotrophs and nitrifiers are involved in their biotransformation in the uninhibited batches. For ibuprofen, the presence of the inhibitor had no significant effect on the rate of transformation. However, for atenolol, the presence of the inhibitor resulted in an increase in the rate of biotransformation, indicating that reduced competition with nitrifiers enabled greater atenolol transformation.

The link between enhanced transformation of several compounds and nitrification could be due to several different factors: first, ammonia oxidizers are directly involved in the

transformation of these compounds. Ammonia monooxygenase is a non-specific enzyme that is capable of oxidizing alternative substrates (Hyman et al., 1994; Keener and Arp, 1994; Roh et al., 2009). Previous studies have demonstrated the ability of ammonia oxidizers to transform EE2 using pure cultures and ATU-inhibited experiments (Shi et al., 2004; Yi and Harper, 2007; Khunjar et al., 2011). Therefore, our results are consistent with previous findings suggesting that ammonia oxidizers are likely major contributors to the biotransformation of these compounds. Another possible explanation is that nitrite oxidizers are involved in the biotransformation of these compounds. Few studies have directly investigated the role of the nitrite oxidizers in pharmaceutical biotransformation, and their contribution is often overlooked as compared to ammonia oxidizers. Inhibition of ammonia oxidation with allylthiourea also ceases the production of nitrite, and therefore decreases the activity of nitrite oxidizers. A final possible explanation of the link between transformation and nitrification is that the products of nitrification (nitrite and nitrate) may be involved in abiotic transformations of these compounds. Previous studies have observed the biologically mediated abiotic transformation of sulfamethoxazole with nitrite under anoxic conditions (Barbieri et al., 2012b; Nödler et al., 2012). Another study demonstrated that EE2 underwent abiotic nitritation in the presence of high nitrite concentrations (10 - 500 mg-NO<sub>2</sub><sup>-</sup>-N/L), and that this reaction was enhanced at low pH (Gaulke et al., 2008). In our experiments, nitrite concentrations were always significantly lower than those reported in these studies (below 2.5 mg-NO<sub>2</sub><sup>-</sup>-N/L) and the pH was near neutral; therefore, nitrite-mediated abiotic transformations are unlikely to be a primary mechanism of transformation.

#### ***4.3.4 Indirect impacts of DO concentration on pharmaceutical transformations***

By comparing biotransformation rates between experiments using biomass from the low versus high DO parent reactor, the indirect impacts of DO on pharmaceutical biotransformation

via changes in microbial community structure were identified. For all of the compounds studied, greater loss of the parent compound (Figure 4-3) and faster biotransformation (Table B3, Appendix B) was observed in batch experiments using low DO parent reactor biomass than the high DO parent (under equivalent batch DO conditions). These results suggest that DO growth condition impacts the microbial community, and that selection in turn impacts the potential for pharmaceutical biotransformation.

One selection impact of long-term low DO growth conditions was reduced specific activity with respect to ammonia oxidation rates in high DO conditions. The observed nitrification rates were comparable between the low and high DO parent reactors under high DO batch conditions because of the increased abundance of ammonia oxidizers in the low DO parent reactor. For ibuprofen, sulfamethoxazole, and acetaminophen, the faster observed biotransformation rates under high DO batch conditions could be explained by the increased biomass concentration in the low DO parent reactor as the VSS-normalized biotransformation rate constants were comparable between the low and high DO parent biomass (Table 4-3). However, for EE2 and atenolol, the specific biotransformation rate constants (VSS-normalized) were greater for the biomass from the low DO parent than the high DO parent reactor. Unlike for ammonia oxidation, these results indicate that low DO conditions selected for a community with comparable or faster specific pharmaceutical biotransformation rates compared to the high DO parent reactor.

Despite identifying similar dominant AOB and NOB genera (*Nitrosomonas*-type and *Nitrospira*-type, respectively) in the low and high DO parent reactors, the communities functioned differently based on nitrification rates. One possible explanation for the differences in specific activity could be microdiveristy (Gruber-Dorninger et al., 2015). The length and region of the 16S rRNA gene that was sequenced only provides resolution at the genus level, and thus diversity

within *Nitrosomonas* and *Nitrospira*-type groupings was not discernable with the methods applied. Sequencing of the ammonia monooxygenase gene would likely better capture diversity within the ammonia oxidizing populations. A number of studies on low DO nitrification systems have reported conflicting results with respect to how DO shifts (or does not shift) the nitrifying microbial community. Several studies have hypothesized that low DO environments select for nitrifier lineages that have high oxygen affinities (Gieseke et al., 2001; Park and Noguera, 2004). The results, however, have been conflicting in terms of the specific lineages of AOBs identified in low DO environments, with several studies identifying AOB belonging to the *Nitrosomonas* genera (Park and Noguera, 2004; Bellucci et al., 2011; Arnaldos et al., 2013) and others finding that *Nitrospira* (Li et al., 2007) dominated in low DO conditions. Further, the recent discovery of organisms within the genus of *Nitrospira* that completely oxidize ammonia to nitrate (comammox) has altered our understanding of the aerobic nitrification process (Daims et al., 2015; van Kessel et al., 2015). It is not yet known how low DO conditions influence the abundance and activity of comammox and whether comammox are involved in pharmaceutical biotransformation. Low DO conditions have been shown to favor the growth of *Nitrospira* sp. over *Nitrobacter* sp. performing nitrite oxidation (Daims et al., 2001; Schramm et al., 1998), and thus could also possibly favor *Nitrospira* that perform complete ammonia oxidation.

An alternative hypothesis for the impact of oxygen limitation on ammonia oxidizing communities is that the community undergoes a physiological, as opposed to structural, adaptation to low DO conditions. Kowalchuk et al. (1998) found no correlation between differences in ammonia oxidizer community structure and oxygen availability in 5 different soil/sediments, and therefore suggested that physiological differences may outplay phylogenetic groupings. In another study by Arnaldos et al. (2013), enhanced expression of a particular heme protein and increased

specific oxygen uptake rates were observed in a nitrifying enrichment culture adapted to low DO conditions in comparison to a high DO enrichment that was operated near saturation. This suggests that microorganisms may ramp up oxygen delivery machinery such as heme proteins that transport oxygen, and key enzymes that use oxygen such as terminal oxidases and oxygenases, in response to oxygen limitation. In this study, it is unclear whether structural or physiological variation is the predominant explanation for the observed differences in specific activity between the low and high DO parent reactors as we were unable to capture sub genera-level diversity with the sequencing effort employed.

Beyond nitrifiers, our results indicated that different DO concentrations in the parent reactors resulted in distinct microbial communities and greater microbial biodiversity in the low DO parent reactor. An additional limiting substrate (in this case, oxygen) can result in greater diversity according to resource competition theory because competition drives diversification (Huston, 1994). Biodiversity is generally believed to positively associate with productivity (Cardinale et al., 2012), but the relationship between biodiversity and function in WWTPs is not well understood. One study of 10 full-scale wastewater treatment systems observed a significant positive association between biodiversity and the collective rate of multiple pharmaceutical biotransformations (Johnson et al., 2014). Conversely, another study of estrogen fate in lab-scale bioreactors found conflicting results with respect to the removal of endocrine disruptors; they observed that a decrease in diversity correlated with an increase in the removal of endocrine disruptors (estrone (E1), 17 $\beta$ -estradiol (E2) and 17 $\alpha$ -ethinylestradiol (EE2)) (Pholchan et al., 2013). This may be due to the choice of compounds in these studies; certain biotransformations might be functionally redundant (catalyzed by many species in the community), and therefore have no association with biodiversity. Conversely, other functions that are performed by few species in

the community would be more likely to have a positive association with biodiversity. Our results support the notion that increased biodiversity may have contributed to the greater collective biotransformation rates observed in the low DO than the high DO parent community, though additional studies are needed to directly test this relationship (investigated in Chapter 6).

#### **4.4 Summary and potential applications**

DO concentration can impact the rate of pharmaceutical biotransformation during wastewater treatment. The results of this study illustrate a nuanced relationship between DO concentration and pharmaceutical biotransformation rates, as DO impacts both microbial physiology and microbial community structure. Short term batch experiments showed that high DO conditions resulted in faster biotransformation rates for ibuprofen, sulfamethoxazole, EE2, and acetaminophen. Atenolol was the one exception for which faster biotransformation occurred in the low than the high DO batch experiments. Long-term low DO growth conditions also selected for a community that had faster net biotransformation rates, but lower specific activity with respect to ammonia oxidation. Long-term low DO growth conditions resulted in a greater biomass concentration, an enrichment of ammonia oxidizers, and increased microbial diversity compared to high DO growth conditions.

Knowledge of oxygen half saturation constants for pharmaceuticals (investigated in Chapter 5) will allow utilities to poise the DO concentration such that it does not drastically impact biotransformation rates, while still saving on aeration energy and taking advantage of other benefits of low DO treatment (e.g. reduced decay and increased microbial diversity). This work and other studies (Liu and Wang, 2013) suggest that despite lower specific rates, reduced decay in low DO conditions that results in an enrichment of ammonia oxidizers can result in comparable nitrification performance to a high DO system. Higher biomass concentrations that could result



from long term low DO conditions could entail greater sludge handling requirements in a full-scale treatment system. If the sludge could be used to generate biogas via anaerobic digestion, benefits from greater sludge production could be realized. An energy balance accounting for aeration energy savings and energy associated with sludge handling should be performed to determine net energy benefits (or losses) of implementing a low DO treatment process. This research also supports a positive association between microbial biodiversity and pharmaceutical biotransformation. DO concentration is one operational parameter that may influence microbial diversity in a treatment system, but there are likely many others, such as solids retention time, substrate quantity and quality, temperature, salinity, and physical configuration. Designing treatment systems that harbor diverse microbial communities may be one way to enhance pharmaceutical biotransformation during treatment. Cycling between low and high DO environments could be one strategy for both enhancing pharmaceutical biotransformation by supporting a diverse microbial community while also providing non oxygen-limiting conditions to enable maximum biotransformation rates.

#### 4.5 Literature cited

APHA; AWWA; WEF, Standard Methods for the Examination of Water and Wastewater. 21st Ed. Washington, D.C., **2005**.

Arnaldos, M.; Pagilla, K. R. Implementation of a Demand-Side Approach to Reduce Aeration Requirements of Activated Sludge Systems: Directed Acclimation of Biomass and Its Effect at the Process Level. *Water Res.* **2014**, *62*, 147–155.

Arnaldos, M.; Kunkel, S.; Stark, B.; Pagilla, K. Enhanced Heme Protein Expression by Ammonia-Oxidizing Communities Acclimated to Low Dissolved Oxygen Conditions. *Appl. Microbiol. Biotechnol.* **2013**, *97* (23), 10211–10221.

Arp, D.; Sayavedra-Soto, L.; Hommes, N. Molecular Biology and Biochemistry of Ammonia Oxidation by *Nitrosomonas europaea*. *Arch. Microbiol.* **2002**, *178* (4), 250–255.

Barbieri, M.; Carrera, J.; Sanchez-Vila, X.; Ayora, C.; Cama, J.; Köck-Schulmeyer, M.; López de Alda, M.; Barceló, D.; Tobella Brunet, J.; Hernández García, M. Microcosm Experiments to Control Anaerobic Redox Conditions When Studying the Fate of Organic Micropollutants in Aquifer Material. *J. Contam. Hydrol.* **2011**, *126* (3-4), 330–345.

Barbieri, M.; Licha, T.; Nödler, K.; Carrera, J.; Ayora, C.; Sanchez-Vila, X. Fate of  $\beta$ -Blockers in Aquifer Material under Nitrate Reducing Conditions: Batch Experiments. *Chemosphere* **2012a**, *89* (11), 1272–1277.

Barbieri, M.; Carrera, J.; Ayora, C.; Sanchez-Vila, X.; Licha, T.; Nödler, K.; Osorio, V.; Pérez, S.; Köck-Schulmeyer, M.; López de Alda, M.; et al. Formation of Diclofenac and Sulfamethoxazole Reversible Transformation Products in Aquifer Material under Denitrifying Conditions: Batch Experiments. *Sci. Total Environ.* **2012b**, *426*, 256–263.

Batt, A. L.; Kim, S.; Aga, D. S. Comparison of the Occurrence of Antibiotics in Four Full-Scale Wastewater Treatment Plants with Varying Designs and Operations. *Chemosphere* **2007**, *68* (3), 428–435.

Bédard, C.; Knowles, R. Physiology, Biochemistry, and Specific Inhibitors of CH<sub>4</sub>, NH<sub>4</sub><sup>+</sup>, and CO Oxidation by Methanotrophs and Nitrifiers. *Microbiol. Rev.* **1989**, *53* (1), 68–84.

Bellucci, M.; Ofițeru, I. D.; Graham, D. W.; Head, I. M.; Curtis, T. P. Low-Dissolved-Oxygen Nitrifying Systems Exploit Ammonia-Oxidizing Bacteria with Unusually High Yields. *Appl. Env. Microbiol.* **2011**, *77* (21), 7787–7796.

Caporaso, J. G.; Lauber, C. L.; Walters, W. A.; Berg-Lyons, D.; Lozupone, C. A.; Turnbaugh, P. J.; Fierer, N.; Knight, R. Global Patterns of 16S rRNA Diversity at a Depth of Millions of Sequences per Sample. *Proc. Natl. Acad. Sci.* **2011**, *108*, 4516–4522.

Cardinale, B. J.; Duffy, J. E.; Gonzalez, A.; Hooper, D. U.; Perrings, C.; Venail, P.; Narwani, A.; Mace, G. M.; Tilman, D.; Wardle, D. A. Biodiversity Loss and Its Impact on Humanity. *Nature* **2012**, *486* (7401), 59–67.

Carucci, A.; Cappai, G.; Piredda, M. Biodegradability and Toxicity of Pharmaceuticals in Biological Wastewater Treatment Plants. *J. Environ. Sci. Heal. Part A* **2006**, *41* (9), 1831–1842.

Cole, J. R.; Wang, Q.; Cardenas, E.; Fish, J.; Chai, B.; Farris, R. J.; Kulam-Syed-Mohideen, A. S.; McGarrell, D. M.; Marsh, T.; Garrity, G. M. The Ribosomal Database Project: Improved Alignments and New Tools for rRNA Analysis. *Nucleic Acids Res.* **2009**, *37* (suppl 1), D141–D145.

Daigger, G. T.; Littleton, H. X. Characterization of Simultaneous Nutrient Removal in Staged, Closed-Loop Bioreactors. *Water Environ. Res.* **2000**, *72* (3), 330–339.

Daims, H.; Lebedeva, E.V.; Pjevac, P.; Han, P.; Herbold, C.; Albertsen, M.; Jehmlich, N.; Palatinszky, M.; Vierheilig, J.; Bulaev, A.; Kirkegaard, R.H.; von Bergen, M.; Rattei, T.; Bendinger, B.; Nielsen, P.H.; Wagner, M. Complete nitrification by *Nitrospira* bacteria. *Nature* **2015**, *528*, 504–509.

Daims, H.; Nielsen, J.L.; Nielsen, P.H.; Schleifer, K.H.; Wagner, M. In situ characterization of *Nitrospira*-like nitrite-oxidizing bacteria active in wastewater treatment plants. *Appl. Environ. Microbiol.* **2001**, *67* (11), 5273–5284.

Elbing, K.; Larsson, C.; Bill, R. M.; Albers, E.; Snoep, J. L.; Boles, E.; Hohmann, S.; Gustafsson, L. Role of Hexose Transport in Control of Glycolytic Flux in *Saccharomyces cerevisiae*. *Appl. Environ. Microbiol.* **2004**, *70* (9), 5323–5330.

Fayad, P. B.; Prévost, M.; Sauv e, S. On-Line Solid-Phase Extraction Coupled to Liquid Chromatography Tandem Mass Spectrometry Optimized for the Analysis of Steroid Hormones in Urban Wastewaters. *Talanta* **2013**, *115*, 349–360.

Flores-Alsina, X.; Corominas, L.; Snip, L.; Vanrolleghem, P. A. Including Greenhouse Gas Emissions during Benchmarking of Wastewater Treatment Plant Control Strategies. *Water Res.* **2011**, *45* (16), 4700–4710.

Gaulke, L. S.; Strand, S. E.; Kalhorn, T. F.; Stensel, H. D. 17 $\alpha$ -Ethinylestradiol Transformation via Abiotic Nitration in the Presence of Ammonia Oxidizing Bacteria. *Environ. Sci. Technol.* **2008**, *42* (20), 7622–7627.

Gieseke, A.; Purkhold, U.; Wagner, M.; Amann, R.; Schramm, A. Community Structure and Activity Dynamics of Nitrifying Bacteria in a Phosphate-Removing Biofilm. *Appl. Env. Microbiol.* **2001**, *67* (3), 1351–1362.

Grady, C. P. L. Jr.; Daigger, G. T.; Love, N. G.; Filipe, C. D. M. Biological Wastewater Treatment,

3rd ed.; CRC Press, **2011**.

Gruber-Dorninger, C.; Pester, M.; Kitzinger, K.; Savio, D. F.; Loy, A.; Rattei, T.; Wagner, M.; Daims, H. Functionally Relevant Diversity of Closely Related *Nitrospira* in Activated Sludge. *ISME J.* **2015**, *9* (3), 643–655.

Gudelj, I.; Beardmore, R. E.; Arkin, S. S.; MacLean, R. C. Constraints on Microbial Metabolism Drive Evolutionary Diversification in Homogeneous Environments. *J. Evol. Biol.* **2007**, *20* (5), 1882–1889.

Habermacher, J.; Benetti, A. D.; Derlon, N.; Morgenroth, E. The Effect of Different Aeration Conditions in Activated Sludge–Side-Stream System on Sludge Production, Sludge Degradation Rates, Active Biomass and Extracellular Polymeric Substances. *Water Res.* **2015**, *85*, 46–56.

He, S.; McMahon, K. D. ‘*Candidatus Accumulibacter*’ Gene Expression in Response to Dynamic EBPR Conditions. *ISME J.* **2011**, *5* (2), 329–340.

Huston, M. A. *Biological Diversity: The Coexistence of Species*; Cambridge University Press, **1994**.

Hyman, M. R.; Page, C. L.; Arp, D. J. Oxidation of Methyl Fluoride and Dimethyl Ether by Ammonia Monooxygenase in *Nitrosomonas europaea*. *Appl. Env. Microbiol.* **1994**, *60* (8), 3033–3035.

Jimenez, J.; Dold, P.; La Motta, E.; Houweling, D.; Bratby, J.; Parker, D. Simultaneous Biological Nutrient Removal in a Single-Stage, Low Oxygen Aerobic Reactor. *Proc. Water Environ. Fed.* **2011**, 31–48.

Johnson, D. R.; Helbling, D. E.; Lee, T. K.; Park, J.; Fenner, K.; Kohler, H. P. E.; Ackermann, M. Association of Biodiversity with the Rates of Micropollutant Biotransformations among Full-Scale Wastewater Treatment Plant Communities. *Appl. Env. Microbiol.* **2015**, *81* (2), 666–675.

Joss, A.; Zabczynski, S.; Göbel, A.; Hoffmann, B.; Löffler, D.; McArdell, C. S.; Ternes, T. A.; Thomsen, A.; Siegrist, H. Biological Degradation of Pharmaceuticals in Municipal Wastewater Treatment: Proposing a Classification Scheme. *Water Res.* **2006**, *40* (8), 1686–1696.

Keener, W. K.; Arp, D. J. Transformations of Aromatic Compounds by *Nitrosomonas europaea*. *Appl. Env. Microbiol.* **1994**, *60* (6), 1914–1920.

Kern, S.; Baumgartner, R.; Helbling, D. E.; Hollender, J.; Singer, H.; Loos, M. J.; Schwarzenbach, R. P.; Fenner, K. A Tiered Procedure for Assessing the Formation of Biotransformation Products of Pharmaceuticals and Biocides during Activated Sludge Treatment. *J. Environ. Monit.* **2010**, *12* (11), 2100–2111.

Khunjar, W. O.; Mackintosh, S. A.; Skotnicka-Pitak, J.; Baik, S.; Aga, D. S.; Yi, T.; Jr., W. F. H.; Love, N. G. Elucidating the Relative Roles of Ammonia Oxidizing and Heterotrophic Bacteria

during the Biotransformation of 17 $\alpha$ -Ethinylestradiol and Trimethoprim. *Environ. Sci. Technol.* **2011**, *45* (8), 3605–3612.

Kowalchuk, G. A.; Bodelier, P. L. E.; Heilig, G. H. J.; Stephen, J. R.; Laanbroek, H. J. Community Analysis of Ammonia-Oxidising Bacteria, in Relation to Oxygen Availability in Soils and Root-Oxygenated Sediments, Using PCR, DGGE and Oligonucleotide Probe Hybridisation. *FEMS Microbiol. Ecol.* **1998**, *27* (4), 339–350.

Lawrence, A. W.; McCarty P. L. Unified Basis for Biological Treatment Design and Operation. *J. San. Eng. Div.* **1970**, *96* (3), 757-778.

Leu, S. Y.; Rosso, D.; Larson, L. E.; Stenstrom, M. K. Real-Time Aeration Efficiency Monitoring in the Activated Sludge Process and Methods to Reduce Energy Consumption and Operating Costs. *Water Environ. Res.* **2009**, *81* (12), 2471–2481.

Li, B.; Irvin, S.; Baker, K. The Variation of Nitrifying Bacterial Population Sizes in a Sequencing Batch Reactor (SBR) Treating Low, Mid, High Concentrated Synthetic Wastewater. *J. Environ. Eng. Sci.* **2007**, *6* (6), 651–663.

Liu, G.; Wang, J. Long-Term Low DO Enriches and Shifts Nitrifier Community in Activated Sludge. *Environ. Sci. Technol.* **2013**, *47* (10), 5109–5117.

Madoni, P. A Sludge Biotic Index (SBI) for the Evaluation of the Biological Performance of Activated Sludge Plants Based on the Microfauna Analysis. *Water Res.* **1994**, *28* (1), 67-75.

Nödler, K.; Licha, T.; Barbieri, M.; Pérez, S. Evidence for the Microbially Mediated Abiotic Formation of Reversible and Non-Reversible Sulfamethoxazole Transformation Products during Denitrification. *Water Res.* **2012**, *46* (7), 2131–2139.

Park, H. D.; Noguera, D. R. Evaluating the Effect of Dissolved Oxygen on Ammonia-Oxidizing Bacterial Communities in Activated Sludge. *Water Res.* **2004**, *38* (14–15), 3275–3286.

Park, N.; Vanderford, B. J.; Snyder, S. A.; Sarp, S.; Kim, S. D.; Cho, J. Effective Controls of Micropollutants Included in Wastewater Effluent Using Constructed Wetlands under Anoxic Condition. *Ecol. Eng.* **2009**, *35* (3), 418–423.

Pholchan, M. K.; Baptista, J. de C.; Davenport, R. J.; Sloan, W. T.; Curtis, T. P. Microbial Community Assembly, Theory and Rare Functions. *Front. Microbiol.* **2013**, *4* (68), 1-9.

Rieger, L.; Jones, R. M.; Dold, P. L.; Bott, C. B. Ammonia-Based Feedforward and Feedback Aeration Control in Activated Sludge Processes. *Water Environ. Res.* **2014**, *86* (1), 63–73.

Roh, H.; Subramanya, N.; Zhao, F.; Yu, C. P.; Sandt, J.; Chu, K. H. Biodegradation Potential of Wastewater Micropollutants by Ammonia-Oxidizing Bacteria. *Chemosphere* **2009**, *77* (8), 1084–1089.

- Rosso, D.; Stenstrom, M. K.; Larson, L. E. Aeration of Large-Scale Municipal Wastewater Treatment Plants: State of the Art. *Water Sci. Technol.* **2008**, *57* (7), 973–978.
- Rothauwe, J. H.; Witzel, K. P.; Liesack, W. The Ammonia Monooxygenase Structural Gene amoA as a Functional Marker: Molecular Fine-Scale Analysis of Natural Ammonia-Oxidizing Populations. *Appl. Env. Microbiol.* **1997**, *63* (12), 4704–4712.
- Schloss, P. D.; Westcott, S. L.; Ryabin, T.; Hall, J. R.; Hartmann, M.; Hollister, E. B.; Lesniewski, R. A.; Oakley, B. B.; Parks, D. H.; Robinson, C. J.; et al. Introducing Mothur: Open-Source, Platform-Independent, Community-Supported Software for Describing and Comparing Microbial Communities. *Appl. Env. Microbiol.* **2009**, *75* (23), 7537–7541.
- Schramm, A.; de Beer, D.; Wagner, M.; Amann, R. Identification and activities in situ of *Nitrosospira* and *Nitrospira* spp. as dominant populations in a nitrifying fluidized bed reactor. *Appl. Environ. Microbiol.* **1998**, *64* (9), 3480–3485.
- Schuyler, R. G.; Tamburini, J. R.; Hogg, S.; Staggs, R. How Low Is Too Low: Several Years of Low Dissolved Oxygen Operations Improve Effluent Quality. *Water Env. Technol.* **2009**, *21*, 32–39.
- Shi, J.; Fujisawa, S.; Nakai, S.; Hosomi, M. Biodegradation of Natural and Synthetic Estrogens by Nitrifying Activated Sludge and Ammonia-Oxidizing Bacterium *Nitrosomonas europaea*. *Water Res.* **2004**, *38* (9), 2323–2330.
- Sonthiphand, P.; Cejudo, E.; Schiff, S. L.; Neufeld, J. D. Wastewater Effluent Impacts Ammonia-Oxidizing Prokaryotes of the Grand River, Canada. *Appl. Environ. Microbiol.* **2013**, *79* (23), 7454–7465.
- Stadler, L. B.; Su, L.; Moline, C. J.; Ernstoff, A. S.; Aga, D. S.; Love, N. G. Effect of Redox Conditions on Pharmaceutical Loss during Biological Wastewater Treatment Using Sequencing Batch Reactors. *J. Hazard. Mater.* **2015**, *282* (23), 106–115.
- Sun, Q.; Li, Y.; Chou, P. H.; Peng, P. Y.; Yu, C. P. Transformation of Bisphenol A and Alkylphenols by Ammonia-Oxidizing Bacteria through Nitration. *Environ. Sci. Technol.* **2012**, *46* (8), 4442–4448.
- Tran, N. H.; Urase, T.; Kusakabe, O. The Characteristics of Enriched Nitrifier Culture in the Degradation of Selected Pharmaceutically Active Compounds. *J. Hazard. Mater.* **2009**, *171* (1–3), 1051–1057.
- Uprety, K.; Balzer, W.; Baurler, R.; Duke, R.; Bott, C. Implementing Ammonia-Based Aeration Control at Biological Nutrient Removing Wastewater Treatment Plants. *Proc. Water Environ. Fed.* **2015**.

van Kessel, M.A.H.J.; Speth, D.R.; Albertsen, M.; Nielsen, P.H.; Op den Camp, H.J.M.; Kartal, B.; Jetten, M.S.M.; Lücker, S. Complete nitrification by a single microorganism. *Nature* **2015**.

WEF. Activated Sludge. In *Operation of Municipal Wastewater Treatment Plants: MoP No. 11, Sixth Edition*; McGraw Hill Professional, Access Engineering: Water Environment Federation, **2008**.

Wirtz, K. W. A Generic Model for Changes in Microbial Kinetic Coefficients. *J. Biotechnol.* **2002**, *97* (2), 147–162.

Yi, T.; Harper, W. F. The Link between Nitrification and Biotransformation of 17 $\alpha$ -Ethinylestradiol. *Environ. Sci. Technol.* **2007**, *41* (12), 4311–4316.

Yu, J. T.; Bouwer, E. J.; Coelhan, M. Occurrence and Biodegradability Studies of Selected Pharmaceuticals and Personal Care Products in Sewage Effluent. *Agric. Water Manag.* **2006**, *86* (1), 72–80.

## **Chapter 5.**

### **Impact of dissolved oxygen on pharmaceutical biotransformation rates and microbial activity in wastewater treatment**

Lauren B. Stadler<sup>1</sup> and Nancy G. Love<sup>1</sup>

<sup>1</sup>Department of Civil and Environmental Engineering, University of Michigan

#### **5.1 Introduction**

Emerging aeration control strategies enabled by innovations in robust, low-cost sensors and real-time feedback control have resulted in substantial reductions in operational bulk liquid dissolved oxygen (DO) concentrations from above 2 mg/L to around 0.5 mg/L. For example, ammonia-based aeration control has resulted in reductions in aeration basin DO concentrations, electricity savings, and methanol savings by supporting simultaneous nitrification-denitrification activity (Uprety et al., 2015). As we move toward low DO treatment processes, there is a need for a better understanding of how low DO environments affect the function and structure of wastewater communities and the fate of micropollutants such as pharmaceuticals. Slowly biodegradable pharmaceutical biotransformation rates can be over three orders of magnitude slower than the rates of conventional pollutant transformations such as ammonia and organic carbon (Joss et al., 2006). Thus, if DO concentration impacts the physiology of the microorganisms involved in biotransformation, it could result in substantial reductions in the removal efficiencies of pharmaceuticals across treatment plants.



In order to predict the fate of pharmaceuticals during wastewater treatment and gain a more resolved understanding of the impact of DO concentration on their biotransformation, we need to establish a database of kinetic parameters such as first order or pseudo first order biotransformation rate constants and oxygen half-saturation constants. Considerable research has been conducted on the former (e.g. Abegglen et al., 2009; Joss et al., 2006; Urase and Kikuta, 2005); classification schemes and modeling efforts have been developed to categorize pharmaceuticals based on their relative biodegradability (Joss et al., 2006) and predict the biodegradability of a compound based on its chemical structure (Khan and Ongerth, 2004). No studies to our knowledge have experimentally determined oxygen half-saturation constants to describe the biotransformation of pharmaceuticals in full-scale wastewater treatment plants.  $K_{O_2}$  values for heterotrophs and nitrifiers, which are commonly used in wastewater treatment plant modeling, are in the range of 0.010 – 0.20 for heterotrophs and 0.74 – 1.8 for ammonia and nitrite oxidizers (Grady et al., 2011). For most pharmaceuticals, there is insufficient knowledge about which microorganisms are responsible for catalyzing their biotransformation. Thus, while the  $K_{O_2}$  values for heterotrophs and nitrifiers might be effective at capturing the impact of oxygen limitation on biotransformation rates, they could also be grossly inaccurate if biotransformation is catalyzed by microorganisms that are particularly sensitive to oxygen limitation or if high DO concentrations inhibit biotransformation rates.

In addition to estimating kinetic parameters that capture community-wide impacts of DO on process rates, we can sequence the 16S rRNA gene and 16S rRNA to characterize the impact of DO on microbial community structure and the activity of individual taxonomic groups. Linking microbial community structure and activity to community function is an active area of research in engineered and natural systems (Harter et al., 2014; Vanwonterghem et al., 2014; Zhi et al., 2014).

For specific processes, such as ammonia oxidation, associations between process rates and the abundance of taxa that perform ammonia oxidation have been observed (Wells et al., 2009). Researchers have proposed frameworks for establishing predictive relationships between microbial activity and biotransformation rates (Helbling et al., 2015), but more research is needed to identify taxonomic groups associated with pharmaceutical biotransformation and validate predictive models.

The objective of this study was to characterize the impact of DO concentration on pharmaceutical biotransformation rates via two approaches: 1) determine oxygen half-saturation constants that can be used to describe the community-wide impact of DO on biotransformation rates; and 2) evaluate shifts in the relative activity of the microbial community due to DO concentration and test for associations between biotransformation rates and the relative activity of specific phylogenetic groups. We performed multiple batch experiments at different DO concentrations using biomass from a full-scale wastewater treatment plant and measured pharmaceutical biotransformation rates. In addition, we characterized the relative activity of the microbial community by performing 16S rRNA sequencing and tested for significant associations between biotransformation rates and the relative activity of phylogenetic groups. The results of this work advance our ability to predict and model the impact of DO concentration on pharmaceutical biotransformation during wastewater treatment and identify taxonomic groups associated with biotransformation.

## **5.2 Materials and methods**

### ***5.2.1 Batch experimental setup***

Six sets of batch experiments were performed at different DO concentrations. Each batch experiment was six hours long and all of the experiments were performed over a period of 19 days

in July and August of 2015. For each experiment, mixed liquor was collected from the end of the aeration basin of the Ann Arbor, MI wastewater treatment plant, which operates a sequential anaerobic/aerobic process that maintains an average DO concentration of 2-3 mg/L during the aerobic phase. The mixed liquor was brought back to the lab where it was immediately centrifuged at 6,200 x g for 5 minutes, the supernatant was discarded, and the biomass was resuspended in effluent. The effluent used in the experiments was final effluent collected before disinfection from a biological nutrient removal facility in Southeastern Virginia. This effluent was chosen because of its low total nitrogen (TN; < 3 mg-N/L) as we intentionally wanted to capture biodegradation rates under low substrate conditions in the batch experiments. The effluent was shipped to Ann Arbor, Michigan overnight, filtered through 0.45 µm filter, aliquoted, and frozen at -20°C until use. An individual aliquot was defrosted for each batch experiment. The defrosted effluent was supplemented with  $\text{KH}_2\text{PO}_4$  and  $\text{K}_2\text{HPO}_4$  to achieve a final concentration of 15 mM phosphate buffer and pH of 7.5.

Batch experiments were performed at target bulk liquid DO concentrations of 6.0, 2.0, 0.5, 0.25, 0.15, and 0.05 mg/L. The DO concentration was controlled by adjusting the airflow rates of air and nitrogen gas being supplied to a manifold that split the flow into the 8 flasks. Two optical DO probes were placed in the flasks and used to monitor the DO concentration during each batch experiment and for making adjustments to the gas flow rates throughout the experiment. Each batch experiment consisted of 8 flasks: 3 replicates with no inhibitors, 3 replicates with 10 mg/L of allylthiourea (ATU) to inhibit ammonia oxidation; and 2 replicates with 0.4% w/v of sodium azide to serve as abiotic controls. ATU was chosen as because it is selective inhibitor of ammonia oxidation that acts by binding to the copper center of ammonia monooxygenase (Bédard and Knowles, 1989). Inhibition of ammonia oxidation was confirmed by measuring the concentrations

of ammonia-N, nitrite-N, and nitrate-N across the batch experiments (Figures C1 and C2, Appendix C). Respirometry was used to determine the minimum concentration of sodium azide needed such that additional sodium azide did not further reduce the specific oxygen uptake rate (detailed in Appendix C). The 0.25 mg-DO/L batch experiment had a different allocation with respect to the 8 flasks: 2 replicates with no inhibitors; 2 replicates with allylthiourea; 2 replicates with sodium azide; and 2 replicates with no biomass (effluent-only controls). The effluent-only controls were only performed once to ensure that no non-biomass associated biotransformation of the pharmaceuticals occurred.

Pharmaceuticals selected for investigation in this study included: acetaminophen, atenolol, 17 $\alpha$ -ethinylestradiol (EE2), sulfamethoxazole, trimethoprim, venlafaxine, ibuprofen, and naproxen. Chemical information about each compound including chemical formula and accurate mass is provided in Table C1 in Appendix C. Compounds were purchased from Sigma Aldrich (Saint Louis, Missouri) and Fischer Scientific (Waltham, Massachusetts). Stock solutions of each individual compound were prepared in methanol and frozen at -20°C until use. A 10 mg/L mixture of all compounds in methanol was prepared and before each batch experiment 150  $\mu$ L of the mixture was added to 250 mL glass flasks and allowed to evaporate until dry. After evaporation, 100 mL of buffered effluent was added to each flask and placed on a stir plate for 1 hour to re-dissolve the dried compounds. The batch experiments were initiated by adding 50 mL of concentrated and washed biomass to each of the flasks, which yielded a target initial concentration of each pharmaceutical of 10  $\mu$ g/L.

### ***5.2.2 Sampling***

Five samples were collected from each flask across the experiment at time points 0, 0.5, 1.5, 3, and 6 hours, with t=0 corresponding to 5 minutes after the biomass was added to the flasks

to ensure it was completely mixed. To sample, 10 mL was collected from each well-mixed flask, spiked with 100  $\mu\text{L}$  of a 500  $\mu\text{g/L}$  stock solution that consisted of a mixture of deuterated analogs of each of the compounds (compounds purchased individually from Toronto Research Chemicals, Toronto, Ontario, Canada) dissolved in water. The samples were then centrifuged at  $4^\circ\text{C}$  for 5 minutes at  $6,200 \times g$ , the supernatants were filtered through 0.3  $\mu\text{m}$  glass fiber filters (Sterlitech Inc., Kent, Washington), and samples were stored at  $4^\circ\text{C}$  until analysis (within 24 hours). Pharmaceutical concentrations were determined in all samples and ammonia-N, nitrite-N, and nitrate-N concentrations were determined according to Standard Methods (methods 4500F-NH<sub>3</sub>, 4500B-NO<sub>2</sub><sup>-</sup>, and 4110; (2005)) in the initial and final samples for each flask. Total and volatile suspended solids (TSS/VSS) concentration was determined for each flask at the end of the experiment (Standard Methods (2005), method 2540). As the batch experiments were only 6 hours and there was no substrate provided aside from what was present in the effluent, it was assumed that no significant growth occurred across the experiment. Pharmaceuticals were quantified in each sample via online solid phase extraction followed by high performance liquid chromatography (HPLC) and high resolution mass spectrometry (HRMS) as detailed in Appendix C.

### ***5.2.3 Pharmaceutical biotransformation rates and determination of oxygen half-saturation constants for pharmaceuticals***

Biotransformation rates were determined by performing a linear fit of the non-substrate limited (zero-order kinetic) portion of the concentration versus time data for each compound in each batch experiment. Biotransformation rates were normalized to the volatile suspended solids (VSS) concentration, which was determined at the end of each batch experiment for each flask. Pharmaceutical quantification data from the batch experiments is provided in Appendix C. Mann-

Whitney  $U$  tests were used to perform pairwise comparisons of the non-inhibited and ATU-inhibited biotransformation rates.

To represent the effect of DO on pharmaceutical biotransformation rates, a Monod-type kinetic equation (equation 1) or Andrews-type equation (equation 2) was used to fit the normalized biotransformation rate data. Kinetic parameters  $q_{max}$  (maximum substrate oxidation rate, ng/mg/hr),  $K_{O_2}$  (oxygen half-saturation constant, mg-DO/L) and  $K_{i,O_2}$  (oxygen inhibition constant, mg-DO/L) were estimated based on the best-fit nonlinear least-squares regression to the experimental data using R (R Core Team, 2012). Measured variables were  $q$  (substrate oxidation rate normalized to biomass VSS concentration, ng/mg/hr) and  $S_{O_2}$  (DO concentration, mg-DO/L).

$$q = \frac{q_{max}S_{O_2}}{K_{O_2}+S_{O_2}} \quad (1)$$

$$q = q_{max} \frac{S_{O_2}}{K_{O_2}+S_{O_2}+\frac{S_{O_2}^2}{K_{i,O_2}}} \quad (2)$$

#### ***5.2.4 Respirometry to determine oxygen half-saturation constants for heterotrophs and nitrifiers***

The oxygen half-saturation constant ( $K_{O_2}$ ) for both nitrifying (lumped AOB and NOB) and heterotrophic populations in Ann Arbor wastewater treatment plant biomass was determined by respirometry. Mixed liquor (ML) collected from the treatment plant for each batch experiment was initially aerated and stirred for at least five minutes to remove extant substrates. The pre-aeration time was determined by measuring the endogenous oxygen uptake rate of the biomass to ensure all extant substrates were completely oxidized (data not shown). A 22-mL aliquot was transferred into a glass vial, placed on a magnetic stir plate, and a real-time DO probe was inserted into the vial with a rubber stopper to seal the vial and eliminate gaseous headspace. This assembly was allowed to stand for 30 seconds to capture the endogenous oxygen uptake rate, before substrate (ammonium chloride for nitrifiers, sodium acetate for heterotrophs) was introduced to the vial via

a syringe such that it was in excess (approximately ten times the calculated stoichiometric amount that would be consumed given the oxygen concentration in the vial). DO concentration was logged every five seconds until it was completely consumed. Trials were run in triplicate and mixed liquor was re-aerated and stirred for three minutes prior to each subsequent trial to ensure oxygen saturation when the trial was initiated.

Data were fitted to an integrated form of the Monod equation for substrate utilization rate (1), using weighted nonlinear least-squares analysis (Smith et al., 1998). To obtain good estimates for  $K_{O_2}$ , we fit the model to the low DO data range where the DO concentration curve transitions from the maximum utilization rate to a slower rate associated with DO-limited growth. We used true growth yield values of 0.24 g biomass COD/g N and 0.67 g biomass COD/g acetate as COD for nitrifiers and heterotrophs, respectively (Grady et al., 2011).

### ***5.2.5 Molecular methods***

Biomass samples were collected for microbial community analysis at the 3-hour time point of the pharmaceutical batch experiments. The pellets resulting from centrifugation were transferred immediately to a -80°C freezer and flash frozen to preserve RNA integrity. RNA extractions and sequencing were only performed on the non-inhibited and allylthiourea-inhibited biomass samples. RNA was extracted with three bead-beating steps and automated extraction using Maxwell simplyRNA tissue kits, according to the manufacturer's instructions (Promega, Madison, Wisconsin) except 10 µL of DNase 1 (increased from 5 µL) was used to remove contaminating DNA. An additional DNase treatment was performed on the RNA extracts using the DNA-free™ DNA Removal Kit (Ambion, Grand Island, New York) according to the manufacturer's "rigorous" procedure. Total RNA concentrations were quantified with the Invitrogen Qubit fluorometer. Quantitative polymerase chain reaction of the 16S rRNA gene (as

described in Chapter 3) was used to confirm that the DNase treatment removed contaminating DNA from the RNA extracts. Reverse transcription to generate single-stranded complementary DNA (cDNA) from RNA extracts was performed using the SuperScript VILO cDNA Synthesis Kit according to manufacturer's instructions (Life Technologies, Grand Island, NY).

Amplicon sequencing of the cDNA extracts was performed at the Host Microbiome Initiative (University of Michigan, Ann Arbor, Michigan) on the Illumina MiSeq platform as described in Chapter 3. Briefly, universal primers F515 and R806 targeting the V4 region of the 16S rRNA gene (Caporaso et al., 2011) as modified by Kozich et al. (2013). Samples were amplified using the Accuprime TAQ (Invitrogen) and amplicons were pooled equally by mass using the SequelPrepNormalization Plate Kit (Life Technologies), multiplexed, and sequencing with the Reagent kit V2. Sequences were processed with Mothur (Schloss et al., 2009) and classified using version 14 of the 16S rRNA gene taxonomy from the Ribosomal Database Project (Cole et al., 2009). Sequencing of 68 samples resulted in 1,178,203 paired-end reads after quality filtering. Sequences were sub-sampled to a depth of 12,294 sequences per sample for subsequent analyses. Operational taxonomic units (OTUs) were defined based on 97% sequence similarity. Yue and Clayton ( $\theta_{yc}$ ) (community structure based) and Jaccard (membership based) indices were calculated as  $\beta$ -diversity metrics.

#### ***5.2.6 Associations between OTU transcript abundances, DO concentration, and pharmaceutical biotransformation rates***

Sequencing of the cDNA samples was used to determine significant associations between OTU abundances, DO concentration, and individual pharmaceutical biotransformation rates. Mothur's `otu.association` command was used with metadata files containing DO concentration and individual pharmaceutical rate data to identify OTUs whose activity (16S rRNA abundance) was



significantly associated with each set of metadata. The Spearman's rank correlation method was selected for the `otu.association` command as it is a non-parametric measure of statistical dependence of two variables. The command generates a Spearman rank correlation coefficient and *p*-value for each individual OTU and the specified metadata.

## 5.3 Results

### 5.3.1 *Pharmaceutical transformation results*

All of the compounds biotransformed to differing extents in the 6-hour batch experiments. A range of biotransformation rates were observed for the compounds studied, with ibuprofen and acetaminophen transformed most rapidly and sulfamethoxazole and trimethoprim most slowly. No loss of any of the compounds was observed in the no-biomass abiotic controls included in the 0.25 mg-DO/L batch experiment (data in Appendix C). Specific biotransformation rates were determined by fitting the linear portion of the concentration versus time data and then normalizing the slope to the VSS concentration of the flask. Figure 5-1 shows the normalized rate for each of the compounds from the 0.5 mg-DO/L batch experiment, which were at or close to the estimated maximum biotransformation rates ( $q_{\max}$ ) for all of the compounds (Figure 5-2). The relative biodegradability of these compounds is consistent with previous studies of these compounds in wastewater systems (Joss et al., 2006).

ATU-inhibited batch experimental results showed no significant difference between ammonia oxidizer-inhibited pharmaceutical biotransformation rates and non-inhibited rates (Mann Whitney *U*,  $p > 0.05$ ). Unlike many previous studies that used ATU to understand the contribution of nitrifiers to pharmaceutical biotransformation (e.g. Batt et al., 2006; Tran et al., 2009), we did not observe a significant contribution by nitrifiers to the biotransformation of the compounds we studied. Notably, the batch experiments we performed were under “starved” conditions as we

initiated the experiments with treated effluent from a treatment plant with low effluent TN (2.98 mg-N/L), and thus only limited ammonia-N was available from the effluent (0.36 mg-NH<sub>3</sub>-N/L) and decay products generated during the batch experiment. Thus, it is possible that if the experiments had been performed under high ammonia-N substrate conditions, we might have observed a greater impact of ATU on pharmaceutical biotransformation rates. There is considerable evidence that AOBs can biotransform pharmaceuticals under ammonium starvation conditions (Forrez et al., 2009; Khunjar et al., 2011; Dawas-Massalha et al., 2014). Previous studies have also found that competitive inhibition can occur such that high concentrations of ammonium repress co-metabolic biotransformations of pharmaceuticals by AOB (Fernandez-Fontaina et al., 2012). However, even under starvation conditions, we did not observe that ammonia oxidizer activity significantly contributed to pharmaceutical biotransformation.

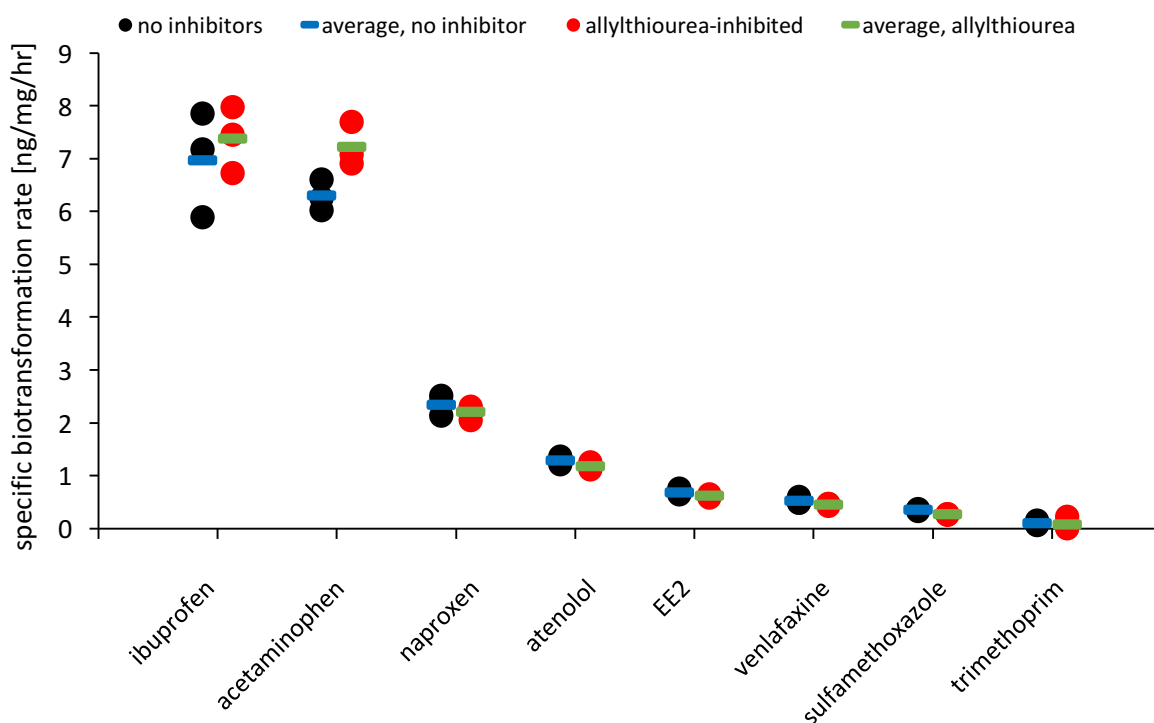


**Figure 5-1.** Specific biotransformation rates observed for each compound in the 0.5 mg-DO/L batch experiment.

### ***5.3.2 Oxygen half-saturation constants for pharmaceutical biotransformations***

The biotransformation rates of all of the compounds investigated were impacted by DO concentration (Figure 5-2). Estimates for  $K_{O_2}$  are provided in Table C3 in Appendix C. All of the compounds except naproxen were better fit with an Andrews-type equation. This suggests that either high concentrations of DO were inhibitory to biotransformation, or that they caused a physiological shift in the enzyme pool of the microbial community that can be described mathematically by an Andrews-type equation. Biotransformation rates decreased relatively sharply for all of the compounds at DO concentrations below about 0.5 mg/L (dotted lines in Figure 5-2), which is consistent with the  $K_{O_2}$  estimates obtained. These results demonstrate that aerobic biotransformation processes were limited by oxygen availability, thereby reducing pharmaceutical biotransformation rates.

In this study we attempted to minimize the contributions of anoxic metabolisms by using an effluent with low TN and low nitrate-N concentrations (2.98 mg-N/L TN and 1.6 mg-N/L as nitrate) as media in the batch experiments. Biotransformation rates due to anoxic metabolisms were not the focus of this study, and the impact of DO concentration on biotransformation rates presented here may be conservative as contributions due to anoxic metabolisms at low DO concentrations were likely nitrate-limited. Interestingly, for 6 of the 8 compounds studied, their maximum biotransformation rate was observed at a DO concentration less than 1 mg/L. Therefore, environments that enable both aerobic and anoxic metabolisms may enhance overall pharmaceutical biotransformation rates. However, several studies have demonstrated slower biotransformation rates of trace contaminants in anoxic versus aerobic environments (Dytczak et al., 2008; Suarez et al., 2010). Thus, while anoxic metabolisms may contribute to

biotransformation, they are likely to be considerably slower than aerobic biotransformation processes.

The oxygen half-saturation constants of  $0.09 \pm 0.3$  for heterotrophs and  $0.38 \pm .09$  for nitrifiers were very similar to previously published values (Grady et al., 2011). Estimated oxygen half-saturation constants ranged between 0.03 and 0.61 across all of the compounds studied (Figure 5-3). Despite variation between  $K_{O_2}$  values of the compounds, the values were almost all lower than the oxygen half-saturation constant for nitrifiers. Ibuprofen was the only compound for which we observed a greater average  $K_{O_2}$  than the nitrifier  $K_{O_2}$ , but the large error associated with the regression suggests it is not significantly different from the  $K_{O_2}$  for nitrifiers. Ibuprofen was also the most rapidly transformed compound (Figure 5-1), so the sensitivity to DO concentration may have little effect on the overall removal of ibuprofen during treatment. These results show that  $K_{O_2}$  values can be used to predict the impact of DO concentration on biotransformation rate and the  $K_{O_2}$  values for the compounds we studied were all within the range of those  $K_{O_2}$  values that we already use to model the impact of DO on heterotrophs and nitrifiers.

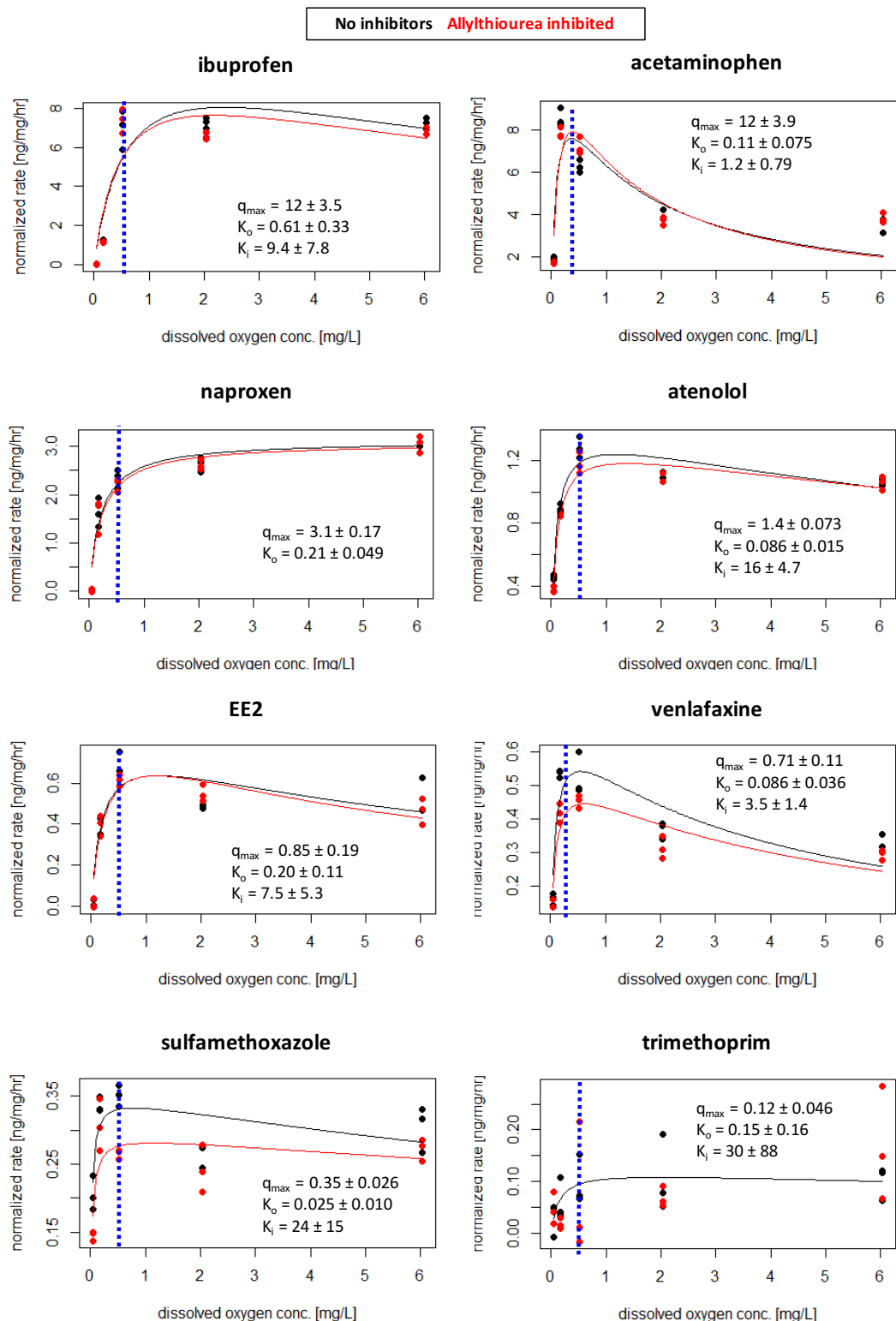


**Figure 5-2.** Pharmaceutical biotransformation rates plotted as a function of DO concentration for each compound. Black and red circles represent non-inhibited and allylthiourea-inhibited values, respectively. Lines represent Andrews and Monod model fitted curves. ATU-inhibited trimethoprim data could not be fitted with either model.

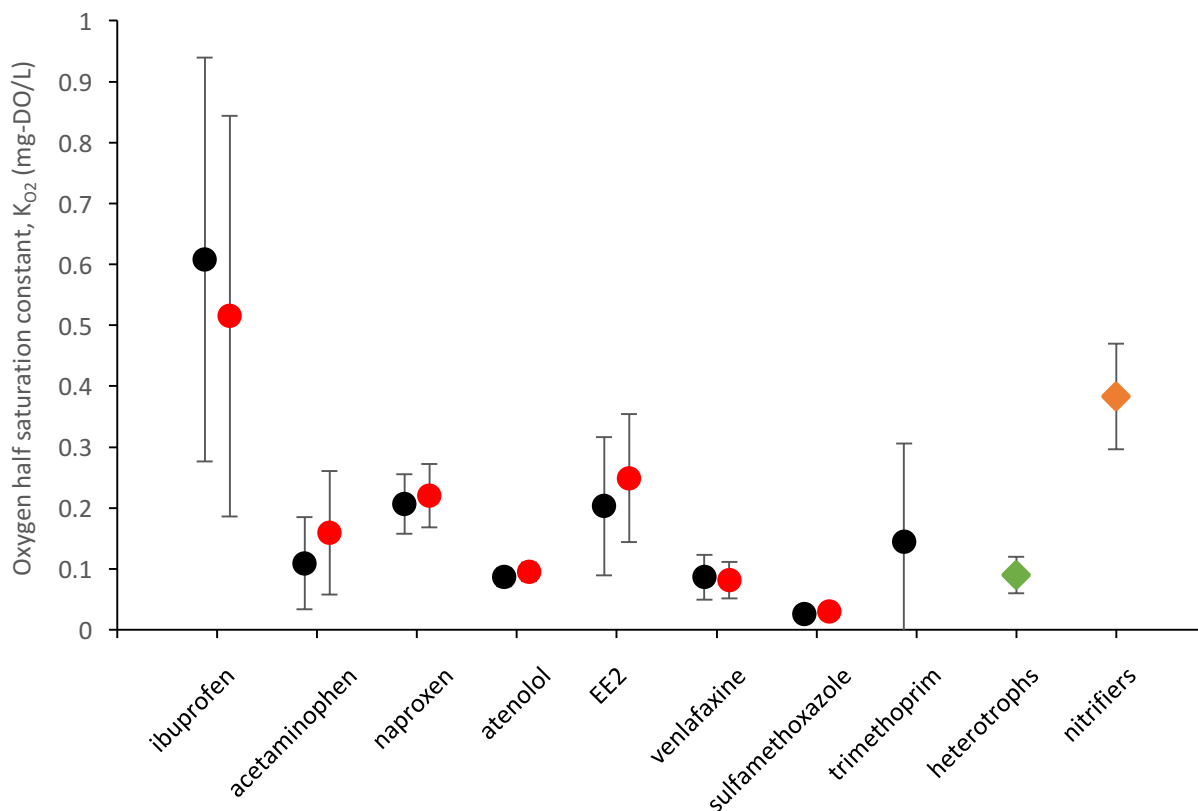


**Figure 5-3.** Oxygen half-saturation constants ( $K_{O_2}$ ) for each pharmaceutical compound and heterotrophs and nitrifiers. Black and red circles represent non-inhibited and allylthiourea-inhibited values, respectively. Trimethoprim rate data for the allylthiourea-inhibited batches could not be fitted with either model. Green and orange diamonds represent heterotroph and nitrifier values, respectively. Error bars represent the standard error of the regression.

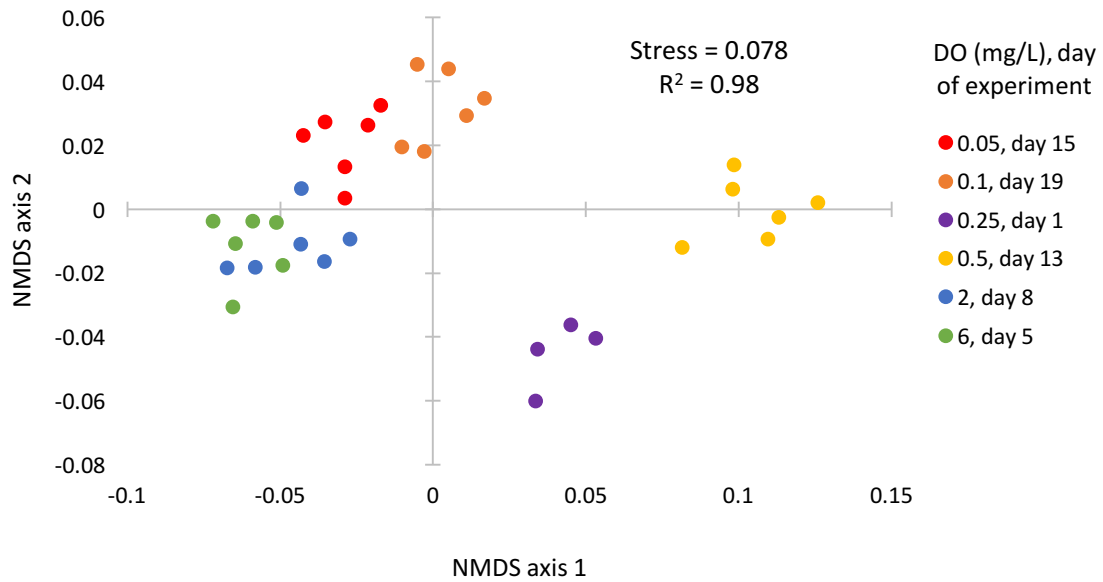
### 5.3.3 Microbial community characteristics

Sequencing of the 16S rRNA was performed to understand how DO concentration shaped the active microbial community during the batch experiments. The wastewater microbial communities from the batch experiments were quite diverse and contained 4,032 OTUs, grouped at 97% similarity, and 497 phylotypes, grouped taxonomically at the genus level. We first tested whether the “active” microbial communities (based on 16S rRNA) from each of the batch experiments were significantly from each other using analysis of molecular variance (AMOVA).

We observed significantly more variation among samples from different batch experiments than within samples from each batch experiment ( $\theta_{yc}$  AMOVA,  $p < 0.001$ ). Pairwise comparisons between each group of samples also showed significantly different active microbial communities ( $\theta_{yc}$  AMOVA,  $p < 0.01$ ). We visualized the differences in community structure using non-metric multidimensional scaling (NMDS) of the  $\theta_{yc}$  index (Figure 5-4). The results confirmed that microbial communities clustered based on batch experiments. Variability in the active microbial communities across each batch experiment is likely due to both differences in batch DO concentration and when the experiment was conducted. These experiments were performed over 19 days and variability in the full-scale WWTP microbial community contributed to the variability in the active microbial communities across the batch experiments. The order and date that each experiment was performed is provided in the legend of Figure 5-4A.

While the microbial communities from the batch experiments were significantly different from one another, they did not obviously cluster based on DO concentration. DO concentration and pharmaceutical biotransformation rates that significantly associated (Spearman,  $p < 0.05$ ) with either of the two NMDS axes are shown in Figure 5-4B as arrows. The 0.5 and 0.25 mg-DO/L batch experiments clustered separately from the rest of the batch experiments, and in the direction that also corresponded to increased biotransformation rates of several of the pharmaceuticals (venlafaxine, acetaminophen, sulfamethoxazole, and atenolol). The NMDS plot also shows that the 2 and 6 mg-DO/L microbial communities are shifted in the direction of increased DO concentration and biotransformation of trimethoprim and naproxen, the only two compounds whose maximum biotransformation rates occurred at DO concentrations greater than 1 mg/L.

(A)



(B)

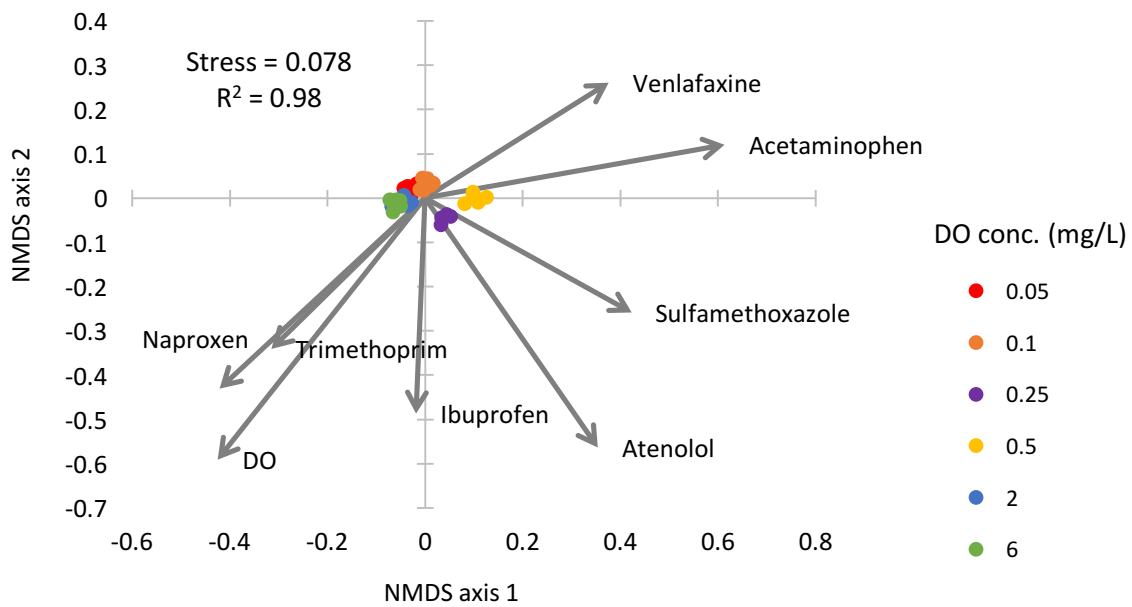


**Figure 5-4.** Non-metric multidimensional scaling biplot showing the active microbial community structures ( $\theta_{yc}$ ) from each of the batch experiments, shown in different colors (A). DO concentration and individual pharmaceutical biotransformation rates that significantly correlated with either of the two axis are shown as arrows (B).



#### 5.3.4 Associations between active OTUs and biotransformation rates

Significant associations between relative activity of individual OTUs and biotransformation rates were observed for each pharmaceutical (Spearman,  $p < 0.01$ ). Classifying sequences based on phylotype (taxonomically based on genera) resulted in significant associations ( $p < 0.01$ ) between phylotypes and biotransformation rates for all compounds except sulfamethoxazole. There was considerable variety across the different compounds with respect to the number and genera of phylotypes with significant positive associations (Table C5, Appendix C). Among the significant and positively associated phylotypes, no individual phylotype's activity was significantly associated with all of the compounds' biotransformation rates. The vast majority (47 of 52) of the significantly associated phylotypes had relative activities of less than 3% (Figure 5-5), indicating that low abundance community members may be major contributors to pharmaceutical biotransformation.

We also tested for associations between phylotypes and DO concentration and found 26 phylotypes that had significant associations with DO concentration (Spearman,  $p < 0.01$ ), 9 of which were positively associated and 17 that were negatively associated. These phylotypes made up between 12 and 16% of the relative activities of their microbial community. As expected, the positively associated phylotypes included genera that were obligate aerobes such as *Bdellovibrio* (Simpson and Robinson, 1968; Varon and Shilo, 1980) and other aerobic organisms such as *Hydrogenophaga* (Willems et al., 1989), while the negatively associated genera included facultative anaerobic organisms such as *Aeromonas* (Seshadri et al., 2006), microaerobic organisms such as *Arcobacter* (Houf et al., 2001), and the denitrifying genera *Paracoccus* (Carlson and Ingraham, 1983). These results demonstrate that significant associations reflect expected shifts in the activity of known genera based on their metabolic lifestyle. In addition, the

compound that had the most number of shared significant associated phylotypes with DO was naproxen (19 shared phylotypes), which was the only compound with biotransformation rates as a function of DO that were best-fit with a Monod-type equation without an inhibition term.

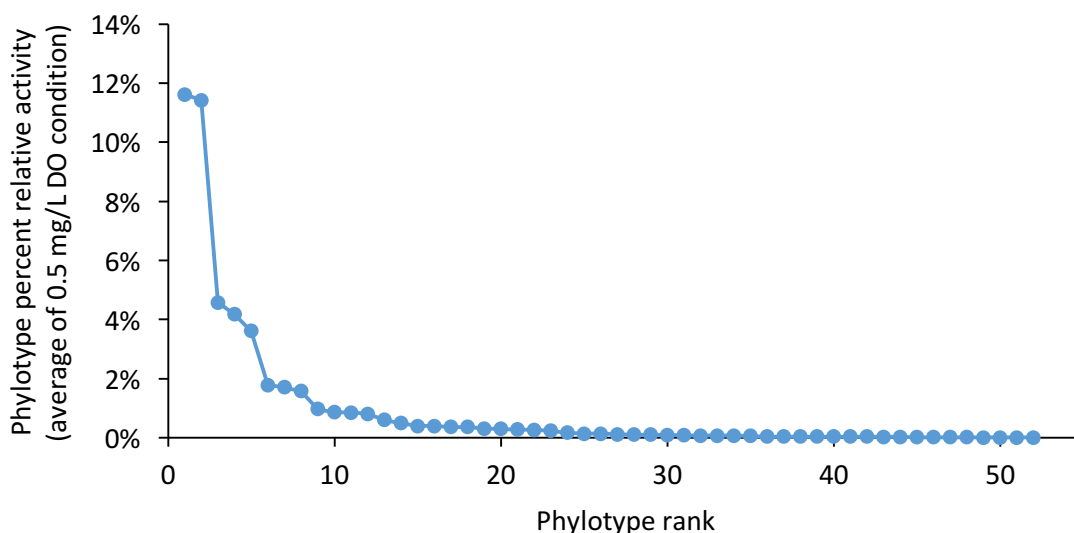


**Figure 5-5.** Rank abundance curve of phylotypes that had significant and positive associations with individual compounds' biotransformation rates (Spearman,  $p < 0.01$ ). The y-axis shows the average relative activity of the phylotype in the 0.5 mg-DO/L batch experiment.

Many compounds shared phylotypes that positively associated (Spearman,  $p < 0.01$ ) with biotransformation rates (Table 5-1 shows the number of phylotypes shared between pairs of compounds). We used the University of Minnesota Pathway Prediction System (UM-PPS), a database for predicting plausible biotransformation pathways for chemical compounds (Gao et al., 2010), to compare whether the predicted possible initial biotransformation pathways were similar between compounds that had shared significant and positively associated phylotypes. We found that for 20 of the 28 pairwise comparisons (approximately 70%) the UM-PPS also predicted either a similar biotransformation pathway when there were shared associated phylotypes or no shared pathways when there were no associated phylotypes. These results indicate that the significant

associations are phylotypes that are involved in catalyzing biotransformation reactions. Positive associations between biotransformation rates and phylotype activity are not unequivocally causal, and there are many scenarios for which non-causal associations could emerge (Johnson et al., 2015). These associations are still valuable as bioindicators and can be used for predicting community functions and biotransformation rates.

**Table 5-1.** Shared phylotypes that associated with biotransformation rates of pairs of compounds and whether the UM-PPS predicted a shared biotransformation pathway (ACE – acetaminophen; VLF – venlafaxine; IBF – ibuprofen; NPX – naproxen; EE2 - 17 $\alpha$ -ethinylestradiol; TMP – trimethoprim; ATE – atenolol; SMX – sulfamethoxazole)

<b>Pairwise comparison</b>	<b>Number of shared phylotypes that were significant and positively associated with biotransformation rate (p&lt;0.01)</b>	<b>UM-PPS predicted similar biotransformation pathway?</b>
ACE vs. VLF	11	no
IBF vs. NPX	4	yes
EE2 vs. VLF	3	yes
TMP vs. IBF	3	yes
EE2 vs. NPX	2	yes
TMP vs. NPX	2	yes
VLF vs. NPX	2	yes
ATE vs. EE2	1	no
ATE vs. TMP	1	yes
ATE vs. IBF	1	no
ACE vs. EE2	1	no
EE2 vs. TMP	1	yes
EE2 vs. IBF	1	yes
ATE vs. ACE	0	no
ATE vs. SMX	0	no
ATE vs. VLF	0	yes
ATE vs. NPX	0	yes
ACE vs. SMX	0	no
ACE vs. TMP	0	no
ACE vs. IBF	0	no
ACE vs. NPX	0	no
EE2 vs. SMX	0	no
SMX vs. TMP	0	no
SMX vs. VLF	0	no

SMX vs. IBF	0	no
SMX vs. NPX	0	no
TMP vs. VLF	0	yes
VLF vs. IBF	0	yes

---

## 5.4 Discussion

The goal of this study was to evaluate the impact of DO concentration on the physiology of the microbial community and the rates of pharmaceutical biotransformations. Our results reveal that substantial reductions in bulk liquid DO concentrations, and therefore energy savings, are possible without compromising pharmaceutical biotransformation. We determined oxygen half-saturation constants for eight compounds using biomass from a full-scale wastewater treatment plant that can be used to model the impact of DO concentration on biotransformation rates. We found that for all of the compounds, a reduction in DO concentration to approximately 0.5 mg/L will not have a major impact on the rate of pharmaceutical biotransformation. Put in other words, the biotransformation rates are at or near their maximum rates at 0.5 mg-DO/L, and increasing aeration will not result in faster biotransformation rates. These results reflect the findings from one wastewater treatment plant, and should be validated by extending this investigation to other treatment plants.

By focusing on a single wastewater treatment plant, we were able to hold the microbial community relatively constant across experiments and identify associations between microbial activity and pharmaceutical biotransformation. The results show that the activity of a number of phylotypes can be used as indicators of biotransformation rates. Linking 16S rRNA gene abundance and activity information to microbial community function is an active area of research. Techniques such as correlation-based network analysis (Ju et al., 2014) and multivariate models (Helbling et al., 2015) have been used to establish predictive relationships between 16S rRNA

gene sequences and community function. We argue that stronger and more mechanistically-relevant associations may be captured by looking at transcript sequences, as the transcript pool is more reflective of the active microbial community.

The phylotypes that significantly associated with DO concentration provide some validation that this approach generates metabolically-relevant phylotypes, as obligate aerobes positively associated with DO concentration and facultative and denitrifying genera had negative associations. It is challenging to validate the phylotypes that associated with pharmaceutical biotransformation rates, as our knowledge of the microorganisms capable of transforming many of the compounds is extremely limited. Notably, for EE2, a compound whose biotransformation has been linked with nitrification in wastewater treatment systems in several studies (Yi and Harper, 2007; Dytczak et al., 2008), its biotransformation rate significantly associated with a phylotype of the *Nitrospira* genera, a group of nitrite oxidizing bacteria. In addition, Helbling et al. (2015) found significant and positive associations between 16S rRNA gene abundances and the transformation of a suite of micropollutants in full-scale wastewater treatment systems. Venlafaxine was the only compound in both their study and ours with significant associations with OTUs, and of the four significant and positively associated OTUs that they observed, we also observed significant and positive associations with two of them (genera *Pirellula* and *Chryseobacterium*). We identified 24 additional phylotypes with significant and positive associations with venlafaxine biotransformation. These associations, as well as the phylotypes identified for the other compounds, adds to the body of knowledge of phylogenetic groups that may be used to predict and potentially enhance specific community functions.

Overall, the phylotypes with associations with biotransformation rates were varied and diverse among the eight compounds studied. There was no single phylotype that was associated

with all compound biotransformation rates, and the maximum number of compounds that a single associated phylotype was shared across was 3 compounds. These results support those found in Chapters 4 and 6 and a previous study (Johnson et al., 2014) that showed that biodiversity is positively associated with the collective rate of pharmaceutical biotransformation. Low DO operation may create niche environments that results in increased biodiversity (as observed in Chapter 4). Thus a reduction in DO concentration could result in a community with faster overall collective rates of pharmaceutical biotransformation by supporting a more diverse microbial community than a fully aerobic, high DO treatment plant.

Long-term low DO operation may select for microorganisms with higher affinities for DO. Previous studies have demonstrated this affect in ammonia oxidizing populations from wastewater treatment systems (Park and Noguera, 2004; Arnaldos and Pagilla, 2014). Arnaldos and Pagilla (2014) observed that AOB had a lower oxygen half-saturation constant (higher affinity) after long-term growth under 0.1 mg/L DO conditions ( $K_{O_2}$  values of 0.23 versus 1.01 mg-DO/L in low versus high DO growth conditions). Park and Noguera (2004) did not observe significant differences in AOB  $K_{O_2}$  values between communities grown under low and high DO conditions, but did observe significantly higher growth rates by the low-DO community at DO concentrations below 4.7 mg/L. Higher oxygen affinities and growth rates for organisms responsible for pharmaceutical biotransformation may also occur after long-term enrichment under low DO conditions. This could result in the potential for even greater energy savings if lower operational DO conditions can be imposed without compromising treatment performance. However, if there is a trade-off between maximal biotransformation rate and substrate affinity, as has been observed in pure cultures (Wirtz, 2002; Elbing et al., 2004), then long-term low DO operation could select for a *K*-strategists over *r*-strategists with overall slower specific pharmaceutical biotransformation

rates (shift from point B to A in Figure 5-6), thus detrimentally impacting removal efficiencies across treatment systems unless biomass concentrations are increased. If low DO operation results in slower decay and thus higher biomass concentrations (as observed in Chapter 4), then the impact of low DO on removal efficiencies may be negligible. This trade-off warrants further investigation as low DO treatment systems become more commonplace.

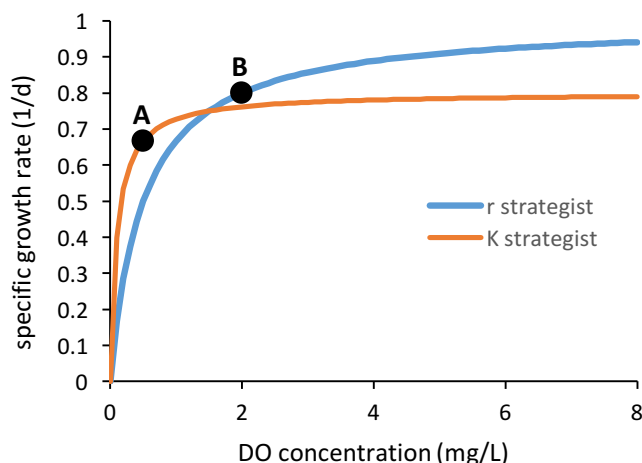


**Figure 5-6.** Specific growth rate versus DO concentration of *r*- versus *K*-strategists according to Monod kinetics. Low DO treatment could theoretically select for *K*-strategists and poise the specific growth rate at point A, while high DO treatment would poise the system at point B.

In conclusion, we determined oxygen half-saturation constants that can be used to describe the impact of DO concentration on the biotransformation rates of several pharmaceuticals. The oxygen half-saturation constants were all within the range or lower than reported half-saturation constants for nitrifiers and heterotrophs. Wastewater models can be modified to incorporate pharmaceutical biotransformation and predict the impact of DO on rates by applying a switching function using  $K_{O_2}$  values. We also found significant associations between the activity of specific phylogenetic groups and specific pharmaceutical biotransformation rates. These phylotypes can serve as indicator organisms to predict biotransformation rates across treatment plants and treatment conditions. We present evidence that bulk kinetic parameters can be linked with

microbial activity measurements, resulting in a biologically-relevant demonstration of community structure/activity and community function relationships.



## 5.5 Literature cited

Abegglen, C.; Joss, A.; McArdell, C. S.; Fink, G.; Schlüsener, M. P.; Ternes, T. A.; Siegrist, H. The Fate of Selected Micropollutants in a Single-House MBR. *Water Res.* **2009**, *43* (7), 2036–2046.

APHA; AWWA; WEF, Standard Methods for the Examination of Water and Wastewater. 21st Ed. Washington, D.C., **2005**.

Arnaldos, M.; Pagilla, K. R. Implementation of a Demand-Side Approach to Reduce Aeration Requirements of Activated Sludge Systems: Directed Acclimation of Biomass and Its Effect at the Process Level. *Water Res.* **2014**, *62*, 147–155.

Batt, A. L.; Kim, S.; Aga, D. S. Enhanced Biodegradation of Iopromide and Trimethoprim in Nitrifying Activated Sludge. *Environ. Sci. Technol.* **2006**, *40* (23), 7367–7373.

Bédard, C.; Knowles, R. Physiology, Biochemistry, and Specific Inhibitors of CH<sub>4</sub>, NH<sub>4</sub><sup>+</sup>, and CO Oxidation by Methanotrophs and Nitrifiers. *Microbiol. Rev.* **1989**, *53* (1), 68–84.

Caporaso, J. G.; Lauber, C. L.; Walters, W. A.; Berg-Lyons, D.; Lozupone, C. A.; Turnbaugh, P. J.; Fierer, N.; Knight, R. Global Patterns of 16S rRNA Diversity at a Depth of Millions of Sequences per Sample. *Proc. Natl. Acad. Sci.* **2011**, *108*, 4516–4522.

Carlson, C. A.; Ingraham, J. L. Comparison of Denitrification by *Pseudomonas Stutzeri*, *Pseudomonas Aeruginosa*, and *Paracoccus Denitrificans*. *Appl. Environ. Microbiol.* **1983**, *45* (4), 1247–1253.

Cole, J. R.; Wang, Q.; Cardenas, E.; Fish, J.; Chai, B.; Farris, R. J.; Kulam-Syed-Mohideen, A. S.; McGarrell, D. M.; Marsh, T.; Garrity, G. M. The Ribosomal Database Project: Improved Alignments and New Tools for rRNA Analysis. *Nucleic Acids Res.* **2009**, *37* (suppl 1), D141–D145.

Dawas-Massalha, A.; Gur-Reznik, S.; Lerman, S.; Sabbah, I.; Dosoretz, C. G. Co-Metabolic Oxidation of Pharmaceutical Compounds by a Nitrifying Bacterial Enrichment. *Bioresour. Technol.* **2014**, *167*, 336–342.

Dytczak, M. A.; Londry, K. L.; Oleszkiewicz, J. A. Biotransformation of Estrogens in Nitrifying Activated Sludge under Aerobic and Alternating Anoxic/aerobic Conditions. *Water Environ. Res.* **2008**, *80* (1), 47–52.

Elbing, K.; Larsson, C.; Bill, R. M.; Albers, E.; Snoep, J. L.; Boles, E.; Hohmann, S.; Gustafsson, L. Role of Hexose Transport in Control of Glycolytic Flux in *Saccharomyces cerevisiae*. *Appl. Environ. Microbiol.* **2004**, *70* (9), 5323–5330.

Fernandez-Fontaina, E.; Omil, F.; Lema, J. M.; Carballa, M. Influence of Nitrifying Conditions on

the Biodegradation and Sorption of Emerging Micropollutants. *Water Res.* **2012**, *46* (16), 5434–5444.

Forrez, I.; Carballa, M.; Boon, N.; Verstraete, W. Biological Removal of 17 $\alpha$ -Ethinylestradiol (EE2) in an Aerated Nitrifying Fixed Bed Reactor during Ammonium Starvation. *J. Chem. Technol. Biotechnol.* **2009**, *84* (1), 119–125.

Gao, J.; Ellis, L. B. M.; Wackett, L. P. The University of Minnesota Biocatalysis/biodegradation Database: Improving Public Access. *Nucleic Acids Res.* **2010**, *38* (suppl 1), D488–D491.

Grady, C. P. L. Jr.; Daigger, G. T.; Love, N. G.; Filipe, C. D. M. *Biological Wastewater Treatment*, 3rd ed.; CRC Press, **2011**.

Harter, J.; Krause, H.-M.; Schuettler, S.; Ruser, R.; Fromme, M.; Scholten, T.; Kappler, A.; Behrens, S. Linking N<sub>2</sub>O Emissions from Biochar-Amended Soil to the Structure and Function of the N-Cycling Microbial Community. *ISME J.* **2014**, *8* (3), 660–674.

Helbling, D. E.; Johnson, D. R.; Lee, T. K.; Scheidegger, A.; Fenner, K. A Framework for Establishing Predictive Relationships between Specific Bacterial 16S rRNA Sequence Abundances and Biotransformation Rates. *Water Res.* **2015**, *70*, 471–484.

Houf, K.; Devriese, L. A.; De Zutter, L.; Van Hoof, J.; Vandamme, P. Development of a New Protocol for the Isolation and Quantification of *Arcobacter* Species from Poultry Products. *Int. J. Food Microbiol.* **2001**, *71* (2–3), 189–196.

Johnson, D. R.; Helbling, D. E.; Lee, T. K.; Park, J.; Fenner, K.; Kohler, H. P. E.; Ackermann, M. Association of Biodiversity with the Rates of Micropollutant Biotransformations among Full-Scale Wastewater Treatment Plant Communities. *Appl. Env. Microbiol.* **2015**, *81* (2), 666–675.

Johnson, D. R.; Helbling, D. E.; Men, Y.; Fenner, K. Can Meta-Omics Help to Establish Causality between Contaminant Biotransformations and Genes or Gene Products? *Environ. Sci. Water Res. Technol.* **2015**, *1* (3), 272–278.

Joss, A.; Zabczynski, S.; Göbel, A.; Hoffmann, B.; Löffler, D.; McArdell, C. S.; Ternes, T. A.; Thomsen, A.; Siegrist, H. Biological Degradation of Pharmaceuticals in Municipal Wastewater Treatment: Proposing a Classification Scheme. *Water Res.* **2006**, *40* (8), 1686–1696.

Ju, F.; Xia, Y.; Guo, F.; Wang, Z.; Zhang, T. Taxonomic Relatedness Shapes Bacterial Assembly in Activated Sludge of Globally Distributed Wastewater Treatment Plants. *Environ. Microbiol.* **2014**, *16* (8), 2421–2432.

Khan, S. J.; Ongerth, J. E. Modelling of Pharmaceutical Residues in Australian Sewage by Quantities of Use and Fugacity Calculations. *Chemosphere* **2004**, *54* (3), 355–367.

Khunjar, W. O.; Mackintosh, S. A.; Skotnicka-Pitak, J.; Baik, S.; Aga, D. S.; Yi, T.; Jr., W. F. H.; Love, N. G. Elucidating the Relative Roles of Ammonia Oxidizing and Heterotrophic Bacteria

during the Biotransformation of 17 $\alpha$ -Ethinylestradiol and Trimethoprim. *Environ. Sci. Technol.* **2011**, *45* (8), 3605–3612.

Kozich, J. J.; Westcott, S. L.; Baxter, N. T.; Highlander, S. K.; Schloss, P. D. Development of a Dual-Index Sequencing Strategy and Curation Pipeline for Analyzing Amplicon Sequence Data on the MiSeq Illumina Sequencing Platform. *Appl. Env. Microbiol.* **2013**, *79* (17), 5112–5120.

Park, H. D.; Noguera, D. R. Evaluating the Effect of Dissolved Oxygen on Ammonia-Oxidizing Bacterial Communities in Activated Sludge. *Water Res.* **2004**, *38* (14–15), 3275–3286.

R Development Core Team. R: A Language and Environment for Statistical Computing. **2012**.

Schloss, P. D.; Westcott, S. L.; Ryabin, T.; Hall, J. R.; Hartmann, M.; Hollister, E. B.; Lesniewski, R. A.; Oakley, B. B.; Parks, D. H.; Robinson, C. J.; et al. Introducing Mothur: Open-Source, Platform-Independent, Community-Supported Software for Describing and Comparing Microbial Communities. *Appl. Env. Microbiol.* **2009**, *75* (23), 7537–7541.

Seshadri, R.; Joseph, S. W.; Chopra, A. K.; Sha, J.; Shaw, J.; Graf, J.; Haft, D.; Wu, M.; Ren, Q.; Rosovitz, M. J. Genome Sequence of *Aeromonas hydrophila* ATCC 7966T: Jack of All Trades. *J. Bacteriol.* **2006**, *188* (23), 8272–8282.

Simpson, F. J.; Robinson, J. Some Energy-Producing Systems in *Bdellovibrio bacteriovorus*, Strain 6-5-S. *Can. J. Biochem.* **1968**, *46* (8), 865–873.

Smith, L. H.; McCarty, P. L.; Kitanidis, P. K. Spreadsheet Method for Evaluation of Biochemical Reaction Rate Coefficients and Their Uncertainties by Weighted Nonlinear Least-Squares Analysis of the Integrated Monod Equation. *Appl. Environ. Microbiol.* **1998**, *64* (6), 2044–2050.

Suarez, S.; Lema, J. M.; Omil, F. Removal of Pharmaceutical and Personal Care Products (PPCPs) under Nitrifying and Denitrifying Conditions. *Water Res.* **2010**, *44* (10), 3214–3224.

Tran, N. H.; Urase, T.; Kusakabe, O. The Characteristics of Enriched Nitrifier Culture in the Degradation of Selected Pharmaceutically Active Compounds. *J. Hazard. Mater.* **2009**, *171* (1–3), 1051–1057.

Uprety, K.; Balzer, W.; Baurner, R.; Duke, R.; Bott, C. Implementing Ammonia-Based Aeration Control at Biological Nutrient Removing Wastewater Treatment Plants. *Proc. Water Environ. Fed.* **2015**.

Urase, T.; Kikuta, T. Separate Estimation of Adsorption and Degradation of Pharmaceutical Substances and Estrogens in the Activated Sludge Process. *Water Res.* **2005**, *39* (7), 1289–1300.

Vanwonterghem, I.; Jensen, P. D.; Ho, D. P.; Batstone, D. J.; Tyson, G. W. Linking Microbial Community Structure, Interactions and Function in Anaerobic Digesters Using New Molecular Techniques. *Curr. Opin. Biotechnol.* **2014**, *27*, 55–64.

Varon, M.; Shilo, M. Ecology of Aquatic Bdellovibrios. *Adv. Aquat. Microbiol.* **1980**, *2*, 1–48.

Wells, G. F.; Park, H.; Yeung, C.; Eggleston, B.; Francis, C. A.; Criddle, C. S. Ammonia-oxidizing Communities in a Highly Aerated Full-scale Activated Sludge Bioreactor: Betaproteobacterial Dynamics and Low Relative Abundance of Crenarchaea. *Environ. Microbiol.* **2009**, *11* (9), 2310–2328.

Willems, A.; Busse, J.; Goor, M.; Pot, B.; Falsen, E.; Jantzen, E.; Hoste, B.; Gillis, M.; Kersters, K.; Auling, G. Hydrogenophaga, a New Genus of Hydrogen-Oxidizing Bacteria That Includes Hydrogenophaga Flava Comb. Nov. (formerly *Pseudomonas flava*), *Hydrogenophaga palleronii* (formerly *Pseudomonas palleronii*), *Hydrogenophaga pseudoflava* (formerly *Pseudomonas pseudoflava*). *Int. J. Syst. Bacteriol.* **1989**, *39* (3), 319–333.

Wirtz, K. W. A Generic Model for Changes in Microbial Kinetic Coefficients. *J. Biotechnol.* **2002**, *97* (2), 147–162.

Yi, T.; Harper, W. F. The Link between Nitrification and Biotransformation of 17 $\alpha$ -Ethinylestradiol. *Environ. Sci. Technol.* **2007**, *41* (12), 4311–4316.

Zhi, W.; Ge, Z.; He, Z.; Zhang, H. Methods for Understanding Microbial Community Structures and Functions in Microbial Fuel Cells: A Review. *Bioresour. Technol.* **2014**, *171*, 461–468.

## Chapter 6.

### **Elucidating the impact of microbial community diversity on pharmaceutical biotransformation during wastewater treatment**

Lauren B. Stadler<sup>1</sup>, Jeseth Delgado Vela<sup>1</sup>, and Nancy G. Love<sup>1</sup>

<sup>1</sup>Department of Civil and Environmental Engineering, University of Michigan

#### **6.1 Introduction**

Wastewater treatment plants (WWTPs) harness microbes to treat our waste, protect our environment from organic pollutants, nutrients, and pathogens. In addition to conventional pollutants, however, thousands of pharmaceuticals are excreted by humans in intact and metabolized forms, reaching WWTPs before being released into the environment (Kolpin et al., 2002). The ability of the microbes in WWTPs to biotransform these chemicals, and thus reduce their associated risk to the environment and human health, is an area of great interest in the scientific community (Carballa et al., 2004; Castiglioni et al., 2005; Nakada et al., 2006; Kasprzyk-Hordern et al., 2009). Substantial research has advanced our knowledge of pharmaceutical biotransformation pathways (Ellis et al., 2006) and the transformation products formed during treatment (Kern et al., 2010). But few studies have linked chemical transformation data with microbial ecology to develop predictive relationships between the characteristics of the microbial community and pharmaceutical biotransformation pathways and rates. A better understanding of

how microbial community characteristics impact pharmaceutical biotransformation could enable the design and operation of WWTPs to reduce pharmaceutical loading in receiving environments.

Biodiversity is one characteristic of wastewater treatment microbial communities that may impact pharmaceutical biotransformation rates (Johnson et al., 2014a). WWTPs harbor extremely diverse microbial communities (Zhang et al., 2011). The relationship between biodiversity and ecosystem function has been an area of considerable debate and interest in ecology (Midgley, 2012). With the emergence of next generation sequencing tools, microbial ecologists have begun to interrogate the relationship between productivity, stability, and diversity (Konopka, 2009; Levine et al., 2011). WWTPs have been studied extensively and serve as a model system for microbial ecology, informing our understanding of mixed-culture microbial assemblages (Pholchan et al., 2013), diversity-function relationships (Johnson et al., 2014b), and ecological consequences of disturbances on ecosystem function (Vuono et al., 2015).

Mounting evidence from studies of microbial systems suggests a positive relationship between biodiversity and community function (Cardinale et al., 2006; Duffy, 2008; Levine et al., 2011). However, functional redundancy, the concept that taxonomically distinct species have the same ecological function, challenges the idea that changes in biodiversity will directly affect community process rates. Processes that are carried out by a large number of taxonomically distinct microorganisms, or broad processes, would not necessarily be impacted by biodiversity losses because the process rate is not limited by the number of species that can perform it. Conversely, narrow processes, or processes performed by few species, would be positively correlated with biodiversity because the process rate is limited by the number of species able to perform the specialized metabolism. Many have argued that diversity based on functional genes, as opposed to taxonomic genes, is more directly associated with ecosystem process rates (Green et al., 2008).

Another source of inconsistency in biodiversity measurements is that microbial biodiversity measurements are typically assessed using DNA-based methods. However, supplementing DNA-based methods with biodiversity estimates using the expressed or active fraction of genes and taxa may result in more positive associations between process rates and biodiversity measurements.

Several studies have evaluated the relationship between biodiversity and community function in wastewater systems. While some studies have shown that WWTP communities are functionally redundant, others have shown that function is dependent on diversity. Franklin and Mills (2006) found wastewater systems to be functionally redundant when community function is defined as consumption of glucose, acetate, citrate, palmitic acid and amino acids. On the other hand, Cook et al. (2006) found that the degradation of a surfactant in industrial wastewater depended on community richness. The discrepancy between these two studies is likely due to how community function was defined: consumption of glucose, acetate, citrate, palmitic acid and amino acids are broad processes, whereas surfactant degradation is a narrow process in WWTP communities. Given the diverse chemical structures of pharmaceuticals, their biotransformation could be catalyzed by either broad or narrow processes. Moreover, pharmaceuticals could undergo multiple transformations ranging in the spectrum of broad to narrow processes. In a study of microbial communities from ten full-scale treatment systems, a positive association between taxonomic and functional biodiversity and the rates of some individual micropollutants was observed (Helbling et al., 2012). However, not all compound biotransformation rates exhibited a positive association with biodiversity, and this can be explained by the fact that those compounds were likely transformed by broad processes. Understanding whether pharmaceutical biotransformations are catalyzed by highly redundant populations, or performed by rare taxa can

help us identify the enzymes that catalyze their transformation and exploit opportunities for enhancing biotransformations during wastewater treatment.

In this study, we examined the relationship between pharmaceutical biotransformations in wastewater microbial communities and both (1) taxonomic and (2) functional diversity. We hypothesized that taxonomic diversity is positively associated with functional diversity in wastewater microbial communities (as was observed previously by Johnson et al., 2014b). Therefore, we expected that the rates of pharmaceutical biotransformation performed by rare taxa would correlate positively with taxonomic and functional diversity in WWTPs. Unlike previous studies on pharmaceutical degradation and activated sludge, we experimentally manipulated an activated sludge community to create communities representing a gradient in diversity to directly test the relationship between diversity and function (here, defined as pharmaceutical biotransformation). With this approach, because the communities were all established from the same original community, we could examine how the loss of specific functions and taxonomic groups impacted pharmaceutical biotransformation. To identify specific functions and taxonomic groups that were lost in the dilution gradient, we used amplicon sequencing of the 16S rRNA gene and 16S rRNA, as well as metagenomics and metatranscriptomics.

## **6.2 Materials and methods**

### ***6.2.1 Experimental design and diversity manipulation***

A gradient in microbial diversity in an activated sludge community was established using a dilution-to-extinction approach (Szabó et al., 2007; Peter et al., 2010; Philippot et al., 2013; Ylla et al., 2013). In this approach, each dilution results in a less diverse subset of the original community by theoretically removing the least abundant species from the previous culture. An 8



L grab sample of activated sludge mixed liquor was collected from the aeration basin of the Ann Arbor WWTP, a facility that performs nitrification and biological phosphorus removal. Before serial dilution, disaggregation of macroflocs in the sample was achieved by blending approximately 500 mL of mixed liquor in an industrial Waring Commercial Blender (Model 516L31) at maximum speed for 10 minutes.

After blending, stepwise dilutions (1:10) were performed by transferring 100 mL into 900 mL of sterile semi-synthetic sewage media (SSM) to achieve dilution conditions from  $10^{-1}$  to  $10^{-7}$ . The SSM was comprised of filtered (0.22  $\mu\text{m}$  Stericup, Millipore, Darmstadt, Germany) and autoclaved primary effluent collected from the Ann Arbor WWTP (detailed in Appendix D). COD and ammonia-N concentrations were determined in the filtered and sterilized primary effluent, and then supplemented with carbon (a mixture of peptone, meat extract, humic acid) and ammonia chloride to achieve a final concentration of 1,850 mg/L as COD and 30 mg-N/L as ammonia. Humics were added such that they made up approximately 10% of the total carbon (Huang et al., 2010), and the remainder of the supplemental carbon was equal parts peptone and meat extract as COD. Micronutrients were also supplemented in proportion to the COD (Grady et al., 2011). After serial dilution, triplicate flasks of 200 mL of the  $10^{-2}$ ,  $10^{-4}$ , and  $10^{-7}$  dilutions were allowed to regrow overnight in an incubator-shaker at 20°C. After the 24-hour regrowth period, the biomass was pelleted via centrifugation and resuspended in 250 mL of fresh SSM.

### ***6.2.2 Pharmaceutical biotransformation batch experiments***

Experiments were initiated by transferring the re-suspended dilution cultures into 500 mL bottles with a mixture of pharmaceuticals pre-dried on the bottom of each bottle (a methanol stock containing a mixture of the compounds was added to each bottle and allowed to evaporate until dry) to achieve a target initial concentration of 10  $\mu\text{g/L}$  of each compound. The compounds

selected for investigation in this study included: atenolol, 17 $\alpha$ -ethinylestradiol (EE2), trimethoprim, venlafaxine, carbamazepine, glyburide, and erythromycin, and additional information about each compound is provided in Table D3 in Appendix D. Compounds were selected to represent a variety of possible initial biotransformation pathways determined using University of Minnesota's Pathway Prediction System (Ellis et al., 2006), which predicts aerobic biodegradation pathways based on chemical structure. For each compound, we counted the number of unique "likely" and "neutral" biotransformation pathways so that for each additional compound included in the study, additional initial biotransformation pathways were being represented (see Appendix D for compound selection approach).

At each dilution level ( $10^{-2}$ ,  $10^{-4}$ ,  $10^{-7}$ ) triplicate batch reactors were prepared. A control batch reactor was also prepared with a mixture of the biomass from each dilution level inactivated with sodium azide (0.2 % w/v). Every 24 hours, an additional 2 mL of 100 g/L sodium azide stock solution was added to the control batch reactor. Beginning and endpoint 20-mL samples were collected from each batch reactor corresponding to time points of 30 minutes and 4 days after initiation, respectively, for pharmaceutical quantification. After collection, samples were spiked with deuterated analogs of the target compounds, filtered through a 0.3  $\mu$ m glass fiber filter (Sterlitech, Kent, WA), and stored at 4°C until analysis (less than 24h after collection). Samples were collected at time points of approximately 30 min, 4h, 8h, 12h, 24h, and 48h and filtered through 0.3  $\mu$ m glass fiber filter (Sterlitech) to determine dissolved organic carbon concentrations (TOC Analyzer, Shimadzu, Kyoto, Japan). Total and volatile suspended solids concentrations were determined according to Standard Methods (2005) at the beginning and end of the experiment (96 hours) for each batch reactor. The average volatile suspended solids concentration between the

beginning and endpoint was used to normalize all carbon oxidation and pharmaceutical transformation rate data.

Pharmaceutical concentrations were determined in each sample via on-line pre-concentration followed by high performance liquid chromatography and high resolution mass spectrometry (details are provided in Appendix D). Background concentrations of pharmaceuticals were considered negligible as compared to the spiked concentrations. Quantification was performed using a matrix-matched calibration curve. Pharmaceutical biotransformation rates and percent loss were calculated for each compound. Rates were calculated using the beginning (30 minute) and end point (4 day) concentrations, without consideration of the shape of the concentration versus time curve.

### ***6.2.3 DNA and RNA sample collection, library preparation, and sequencing***

Duplicate 15 mL samples from each batch reactor were collected for DNA analysis from each of the triplicate dilution cultures between 4h20min and 5h40min after initiating the batch experiments. The biomass was pelleted via centrifugation at 6,200 x g, supernatant discarded, and the pellet was stored at -80°C until DNA extraction. Duplicate 15 mL samples were collected for RNA analysis from each of the triplicate dilution cultures between 5h30min and 7h50min after initiating the batch experiments. The biomass was pelleted via centrifugation (4°C, 5min), supernatant discarded, and the pellet was re-suspended in 2 mL of RNALater (Qiagen, Valencia, CA) and stored at -80°C until RNA extraction. RNA samples were collected in this timeframe to get a representative sample of microbial activity at a time when there were residual organic carbon and pharmaceutical concentrations.

DNA and RNA extraction were performed with three bead beading steps followed by automated extraction using a Maxwell 16 automated nucleic acid extractor (Promega, Madison, WI) using the DNA blood and simplyRNA tissue kits, respectively. Extractions were conducted according to the manufacturer's instructions except 10  $\mu$ L of DNase 1 (increased from 5  $\mu$ L) was used to remove contaminating DNA during RNA extractions. Total DNA and RNA concentration in each sample were fluorometrically quantified with the Quantifluor DNA and RNA sample kits (Promega, Madison, WI). Reverse transcription to generate single-stranded complementary DNA (cDNA) from RNA extracts was performed using the SuperScript VILO cDNA Synthesis Kit according to manufacturer's instruction (Life Technologies, Grand Island, NY). Amplicon sequencing of the 16S rRNA gene and cDNA were performed on Illumina MiSeq (Illumina Inc., San Diego, CA) using universal primers for bacteria and archaea targeting the V4 region of the 16S rRNA gene (Kozich et al., 2013).

DNA samples were prepared for shotgun metagenomic sequencing at the University of Michigan DNA Sequencing Core. DNA was fragmented to 400 bp using standard Covaris sonication (Covaris, Woburn, MA). Fragmented DNA was then prepared as a standard Illumina library using Kapa reagents (Kapa Biosystems, Wilmington MA) on an Apollo instrument (WalterGen Bio-systems, Fremont, CA), where the fragments were end-repaired, A-tailed, and adapter-ligated. The samples were then PCR amplified and pooled. The high diversity samples ( $10^{-2}$ ) were sequenced on a single lane of a HiSeq Flow Cell (version 3, Illumina) and the medium ( $10^{-4}$ ) and low ( $10^{-7}$ ) diversity samples were sequenced on a second lane, with the medium diversity samples being weighted 2x the low diversity samples. The weighted pooling was chosen in order to achieve greater sequencing depth on the more diverse samples. Final libraries were checked for quality and quantity by TapeStation (Agilent, Santa Clara, CA) and qPCR using Kapa's library

quantification kit for Illumina Sequencing platforms (catalog #KK4835) (Kapa Biosystems). They were clustered on the cBot (Illumina) and sequenced on a 100-cycle paired end run on a HiSeq 2500 in High Output mode using version 3 reagents according to manufacturer's protocols (Illumina).

RNA samples were prepared for shotgun metatranscriptomic sequencing by first enriching the mRNA from the total RNA extracts using the MICROBExpress Bacterial mRNA Enrichment Kit (Invitrogen, Carlsbad, CA) based on previous studies that reported that subtractive hybridization kits using rRNA specific probes are the most effective available kits for enriching mRNA from total rRNA from environmental samples (He et al., 2010; Mettel et al., 2010). Individual libraries were prepared for each sample as for the DNA samples and the samples were multiplexed using sample-specific adaptors on a single lane of a HiSeq Flow Cell (Illumina, Inc.). No sample-based weighting was employed for the metatranscriptomic sequencing.

#### ***6.2.4 Sequencing analysis and biodiversity measurements***

Amplicon sequencing reads were analyzed using Mothur (version 1.33.3) (Schloss et al., 2009) and classified using the 16S rRNA gene taxonomy from the Ribosomal Database Project (Cole et al., 2009). Differences in sequencing depth were corrected for by subsampling to the lowest number of sequences per sample for all samples (19,681 for DNA, and 29,428 for cDNA). Sequences were binned into operational taxonomic units (OTUs) based on sequence similarity of greater or equal to 97%. Taxonomic biodiversity measurements were calculated based on OTUs.

Raw shotgun sequencing reads were dereplicated (100% identity over 100% of the length) and trimmed using Sickle (Joshi and Fass, 2011). Adaptors were removed using Scythe version 0.993b (<https://github.com/Geo-omics/scripts/tree/master/DerepTools>). Trimming removed 8-19% of the data. Whole genome de novo assembly was performed by pooling all reads from the

dilution cultures and using IDBA-UD (Peng et al., 2012) with the following parameters: mink 52, maxk 93, step 8. Assembled data was submitted to the DOE JGI-IMG/MER annotation pipeline (Taxon Object ID 3300005080). KEGG KO annotations from the IMG analysis were screened to retain those above a threshold of an e-value less than  $10^{-5}$ , bit score greater than 50, and percent identity greater than 60%.

Paired-end transcriptomic reads were mapped to assembled contigs using the Burrows-Wheeler Aligner (BWA version 0.7.10; Li and Durbin, 2009). Each replicate was mapped to the pooled assembly separately. Paired forward and reverse read alignments were generated in the SAM format using BWASAMPE algorithm. The mapped read counts were extracted using SAMtools (Li et al., 2009). HTSeq count was used to obtain the raw counts per gene for each sample, which was used for all subsequent analyses (Anders et al., 2014). Functional diversity metrics were calculating after subsampling to the lowest number of sequences per sample (1,233,846 and 624,845 for the metagenomic and metatranscriptomic reads, respectively) to correct for differences in sequencing depth.

### ***6.2.5 Statistical analyses***

Statistical analysis were performed in the R environment using the stats (R Development Core team, 2013) and vegan (Oksanen et al., 2007) packages. Non-parametric statistical methods were used for pairwise tests and associations between biotransformation rates and biodiversity measurements as they do not assume any underlying form for the distribution of the data. Mann-Whitney *U* test was used to perform pairwise tests of biotransformation rates and pairwise tests of taxonomic and functional diversity measurements between the different dilution conditions. Spearman rank correlation was used to test associations between biodiversity and pharmaceutical biotransformation rates.

Metatranscriptomic mapped reads were analyzed using the Bioconductor DESeq2 package based on the negative binomial model (Love et al., 2014). For differential expression analysis, raw counts were normalized using relative library sizes, and significant differential expression was tested using the likelihood ratio test. The association between the normalized expression of each gene and biotransformation rate of each pharmaceutical was tested using the two-sided Spearman's rank correlation.

## 6.3 Results

### 6.3.1 Dilution resulted in communities with a gradient of taxonomic and functional diversity

With increased dilution, the richness of the activated sludge microbial community decreased. Rarefaction curves of unique OTUs versus sequences sampled show distinct clustering of the dilution cultures, with samples from the most diverse culture ( $10^{-2}$ ) having the greatest number of unique OTUs, followed by the medium-diversity culture ( $10^{-4}$ ), and the low-diversity culture ( $10^{-7}$ ) that plateaued with the lowest number of unique OTUs (Figure 6-1). Differences in taxonomic richness and diversity between the dilution cultures are supported by various biodiversity measurements based on the 16S rRNA gene sequence data (Table 6-1). DNA-based functional richness, the number of unique annotated functions, was not significantly different between the  $10^{-2}$  and  $10^{-4}$  dilution batches (Mann-Whitney  $U$ ,  $p = 0.19$ ). It was significantly different between the most diluted batch ( $10^{-7}$ ) and the other conditions (Mann-Whitney  $U$ ,  $p < 0.05$  for both). The loss of taxa was not proportional to the loss of functional genes across the dilution cultures, as there was a significant difference in taxonomic richness but not functional richness between the  $10^{-2}$  and  $10^{-4}$  conditions, indicative of some functional redundancy within the community.

The Shannon taxonomic diversity measurements based on DNA and RNA were significantly different between the conditions (Mann-Whitney  $U$ ,  $p < 0.05$ ). The Shannon taxonomic index accounts for the relative abundances of the functional genes, and places less weight on the least-abundant functions. With this index, greater evenness in a community corresponds to a higher Shannon diversity index. The Shannon indices show that  $10^{-2}$  community was more even than the  $10^{-4}$  and  $10^{-7}$  communities, and this was also supported by the Shannon evenness indices (data not shown). These results indicate that the dilution approach creates a gradient in diversity by not only reducing the total number of unique OTUs and functions, but also by reducing the evenness of the microbial community. Conversely, the RNA-based functional diversity indices showed that the Shannon functional index did not decrease with increased dilution. In other words, dilution resulted in a community that remained relatively even with respect to expressed functional genes, despite being less even with respect to active taxa, again supporting the notion that there was functional redundancy in the communities.



**Table 6-1.** Biodiversity indices based on 16S rRNA gene, 16S rRNA, metagenomic, and metatranscriptomic sequencing of biomass from the dilution cultures.

Biodiversity index	Dilution condition		
	$10^{-2}$	$10^{-4}$	$10^{-7}$
<b>DNA</b>			
Taxonomic richness (unique OTUs)	311 ± 63	123 ± 7	51 ± 21
Chao1 extrapolated taxonomic richness	358 ± 68	136 ± 4	64 ± 23
Shannon taxonomic diversity	2.67 ± 0.19	2.02 ± 0.06	1.37 ± 0.06
Functional richness (unique functional genes)	4686 ± 48	4643 ± 21	4219 ± 229
Chao1 extrapolated functional richness	4863 ± 49	4809 ± 46	4328 ± 199
Shannon functional diversity	7.66 ± 0.01	7.63 ± 0.00	7.57 ± 0.01
<b>RNA</b>			
Taxonomic richness (unique OTUs)	512 ± 10	190 ± 22	109 ± 36
Chao1 extrapolated taxonomic richness	983 ± 62	354 ± 32	208 ± 84
Shannon taxonomic diversity	2.71 ± 0.04	1.95 ± 0.04	1.62 ± 0.12
Functional richness (unique functional genes)	4013 ± 26	3916 ± 15	3501 ± 113
Chao1 extrapolated functional richness	4300 ± 16	4214 ± 49	3695 ± 130
Shannon functional diversity	6.57 ± 0.06	6.63 ± 0.11	6.60 ± 0.03

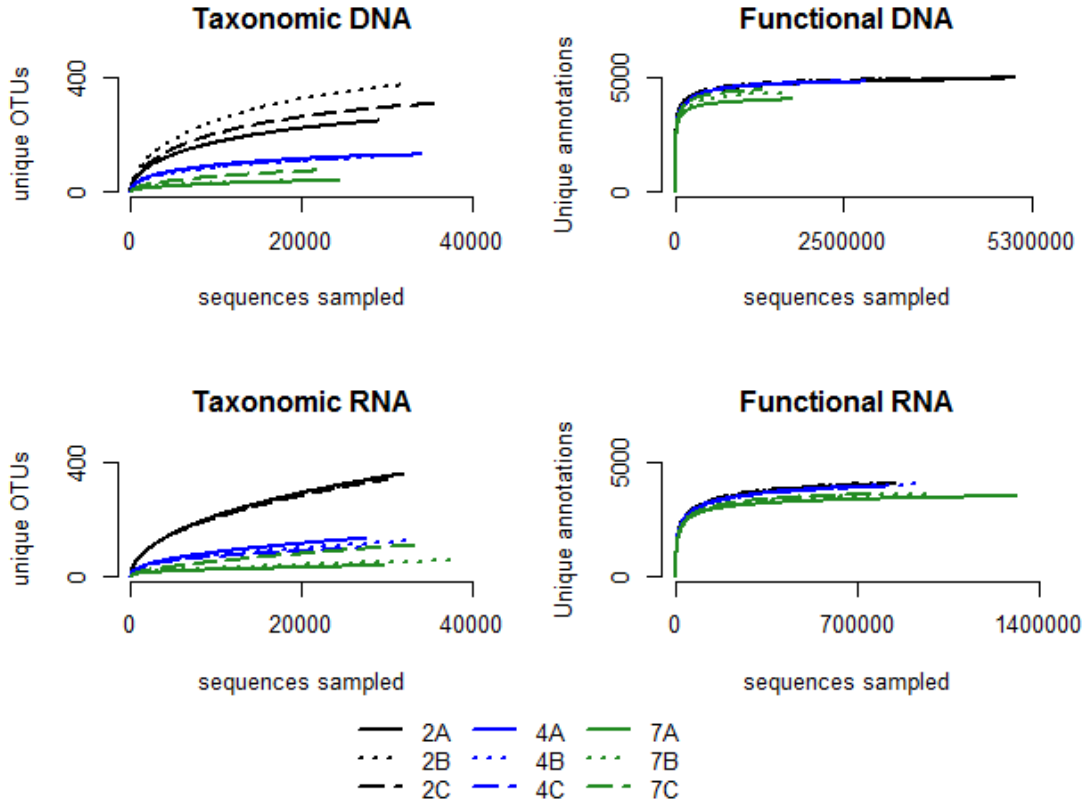


**Figure 6-1.** Rarefaction plots for the dilution cultures based on 16S rRNA gene and 16S rRNA sequencing (taxonomic) and whole genome and metagenome sequencing (functional). The dilution conditions are shown in black ( $10^{-2}$ ), blue ( $10^{-4}$ ) and green ( $10^{-7}$ ).

### 6.3.2 Taxonomic and functional diversity positively associated with one another

In order to understand if greater unique taxa corresponded to increased functional-traits in the wastewater microbial communities, we first tested whether taxonomic richness was positively associated with functional richness. We found that for both the DNA- and RNA-based annotations, that there was a significant positive association between taxonomic and functional richness (Figure 6-2). The shape of the data in Figure 6-2 suggests that the number of unique functions does not increase linearly with the number of unique OTUs. This is consistent with the idea that the most

diverse communities are also the most functionally redundant and that the unique OTUs contain many of the same functional genes.

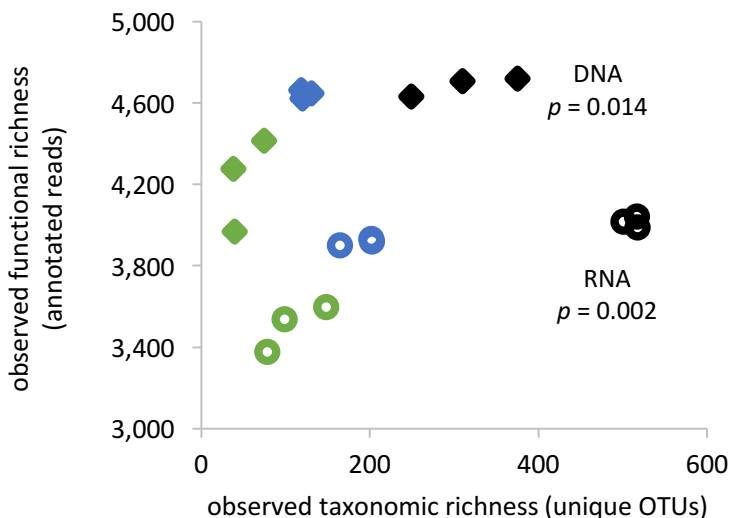


**Figure 6-2.** Observed functional richness versus taxonomic richness. DNA-based annotations are shown in filled markers and RNA-based annotations in open markers. 10<sup>-2</sup>, 10<sup>-4</sup>, and 10<sup>-7</sup> samples are represented by black, blue, and green markers, respectively. Reported *p*-values are based on the two-sided Spearman rank correlation test and indicate significant positive association between taxonomic and functional richness for both DNA and RNA-based annotations.

### 6.3.3 Carbon oxidation and pharmaceutical transformations

Carbon utilization, a process that is widespread across all forms of life, is a function that we expected to be functionally redundant across all of the dilution conditions. Thus we hypothesized that there would not be a significant difference between carbon oxidation rate or extent between the dilution conditions. To test this, dissolved organic carbon was measured in samples across the experiment to determine carbon oxidation rates (Figure D1, Appendix D). We found no significant difference between normalized carbon oxidation rates (normalized by VSS concentration) between the dilution conditions (Mann Whitney *U*, *p* > 0.19). Further, we found no significant association between carbon oxidation rate and taxonomic or functional richness

(Spearman,  $p > 0.8$ ). Dissolved organic carbon remained constant throughout the batch experiment in the control flask, indicating that the sodium azide-supplemented control served to sufficiently inactivate carbon oxidation activity throughout the experiment.

Pharmaceutical biotransformation rates were determined for 8 compounds. Average percent loss normalized by volatile suspended solids concentration, a surrogate for specific biotransformation activity, is shown in Figure 6-3 for each compound and each dilution condition. Significant differences between the degree of biotransformation and the dilution condition were observed for 6 of the 8 compounds, with greater extents of biotransformation observed in the most diverse culture (Mann-Whitney  $U$ ,  $p < 0.05$ ). Two compounds did not follow the same pattern as the rest: for glyburide, no significant differences in extent or rate of biotransformation between the dilution cultures were observed as very limited loss of the parent compound occurred across the experiment; and for erythromycin, the greatest loss was observed in the  $10^{-4}$  condition. Atenolol and venlafaxine were the only compounds for which the stepwise dilution resulted in a corresponding stepwise reduction in biotransformation rate. For all of the other compounds there was only a significant difference in biotransformation rate between two of the dilutions conditions. One possible explanation is that the loss in taxonomic diversity that occurred during dilution resulted in a loss of the specific OTUs involved in the biotransformation of that compound. Once those responsible community members were lost, additional dilution did not significantly affect the observed biotransformation rate.

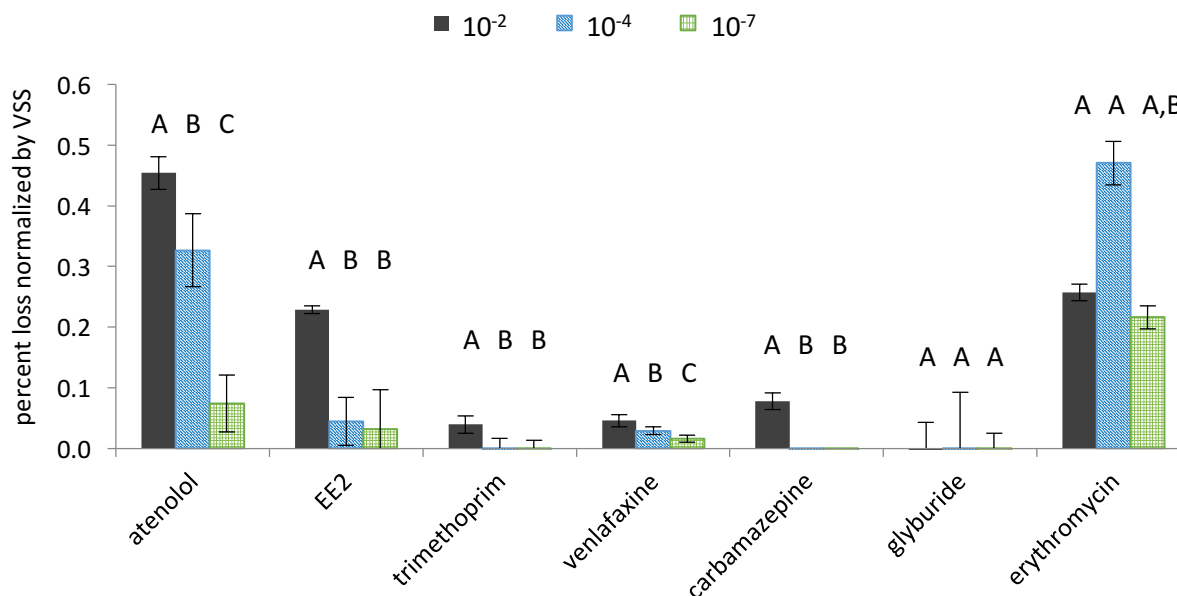


**Figure 6-3.** Average pharmaceutical loss (disappearance of the parent compound) normalized to volatile suspended solids concentration for each dilution condition (black: 10<sup>-2</sup>; blue: 10<sup>-4</sup>; green: 10<sup>-7</sup>). The same letter above the bars indicate treatments without significant differences (Mann-Whitney  $U$ ,  $p > 0.05$ ) between biotransformation rates.

#### 6.3.4 Significant associations between functional richness and pharmaceutical biotransformation rate were observed

We directly tested for associations between individual pharmaceutical biotransformation rates and biodiversity measurements. We also assessed associations between the collective rates of pharmaceutical biotransformation and biodiversity by scaling each compound's normalized rate (mean of 0, standard deviation of 1) and taking the average of the scaled rates to generate a collective average rate for each condition (Zavaleta et al., 2010; Johnson et al., 2014a). We calculated richness using DNA- and RNA- based taxonomic and functional data, allowing comparisons between associations using DNA versus RNA and taxonomic versus functional richness. We observed a strong positive correlation between richness and several individual pharmaceutical biotransformation rates (Figure D2, Appendix D). The Spearman correlation  $p$ -

values resulting from these associations are shown in Figure 6-4. Atenolol, trimethoprim, venlafaxine, carbamazepine, and the collective compound rates were significantly associated with both a taxonomic and functional richness measurement. Notably, associations with functional richness were always stronger with RNA- than DNA-based richness measurements. This indicates that expressed genes are better predictors of pharmaceutical biotransformation and supports the notion that metagenomic datasets may mask significant associations with process rates as they include non-expressed traits. Differences in the strength of associations between rates and DNA- versus RNA-based taxonomic richness measurements were less pronounced than for functional richness. This can be explained in part by the experimental conditions, which were fed batch reactors and the biomass samples were collected when the microbial community was actively growing. If the communities were in an exponential growth phase, it is not surprising that the associations between biotransformation rates and DNA and RNA-based taxonomic richness were similar (Varricchio and Monier, 1971; Pérez-Osorio et al., 2010).

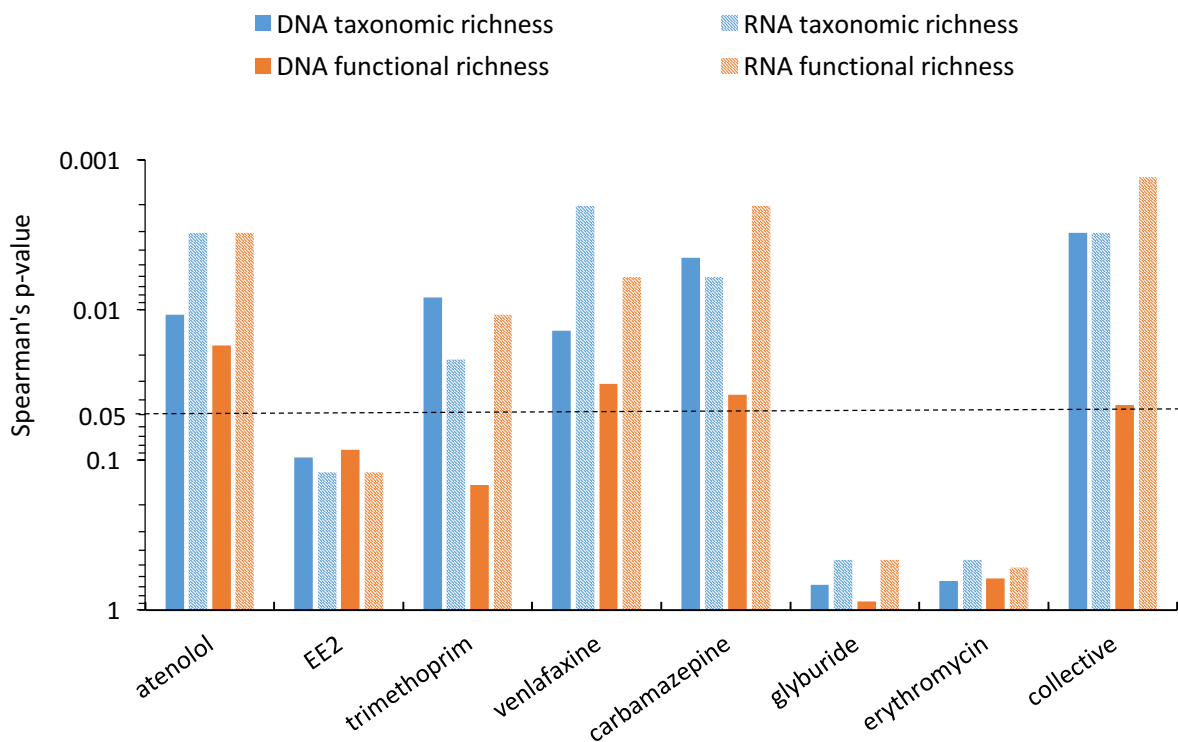


**Figure 6-4.** Spearman correlation p-values for associations between richness and pharmaceutical biotransformation rates. Biodiversity measurements were calculated based on taxonomic (blue bars) and functional (orange bars) sequencing data using both the DNA (solid bars) and RNA (patterned bars). Dashed line signifies  $p = 0.05$ .

We compared associations of pharmaceutical biotransformation rates with richness calculated using all expressed genes to associations calculated with only metabolism-related genes, as we expected those genes were likely responsible for differences in biotransformation rates. For most compounds and for the collective pharmaceutical biotransformation rates, a stronger association was determined with richness accounting for all genes as opposed to only metabolic genes (Figure D3, Appendix D). This may be because by only focusing on known metabolic genes, we are potentially substantially underestimating the functional richness of the communities.

### 6.3.5 Differential expression of functional genes suggests potential enzymes associated with biodegradation

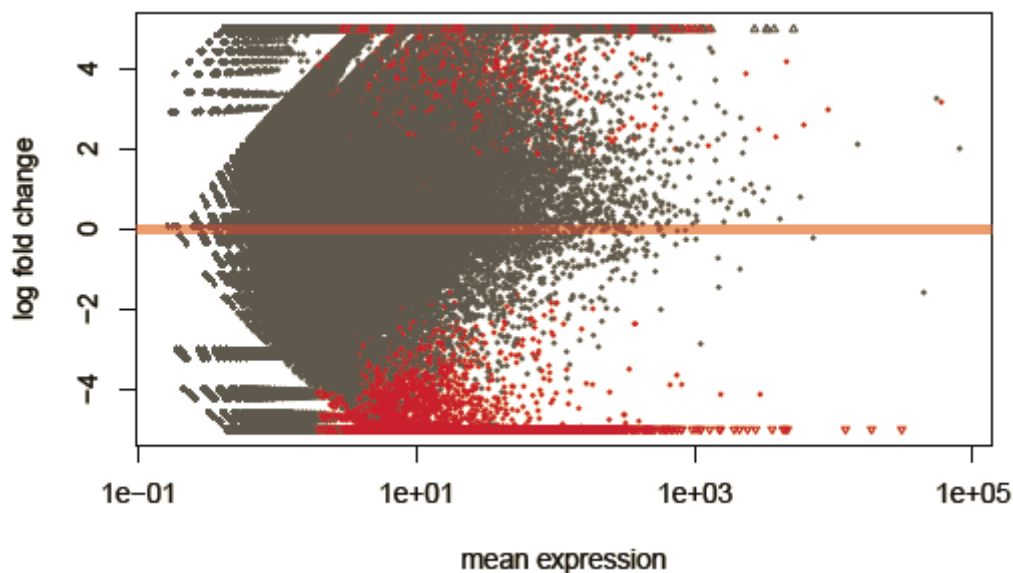


**Figure 6-5.** The relationship between the mean expression across all of the samples, and the log change in expression between the  $10^{-2}$  and  $10^{-7}$  cultures. Each gene is shown in grey. Statistically significant (likelihood ratio  $p_{adj} < 0.05$ ) differentially expressed genes are shown in red.

After establishing that there were significant positive associations between biodiversity and pharmaceutical biotransformation rates, we asked which functions were differentially expressed across the dilution cultures, and specifically which functions were lost? Of the 710,402 functions analyzed, 45,840 were found to be differentially expressed between the three dilution conditions ( $p_{adj} < 0.05$ ), and 15,290 of those were found to be good hits to the KEGG Orthology database. The majority of the significant differentially expressed functions were lost with dilution from the  $10^{-2}$  to the  $10^{-7}$  cultures (negative log fold change, Figure 6-5). Thus, a loss of biodiversity corresponded to a loss of expression of these functions. For the compounds that were transformed to different extents across the three dilution conditions, the genes that had a lower level of



expression in the least diverse culture ( $10^{-7}$ ) could be responsible for pharmaceutical biotransformation.

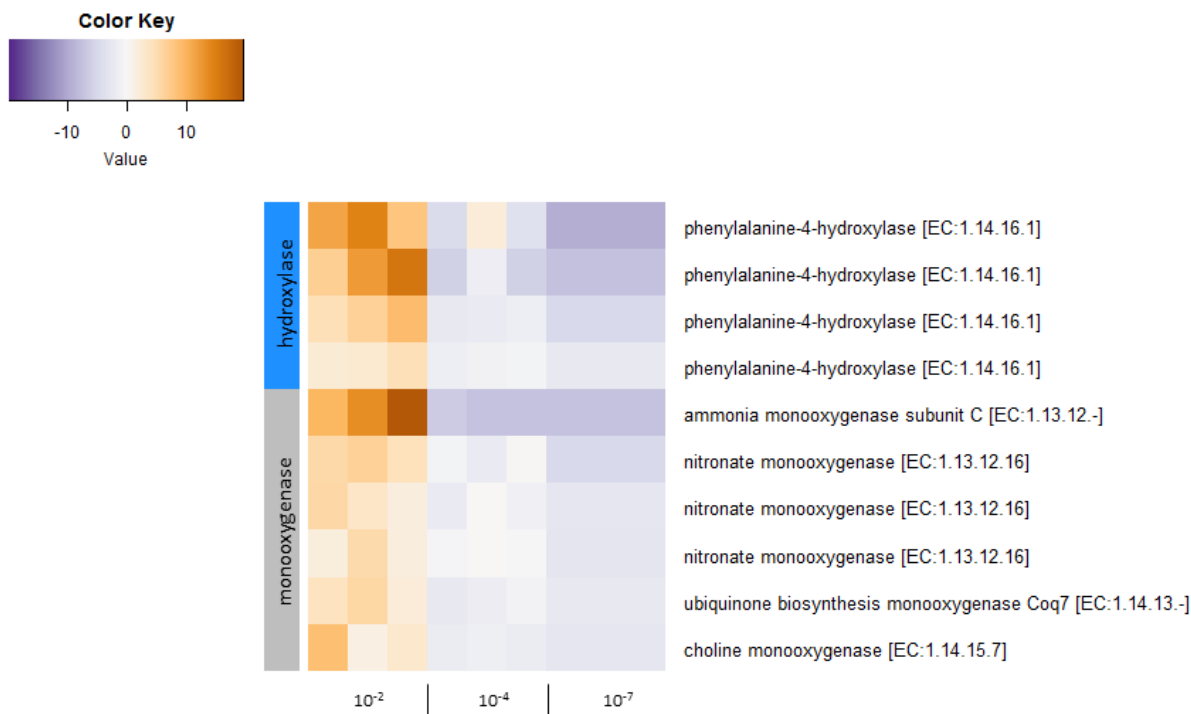


**Figure 6-6.** Relative expression of significantly differentially expressed genes (likelihood ratio,  $p_{adj} < 0.05$ ) that were also significantly associated with EE2 biotransformation (Spearman,  $p < 0.05$ ). The vertical bar on the left shows monooxygenase genes and hydroxylase genes. Expression value is relative to the average expression of that gene in all conditions. Genes with the same name are unique sequences that were annotated with the same KEGG Orthology.

We sought to establish whether genes that might have been involved in pharmaceutical biotransformation were lost across the dilution conditions. We conducted a two-sided Spearman's rank correlation test between the normalized expression of each gene and each compound's biotransformation rate to identify genes whose expression pattern was significantly associated with biotransformation rate. We then narrowed the list of genes by focusing on classes of metabolic genes that were predicted, according to the University of Minnesota's Pathway Prediction System (Ellis et al., 2006), to be involved in the compound's biotransformation. We focused on the

compounds that were transformed to a different extent with increased dilution (atenolol, EE2, trimethoprim, venlafaxine, and carbamazepine) and further narrowed the list of genes relevant to those compounds by selecting genes only if they were lost with increased dilution. The genes identified for each compound are provided in Appendix D. To illustrate the analysis with one compound, Figure 6-6 shows the genes that were significantly associated with EE2 biotransformation, predicted to be involved in EE2 transformation, and lost between the  $10^{-2}$  and the  $10^{-7}$  conditions. As expected, there were many monooxygenase and hydroxylase genes lost between the  $10^{-2}$  and the  $10^{-7}$  cultures that were positively associated with the rate of EE2 transformation. One specific gene that was lost was ammonia monooxygenase, which encodes for an enzyme that has previously been associated with catalyzing EE2 transformation in both pure (Khunjar et al., 2011) and mixed communities (Tran et al., 2009). We found the subunit C of the ammonia monooxygenase gene, which had 99% identity to ammonia monooxygenase of *Nitrosomonas* sp. Is79A3 over 270 amino acids, was both significantly differentially expressed across the dilution conditions (likelihood ratio,  $p_{\text{adj}} = 0.0003$ ) and significantly associated with EE2 biotransformation (Spearman,  $p = 0.038$ ). An OTU was also identified in the 16S rRNA data that was 99% similar over 253 nucleotides to *Nitrosomonas* sp. Is79A3. Additionally, the activity of this OTU decreased across the dilution conditions, and its relative activity significantly correlated with ammonia monooxygenase expression (Spearman,  $p = 0.017$ ). This demonstrates that statistical tests yielded genes encoding enzymes that may be mechanistically involved in pharmaceutical biotransformation. We further reasoned that this approach using statistical associations and knowledge of likely biochemical pathways could yield candidate genes linked to biotransformation for all of the compounds investigated. Candidate gene lists for each compound with KEGG Orthology numbers and descriptions, and heatmaps are provided in Appendix D.

## 6.4 Discussion

Our results provide further evidence that there is a strong positive association between taxonomic and functional diversity in wastewater microbial communities (Helbling et al., 2012). These results are consistent with a previous study on wastewater treatment plant microbial communities (Johnson et al., 2014a), and several other studies on microbial communities in other environments, which showed that communities with more taxa are likely to have more functional traits (Gilbert et al., 2010; Bryant et al., 2012). However, there are several other studies involving aquatic and soil microbial communities that observed inconsistent associations between taxonomic and functional richness (Fierer et al., 2012; Yergeau et al., 2012). This could be due in part to functional redundancy. We also observed this phenomenon as the shape of the association between taxonomic and functional genes was not linear; the number of functional genes did not increase at the same rate as the number of OTUs. This pattern indicated that there was a great deal of redundancy in the most diverse communities with respect to functional genes. Despite the functional redundancy, we observed that the functions responsible for the biotransformation of several compounds (atenolol, EE2, trimethoprim, and carbamazepine) were relatively rare because even with less than a 2.5% loss of expressed functional genes observed between the  $10^{-2}$  and  $10^{-4}$  dilution cultures, we found a significant reduction in the biotransformation rates.

For all of the compounds with significant associations with expressed functional genes (atenolol, trimethoprim, carbamazepine, venlafaxine, and collective; Figure 6-4), we also saw significant associations with RNA-based taxonomic richness. This indicates that for the purpose of understanding the relationship between biodiversity and function, amplicon sequencing of the 16S rRNA was a sufficient measure of biodiversity to test associations with process rates. This may not hold true in highly functionally redundant microbial communities, where expressed

taxonomic and functional diversity are not strongly associated with one another (e.g. a lake microbial community as observed by Ylla et al. (2013)). Using 16S rRNA to test relationships with biodiversity is advantageous because amplicon sequencing is more affordable, less computationally intensive because it generates a fraction of the data, easier to analyze, and has more developed reference databases compared with functional genes. But only by performing omics sequencing is it possible to test associations with specific genes and generate candidate gene lists that can be used to discover mechanistic links with biotransformation.

Despite not finding significant associations between biodiversity and pharmaceutical biotransformation rate for all the compounds studied, we were able to use statistical associations and biochemical knowledge about transformation pathways to identify candidate genes that could mediate transformation. For EE2, the biotransformation rate was significantly different between the  $10^{-2}$  and the  $10^{-4}$  dilution conditions (Figure 6-3), but there was not a significant association between taxonomic or functional richness and biotransformation rates (Figure 6-4). For this compound, we suspect that specific taxa and functional genes were lost between the  $10^{-2}$  and the  $10^{-4}$  conditions that were responsible for EE2 biotransformation, and thus additional dilution and reductions in diversity resulted in no further impact on EE2 biotransformation. We were able to identify *Nitrosomonas* sp. monooxygenase genes whose expression patterns co-varied significantly with EE2 biotransformation rates (Spearman,  $p < 0.05$ ; Figure 6-6), and thus corroborate this hypothesis. We therefore can conclude that EE2 biotransformation is a narrow process catalyzed by rare taxa expressing rare functions in the wastewater microbial community. Other compounds, such as erythromycin showed no significant associations with biodiversity and biotransformation rate. Biotransformation of erythromycin is therefore a broad process catalyzed by more abundant taxa or widespread functions in the wastewater microbial community.

We used gene expression to identify candidate metabolisms involved in biotransformation, but there were many challenges associated with this approach. Namely the number of significant associations that are generated with this approach yielded many candidate metabolisms and enzymes that are likely not directly involved in biotransformation. While statistical methods and knowledge of the metabolisms and compounds can be used to reduce the number of candidate genes, the list of candidate genes was nevertheless vast. Candidate genes require more controlled experiments in order to validate their direct (or indirect) involvement in biotransformation. Furthermore, because a loss of expression does not directly correlate with enzymatic activity (Maier et al., 2009; Vogel and Marcotte, 2012), candidate genes may not represent the proteins that were active in the experiment. Nevertheless, all of the compounds that had significant associations with richness had stronger associations with transcriptomic richness than genomic richness. Therefore, despite the limitations associated with this approach, transcriptomic data can be more powerful for generating predictive associations between enzymes and pharmaceutical biotransformation than genomic data.

One additional limitation of our omics data analysis was that the annotations were database dependent as we only included genes that could be annotated with the KEGG Orthology gene database. Only 33% of our significantly differentially expressed genes were annotated using this database. In reducing our data to those functions that have been annotated, we made the data analysis more manageable but also potentially underestimated functional diversity and richness. It also precluded our ability to identify novel functions that might be associated with pharmaceutical biotransformation.

In conclusion, we observed significant positive associations between biodiversity of wastewater treatment plant microbial communities and the rates of some individual

pharmaceuticals as well as the collective pharmaceutical biotransformation rates. By linking gene expression with individual pharmaceutical biotransformation rates, we identified metabolic genes that potentially encode for enzymes that were responsible catalyzing biotransformation. Further experimentation is needed to conclusively link those functions to biotransformation reactions. As models are developed to link microbial sequencing data to process rates in wastewater treatment, the associated genes may also be useful as biomarkers for predicting pharmaceutical biotransformation rates. The strong positive association between biodiversity and the collective rate of pharmaceutical biotransformation has implications for the design and operation of WWTPs to increase pharmaceutical removal. Specifically, creating niche environments that support the growth of diverse microbial communities could result in better overall performance with respect to pharmaceutical removal. Understanding the factors that drive microbial biodiversity in WWTPs such as redox environment, influent composition, solids residence time, and reactor configuration, and their impact on pharmaceutical biotransformation rates is needed to harness the benefits of biodiversity for wastewater treatment.

## 6.5 Literature cited

Anders, S.; Pyl, P. T.; Huber, W. HTSeq A Python Framework to Work with High-Throughput Sequencing Data. *Bioinformatics* **2014**, *31* (2), 166–169.

APHA; AWWA; WEF, Standard Methods for the Examination of Water and Wastewater. 21st Ed. Washington, D.C., **2005**.

Bryant, J. A.; Stewart, F. J.; Eppley, J. M.; DeLong, E. F. Microbial Community Phylogenetic and Trait Diversity Declines with Depth in a Marine Oxygen Minimum Zone. *Ecology* **2012**, *93* (7), 1659–1673.

Carballa, M.; Omil, F.; Lema, J. M.; Llompart, M.; García-Jares, C.; Rodríguez, I.; Gomez, M.; Ternes, T. Behavior of Pharmaceuticals, Cosmetics and Hormones in a Sewage Treatment Plant. *Water Res.* **2004**, *38* (12), 2918–2926.

Cardinale, B. J.; Srivastava, D. S.; Emmett Duffy, J.; Wright, J. P.; Downing, A. L.; Sankaran, M.; Jouseau, C. Effects of Biodiversity on the Functioning of Trophic Groups and Ecosystems. *Nature* **2006**, *443* (7114), 989–992.

Castiglioni, S.; Bagnati, R.; Fanelli, R.; Pomati, F.; Calamari, D.; Zuccato, E. Removal of Pharmaceuticals in Sewage Treatment Plants in Italy. *Environ. Sci. Technol.* **2005**, *40* (1), 357–363.

Cole, J. R.; Wang, Q.; Cardenas, E.; Fish, J.; Chai, B.; Farris, R. J.; Kulam-Syed-Mohideen, A. S.; McGarrell, D. M.; Marsh, T.; Garrity, G. M.; et al. The Ribosomal Database Project: Improved Alignments and New Tools for rRNA Analysis. *Nucleic Acids Res.* **2009**, *37*, D141–D145.

Cook, K. L.; Garland, J. L.; Layton, A. C.; Dionisi, H. M.; Levine, L. H.; Sayler, G. S. Effect of Microbial Species Richness on Community Stability and Community Function in a Model Plant-Based Wastewater Processing System. *Microb. Ecol.* **2006**, *52* (4), 725–737.

Duffy, J. E. Why Biodiversity Is Important to the Functioning of Real-World Ecosystems. *Front. Ecol. Environ.* **2008**, *7* (8), 437–444.

Ellis, L. B. M.; Roe, D.; Wackett, L. P. The University of Minnesota Biocatalysis/biodegradation Database: The First Decade. *Nucleic Acids Res.* **2006**, *34* (suppl 1), D517–D521.

Fierer, N.; Leff, J. W.; Adams, B. J.; Nielsen, U. N.; Bates, S. T.; Lauber, C. L.; Owens, S.; Gilbert, J. A.; Wall, D. H.; Caporaso, J. G. Cross-Biome Metagenomic Analyses of Soil Microbial Communities and Their Functional Attributes. *Proc. Natl. Acad. Sci.* **2012**, *109* (52), 21390–21395.

Franklin, R. B.; Mills, A. L. Structural and Functional Responses of a Sewage Microbial Community to Dilution-Induced Reductions in Diversity. *Microb. Ecol.* **2006**, *52* (2), 280–288.

- Gilbert, J. A.; Field, D.; Swift, P.; Thomas, S.; Cummings, D.; Temperton, B.; Weynberg, K.; Huse, S.; Hughes, M.; Joint, I. The Taxonomic and Functional Diversity of Microbes at a Temperate Coastal Site: A “Multi-Omic”study of Seasonal and Diel Temporal Variation. *PLoS One* **2010**, *5* (11), e15545.
- Grady, C. P. L. Jr.; Daigger, G. T.; Love, N. G.; Filipe, C. D. M. *Biological Wastewater Treatment*, 3rd ed.; CRC Press, **2011**.
- Green, J. L.; Bohannon, B. J. M.; Whitaker, R. J. Microbial Biogeography: From Taxonomy to Traits. *Science* **2008**, *320* (5879), 1039–1043.
- He, S.; Wurtzel, O.; Singh, K.; Froula, J. L.; Yilmaz, S.; Tringe, S. G.; Wang, Z.; Chen, F.; Lindquist, E. A.; Sorek, R. Validation of Two Ribosomal RNA Removal Methods for Microbial Metatranscriptomics. *Nat. Methods* **2010**, *7* (10), 807–812.
- Helbling, D. E.; Johnson, D. R.; Honti, M.; Fenner, K. Micropollutant Biotransformation Kinetics Associate with WWTP Process Parameters and Microbial Community Characteristics. *Environ. Sci. Technol.* **2012**, *46* (19), 10579–10588.
- Huang, M.; Li, Y.; Gu, G. Chemical Composition of Organic Matters in Domestic Wastewater. *Desalination* **2010**, *262* (1), 36–42.
- Johnson, D. R.; Helbling, D. E.; Lee, T. K.; Park, J.; Fenner, K.; Kohler, H. P. E.; Ackermann, M. Association of Biodiversity with the Rates of Micropollutant Biotransformations among Full-Scale Wastewater Treatment Plant Communities. *Appl. Env. Microbiol.* **2015**, *81* (2), 666–675.
- Johnson, D. R.; Lee, T. K.; Park, J.; Fenner, K.; Helbling, D. E. The Functional and Taxonomic Richness of Wastewater Treatment Plant Microbial Communities Are Associated with Each Other and with Ambient Nitrogen and Carbon Availability. *Environ. Microbiol.* **2014**, *17* (12), 4851–4860.
- Joshi, N. A.; Fass, J. N. Sickel: A Sliding-Window, Adaptive, Quality-Based Trimming Tool for FastQ Files. Version 1.33, **2011**.
- Kasprzyk-Hordern, B.; Dinsdale, R. M.; Guwy, A. J. The Removal of Pharmaceuticals, Personal Care Products, Endocrine Disruptors and Illicit Drugs during Wastewater Treatment and Its Impact on the Quality of Receiving Waters. *Water Res.* **2009**, *43* (2), 363–380.
- Kern, S.; Baumgartner, R.; Helbling, D. E.; Hollender, J.; Singer, H.; Loos, M. J.; Schwarzenbach, R. P.; Fenner, K. A Tiered Procedure for Assessing the Formation of Biotransformation Products of Pharmaceuticals and Biocides during Activated Sludge Treatment. *J. Environ. Monit.* **2010**, *12* (11), 2100–2111.
- Khunjar, W. O.; Mackintosh, S. A.; Skotnicka-Pitak, J.; Baik, S.; Aga, D. S.; Yi, T.; Jr., W. F. H.; Love, N. G. Elucidating the Relative Roles of Ammonia Oxidizing and Heterotrophic Bacteria



during the Biotransformation of 17 $\alpha$ -Ethinylestradiol and Trimethoprim. *Environ. Sci. Technol.* **2011**, *45* (8), 3605–3612.

Kolpin, D. W.; Furlong, E. T.; Meyer, M. T.; Thurman, E. M.; Zaugg, S. D.; Barber, L. B.; Buxton, H. T. Pharmaceuticals, Hormones, and Other Organic Wastewater Contaminants in U.S. Streams, 1999–2000: A National Reconnaissance. *Environ. Sci. Technol.* **2002**, *36* (6), 1202–1211.

Konopka, A. What Is Microbial Community Ecology? *ISME J.* **2009**, *3* (11), 1223–1230.

Kozich, J. J.; Westcott, S. L.; Baxter, N. T.; Highlander, S. K.; Schloss, P. D. Development of a Dual-Index Sequencing Strategy and Curation Pipeline for Analyzing Amplicon Sequence Data on the MiSeq Illumina Sequencing Platform. *Appl. Environ. Microbiol.* **2013**, *79* (17), 5112–5120.

Levine, U. Y.; Teal, T. K.; Robertson, G. P.; Schmidt, T. M. Agriculture's Impact on Microbial Diversity and Associated Fluxes of Carbon Dioxide and Methane. *ISME J.* **2011**, *5* (10), 1683–1691.

Li, H.; Durbin, R. Fast and Accurate Short Read Alignment with Burrows-Wheeler Transform. *Bioinformatics* **2009**, *25* (14), 1754–1760.

Li, H.; Handsaker, B.; Wysoker, A.; Fennell, T.; Ruan, J.; Homer, N.; Marth, G.; Abecasis, G.; Durbin, R.; Subgroup, 1000 Genome Project Data Processing. The Sequence Alignment/Map Format and SAMtools. *Bioinformatics* **2009**, *25* (16), 2078–2079.

Love, M. I.; Huber, W.; Anders, S. Moderated Estimation of Fold Change and Dispersion for RNA-Seq Data with DESeq2. *Genome Biol.* **2014**, *15* (12), 550.

Maier, T.; Güell, M.; Serrano, L. Correlation of mRNA and Protein in Complex Biological Samples. *FEBS Lett.* **2009**, *583* (24), 3966–3973.

Mettel, C.; Kim, Y.; Shrestha, P. M.; Liesack, W. Extraction of mRNA from Soil. *Appl. Environ. Microbiol.* **2010**, *76* (17), 5995–6000.

Midgley, G. F. Biodiversity and Ecosystem Function. *Science* **2012**, *335* (6065), 174–175.

Nakada, N.; Tanishima, T.; Shinohara, H.; Kiri, K.; Takada, H. Pharmaceutical Chemicals and Endocrine Disruptors in Municipal Wastewater in Tokyo and Their Removal during Activated Sludge Treatment. *Water Res.* **2006**, *40* (17), 3297–3303.

Oksanen, J.; Kindt, R.; Legendre, P.; O'Hara, B.; Stevens, M. H. H.; Oksanen, M. J.; Suggests, M. The Vegan Package. *Community Ecol. Packag.* **2007**.

Peng, Y.; Leung, H. C. M.; Yiu, S. M.; Chin, F. Y. L. IDBA-UD: A de Novo Assembler for Single-Cell and Metagenomic Sequencing Data with Highly Uneven Depth. *Bioinformatics* **2012**, *28* (11), 1420–1428.

Pérez-Osorio, A. C.; Williamson, K. S.; Franklin, M. J. Heterogeneous rpoS and rhlR mRNA

Levels and 16S rRNA/rDNA (rRNA Gene) Ratios within *Pseudomonas aeruginosa* Biofilms, Sampled by Laser Capture Microdissection. *J. Bacteriol.* **2010**, *192* (12), 2991–3000.

Peter, H.; Beier, S.; Bertilsson, S.; Lindström, E. S.; Langenheder, S.; Tranvik, L. J. Function-Specific Response to Depletion of Microbial Diversity. *ISME J.* **2010**, *5* (2), 351–361.

Philippot, L.; Spor, A.; Hénault, C.; Bru, D.; Bizouard, F.; Jones, C. M.; Sarr, A.; Maron, P.-A. Loss in Microbial Diversity Affects Nitrogen Cycling in Soil. *ISME J.* **2013**, *7* (8), 1609–1619.

Pholchan, M. K.; Baptista, J. de C.; Davenport, R. J.; Sloan, W. T.; Curtis, T. P. Microbial Community Assembly, Theory and Rare Functions. *Front. Microbiol.* **2013**, *4* (68), 1-9.

Schloss, P. D.; Westcott, S. L.; Ryabin, T.; Hall, J. R.; Hartmann, M.; Hollister, E. B.; Lesniewski, R. A.; Oakley, B. B.; Parks, D. H.; Robinson, C. J.; et al. Introducing Mothur: Open-Source, Platform-Independent, Community-Supported Software for Describing and Comparing Microbial Communities. *Appl. Env. Microbiol.* **2009**, *75* (23), 7537–7541.

Szabó, K. É.; Itor, P. O. B.; Bertilsson, S.; Tranvik, L.; Eiler, A. Importance of Rare and Abundant Populations for the Structure and Functional Potential of Freshwater Bacterial Communities. *Aquat. Microb. Ecol.* **2007**, *47* (1), 1–10.

Tran, N. H.; Urase, T.; Kusakabe, O. The Characteristics of Enriched Nitrifier Culture in the Degradation of Selected Pharmaceutically Active Compounds. *J. Hazard. Mater.* **2009**, *171* (1–3), 1051–1057.

Varricchio, F.; Monier, R. Ribosome Patterns in *Escherichia Coli* Growing at Various Rates. *J. Bacteriol.* **1971**, *108* (1), 105–110.

Vogel, C.; Marcotte, E. M. Insights into the Regulation of Protein Abundance from Proteomic and Transcriptomic Analyses. *Nat. Rev. Genet.* **2012**, *13* (4), 227–232.

Vuono, D. C.; Benecke, J.; Henkel, J.; Navidi, W. C.; Cath, T. Y.; Munakata-Marr, J.; Spear, J. R.; Drewes, J. E. Disturbance and Temporal Partitioning of the Activated Sludge Metacommunity. *ISME J.* **2015**, *9* (2), 425–435.

Yergeau, E.; Bokhorst, S.; Kang, S.; Zhou, J.; Greer, C. W.; Aerts, R.; Kowalchuk, G. A. Shifts in Soil Microorganisms in Response to Warming Are Consistent across a Range of Antarctic Environments. *ISME J.* **2012**, *6* (3), 692–702.

Ylla, I.; Peter, H.; Romani, A. M.; Tranvik, L. J. Different Diversity-Functioning Relationship in Lake and Stream Bacterial Communities. *FEMS Microbiol. Ecol.* **2013**, *85* (1), 95–103.

Zavaleta, E. S.; Pasari, J. R.; Hulvey, K. B.; Tilman, G. D. Sustaining Multiple Ecosystem Functions in Grassland Communities Requires Higher Biodiversity. *Proc. Natl. Acad. Sci.* **2010**, *107* (4), 1443–1446.

Zhang, T.; Shao, M.-F.; Ye, L. 454 Pyrosequencing Reveals Bacterial Diversity of Activated Sludge from 14 Sewage Treatment Plants. *ISME J.* **2011**, 6 (6), 1137–1147.

## **Chapter 7.**

### **Conclusions and Engineering Significance**

#### **7.1 Overview**

This dissertation evaluated the impact of DO concentration on pharmaceutical biotransformation during wastewater treatment. The objectives of this research align with a broader goal of advancing the sustainability of wastewater treatment systems, and navigating potential tradeoffs between energy use and water quality. This work began by demonstrating with bench-scale reactors that redox environment impacts the degree of pharmaceutical loss during treatment (Chapter 3). To better understand the mechanisms responsible for the observed differences between fully aerobic and low DO treatment, Chapters 4 – 6 focused on elucidating both direct and indirect impacts of DO concentration on pharmaceutical biotransformation rates. Bench-scale nitrifying bioreactors were used to demonstrate that DO concentration impacts microbial physiology and microbial community structure, and both of those in turn impact pharmaceutical biotransformation rates (Chapter 4). Chapter 5 focused on physiological impacts of DO concentration on pharmaceutical biotransformation, and Chapter 6 focused on the impact of biodiversity, one aspect of microbial community structure, on pharmaceutical biotransformation. Throughout this research, methods from analytical chemistry, microbial ecology, and process engineering were integrated to understand relationships between microbial

community characteristics and kinetics of microbial metabolism. The cumulative results of this dissertation show that it is possible to operate at lower bulk liquid DO concentrations (0.5 - 1 mg/L) without compromising pharmaceutical biotransformation. An outcome of this research is the opportunity to reduce the energy footprint of treatment. Major findings and their engineering significance are discussed in more detail below.

## **7.2 Main findings and significance**

### ***7.2.1 Direct impacts of DO concentration on pharmaceutical biotransformation rates***

DO can act as a limiting substrate and slow the rate of microbial metabolism, thereby reducing the rate of pharmaceutical biotransformations. Affinity constants, such as the oxygen half saturation constants ( $K_{O_2}$ ), are used to model the effect of substrate limitation on process rates. Oxygen half saturation constants for heterotrophs and nitrifiers are commonly used in wastewater treatment plant models such as the Activated Sludge Model (Henze, 2000). Incorporating pharmaceutical fate into existing activated sludge models is an active area of research (Plósz et al., 2012; Clouzot et al., 2013) and the utility of these models is a function of the kinetic parameters that they employ. To our knowledge, no previous studies have published oxygen half saturation constants to describe pharmaceutical biotransformation rates. The values presented in Chapter 5 were all within the range or lower than the values used for heterotrophs and nitrifiers, suggesting that DO concentration will not disproportionately impact pharmaceutical biotransformation rates and operating at a high DO concentration will not result in greater overall pharmaceutical removal.

While pharmaceuticals are not currently regulated pollutants in the U.S., their presence in wastewater effluents has garnered public attention (Dean, 2007; Israel, 2010), and even stalled water reuse projects (Macmillan, 2012). Utilities and consulting firms performed monitoring studies in response to concerns over the wide proliferation of pharmaceuticals and other trace

organic compounds in wastewater effluents (e.g. U.S. EPA, 2009). As utilities aim to minimize the discharge of these compounds into the environment or consider water reuse schemes, the ability to use modeling to inform pharmaceutical fate during wastewater treatment will become increasingly powerful. Time and resource intensive monitoring studies could be supplemented with modeling approaches to evaluate and optimize treatment scenarios and minimize impacts on receiving waters. Integrated wastewater process models and ecotoxicity models are also increasingly being used to inform regulatory decisions (Clouzot et al., 2013). With validated models that predict pharmaceutical fate, regulators will be better suited to develop policies and guidelines to control pharmaceutical emissions and support technologies that reduce environmental impacts (Stadler et al., 2012). The results of Chapter 5 have the opportunity to be incorporated into existing pharmaceutical fate models and in particular to inform utilities that are using or considering low DO treatment processes.

We also identified specific phylogenetic groups that significantly associated with individual pharmaceutical biotransformation rates. Engineering wastewater treatment processes to enhance biotransformation of specific or groups of pharmaceuticals requires knowledge about which organisms are involved or strongly correlated with their removal, and how treatment process environments influence their abundance and activity. Genomic methods have advanced our understanding of the microorganisms responsible for carbon, nitrogen, and phosphorus transformations and led to improved process designs (e.g. Martin et al., 2006; Yu et al., 2010; Smith et al., 2015). The use of these methods to advance pharmaceutical biotransformation during treatment is, in comparison, in its infancy. The results of this dissertation add to the existing (and currently limited) body of knowledge of specific phylogenetic groups that are strongly associated with pharmaceutical removal and how DO concentration impacts their activity.

### ***7.2.2 Indirect impacts of DO on pharmaceutical biotransformation rates***

Long-term DO concentration shapes the microbial community, thereby impacting pharmaceutical biotransformation rates. In Chapter 4 we found that long-term low DO conditions resulted in a greater biomass concentration than fully aerobic conditions, likely due to reduced biomass decay. Greater overall biomass in the low DO reactor resulted in net biotransformation rates comparable to those under non-limiting DO conditions, despite lower specific activity with respect to ammonia oxidation and pharmaceutical biotransformation rates. In addition, we found that the low DO reactor supported the growth of a more diverse microbial community. We further showed that microbial diversity was strongly correlated with the collective rate of pharmaceutical biotransformation in Chapter 6.

These results have important implications for the design and operation of WWTPs. First, the results support those of other studies (Bellucci et al., 2011; Jimenez et al., 2011; Liu and Wang, 2013) that show that stable and complete nitrification is possible at a DO concentration less than 0.5 mg/L, suggesting substantial energy savings are possible by reducing aeration. While energy savings are possible, reduced aeration may also mean a loss of capacity for many nitrifying WWTPs. Operating at a DO concentration close to the nitrifier oxygen half saturation constant will result in reduced specific growth rates, and thus require an increase in SRT to achieve the same effluent quality. If SRT must increase to enable reductions in aeration, then capacity is lost in terms of aeration tank and clarifier volume. WWTPs at or near their design capacity are thus unlikely to adopt low DO treatment strategies, while smaller WWTPs with large SRT safety factors are better suited to implement reduced aeration at the expense of a loss of capacity.

Another impact of long-term low DO treatment is that it could select for high-oxygen affinity organisms at the expense of lower substrate utilization rates if there is a biochemical

tradeoff between substrate affinity and maximum substrate utilization rate (Gudelj et al., 2007). If this occurs, then biomass concentrations will have to be greater to achieve the same level of treatment. In addition, reduced decay in low DO conditions could also result in biomass with lower specific activity if low DO inhibits the hydrolysis of cell debris as opposed to the endogenous decay rate (Liu and Wang, 2015). Increasing biomass concentrations will result in greater sludge handling requirements. Therefore, increased sludge production and its associated energy inputs and costs need to be balanced against energy savings from aeration.

Our findings also show that limiting DO can be a driver of microbial biodiversity, and thus result in a greater collective rate of pharmaceutical biotransformation. Additional research is needed to understand what the main drivers of microbial biodiversity are in wastewater treatment systems. In addition to redox conditions, many other factors may influence the biodiversity of a treatment system such as SRT, influent substrate composition and concentration, temperature, and reactor configuration. The relative importance of DO as a driver of biodiversity is not known. The results of this research align with previous research that shows biodiversity is linked to enhanced productivity, resilience, and resistance to disturbances (Cardinale et al., 2006, 2012; Allison and Martiny, 2008). Identifying specific taxa and enzymes that are responsible for contaminant transformations is one outcome of this research, but the importance of supporting a diverse microbial community must not be overlooked. Lessons learned from bioremediation efforts continue to ring true; for example, an understanding of the whole microbial community is essential, not just the microorganisms responsible for contaminant transformations, as the community can affect the behavior of an individual microorganisms through synergistic and competitive interactions. An outcome of this research is to link the design and operation of WWTPs with the microbial communities they support to enhance treatment performance.



### 7.3 Future research

The studies presented in this dissertation could enable engineers to responsibly implement energy-saving strategies that employ reduced aeration and predict its consequences on pharmaceutical biotransformation during treatment. Additional research on aeration strategies and control systems is needed to optimize the benefits of biodiversity while avoiding conditions that reduce biotransformation rates due to oxygen limitation. Cycling between low and high DO environments is one possible strategy for both enhancing pharmaceutical biotransformation by supporting a diverse microbial community while also providing non oxygen-limiting conditions to enable maximum biotransformation rates. With advances in dissolved oxygen probes and aeration feedback control systems, these strategies will become more feasible for WWTPs to implement.

Additional research is needed to understand how low DO treatment impacts biotransformation pathways and the resulting transformation products. A better understanding of the stability and ecotoxicity of transformation products formed in low DO environments and how they differ from high DO systems is needed to ensure that energy saving strategies that exacerbate effluent ecotoxicity are not implemented. Future research should focus on comparing the toxicity of effluents from WWTPs employing different aeration strategies, identifying specific transformation products of environmental concern, and designing treatment strategies that result in mineralization or benign and environmentally stable products.

Wastewater treatment systems are model systems for microbial ecology, and this research has potential to spark further research on the ecology of wastewater microbial communities, such as the biochemical tradeoff between substrate affinity and maximum substrate utilization rate as a driver of diversification, and the relationship between functional redundancy and process stability. Ultimately, a deeper understanding of the microorganisms that are central to the success of

wastewater treatment will empower engineers to design more sustainable and resilient treatment systems.

## 7.4 Literature cited

- Allison, S. D.; Martiny, J. B. H. Resistance, Resilience, and Redundancy in Microbial Communities. *Proc. Natl. Acad. Sci.* **2008**, *105* (Supplement 1), 11512–11519.
- Bellucci, M.; Ofițeru, I. D.; Graham, D. W.; Head, I. M.; Curtis, T. P. Low-Dissolved-Oxygen Nitrifying Systems Exploit Ammonia-Oxidizing Bacteria with Unusually High Yields. *Appl. Env. Microbiol.* **2011**, *77* (21), 7787–7796.
- Cardinale, B. J.; Srivastava, D. S.; Emmett Duffy, J.; Wright, J. P.; Downing, A. L.; Sankaran, M.; Jouseau, C. Effects of Biodiversity on the Functioning of Trophic Groups and Ecosystems. *Nature* **2006**, *443* (7114), 989–992.
- Cardinale, B. J.; Duffy, J. E.; Gonzalez, A.; Hooper, D. U.; Perrings, C.; Venail, P.; Narwani, A.; Mace, G. M.; Tilman, D.; Wardle, D. A. Biodiversity Loss and Its Impact on Humanity. *Nature* **2012**, *486* (7401), 59–67.
- Clouzot, L.; Choubert, J.-M.; Cloutier, F.; Goel, R.; Love, N. G.; Melcer, H.; Ort, C.; Patureau, D.; Plósz, B. G.; Pomiès, M. Perspectives on Modelling Micropollutants in Wastewater Treatment Plants. *Water Sci. Technol.* **2013**, *68* (2), 448–461.
- Dean, C. Drugs Are in the Water. Does It Matter? *New York Times*. April 3, 2007.
- Gudelj, I.; Beardmore, R. E.; Arkin, S. S.; MacLean, R. C. Constraints on Microbial Metabolism Drive Evolutionary Diversification in Homogeneous Environments. *J. Evol. Biol.* **2007**, *20* (5), 1882–1889.
- Henze, M. *Activated Sludge Models ASM1, ASM2, ASM2d and ASM3*; IWA publishing, **2000**.
- Israel, B. Pharmaceutical Waste Seeping into Environment. *LiveScience*. June 4, 2010.
- Jimenez, J.; Dold, P.; La Motta, E.; Houweling, D.; Bratby, J.; Parker, D. Simultaneous Biological Nutrient Removal in a Single-Stage, Low Oxygen Aerobic Reactor. *Proc. Water Environ. Fed.* **2011**, 31–48.
- Liu, G.; Wang, J. Long-Term Low DO Enriches and Shifts Nitrifier Community in Activated Sludge. *Environ. Sci. Technol.* **2013**, *47* (10), 5109–5117.
- Liu, G.; Wang, J. Modeling Effects of DO and SRT on Activated Sludge Decay and Production. *Water Res.* **2015**, *80*, 169–178.
- Macmillan, L. Those Snowy Slopes, Sprayed With Wastewater. *New York Times*. Oct. 10, 2012.
- Martin, H. G.; Ivanova, N.; Kunin, V.; Warnecke, F.; Barry, K. W.; McHardy, A. C.; Yeates, C.; He, S.; Salamov, A. A.; Szeto, E.; et al. Metagenomic Analysis of Two Enhanced Biological Phosphorus Removal (EBPR) Sludge Communities. *Nat. Biotechnol.* **2006**, *24* (10), 1263–1269.

Plósz, B. G.; Langford, K. H.; Thomas, K. V. An Activated Sludge Modeling Framework for Xenobiotic Trace Chemicals (ASM-X): Assessment of Diclofenac and Carbamazepine. *Biotechnol. Bioeng.* **2012**, *109* (11), 2757–2769.

Smith, A. L.; Skerlos, S. J.; Raskin, L. Membrane Biofilm Development Improves COD Removal in Anaerobic Membrane Bioreactor Wastewater Treatment. *Microb. Biotechnol.* **2015**, *8* (5), 883–894.

Stadler, L. B.; Ernstoff, A. S.; Aga, D. S.; Love, N. G. Micropollutant Fate in Wastewater Treatment: Redefining “Removal.” *Environ. Sci. Technol.* **2012**, *46* (19), 10485–10486.

U.S. EPA. Occurrence of Contaminants of Emerging Concern in Wastewater From Nine Publicly Owned Treatment Works, *EPA-821-R-09-009*; **2009**.

Yu, R.; Kampschreur, M. J.; Loosdrecht, M. C. M. van; Chandran, K. Mechanisms and Specific Directionality of Autotrophic Nitrous Oxide and Nitric Oxide Generation during Transient Anoxia. *Environ. Sci. Technol.* **2010**, *44* (4), 1313–1319.

## **Appendices**

## Appendix A.

### Supplementary Information for Chapter 3

#### Effect of Redox Conditions on Pharmaceutical Loss during Biological Wastewater Treatment using Sequencing Batch Reactors

##### A1. Reactor influent preparation

Primary effluent collected from the local wastewater treatment plant was supplemented with acetate, glycerol, and yeast extract (equal parts as COD) and ammonium chloride to reach a soluble COD (sCOD) concentration of 250 mg/L and 25 mg-NH<sub>4</sub>-N/L. Micronutrients were added in proportion to the sCOD supplement according to Grady et al. (2011) (Table A1).

**Table A1.** Micronutrient solution used to supplement influent feed, 5 mL added per 100 mg-COD/L supplemented.

Mineral Salt	Concentration in micronutrient stock (g/L)
MgSO <sub>4</sub> *7H <sub>2</sub> O	1.8
MnSO <sub>4</sub> *H <sub>2</sub> O	0.054
ZnCl <sub>2</sub>	0.018
CuCl <sub>2</sub> *2H <sub>2</sub> O	0.006
CoCl <sub>2</sub> *6H <sub>2</sub> O	0.0002
Na <sub>2</sub> MoO <sub>4</sub> *2H <sub>2</sub> O	0.0003
CaCl <sub>2</sub>	0.72
FeCl <sub>2</sub> *4H <sub>2</sub> O	0.187
K <sub>2</sub> HPO <sub>4</sub> *3H <sub>2</sub> O	3.4

## A2. LC/MS/MS analysis of pharmaceuticals

**Table A2.** Multiple reaction monitoring (MRM) parameters with retention times for each target compound (CE = collision energy)

Compound Name	Retention Time (min)	Precursor Ion ( <i>m/z</i> )	Primary Product Ion ( <i>m/z</i> )	Secondary Product Ion ( <i>m/z</i> )	Fragmentor (V)	CE (eV)
Atenolol	2.2	267	145.1	74	155	27/23
d <sub>7</sub> -Atenolol	2.2	274.3	145.1	79.1	157	26/22
Trimethoprim	6.5	291.2	230.1	123	155	23/27
d <sub>9</sub> -Trimethoprim	6.3	300.2	234.2	123.1	160	26/26
Desvenlafaxine	9.4	264.4	246.2	58.1	74	7/19
d <sub>6</sub> -Desvenlafaxine	9.4	270.4	252.3	58.1	99	10/18
Sulfamethoxazole	10.8	254.1	108	92	64	23/23
d <sub>4</sub> -Sulfamethoxazole	10.8	258.1	111.9	96.3	107	26/30
Phenytoin	12.6	253.1	182.1	104	104	15/39
d <sub>10</sub> -Phenytoin	12.6	263.2	192.1	109.1	32	18/38

**Gradient used for compound separation:** The mobile phase A was water+0.3% formic acid and B was acetonitrile. The gradient profile used was as follows: 90% A was held for 1.5 min, ramped to 95% of B over 10.5 min, held at 95% B for 2 minutes, and finally returned to 100% of A over 1 min.

**Instrument detection limits:** A series of standard solutions with concentrations of 0.1, 0.5, 1, 5 and 10 ppb were prepared and run on LC/MS/MS using the method we developed. Peaks were checked to see if they were well defined based on the shape, retention time, ratio of qualifier and quantifier. A range of instrument detection limit for each compound was determined based on the lowest detectable concentration and highest non-detectable concentration (Table A2).

**Method detection limit:** Because there are always native forms of pharmaceuticals in the real wastewater samples, the method detection limits for pharmaceuticals cannot be measured directly. In fact, the method detection limits were explored based on the assumption that the deuterated form of compounds has the same value as the native form. The signal of deuterated

pharmaceuticals from 7 blank samples (influent and effluent matrix without spiking deuterated pharmaceuticals) were measured, and the mean value ( $y_{\text{blank}}$ ) was calculated. Samples with concentrations of deuterated compounds about 1 to 5 times higher than the estimated instrument detection limits were prepared, and signal from 7 replicates ( $y_{\text{sample}}$ ) were measured. The standard deviation ( $s$ ) of the 7 measurements was computed.

The minimum detectable signal,  $y_{\text{dl}}$ , is defined as:  $y_{\text{dl}} = y_{\text{blank}} + 3s$

The corrected signal,  $y_{\text{sample}} - y_{\text{blank}}$ , is proportional to sample concentration:

$$y_{\text{sample}} - y_{\text{blank}} = m \times [\text{sample concentration}]$$

With  $y_{\text{sample}}$ ,  $y_{\text{blank}}$  measured and sample concentration known,  $m$  can be calculated.

Detection limit: Minimum detectable concentration =  $\frac{3s}{m}$

Then we convert the minimum detectable concentration into the original concentration before SPE to get the method detection limit (Table A3).

**Table A3.** Method detection limit using 100 mL for solid phase extraction (LOD = limit of detection)

Compounds	Estimated Instrument LOD for Native Form Compounds (ppb)	Method LOD for Primary Samples (ppt)	Method LOD for Samples from Reactor A (ppt)	Method LOD for Samples from Reactor C (ppt)
d <sub>7</sub> -Atenolol	0.5~1	62.2	36.0	26.6
d <sub>9</sub> -Trimethoprim	0.1~0.5	46.9	24.5	21.5
d <sub>6</sub> -Desvenlafaxine	<0.1	6.7	6.8	9.3
d <sub>4</sub> -Sulfamethoxazole	~0.1	48.5	80.5	22.0
d <sub>10</sub> -Phenytoin	0.5~1	25.4	43.3	38.0



### A3. Cross-cycle profile of atenolol in anoxic/aerobic reactor (A)

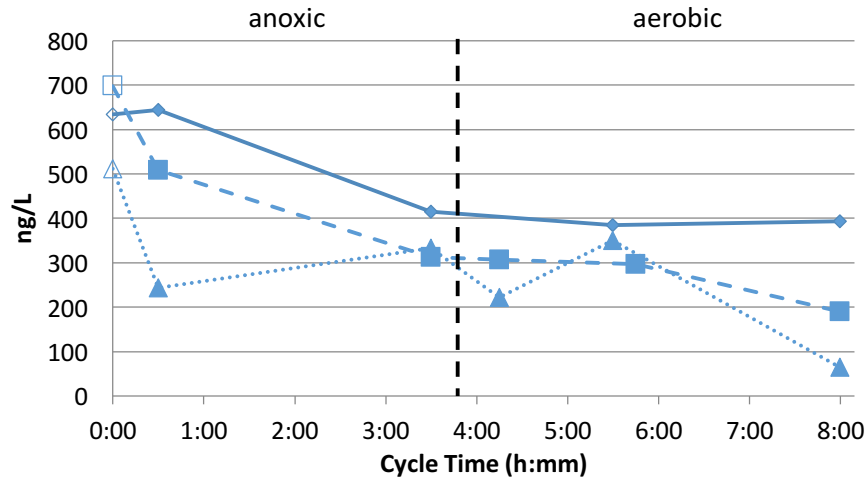


**Figure A1.** Cross-cycle concentrations of atenolol in the anoxic/aerobic SBR (reactor A) collected on three separate dates (day 287, 331, and 349 of operation shown as diamonds, squares, and triangles, respectively). Open symbols are calculated theoretical values based on influent concentration\*(2/3) + previous cycle effluent concentration\*(1/3). Dashed line indicates where aeration began during the reaction cycle.

**Table A4.** Percent loss across reaction cycle for atenolol and sulfamethoxazole where percent loss is calculated as ((concentration at cycle time=0) – (concentration at cycle time=8hr))/(concentration at cycle time=0)\*100% based on cross-cycle sampling

	Anoxic/Aerobic (A) (n=3)	Aerobic (B) (n=2)	Microaerobic (C) (n=3)	Microaerobic (D) (n=3)
Atenolol	66 ± 25	85 ± 22	53 ± 8	52 ± 1
Sulfamethoxazole	24 ± 10	29 ± 26	39 ± 31	45 ± 14

#### A4. Conjugated forms of sulfamethoxazole and desvenlafaxine

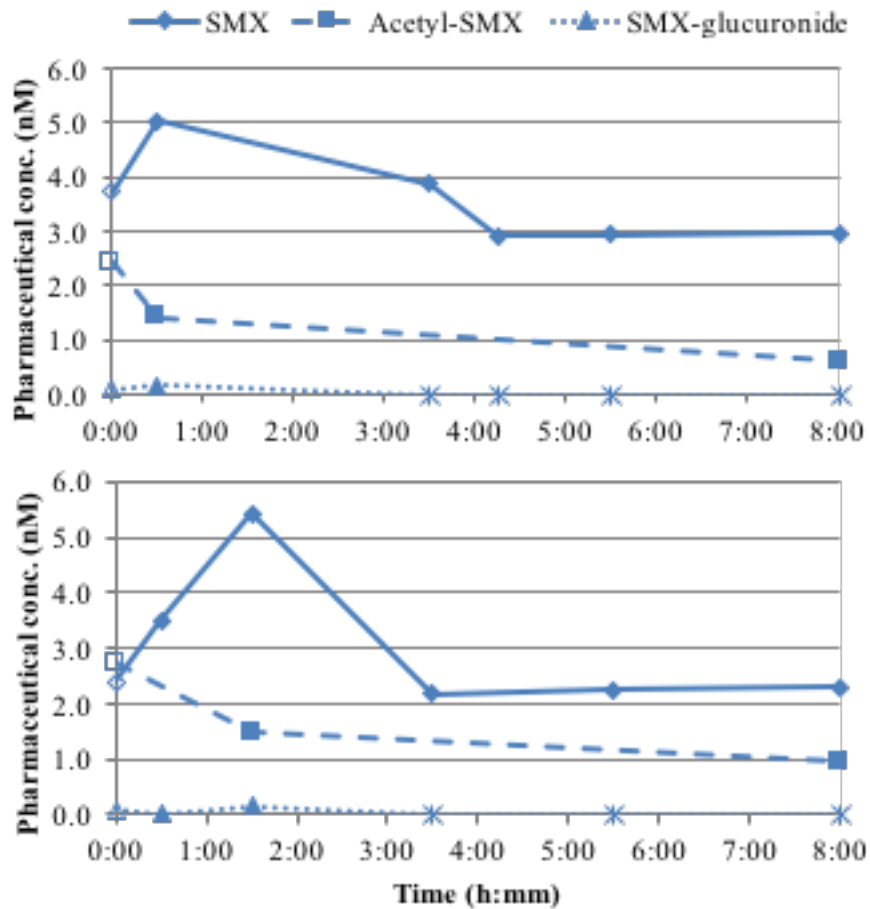


**Figure A2.** Cross-cycle concentrations of sulfamethoxazole (SMX), acetyl-sulfamethoxazole (acetyl-SMX), and sulfamethoxazole-glucuronide (SMX-gluc) in select samples from the anoxic/aerobic SBR (reactor A; top) and the microaerobic SBR (reactor C; bottom). Open symbols are calculated theoretical values based on influent concentration\*(2/3) + previous cycle effluent concentration\*(1/3) and asterisks signify values that were below the detection limit. Table A5. Average system removal (%) of venlafaxine-family compounds (DVF = desvenlafaxine; DVF-glu = desvenlafaxine-glucuronide; VLF = venlafaxine)

**Table A5.** Average system removal (%) of venlafaxine-family compounds (DVF = desvenlafaxine; DVF-glu = desvenlafaxine-glucuronide; VLF = venlafaxine)

	Anoxic/Aerobic (A)	Aerobic (B)	Microaerobic (C)	Microaerobic (D)
DVF	-20 ± 17	-16 ± 15	-26 ± 12	-18 ± 14
DVG*	>99	>99	>99	>99
VLF	1.2 ± 20	8.5 ± 12	1.2 ± 23	6.0 ± 10
DVF+DVG+VLF	-5.3 ± 16	0.1 ± 12	-8.4 ± 14	-1.1 ± 10

\*No standard deviation reported for DVG because of concentrations were below detection for majority of reactor effluent samples.

### Literature cited

Grady, C. P. L. Jr.; Daigger, G. T.; Love, N. G.; Filipe, C. D. M. *Biological Wastewater Treatment*, 3rd ed.; CRC Press, **2011**.

## Appendix B.

### Supplementary Information for Chapter 4

#### Impact of microbial physiology and microbial community structure on pharmaceutical fate driven by dissolved oxygen concentration in nitrifying bioreactors

##### Parent reactor influent media recipe

**Table B1.** Parent reactor influent media

<b>Compound</b>	<b>Concentration (mg/L)</b>
(NH <sub>4</sub> )HCO <sub>3</sub>	1110
MgSO <sub>4</sub> *7H <sub>2</sub> O	6.6
MgCl <sub>2</sub> *6H <sub>2</sub> O	5.0
CaCl <sub>2</sub> *2H <sub>2</sub> O	6.0
K <sub>2</sub> HPO <sub>4</sub> (dibasic)	16
Na <sub>2</sub> MoO <sub>4</sub> *2H <sub>2</sub> O	0.010
MnSO <sub>4</sub> *H <sub>2</sub> O	0.045
CoCl <sub>2</sub> *7H <sub>2</sub> O	0.00040
ZnCl <sub>2</sub>	0.060
CuCl <sub>2</sub> *2H <sub>2</sub> O	0.17
Chelated iron	0.44
H <sub>3</sub> BO <sub>3</sub>	0.013

##### Nitrate-N method

Nitrate samples were stored in plastic centrifuge tubes at 4°C until analysis, which was performed within 1 week of sampling. Nitrate concentrations were determined via duplicate

injections using a DX-100 Ion Chromatograph (Dionex; Sunnyvale, California) with RFIC IonPac AG16 guard column, an IonPac AS14 analytical column, and eluent containing 3.5 mM Na<sub>2</sub>CO<sub>3</sub> and 1.0 mM NaHCO<sub>3</sub>.

### **qPCR standard curve generation**

qPCR standards were prepared by collecting three 50 mL samples from both parent reactors over two weeks of stable operation, extracting DNA from the biomass samples, and subsequently combining the DNA extracts at equal concentrations to generate a community DNA pool. PCR was used to amplify the *amoA* gene in the pooled DNA sample using the primers amoA-1F (5'-GGGGTTTCTACTGGTGGT-3') and amoA-2R (5'-CCCCTCKGSAAAGCCTTCTTC-3') (Rotthauwe et al., 1997). Each 20 µL reaction volume consisted of 10 µL of 2x Phusion Flash High-Fidelity PCR Master Mix (Thermo Fisher Scientific, Waltham, MA), 0.2 µL each of 50 µM forward and reverse primer (final concentration of 50 µM), 0.12 µL of 50 mg/mL bovine serum albumin (final concentration of 0.3 mg/mL), 7.48 µL of nuclease-free water, and 2 µL of a mixture of the DNA extracts and nuclease free water that resulted in a final DNA concentration of approximately 2 ng per reaction. Thermocycling conditions were as follows: 5 minutes at 95°C, followed by 35 cycles of 45 seconds at 95°C, 45 seconds at 55°C, and 45 seconds at 72°C, and a final extension of 5 minutes at 72°C. The PCR products (amplified *amoA* gene) was visualized by 1.5% agarose gel electrophoresis and resulted in a single band at the expected amplicon size (491 bp). The band was excised from the gel using a sterile scalpel and the PCR products were purified using the QIAquick Gel Extraction Kit (Qiagen, Valencia, CA). The DNA concentration of the purified amplicon pool was determined via Quantifluor dsDNA and fluorospectrometry. Serial dilutions of the purified amplicon pool were used as qPCR standards ranging from 10<sup>8</sup> to 10<sup>2</sup> copies.

## LC/HRMS analysis of pharmaceuticals

**Table B2.** Target compounds with accurate mass and retention times used for quantification

Compound	Formula	Accurate mass (m/z)	Retention time (min)	ESI mode
Trimethoprim	C14H18N4O3	291.14516	6.67	positive
d9-trimethoprim	C14H9D9N4O3	300.20165	6.62	positive
Sulfamethoxazole	C10H11N3O3S	254.05938	7.23	positive
d4-sulfamethoxazole	C10H7D4N3O3S	258.08449	7.22	positive
EE2	C20H24O2	279.17434	10.96	positive
d4-EE2	C20H20D4O2	283.19944	10.95	positive
Atenolol	C14H22N2O3	267.17031	4.92	positive
d7-atenolol	C14H15D7N2O3	274.21425	4.88	positive
Venlafaxine	C17H27NO2	278.21145	8.97	positive
d6-venlafaxine	C17H21D6NO2	284.24911	8.94	positive
Caffeine	C8H10N4O2	195.08765	6.83	positive
d9-Caffeine	C8HD9N4O2	204.14414	6.80	positive
Carbamazepine	C15H12N2O	237.10223	9.59	positive
d8-Carbamazepine	C15H4D8N2O	245.15245	9.54	positive
Glyburide	C23H28CIN3O5S	494.15109	11.23	positive
d11-Glyburide	C23H17D11CIN3O5S	505.22014	11.20	positive
Acetaminophen	C8H9NO2	152.07060	5.25	positive
d3-Acetaminophen	C8H6D3NO2	155.08943	5.22	positive
Acetyl-sulfamethoxazole	C12H13N3O4S	296.06995	8.11	positive
Ibuprofen	C13H18O2	205.12231	11.61	negative
d3-ibuprofen	C13H15D3O2	208.14241	11.60	negative
Naproxen	C14H14O3	229.08592	10.64	negative
d3-Naproxen	C14H11D3O3	232.10475	10.62	negative

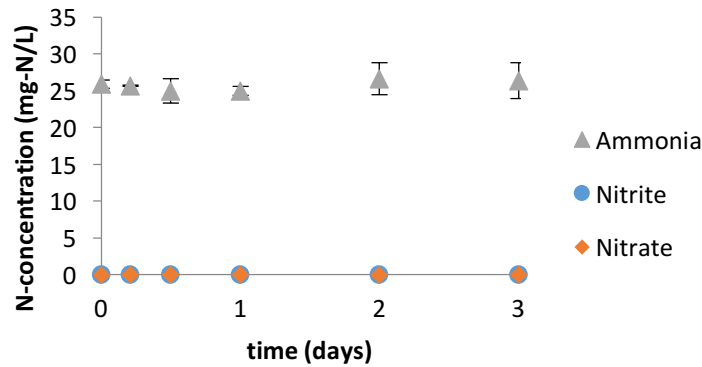
### Gradient used for compound separation

The mobile phase A was water + 0.1% formic acid and B was methanol + 0.1 % formic acid. The flow rate was 0.175 mL/min and the gradient profile used was as follows: 90% A was held for 3 min, ramped to 90% of B over 8 min, held at 90% B for 1 minutes, flow rate increased to 0.25 mL/min over 0.2 minutes and held at 0.25 ml/min for 1.8 minutes, and finally returned to 90% of A and 0.175 mL/min over 0.2 min.

## Allylthiourea inhibited batches

Duplicate batch reactors were supplemented with 10 mg/L of allylthiourea (ATU) to inhibit ammonia oxidation. Complete ammonia oxidation inhibition was confirmed by measuring the concentration of ammonia, nitrite, and nitrate-N across the batch experiments (Figures B1-a and B1-b). Ammonia concentrations did not change significantly across the batch experiments and no production of nitrite or nitrate was observed, indicating ATU halted ammonia oxidation.

a.



b.

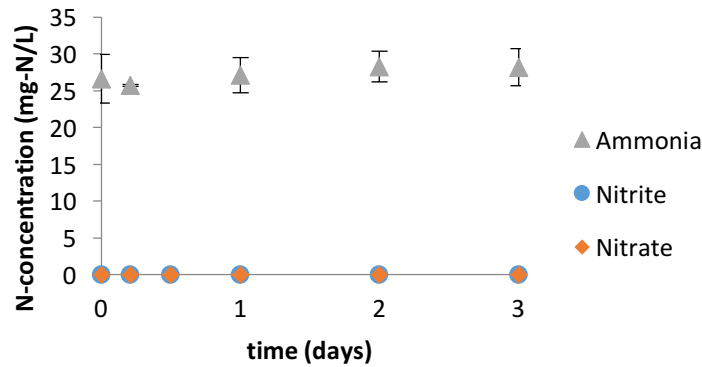
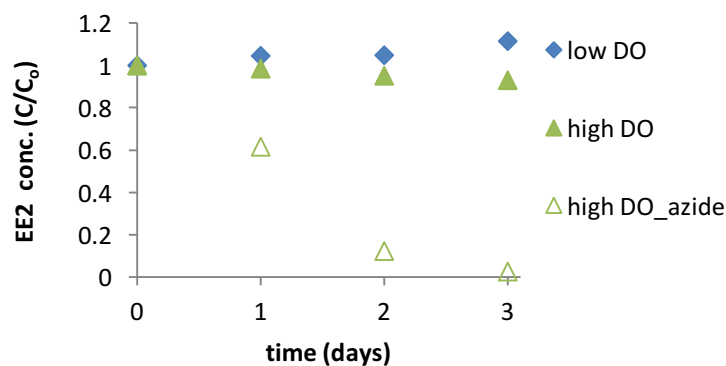


**Figure B1.** Concentration profiles of ammonia-, nitrite-, and nitrate-N in batch reactors supplemented with 10 mg/L ATU using biomass from the low DO (a) and high DO (b) parent reactors. Markers represent the average concentration of the duplicate batch reactors and error bars represent the concentration range.

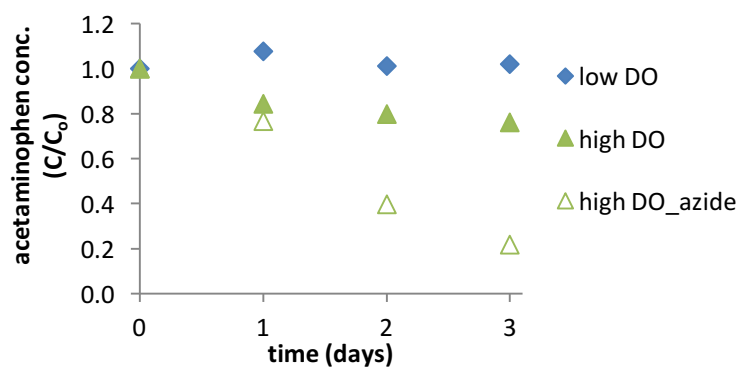
## Abiotic reactions with sodium azide under high DO conditions

Abiotic reactions with the pharmaceuticals were investigated by performing batch experiments without biomass, using media with and without sodium azide present (0.1 % w/v). We observed losses of EE2 and acetaminophen in the presence of sodium azide, indicating abiotic reactions occurred between sodium azide and those compounds (Figures B2-a and B2-b). Thus, losses in the azide-inactivated flasks should not be considered true controls.

a.

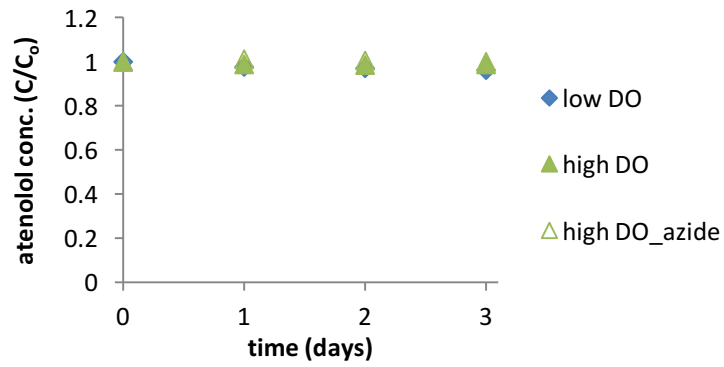


b.





c.



d.

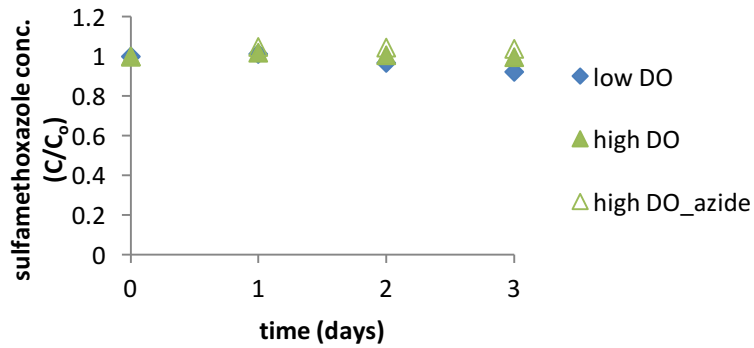
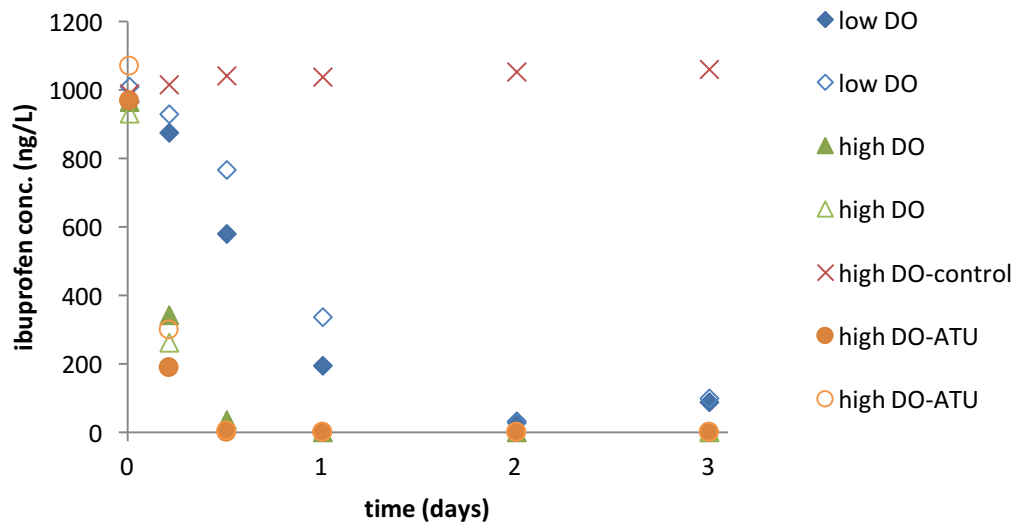


**Figure B2.** Concentration profiles of EE2 (a), acetaminophen (b), atenolol (c), and sulfamethoxazole (d) in abiotic batch experiments performed with media and sodium azide. Blue markers represent low DO batch conditions ( $DO = 0.2 - 0.3$  mg/L) and green markers represent high DO batch conditions (fully aerated,  $DO > 4$  mg/L)

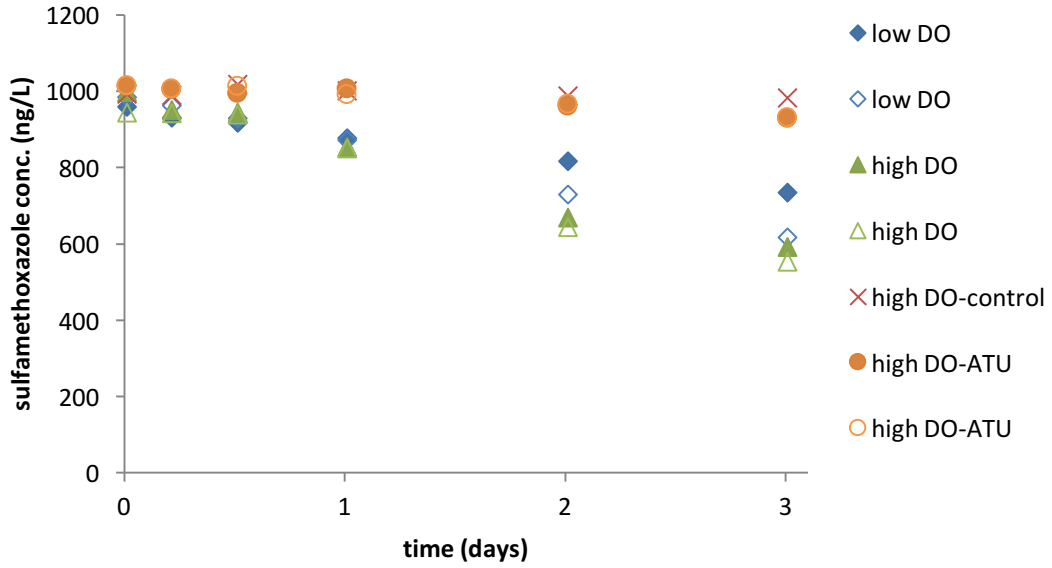
### Low DO parent reactor batch experiments

Concentration profiles for batch experiments using the low DO parent reactor biomass are presented in Figure B3.

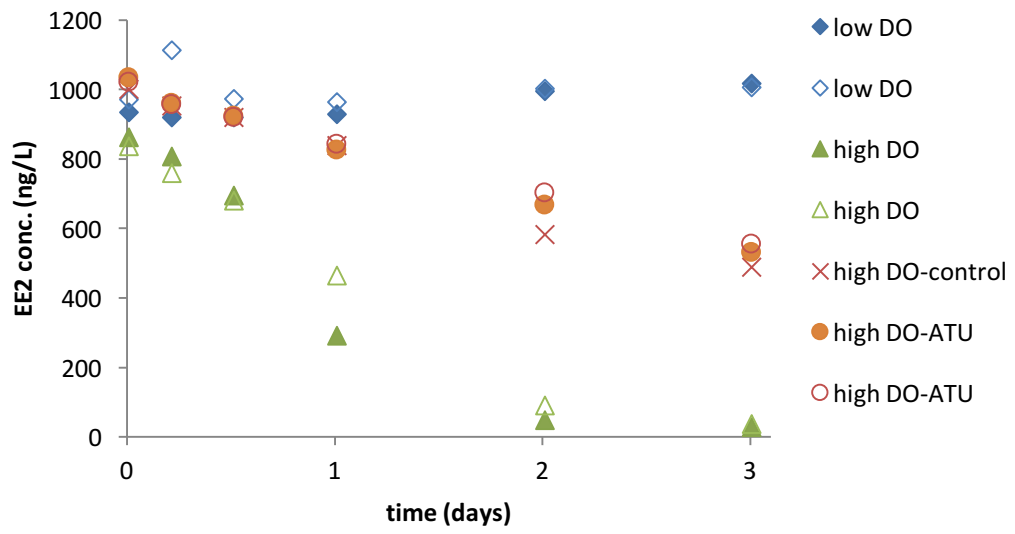
a.



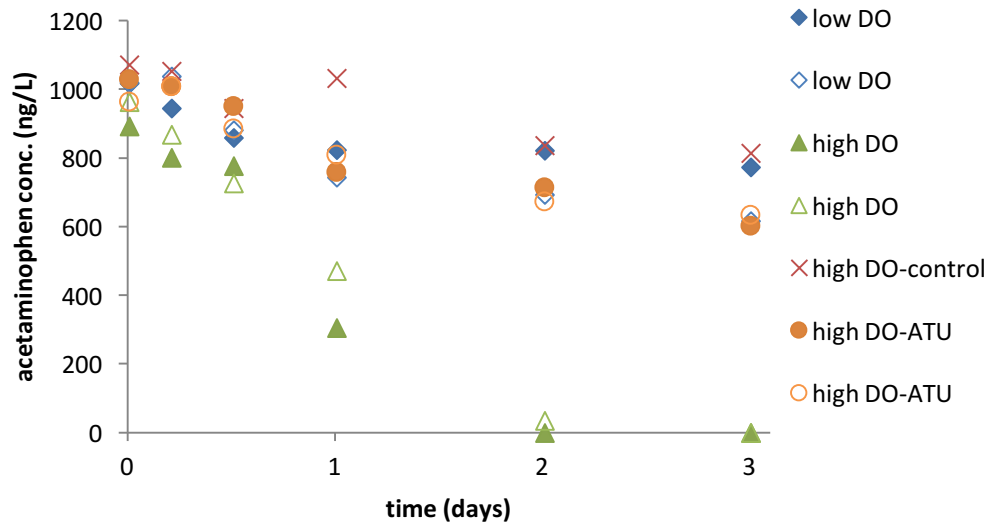
b.



c.



d.



e.

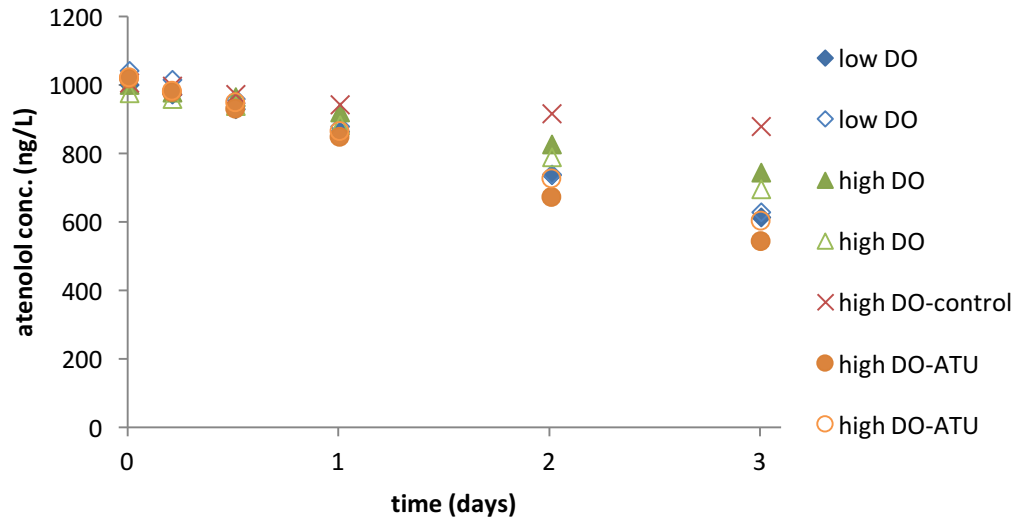
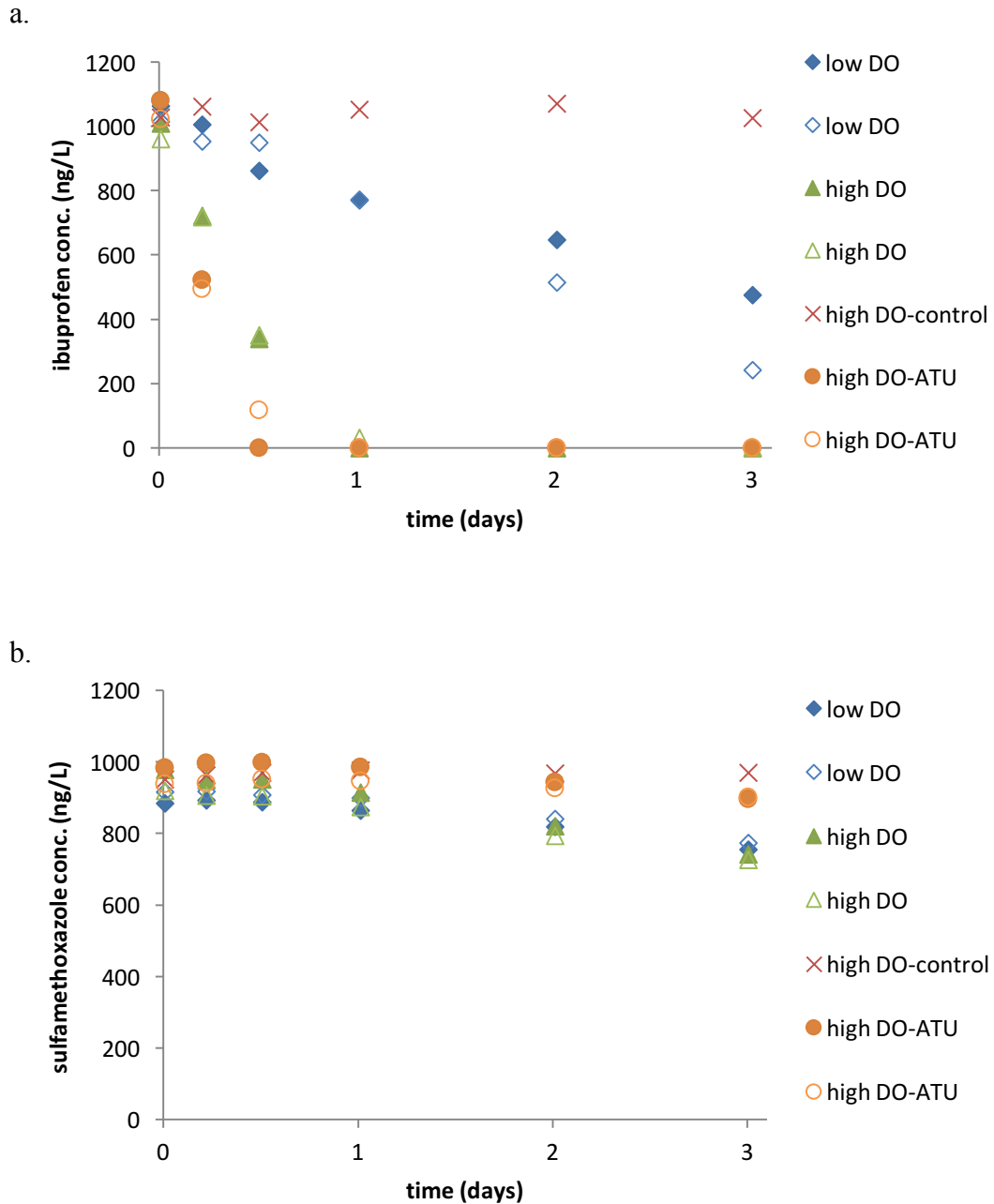


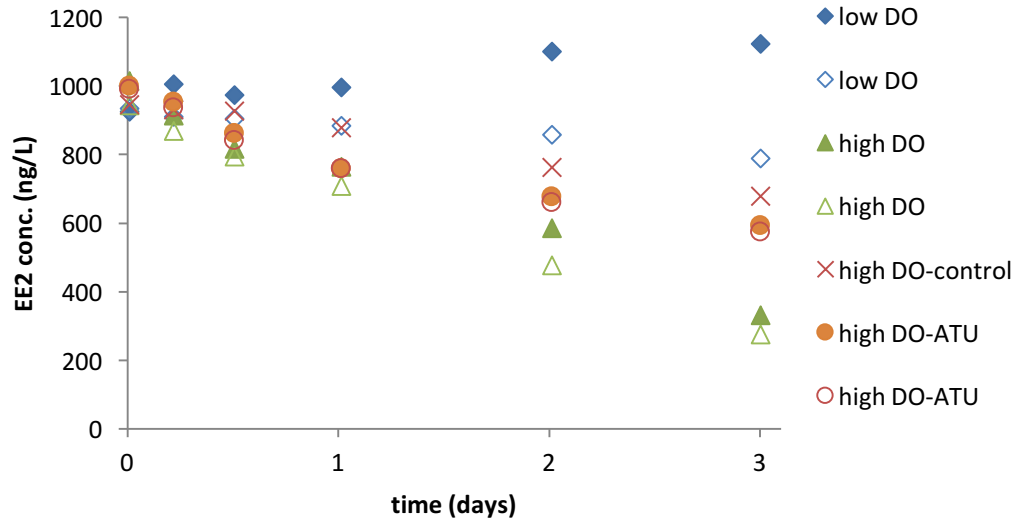
**Figure B3.** Concentration profiles of ibuprofen (a), sulfamethoxazole (b), EE2 (c), acetaminophen (d), and atenolol (e) in batch experiments performed with low DO parent biomass.

## High DO parent batch experiments

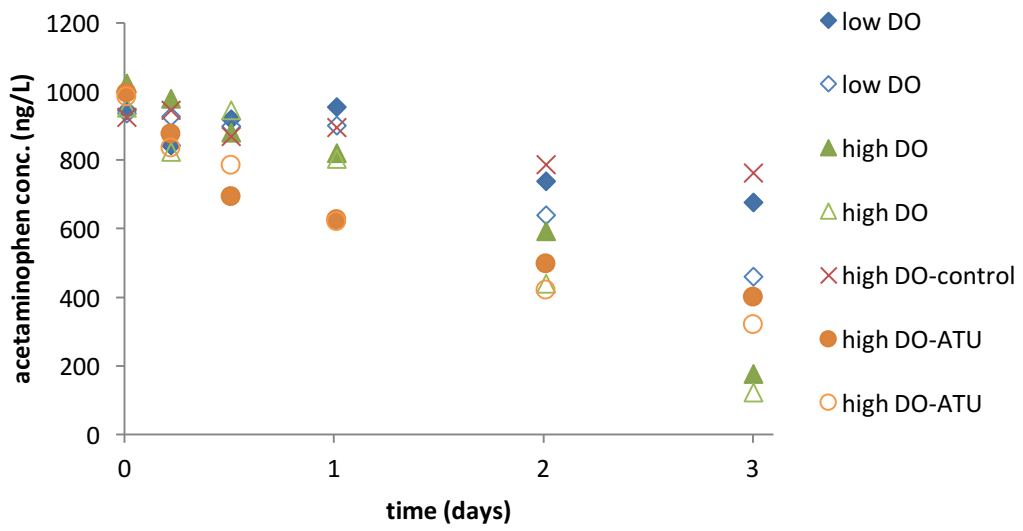
Concentration profiles for batch experiments using the high DO parent reactor biomass are presented in Figure B4.



c.



d.



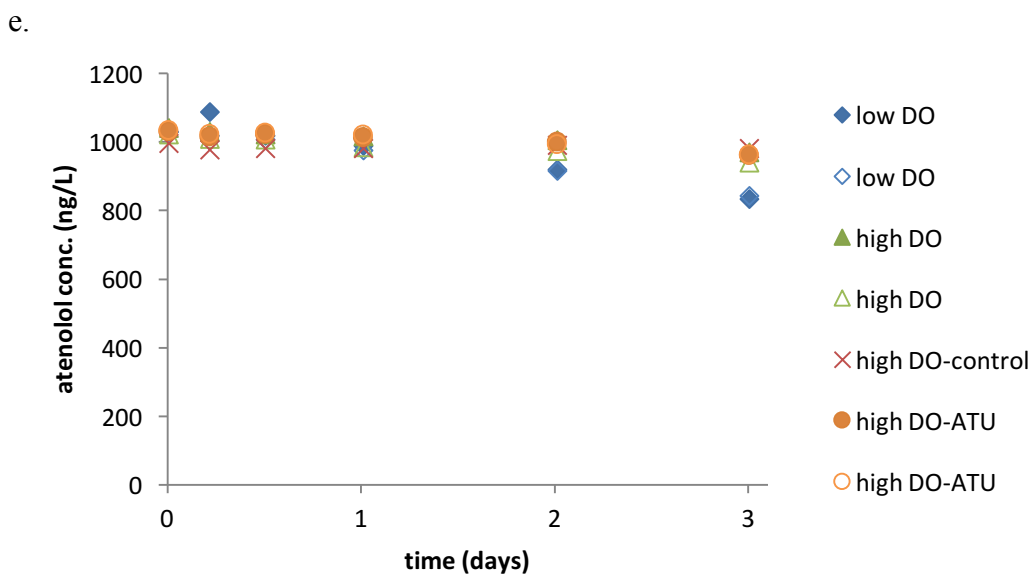


**Figure B4.** Concentration profiles of ibuprofen (a), sulfamethoxazole (b), EE2 (c), acetaminophen (d), and atenolol (e) in batch experiments performed with high DO parent biomass.

### Biotransformation rate constants

**Table B3.** Observed kinetic biotransformation rate constants for ibuprofen, EE2, sulfamethoxazole, acetaminophen, and atenolol. No biotransformation rate is reported for EE2 for low DO batch conditions because no significant biotransformation occurred.

	$k_{obs}$ [day <sup>-1</sup> ]				
	Ibuprofen	EE2	Sulfamethoxazole	Acetaminophen	Atenolol
Low DO parent & low DO batch	1.0 E00 ± 2.1E-02	N.A.	1.2E-01 ± 5.1E-02	1.2E-01 ± 6.9E-02	1.7E-01 ± 6.1E-03
Low DO parent & high DO batch	6.4 E00 ± 2.6E-01	1.2 E00 ± 2.8E-02	1.9E-01 ± 9.0E-03	1.4 E00 ± 4.3E-01	1.1E-01 ± 1.0E-02
High DO parent & low DO batch	3.6E-01 ± 1.5E-01	N.A.	5.6E-02 ± 1.6E-03	1.7E-01 ± 9.4E-02	7.3E-02 ± 9.0E-03
High DO parent & high DO batch	2.9 E00 ± 8.3E-03	3.7E-01 ± 4.0E-02	8.6E-02 ± 8.3E-03	5.9E-01 ± 1.3E-02	2.3E-02 ± 3.7E-03

## Ammonia and nitrite oxidizer populations in low and high DO parent reactors

Ammonia oxidizing bacteria (AOB) and nitrite oxidizing bacteria (NOB) were identified in the parent reactors by performing a BLASTN of each OTU's representative sequence (outputted from Mothur) against a custom database of full length 16S sequences of AOB and NOB downloaded from NCBI (Table B4).

**Table B4.** Ammonia oxidizing bacterial (AOB) and nitrite oxidizing bacteria (NOB) identified in the low and high DO parent reactors. Percent identity is the percent of the queried sequence that was identical to the database sequence listed in the left column.

	Percent identity (%)	Relative abundance (%)	
		Low DO parent	High DO parent
<b>Ammonia oxidizing bacteria</b>			
<i>Nitrosomonas</i> sp. JL21	99.2	4.311	8.695
<i>Nitrosomonas</i> sp. ls79A3	98.0	1.930	3.121
<i>Nitrosomonas ureae</i> strain Nm10	97.2	0.012	0.433
<i>Nitrosomonas europaea</i>	98.0	0.428	0.000
<i>Nitrosomonas oligotropha</i> strain Nm10	99.6	0.004	0.000
<i>Nitrosococcus mobilis</i> Nc2	99.2	0.089	0.000
<b>Nitrite oxidizing bacteria</b>			
<i>Nitrospira defluvii</i>	100.0	6.066	6.697
<i>Nitrobacter winogradskyi</i>	100.0	0.016	1.500
<i>Nitrospira moscoviensis</i>	98.4	0.759	0.206

## Literature cited

Rotthauwe, J. H.; Witzel, K. P.; Liesack, W. The Ammonia Monooxygenase Structural Gene *amoA* as a Functional Marker: Molecular Fine-Scale Analysis of Natural Ammonia-Oxidizing Populations. *Appl. Env. Microbiol.* **1997**, *63* (12), 4704–4712.



## **Appendix C.**

### **Supplementary Information for Chapter 5**

#### **Impact of dissolved oxygen on pharmaceutical biotransformation rates and microbial activity in wastewater treatment**

##### **Pharmaceutical quantification via liquid chromatography and high resolution mass spectrometry**

Pharmaceuticals were quantified via on-line pre-concentration followed by high performance liquid chromatography (HPLC) and high resolution mass spectrometry (HRMS). Matrix-matched external calibration curves containing a mixture of the target compounds and deuterated analogs were used for quantification. On-line pre-concentration of the compounds of interest was performed using the Equan™ (Thermo Fisher Scientific, Grand Island, New York) system (system details are provided in Fayad et al., 2013). The on-line pre-concentration was performed using a Hypersil Gold aQ trapping column (20 x 2.1 mm, 12 µM particle size; Thermo Fisher Scientific) and chromatographic separation was done with an Accucore aQ column (50 x 2.1 mm, 2.6 µm particle size; Thermo Fisher Scientific). A 500 µL sample was injected onto the trapping column. A mobile phase containing water with 0.1% formic acid and methanol with 0.1% formic acid was applied via gradient flow to elute all compounds with minimal overlap. The mobile phase A was water + 0.1% formic acid and B was methanol + 0.1 % formic acid. The flow rate was 0.175 mL/min and the gradient profile used was as follows: 90% A was held for 3 min, ramped

to 90% of B over 8 min, held at 90% B for 1 minutes, flow rate increased to 0.25 mL/min over 0.2 minutes and held at 0.25 ml/min for 1.8 minutes, and finally returned to 90% of A and 0.175 mL/min over 0.2 min. Total run time for one sample was 16 minutes at a flow rate of 1 mL/min on the trapping column and 0.175 – 0.250 mL/min on the analytical column.

Ionization was achieved by positive electron spray ionization (ESI) for the following compounds: atenolol, 17 $\alpha$ -ethinylestradiol (EE2), sulfamethoxazole, trimethoprim, venlafaxine, and acetaminophen; negative ESI was used for: ibuprofen and naproxen. The following source parameters were used: capillary temperature of 250 °C, auxillary gas heater temperature of 275 °C, a spray voltage of 3.5 kV, sheath gas flow rate of 30 arbitrary units, auxillary gas flow rate of 20 arbitrary units, and sweep gas flow rate of 1 arbitrary unit. A full scan ranging from 150 to 750 m/z was performed at a resolution of 70,000 and target automatic gain control (AGC) of  $1 \times 10^{-6}$ . All data were collected and processed using the Thermo TraceFinder Software Version 3.2 (Thermo Fisher Scientific).

**Table C1.** Target compounds with accurate mass and retention times used for quantification

Compound	Formula	Accurate mass (m/z)	Retention time (min)	ESI mode
Trimethoprim	C14H18N4O3	291.14516	6.67	positive
d9-trimethoprim	C14H9D9N4O3	300.20165	6.62	positive
Sulfamethoxazole	C10H11N3O3S	254.05938	7.23	positive
d4-sulfamethoxazole	C10H7D4N3O3S	258.08449	7.22	positive
EE2	C20H24O2	279.17434	10.96	positive
d4-EE2	C20H20D4O2	283.19944	10.95	positive
Atenolol	C14H22N2O3	267.17031	4.92	positive
d7-atenolol	C14H15D7N2O3	274.21425	4.88	positive
Venlafaxine	C17H27NO2	278.21145	8.97	positive
d6-venlafaxine	C17H21D6NO2	284.24911	8.94	positive
Acetaminophen	C8H9NO2	152.07060	5.25	positive
d3-Acetaminophen	C8H6D3NO2	155.08943	5.22	positive
Ibuprofen	C13H18O2	205.12231	11.61	negative
d3-ibuprofen	C13H15D3O2	208.14241	11.60	negative
Naproxen	C14H14O3	229.08592	10.64	negative
d3-Naproxen	C14H11D3O3	232.10475	10.62	negative

### Allylthiourea inhibited batches

Triplicate batch reactors were supplemented with 10 mg/L of allylthiourea (ATU) to inhibit ammonia oxidation. A preliminary experiment was performed to assess whether 10 mg/L was sufficient to inhibit ammonia oxidation. The experiment involved four batch reactors: one supplemented with 0.4% w/v sodium azide, one with 10 mg/L ATU, and two uninhibited batch reactors. The effluent used to re-suspend the biomass in these experiments was filtered final effluent from the Ann Arbor wastewater treatment plant, the experiment was run for 24 hours, and the DO was maintained at approximately 1.0 mg/L. Ammonia oxidation inhibition was confirmed by measuring the concentration of ammonia-N across the batch experiments. In the azide and ATU-inhibited batch reactors, ammonia-N concentrations increased due to and ammonia release from decay over the 24 hours, and that ammonia was not oxidized due to inhibition (Figure C1).

In the uninhibited batches, the 24-hour ammonia-N concentrations were significantly less than the inhibited batches as nitrification was not inhibited, demonstrating that the nitrifiers were active and oxidized the ammonia released due to decay over the 24 hour experiment. Ammonia-, nitrite-, and nitrate-N concentrations were also measured across the 6 hour pharmaceutical biotransformation batch experiments to ensure ATU resulted in ammonia oxidation inhibition. Similar to the preliminary test experiment, ammonia-N concentrations increased during the 6-hour experiment due to release from decay in the azide and ATU-inhibited batches, while they remained low in the uninhibited batches due to active nitrification (Figure C2 shows 2 mg-DO/L batch experiment results). Nitrate-N concentrations at the beginning and end of the 6-hour batch experiments also showed an increase in nitrate-N in the uninhibited batch reactors and no change in nitrate-N in the inhibited reactors, confirming that there was active nitrification occurring in the uninhibited batch reactors and no nitrification in the azide and ATU inhibited reactors (Figure C2).

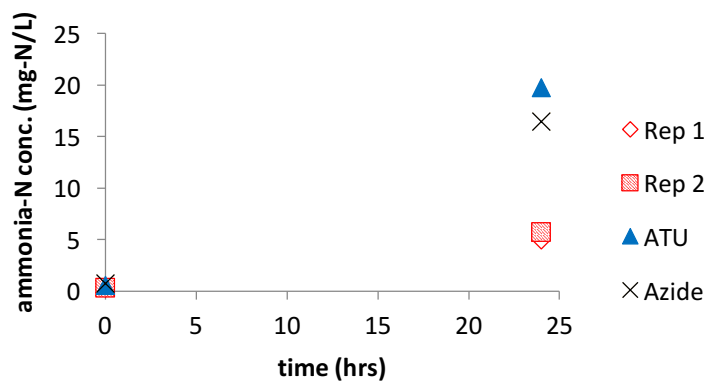
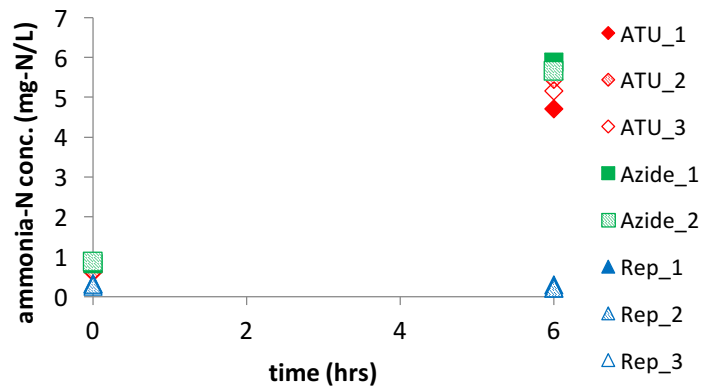


**Figure C1.** Initial and final concentrations of ammonia-N in batch reactors from preliminary batch experiment.

a.



b.

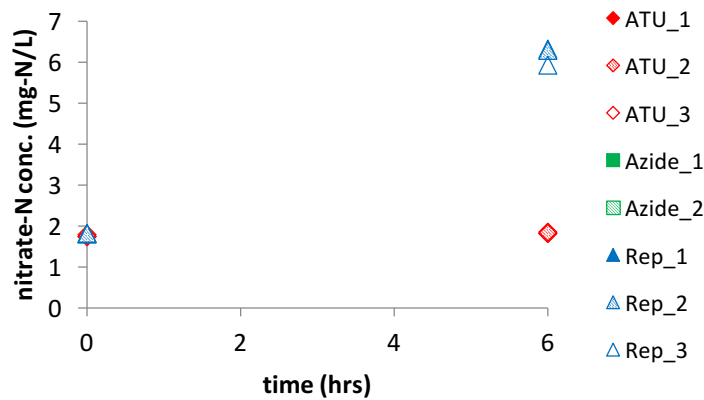


**Figure C2.** Initial and final concentrations of ammonia-N (a) and nitrate-N (b) from the 2.0 mg-DO/L batch experiment.

### Sodium azide concentration determination

We determined the sodium azide concentration to use for the controls by performing respirometry using biomass from the full-scale wastewater treatment plant. Respirometry was performed as described in the Chapter 5, section 5.2.4 and the maximum oxygen uptake rate (OUR) was determined for heterotrophs using several different concentrations of sodium azide: 0, 0.05, 0.2, 0.4, and 0.6 % w/v. For each respirometry experiment, biomass was allowed to sit with the

sodium azide for 10 minutes prior to substrate addition. Figure C3 shows sodium azide concentration used versus the maximum OUR. We selected 0.4% w/v as the concentration to use in batch experiments as the max OUR has plateaued at that concentration.

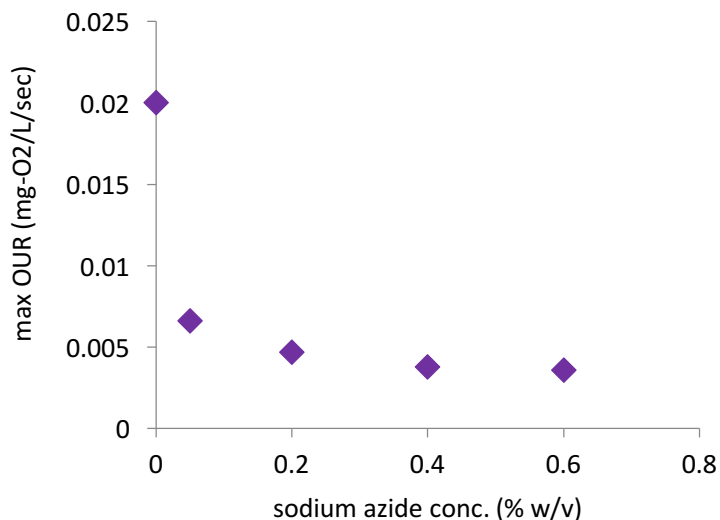


**Figure C3.** Sodium azide concentration used in respirometry versus maximum oxygen uptake rate. Based on this data, we selected a sodium azide concentration of 0.4 % w/v to use in the batch experiments for the controls.

### Pharmaceutical biotransformation data

Raw pharmaceutical data is show in Table C2. Concentrations are shown in ng/L. The lowest standard used for quantification was 50 ng/L, and concentrations below 50 ng/L are below the limit of detection. No-biomass abiotic controls were performed in the 0.25 mg-DO/L batch experiments (designated Abiotic\_1 and Abiotic\_2).

**Table C2.** Pharmaceutical concentrations in biotransformation batch experiments performed at different DO concentrations (6.0, 2.0, 0.5, 0.25, 0.15, and 0.05 mg/L). The first row of each table section is the sampling time in hours. Concentration units are ng/L.

<b>Ibuprofen</b>					
<b>6.0 mg-DO/L</b>	0	0.5	1.5	3	6
Rep_1	8534	563	26	7	21
Rep_2	8615	466	37	16	0
Rep_3	8483	487	12	21	0
ATU_1	7480	547	50	12	0
ATU_2	7430	431	10	16	0
ATU_3	7523	427	0	13	0
Azide_1	11625	11478	11403	10894	11405
Azide_2	11468	11231	11189	11108	11264
<b>2.0 mg-DO/L</b>	0	0.5	1.5	3	6
Rep_1	8342	590	76	68	58
Rep_2	8403	582	87	85	42
Rep_3	8112	533	86	66	50
ATU_1	7131	555	67	85	36
ATU_2	7398	436	64	50	43
ATU_3	7335	459	83	36	34
Azide_1	11630	10953	10868	11283	10768
Azide_2	11545	11205	11023	11213	11073
<b>0.5 mg-DO/L</b>	0	0.5	1.5	3	6
Rep_1	10804	4166	124	55	30
Rep_2	10685	5239	127	47	30
Rep_3	10947	4076	68	80	14
ATU_1	11127	4141	176	34	8
ATU_2	11091	4115	125	24	41
ATU_3	10937	4802	89	39	25
Azide_1	12097	11675	11611	11512	11773
Azide_2	11898	11847	11794	11837	11273
<b>0.25 mg-DO/L</b>	0	0.5	1.5	3	6
ATU_1	10949	9203	2785	825	389
ATU_2	12115	10599	4381	833	741
Rep_1	11278	9719	600	578	389
Rep_2	10897	9496	3852	879	743
Azide_1	11606	11425	11198	11303	11768

Azide_2	11588	11467	11097	10900	11145
Abiotic_1	11541	11902	11721	11920	11765
Abiotic_2	11816	11882	11659	11934	12025

<b>0.15 mg-DO/L</b>	0	0.5	1.5	3	6
Rep_1	12417	10087	749	100	54
Rep_2	11946	11191	6291	530	76
Rep_3	12219	10607	1747	144	82
ATU_1	11999	10317	701	119	30
ATU_2	12110	9908	731	67	37
ATU_3	12000	11360	5534	411	56
Azide_1	12379	12240	12264	12041	12322
Azide_2	12629	12259	12526	12025	11811

<b>0.05 mg-DO/L</b>	0	0.5	1.5	3	6
Rep_1	12026	11843	12162	11935	11647
Rep_2	12011	12345	12177	12129	12026
Rep_3	11910	11987	12084	12003	11713
ATU_1	11913	11998	11709	11828	12017
ATU_2	12108	11944	12419	11764	11907
ATU_3	11821	11721	11966	11975	12041
Azide_1	12626	12845	12613	12180	12364
Azide_2	12176	11780	12789	12595	12654

---

**Acetaminophen**

---

<b>6.0 mg-DO/L</b>	0	0.5	1.5	3	6
Rep_1	3454	0	0	0	0
Rep_2	4434	0	0	0	0
Rep_3	4365	0	0	0	0
ATU_1	3781	48	0	38	0
ATU_2	3819	0	0	26	0
ATU_3	4129	0	0	50	0
Azide_1	9056	6880	3430	626	21
Azide_2	9288	6820	2979	726	16

<b>2.0 mg-DO/L</b>	0	0.5	1.5	3	6
Rep_1	4086	0	0	0	0
Rep_2	4390	0	0	0	0
Rep_3	4204	0	0	0	0



ATU_1	3575	0	0	0	0
ATU_2	3886	0	0	0	0
ATU_3	4050	0	0	0	0
Azide_1	9436	6847	3118	591	105
Azide_2	9292	6521	3387	557	68
<b>0.5 mg-DO/L</b>	<b>0</b>	<b>0.5</b>	<b>1.5</b>	<b>3</b>	<b>6</b>
Rep_1	5897	109	0	0	0
Rep_2	5608	36	0	0	0
Rep_3	5815	34	0	0	0
ATU_1	6849	219	0	0	0
ATU_2	6996	268	0	0	0
ATU_3	6498	196	0	0	0
Azide_1	9766	8036	5485	2943	922
Azide_2	10069	8629	5618	3155	906
<b>0.25 mg-DO/L</b>	<b>0</b>	<b>0.5</b>	<b>1.5</b>	<b>3</b>	<b>6</b>
ATU_1	7297	100	0	0	0
ATU_2	8499	890	29	119	105
Rep_1	7137	211	0	0	141
Rep_2	7102	0	0	0	258
Azide_1	9794	6933	2570	1087	0
Azide_2	10374	6715	2286	813	159
Abiotic_1	10430	10414	10242	10431	10281
Abiotic_2	10432	10650	10407	10445	10342
<b>0.15 mg-DO/L</b>	<b>0</b>	<b>0.5</b>	<b>1.5</b>	<b>3</b>	<b>6</b>
Rep_1	8162	678	13	0	0
Rep_2	7964	861	0	0	0
Rep_3	7627	597	0	0	0
ATU_1	7913	1146	0	7	0
ATU_2	8124	881	0	22	0
ATU_3	7843	1286	0	0	0
Azide_1	10173	8431	5059	1879	145
Azide_2	10241	8430	5240	2006	6
<b>0.05 mg-DO/L</b>	<b>0</b>	<b>0.5</b>	<b>1.5</b>	<b>3</b>	<b>6</b>
Rep_1	7817	4795	1976	405	100
Rep_2	7587	4732	2077	645	78
Rep_3	7301	4373	1960	470	0

ATU_1	7695	4653	2014	533	0
ATU_2	7657	4891	2057	548	0
ATU_3	7417	4647	2060	651	98
Azide_1	9932	8017	4895	1834	263
Azide_2	9911	8017	4876	1996	129

<b>Naproxen</b>					
<b>6.0 mg-DO/L</b>	0	0.5	1.5	3	6
Rep_1	10752	7225	1746	75	61
Rep_2	10794	7174	1683	62	26
Rep_3	10580	7385	1792	68	0
ATU_1	9956	7087	1793	91	20
ATU_2	10310	7078	1879	72	26
ATU_3	10278	7026	1766	74	8
Azide_1	10743	11265	10678	10815	10965
Azide_2	10834	10883	10914	10803	11048
<b>2.0 mg-DO/L</b>	0	0.5	1.5	3	6
Rep_1	11333	8565	2527	146	20
Rep_2	11020	8343	2693	118	66
Rep_3	10557	8534	2529	151	18
ATU_1	10322	8050	2547	171	16
ATU_2	10826	8107	2457	88	96
ATU_3	10706	8035	2549	103	43
Azide_1	11131	11125	11136	11142	10614
Azide_2	10731	11207	11270	11251	10755
<b>0.5 mg-DO/L</b>	0	0.5	1.5	3	6
Rep_1	11064	9350	4450	483	40
Rep_2	10994	9312	5082	811	85
Rep_3	11086	9434	4493	595	26
ATU_1	10961	8950	4600	679	46
ATU_2	10732	9114	4690	585	16
ATU_3	10552	9371	4950	718	44
Azide_1	11120	10867	10998	11013	10789
Azide_2	11002	10958	10931	10872	11096
<b>0.25 mg-DO/L</b>	0	0.5	1.5	3	6
ATU_1	10309	9847	7497	1318	0

ATU_2	11215	11027	8384	3095	0
Rep_1	11079	10830	4296	189	0
Rep_2	10848	10542	7932	2846	0
Azide_1	10963	10972	10844	11120	11405
Azide_2	11056	11137	10805	11059	11271
Abiotic_1	11147	10986	10997	10782	11131
Abiotic_2	11053	11442	11179	11244	11018

<b>0.15 mg-DO/L</b>	0	0.5	1.5	3	6
Rep_1	11104	10582	6820	1498	75
Rep_2	11414	10787	8892	4557	254
Rep_3	11540	10992	7637	3380	128
ATU_1	10897	10646	6791	1556	33
ATU_2	11160	10611	7078	1523	83
ATU_3	11173	11130	8808	5174	141
Azide_1	11393	11487	11209	11604	11972
Azide_2	11346	11526	11057	11359	11681

<b>0.05 mg-DO/L</b>	0	0.5	1.5	3	6
Rep_1	11338	11512	11049	11161	10910
Rep_2	11166	11006	11383	11620	10987
Rep_3	11350	11020	11273	11348	11057
ATU_1	11309	11264	11077	11129	10772
ATU_2	11196	11012	11099	10701	11021
ATU_3	10953	11288	11331	11277	11151
Azide_1	11142	11276	11737	11211	11203
Azide_2	11302	11128	10814	11299	11558

<b>Atenolol</b>					
<b>6.0 mg-DO/L</b>	0	0.5	1.5	3	6
Rep_1	9681	8851	5966	2794	354
Rep_2	10313	8724	6032	2830	330
Rep_3	9723	8699	6019	2815	348
ATU_1	9373	8492	6066	2989	386
ATU_2	9490	8714	6186	3129	441
ATU_3	9714	8527	6209	3050	468
Azide_1	10271	10158	9607	8928	7922
Azide_2	10403	10031	9748	8918	7986

<b>2.0 mg-DO/L</b>	0	0.5	1.5	3	6
Rep_1	9815	8687	5782	2653	275
Rep_2	9752	8645	5897	2717	299
Rep_3	9615	8842	5762	2519	279
ATU_1	9334	8330	5858	2787	396
ATU_2	9772	8475	5825	3223	328
ATU_3	9909	8682	5952	2849	346
Azide_1	10465	10106	9633	9114	7876
Azide_2	10390	10183	9648	9116	8021

<b>0.5 mg-DO/L</b>	0	0.5	1.5	3	6
Rep_1	9888	8645	5851	2828	435
Rep_2	9904	8750	6020	3142	555
Rep_3	9919	8700	5798	2806	435
ATU_1	9419	8435	5980	3113	574
ATU_2	9685	8593	5988	3103	527
ATU_3	9625	8674	6271	3242	552
Azide_1	10312	10136	9683	8715	7501
Azide_2	10250	10070	9493	8653	7393

<b>0.25 mg-DO/L</b>	0	0.5	1.5	3	6
ATU_1	8983	7738	5477	2701	167
ATU_2	10235	8348	6100	3285	240
Rep_1	10241	8337	5072	2153	125
Rep_2	9934	8462	5558	2862	321
Azide_1	10141	9668	8526	7325	5823
Azide_2	10100	9556	8500	7377	5802
Abiotic_1	10201	10227	10189	10332	10291
Abiotic_2	10371	10403	10382	10415	10423

<b>0.15 mg-DO/L</b>	0	0.5	1.5	3	6
Rep_1	10088	9371	7130	3975	953
Rep_2	10165	9337	7598	4459	1305
Rep_3	10281	9417	7532	4357	1193
ATU_1	9911	9279	7121	4181	1056
ATU_2	10064	9327	7290	4246	994
ATU_3	10180	9427	7570	4894	1432
Azide_1	10812	10620	10277	9441	7855
Azide_2	10869	10626	10312	9455	7921

<b>0.05 mg-DO/L</b>	0	0.5	1.5	3	6
Rep_1	10135	9242	8247	6872	4606
Rep_2	10089	9435	8343	6960	4857
Rep_3	9973	9316	8283	6850	4693
ATU_1	9949	9253	8320	6916	5065
ATU_2	9944	9454	8550	7195	5057
ATU_3	9961	9298	8482	7120	5136
Azide_1	10733	10544	10221	9566	8176
Azide_2	10585	10451	10187	9457	8240

<b>EE2</b>					
<b>6.0 mg-DO/L</b>	0	0.5	1.5	3	6
Rep_1	7700	7264	6139	4612	2779
Rep_2	9052	7179	6121	4614	2716
Rep_3	7702	7120	5982	4682	2826
ATU_1	7641	7273	6052	4796	3108
ATU_2	7312	7269	6065	4817	3033
ATU_3	7867	6888	6156	4673	3113
Azide_1	7413	7321	7383	6963	6891
Azide_2	7580	7189	7301	7416	7150

<b>2.0 mg-DO/L</b>	0	0.5	1.5	3	6
Rep_1	7720	6929	5746	4604	2693
Rep_2	7491	6797	5926	4517	2575
Rep_3	7456	7319	5815	4215	2456
ATU_1	7414	6691	5843	4257	2610
ATU_2	7878	6624	5629	4568	2719
ATU_3	8103	7000	5759	4375	2501
Azide_1	7890	7220	6776	6297	5137
Azide_2	7853	7483	7004	6574	5554

<b>0.5 mg-DO/L</b>	0	0.5	1.5	3	6
Rep_1	8040	7309	5705	4389	2398
Rep_2	8146	7331	5952	4588	2488
Rep_3	8111	7385	5749	4147	2147
ATU_1	7831	6932	6007	4361	2436
ATU_2	7819	7225	5958	4454	2488
ATU_3	7680	7217	6156	4466	2436
Azide_1	7886	7777	7341	5982	3729

Azide_2	7844	7690	6937	5822	3957
<b>0.25 mg-DO/L</b>	<b>0</b>	<b>0.5</b>	<b>1.5</b>	<b>3</b>	<b>6</b>
ATU_1	7047	6789	6533	6806	3656
ATU_2	9256	7267	7389	7473	4503
Rep_1	9379	7442	6525	6244	3895
Rep_2	8309	8386	6855	7217	5299
Azide_1	7671	7605	7325	8399	7717
Azide_2	8289	7764	7552	8323	7747
Abiotic_1	10120	10207	10292	10363	10305
Abiotic_2	10466	10430	10341	10315	10546
<b>0.15 mg-DO/L</b>	<b>0</b>	<b>0.5</b>	<b>1.5</b>	<b>3</b>	<b>6</b>
Rep_1	8002	7689	6891	5634	3744
Rep_2	8083	7763	7973	6256	4515
Rep_3	8340	7928	8168	5848	4199
ATU_1	8356	7776	6909	5600	3735
ATU_2	8146	7631	7053	5901	3822
ATU_3	8353	7840	7379	6552	4876
Azide_1	8143	7541	7538	6781	5009
Azide_2	8105	7611	7290	6711	5240
<b>0.05 mg-DO/L</b>	<b>0</b>	<b>0.5</b>	<b>1.5</b>	<b>3</b>	<b>6</b>
Rep_1	8125	7986	7951	7846	7747
Rep_2	8036	7909	7897	8018	7980
Rep_3	8067	7782	8123	8164	7998
ATU_1	8401	8186	8044	7604	7935
ATU_2	7943	7897	7861	7884	7960
ATU_3	8216	7787	8093	7854	8282
Azide_1	8086	8034	7728	7279	6602
Azide_2	7586	7665	7692	7317	6671

---

**Venlafaxine**

---

<b>6.0 mg-DO/L</b>	<b>0</b>	<b>0.5</b>	<b>1.5</b>	<b>3</b>	<b>6</b>
Rep_1	10110	9772	8636	7772	7473
Rep_2	10371	9534	8807	8224	7875
Rep_3	10145	9584	8617	8117	8156
ATU_1	9911	9453	8717	8083	8157
ATU_2	9928	9561	8714	8178	7916

ATU_3	10033	9555	8866	8203	8318
Azide_1	10208	10273	10195	10011	10451
Azide_2	10220	10076	10025	9763	9939
<b>2.0 mg-DO/L</b>	<b>0</b>	<b>0.5</b>	<b>1.5</b>	<b>3</b>	<b>6</b>
Rep_1	10319	9935	8869	8155	8153
Rep_2	10511	9785	8813	8111	8003
Rep_3	10294	9822	8617	7814	7886
ATU_1	10388	9742	9064	8240	8292
ATU_2	10302	9800	9024	8559	8674
ATU_3	10464	9925	9085	8509	8502
Azide_1	10600	10567	10586	10736	10797
Azide_2	10524	10453	10520	10667	10794
<b>0.5 mg-DO/L</b>	<b>0</b>	<b>0.5</b>	<b>1.5</b>	<b>3</b>	<b>6</b>
Rep_1	10233	9312	8135	7503	8032
Rep_2	10230	9384	8218	7535	7736
Rep_3	10267	9268	7958	7115	7513
ATU_1	9969	9117	8236	7396	7531
ATU_2	10103	9282	8338	7646	7629
ATU_3	9944	9466	8427	7582	7728
Azide_1	10492	10434	10484	10476	10527
Azide_2	10316	10305	10289	10289	10326
<b>0.25 mg-DO/L</b>	<b>0</b>	<b>0.5</b>	<b>1.5</b>	<b>3</b>	<b>6</b>
ATU_1	9403	9065	8873	8619	8645
ATU_2	10173	9656	9483	9078	9214
Rep_1	10305	9614	8964	8668	8831
Rep_2	10098	9734	9175	9157	9287
Azide_1	10146	10281	10217	10387	10608
Azide_2	10044	10220	10375	10589	10540
Abiotic_1	10228	10278	10274	10225	10282
Abiotic_2	10275	10401	10408	10409	10521
<b>0.15 mg-DO/L</b>	<b>0</b>	<b>0.5</b>	<b>1.5</b>	<b>3</b>	<b>6</b>
Rep_1	10440	9922	8648	7767	7617
Rep_2	10627	9895	8895	7862	7429
Rep_3	10623	10048	8801	7954	7388
ATU_1	10396	9894	8809	8052	7884
ATU_2	10509	9986	9075	8291	8209

ATU_3	10565	10185	9273	8586	8490
Azide_1	10796	10739	10886	10903	10915
Azide_2	10727	10625	10773	10763	10890

<b>0.05 mg-DO/L</b>	0	0.5	1.5	3	6
Rep_1	10435	9971	9497	9399	9564
Rep_2	10364	10084	9567	9412	9529
Rep_3	10317	9957	9628	9472	9511
ATU_1	10351	9977	9651	9271	9476
ATU_2	10295	10118	9755	9377	9578
ATU_3	10296	9937	9752	9466	9788
Azide_1	10671	10708	10704	10769	10791
Azide_2	10523	10487	10498	10461	10600

---

**Sulfamethoxazole**

---

<b>6.0 mg-DO/L</b>	0	0.5	1.5	3	6
Rep_1	11154	10850	10307	9395	7818
Rep_2	11252	10777	10201	9028	6962
Rep_3	11087	10772	10222	8980	6702
ATU_1	10670	10485	9935	9008	7297
ATU_2	10870	10655	10192	9266	7256
ATU_3	10911	10638	10170	9183	7872
Azide_1	11161	11016	10714	10263	10197
Azide_2	11144	10926	10258	9521	10103

<b>2.0 mg-DO/L</b>	0	0.5	1.5	3	6
Rep_1	11202	10991	10462	9458	7810
Rep_2	11227	11019	10465	9521	7907
Rep_3	11087	11019	10505	9490	7984
ATU_1	10789	10611	10288	9506	8095
ATU_2	11096	10880	10361	9385	7691
ATU_3	11154	10889	10486	9649	8141
Azide_1	11175	10997	10792	10398	9943
Azide_2	11131	11086	10732	10419	10035

<b>0.5 mg-DO/L</b>	0	0.5	1.5	3	6
Rep_1	10997	10526	9919	8967	7363
Rep_2	11001	10596	9877	9051	7396
Rep_3	11042	10662	10104	9285	7678



ATU_1	10564	10245	9788	9118	7673
ATU_2	10789	10450	10032	9380	7900
ATU_3	10763	10500	10032	9287	7720
Azide_1	10981	10845	10628	10341	10006
Azide_2	10833	10880	10642	10373	9988

---

<b>0.25 mg-DO/L</b>	<b>0</b>	<b>0.5</b>	<b>1.5</b>	<b>3</b>	<b>6</b>
---------------------	----------	------------	------------	----------	----------

---

ATU_1	10572	10079	9486	8642	6850
ATU_2	11228	10495	9443	8380	6410
Rep_1	11243	10558	9673	8538	6654
Rep_2	11221	10560	9500	8184	6000
Azide_1	11047	10869	10462	10266	9748
Azide_2	10974	10789	10418	10186	9610
Abiotic_1	11060	11104	11083	11269	11272
Abiotic_2	11169	11230	11330	11286	11388

---

<b>0.15 mg-DO/L</b>	<b>0</b>	<b>0.5</b>	<b>1.5</b>	<b>3</b>	<b>6</b>
---------------------	----------	------------	------------	----------	----------

---

Rep_1	11311	10991	10461	9409	7862
Rep_2	11344	10938	10373	9398	7976
Rep_3	11449	11075	10552	9529	8095
ATU_1	10945	10730	10277	9514	8109
ATU_2	11235	10916	10425	9572	8011
ATU_3	11291	11040	10282	9349	7759
Azide_1	11354	11219	11102	10769	10313
Azide_2	11366	11311	11050	10755	10377

---

<b>0.05 mg-DO/L</b>	<b>0</b>	<b>0.5</b>	<b>1.5</b>	<b>3</b>	<b>6</b>
---------------------	----------	------------	------------	----------	----------

---

Rep_1	11359	11053	10793	10130	8637
Rep_2	11243	11140	10833	10266	9157
Rep_3	11247	11036	10882	10023	8874
ATU_1	11109	10885	10796	10179	9088
ATU_2	11166	11066	10942	10267	9173
ATU_3	11039	10926	10878	10343	9395
Azide_1	11336	11264	11053	10767	10149
Azide_2	11130	11079	10928	10538	10102

---

**Trimethoprim**

---

<b>6.0 mg-DO/L</b>	<b>0</b>	<b>0.5</b>	<b>1.5</b>	<b>3</b>	<b>6</b>
Rep_1	10516	10205	10116	9738	9333

Rep_2	10539	10243	9911	9694	9324
Rep_3	9774	9953	9934	9375	9171
ATU_1	10846	9753	9659	9134	9082
ATU_2	9969	10013	9550	9548	9338
ATU_3	10005	9823	9569	9104	9145
Azide_1	11415	10720	10865	10315	10194
Azide_2	10870	10581	10641	10415	10384

<b>2.0 mg-DO/L</b>	0	0.5	1.5	3	6
Rep_1	11048	10136	10025	9827	9635
Rep_2	10272	9935	9997	9787	9596
Rep_3	10051	10171	9937	9712	9471
ATU_1	9932	9586	9578	9371	9202
ATU_2	9993	9740	9750	9613	9675
ATU_3	9995	9859	9674	9656	9518
Azide_1	10995	10488	10600	10593	10512
Azide_2	10597	10551	10678	10726	10618

<b>0.5 mg-DO/L</b>	0	0.5	1.5	3	6
Rep_1	9925	9725	9648	9528	9371
Rep_2	9809	9666	9625	9445	9179
Rep_3	10288	9705	9568	9492	9183
ATU_1	10217	9081	9248	9001	8820
ATU_2	9402	9253	9387	9347	9245
ATU_3	9305	9277	9360	9399	9223
Azide_1	10805	10283	10423	10419	10345
Azide_2	10062	10174	10475	10378	10250

<b>0.25 mg-DO/L</b>	0	0.5	1.5	3	6
ATU_1	9478	9483	9580	9504	9356
ATU_2	10365	9645	9536	9756	9825
Rep_1	10954	10408	9762	10029	9677
Rep_2	10319	10439	9622	9982	9760
Azide_1	10611	10776	10629	10629	10400
Azide_2	10618	10577	10432	10597	10507
Abiotic_1	10854	10414	10254	10536	10602
Abiotic_2	10617	10547	10560	10707	10796

<b>0.15 mg-DO/L</b>	0	0.5	1.5	3	6
Rep_1	9982	9782	9979	9855	9629

Rep_2	9942	10476	9923	9790	9526
Rep_3	10520	9899	10217	9532	9420
ATU_1	9860	9613	9497	9501	9546
ATU_2	9873	9983	9877	9823	9768
ATU_3	10025	9943	9837	9809	9887
Azide_1	10528	10600	10740	10659	10611
Azide_2	11127	10585	10700	10656	10621

<b>0.05 mg-DO/L</b>	0	0.5	1.5	3	6
Rep_1	10536	9986	10105	10236	9961
Rep_2	9940	10272	9920	10042	10030
Rep_3	10561	9834	9877	10040	9954
ATU_1	10938	9839	9650	9757	9873
ATU_2	10492	10345	10071	10010	9955
ATU_3	10177	9668	10052	9948	9958
Azide_1	10988	11043	10608	10532	10435
Azide_2	10876	10265	10523	10312	10293

## Fitting parameters for Monod and Andrews type model fits to experimental data

Curve fitting was performed in R using non-linear least squares regression to find parameter values. Parameters and a summary of the fitting data is provided in Table C3. The units of  $K_0$  and  $K_i$  are mg-DO/L and the units of  $u_{max}$  are ng-pharmaceutical/mg-biomass/hour.

**Table C3.** Kinetic parameters from curve fitting Monod or Andrews equations to experimental data using non-linear least squares regression analysis.  $K_0$  and  $K_i$  units are mg-DO/L and the units of  $u_{max}$  are ng-pharmaceutical/mg-biomass/hour.

**Significance codes:** 0 ‘\*\*\*’ 0.001 ‘\*\*’ 0.01 ‘\*’ 0.05 ‘.’ 0.1 ‘ ’ 1

---

**Formula:**  $\text{rate\_ibuprofen} \sim u_{max} * (S/(K_0 + S + (S^2/K_i)))$

	Estimate	Std. error	t	value	Pr(> t )
umax	12.1669	3.4576	3.519	0.00423	**
Ko	0.6082	0.3317	1.834	0.0916	.
Ki	9.3801	7.7864	1.205	0.25155	

Residual standard error: 1.23 on 12 degrees of freedom

Number of iterations to convergence: 18

Achieved convergence tolerance: 8.27e-06

---

**Formula:**  $\text{rate\_ibuprofen\_ATU} \sim u_{max} * (S/(K_0 + S + (S^2/K_i)))$

	Estimate	Std. error	t	value	Pr(> t )
umax	11.2524	3.6179	3.11	0.00902	**
Ko	0.515	0.3291	1.565	0.14363	
Ki	9.2935	8.919	1.042	0.31796	

Residual standard error: 1.428 on 12 degrees of freedom

Number of iterations to convergence: 28

Achieved convergence tolerance: 7.79e-06

---

**Formula:**  $\text{rate\_acetaminophen} \sim u_{max} * (S/(K_0 + S + (S^2/K_i)))$

	Estimate	Std. error	t	value	Pr(> t )
umax	12.13052	3.85814	3.144	0.00847	**
Ko	0.10907	0.07542	1.446	0.17375	
Ki	1.23421	0.79372	1.555	0.14592	

Residual standard error: 1.604 on 12 degrees of freedom

Number of iterations to convergence: 17

Achieved convergence tolerance: 8.606e-06

---

**Formula: rate\_acetaminophen\_ATU ~ umax \* (S/(Ko + S + (S^2/Ki)))**

	Estimate	Std. error	t	value	Pr(> t )
umax	14.2684	4.8085	2.967	0.0118	*
Ko	0.1591	0.1017	1.565	0.1436	
Ki	0.9828	0.5981	1.643	0.1263	

Residual standard error: 1.396 on 12 degrees of freedom

Number of iterations to convergence: 12

Achieved convergence tolerance: 8.456e-06

---

**Formula: rate\_naproxen ~ umax \* S/(Ko + S)**

	Estimate	Std. error	t	value	Pr(> t )
umax	3.12156	0.16815	18.564	9.70E-11	***
Ko	0.20655	0.04865	4.245	0.000955	***

Residual standard error: 0.3392 on 13 degrees of freedom

Number of iterations to convergence: 8

Achieved convergence tolerance: 6.461e-06

---

**Formula: rate\_naproxen\_ATU ~ umax \* S/(Ko + S)**

	Estimate	Std. error	t	value	Pr(> t )
umax	3.0785	0.16874	18.244	1.21E-10	***
Ko	0.2197	0.05207	4.219	0.001	**

Residual standard error: 0.3351 on 13 degrees of freedom

Number of iterations to convergence: 7

Achieved convergence tolerance: 7.282e-06

---

**Formula: rate\_atenolol ~ umax \* (S/(Ko + S + (S^2/Ki)))**

	Estimate	Std. error	t	value	Pr(> t )
umax	1.42071	0.07344	19.346	2.05E-10	***
Ko	0.08622	0.01479	5.828	8.11E-05	***

Ki	16.23281	4.66895	3.477	0.00457	**
----	----------	---------	-------	---------	----

Residual standard error: 0.08108 on 12 degrees of freedom

Number of iterations to convergence: 7

Achieved convergence tolerance: 9.224e-07

---

**Formula: rate\_atenolol\_ATU ~ umax \* (S/(Ko + S + (S^2/Ki)))**

	Estimate	Std. error	t	value	Pr(> t )
umax	1.34143	0.06574	20.405	1.10E-10	***
Ko	0.09489	0.01525	6.224	4.43E-05	***
Ki	20.67147	6.55295	3.155	0.0083	**

Residual standard error: 0.07216 on 12 degrees of freedom

Number of iterations to convergence: 7

Achieved convergence tolerance: 1.399e-06

---

**Formula: rate\_EE2 ~ umax \* (S/(Ko + S + (S^2/Ki)))**

	Estimate	Std. error	t	value	Pr(> t )
umax	0.8466	0.1937	4.372	0.00091	***
Ko	0.2031	0.1133	1.794	0.09811	.
Ki	7.4858	5.3295	1.405	0.1855	.

Residual standard error: 0.1221 on 12 degrees of freedom

Number of iterations to convergence: 21

Achieved convergence tolerance: 8.456e-06

---

**Formula: rate\_EE2\_ATU ~ umax \* (S/(Ko + S + (S^2/Ki)))**

	Estimate	Std. error	t	value	Pr(> t )
umax	0.9023	0.1705	5.294	0.00019	***
Ko	0.249	0.1052	2.367	0.03561	*
Ki	5.7065	2.8688	1.989	0.06997	.

Residual standard error: 0.08754 on 12 degrees of freedom

Number of iterations to convergence: 13

Achieved convergence tolerance: 7.105e-06

---

---

**Formula: rate\_venlafaxine ~ umax \* (S/(Ko + S + (S^2/Ki)))**

	Estimate	Std. error	t	value	Pr(> t )
umax	0.711	0.10748	6.615	2.48E-05	***
Ko	0.08628	0.0364	2.37	0.0354	*
Ki	3.50043	1.43173	2.445	0.0309	*

Residual standard error: 0.08092 on 12 degrees of freedom

Number of iterations to convergence: 10

Achieved convergence tolerance: 4.328e-06

---

---

**Formula: rate\_venlafaxine\_ATU ~ umax \* (S/(Ko + S + (S^2/Ki)))**

	Estimate	Std. error	t	value	Pr(> t )
umax	0.56184	0.06923	8.115	3.25E-06	***
Ko	0.08117	0.02969	2.734	0.0181	*
Ki	4.70827	1.75082	2.689	0.0197	*

Residual standard error: 0.05922 on 12 degrees of freedom

Number of iterations to convergence: 9

Achieved convergence tolerance: 7.463e-06

---

---

**Formula: rate\_sulfamethoxazole ~ umax \* (S/(Ko + S + (S^2/Ki)))**

	Estimate	Std. error	t	value	Pr(> t )
umax	0.3537	0.02624	13.478	1.31E-08	***
Ko	0.02524	0.01004	2.513	0.0272	*
Ki	24.15272	15.24334	1.584	0.1391	

---

Residual standard error: 0.04242 on 12 degrees of freedom

Number of iterations to convergence: 9

Achieved convergence tolerance: 4.376e-06

---

---

**Formula: rate\_sulfamethoxazole\_ATU ~ umax \* (S/(Ko + S + (S^2/Ki)))**

	Estimate	Std. error	t	value	Pr(> t )
umax	0.2958	0.02732	10.827	1.51E-07	***
Ko	0.03034	0.01406	2.158	0.0519	.
Ki	42.65404	51.47901	0.829	0.4235	

Residual standard error: 0.04432 on 12 degrees of freedom

Number of iterations to convergence: 10

Achieved convergence tolerance: 6.436e-06

---

**Formula: rate\_trimethoprim ~ umax \* (S/(Ko + S + (S^2/Ki)))**

	Estimate	Std. error	t	value	Pr(> t )
umax	0.12305	0.04612	2.668	0.0205	*
Ko	0.14465	0.16093	0.899	0.3864	
Ki	29.58847	87.96993	0.336	0.7424	

Residual standard error: 0.04409 on 12 degrees of freedom

Number of iterations to convergence: 6

Achieved convergence tolerance: 1.095e-06

---



### Phylotypes that had significant associations (Spearman, $p < 0.01$ ) with DO concentration

Associations between phylotypes (OTUs grouped by genus) and DO concentration were tested using Mothur's `otu.association` command using the `metadata` option, which performs a Spearman's rank correlation test between the transcript abundance of each phylotype and the DO concentration of the batch experiment. Positive and negative associations are provided in Table C4.

**Table C4.** Phylotypes with significant associations (Spearman,  $p < 0.01$ ) with DO concentration.

Positively associated with DO concentration						
OTU	Kingdom	Phylum	Class	Order	Family	Genus
Otu028	Bacteria	Bacteroidetes	Sphingobacteriia	Sphingobacteriales	unclassified	unclassified
Otu029	Bacteria	Planctomycetes	Planctomycetia	Planctomycetales	Planctomycetaceae	Planctomyces
Otu033	Bacteria	Chloroflexi	Caldilineae	Caldilineales	Caldilineaceae	unclassified
Otu035	Bacteria	Proteobacteria	Gammaproteobacteria	Xanthomonadales	Xanthomonadaceae	unclassified
Otu048	Bacteria	Proteobacteria	Deltaproteobacteria	Bdellovibrionales	Bdellovibrionaceae	Bdellovibrio
Otu086	Bacteria	Bacteroidetes	Bacteroidetes_incertae_sedis	Ohtaekwangia	unclassified	unclassified
Otu089	Bacteria	Bacteroidetes	Sphingobacteriia	Sphingobacteriales	Chitinophagaceae	Terrimonas
Otu174	Bacteria	Proteobacteria	Betaproteobacteria	Burkholderiales	Comamonadaceae	Hydrogenophaga
Otu190	Bacteria	Proteobacteria	Alphaproteobacteria	Caulobacterales	Caulobacteraceae	unclassified

Negatively associated with DO concentration						
OTU	Kingdom	Phylum	Class	Order	Family	Genus
Otu009	Bacteria	Actinobacteria	Actinobacteria	Actinomycetales	unclassified	unclassified
Otu016	Bacteria	Proteobacteria	Alphaproteobacteria	Rhodobacterales	Rhodobacteraceae	unclassified
Otu017	Bacteria	Proteobacteria	Deltaproteobacteria	Myxococcales	Polyangiaceae	Byssovorax
Otu020	Bacteria	Proteobacteria	Deltaproteobacteria	unclassified	unclassified	unclassified
Otu022	Bacteria	Firmicutes	Clostridia	Clostridiales	Ruminococcaceae	unclassified

Otu024	Bacteria	Actinobacteria	Actinobacteria	unclassified	unclassified	unclassified
Otu032	Bacteria	Firmicutes	Clostridia	Clostridiales	Lachnospiraceae	unclassified
Otu043	Bacteria	Proteobacteria	Epsilonproteobacteria	Campylobacterales	Campylobacteraceae	Arcobacter
Otu052	Bacteria	Proteobacteria	Alphaproteobacteria	Rhodobacterales	Rhodobacteraceae	Paracoccus
Otu066	Bacteria	Firmicutes	Bacilli	Lactobacillales	Streptococcaceae	Streptococcus
Otu091	Bacteria	Firmicutes	Clostridia	Clostridiales	Lachnospiraceae	Ruminococcus2
Otu105	Bacteria	Bacteroidetes	Flavobacteriia	Flavobacteriales	Flavobacteriaceae	Chryseobacterium
Otu108	Bacteria	Nitrospirae	Nitrospira	Nitrospirales	Nitrospiraceae	Nitrospira
Otu109	Bacteria	Firmicutes	Bacilli	Lactobacillales	Streptococcaceae	Lactococcus
Otu118	Bacteria	Bacteroidetes	Flavobacteriia	Flavobacteriales	Flavobacteriaceae	Cloacibacterium
Otu150	Bacteria	Proteobacteria	Gammaproteobacteria	Aeromonadales	Aeromonadaceae	Aeromonas
Otu196	Bacteria	Bacteroidetes	Cytophagia	Cytophagales	unclassified	unclassified

### **Phylotypes that had positive and significant associations (Spearman, $p < 0.01$ ) with pharmaceutical biotransformation rates**

Positive associations between phylotypes and biotransformation rates for each compound were identified using Mothur's `otu.association` command using the `metadata` option and Spearman's rank correlation method (Table E5). The number and relative activity of the significantly associated phylotypes differed between the compounds, as no single significantly associated phylotype was shared among more than 3 compounds (Figure C4).

**Table C5.** Phylotypes with significant associations (Spearman,  $p < 0.01$ ) with biotransformation rates for each compound.

<b>Ibuprofen</b>						
<b>OTU</b>	<b>Kingdom</b>	<b>Phylum</b>	<b>Class</b>	<b>Order</b>	<b>Family</b>	<b>Genus</b>
Otu009	Bacteria	Actinobacteria	Actinobacteria	Actinomycetales	unclassified	unclassified
Otu016	Bacteria	Proteobacteria	Alphaproteobacteria	Rhodobacterales	Rhodobacteraceae	unclassified
Otu043	Bacteria	Proteobacteria	Epsilonproteobacteria	Campylobacterales	Campylobacteraceae	Arcobacter
Otu109	Bacteria	Firmicutes	Bacilli	Lactobacillales	Streptococcaceae	Lactococcus
Otu151	Bacteria	Proteobacteria	Gammaproteobacteria	Pseudomonadales	Moraxellaceae	Enhydrobacter
Otu205	Bacteria	Actinobacteria	Actinobacteria	Actinomycetales	Intrasporangiaceae	Phycococcus

<b>Acetaminophen</b>						
<b>OTU</b>	<b>Kingdom</b>	<b>Phylum</b>	<b>Class</b>	<b>Order</b>	<b>Family</b>	<b>Genus</b>
Otu001	Bacteria	unclassified	unclassified	unclassified	unclassified	unclassified
Otu011	Bacteria	Proteobacteria	Deltaproteobacteria	Myxococcales	Nannocystaceae	unclassified
Otu014	Bacteria	Proteobacteria	Alphaproteobacteria	unclassified	unclassified	unclassified
Otu026	Bacteria	Actinobacteria	Actinobacteria	Actinomycetales	Mycobacteriaceae	Mycobacterium
Otu029	Bacteria	Planctomycetes	Planctomycetia	Planctomycetales	Planctomycetaceae	Planctomyces
Otu080	Bacteria	Bacteroidetes	Sphingobacteriia	Sphingobacteriales	Chitinophagaceae	Ferruginibacter
Otu131	Bacteria	Gemmatimonadetes	Gemmatimonadetes	Gemmatimonadales	Gemmatimonadaceae	Gemmatimonas
Otu137	Bacteria	Acidobacteria	Acidobacteria_Gp10	Gp10	unclassified	unclassified
Otu142	Bacteria	Proteobacteria	Gammaproteobacteria	Xanthomonadales	Xanthomonadaceae	Pseudoxanthomonas
Otu152	Bacteria	Proteobacteria	Alphaproteobacteria	Caulobacterales	Hyphomonadaceae	Hyphomonas
Otu158	Bacteria	Proteobacteria	Gammaproteobacteria	Xanthomonadales	Xanthomonadaceae	Dokdonella
Otu200	Bacteria	Acidobacteria	Acidobacteria_Gp4	unclassified	unclassified	unclassified
Otu204	Bacteria	candidate_division_WPS-2	unclassified	unclassified	unclassified	unclassified
Otu271	Bacteria	Proteobacteria	Betaproteobacteria	Burkholderiales	Alcaligenaceae	Azohydromonas
Otu382	Archaea	Euryarchaeota	Thermoplasmata	Methanomassiliococcales	Methanomassiliococcaceae	Methanomassiliococcus

Otu449 Bacteria Proteobacteria Betaproteobacteria Burkholderiales Oxalobacteraceae Massilia

**Naproxen**

<b>OTU</b>	<b>Kingdom</b>	<b>Phylum</b>	<b>Class</b>	<b>Order</b>	<b>Family</b>	<b>Genus</b>
Otu009	Bacteria	Actinobacteria	Actinobacteria	Actinomycetales	unclassified	unclassified
Otu016	Bacteria	Proteobacteria	Alphaproteobacteria	Rhodobacterales	Rhodobacteraceae	unclassified
Otu017	Bacteria	Proteobacteria	Deltaproteobacteria	Myxococcales	Polyangiaceae	Byssovorax
Otu022	Bacteria	Firmicutes	Clostridia	Clostridiales	Ruminococcaceae	unclassified
Otu024	Bacteria	Actinobacteria	Actinobacteria	unclassified	unclassified	unclassified
Otu043	Bacteria	Proteobacteria	Epsilonproteobacteria	Campylobacterales	Campylobacteraceae	Arcobacter
Otu052	Bacteria	Proteobacteria	Alphaproteobacteria	Rhodobacterales	Rhodobacteraceae	Paracoccus
Otu066	Bacteria	Firmicutes	Bacilli	Lactobacillales	Streptococcaceae	Streptococcus
Otu105	Bacteria	Bacteroidetes	Flavobacteriia	Flavobacteriales	Flavobacteriaceae	Chryseobacterium
Otu108	Bacteria	Nitrospirae	Nitrospira	Nitrospirales	Nitrospiraceae	Nitrospira
Otu109	Bacteria	Firmicutes	Bacilli	Lactobacillales	Streptococcaceae	Lactococcus
Otu118	Bacteria	Bacteroidetes	Flavobacteriia	Flavobacteriales	Flavobacteriaceae	Cloacibacterium
Otu150	Bacteria	Proteobacteria	Gammaproteobacteria	Aeromonadales	Aeromonadaceae	Aeromonas
Otu172	Archaea	Euryarchaeota	Methanomicrobia	Methanosarcinales	Methanosarcinaceae	Methanosarcina

**Atenolol**

<b>OTU</b>	<b>Kingdom</b>	<b>Phylum</b>	<b>Class</b>	<b>Order</b>	<b>Family</b>	<b>Genus</b>
Otu068	Bacteria	Proteobacteria	Alphaproteobacteria	Rhizobiales	Phyllobacteriaceae	unclassified
Otu205	Bacteria	Actinobacteria	Actinobacteria	Actinomycetales	Intrasporangiaceae	Phycococcus
Otu241	Bacteria	Fusobacteria	Fusobacteriia	Fusobacteriales	Leptotrichiaceae	unclassified

**EE2**

<b>OTU</b>	<b>Kingdom</b>	<b>Phylum</b>	<b>Class</b>	<b>Order</b>	<b>Family</b>	<b>Genus</b>
Otu014	Bacteria	Proteobacteria	Alphaproteobacteria	unclassified	unclassified	unclassified
Otu091	Bacteria	Firmicutes	Clostridia	Clostridiales	Lachnospiraceae	Ruminococcus2

Otu105	Bacteria	Bacteroidetes	Flavobacteriia	Flavobacteriales	Flavobacteriaceae	Chryseobacterium
Otu108	Bacteria	Nitrospirae	Nitrospira	Nitrospirales	Nitrospiraceae	Nitrospira
Otu193	Bacteria	Deinococcus-Thermus	Deinococci	Deinococcales	Deinococcaceae	unclassified
Otu205	Bacteria	Actinobacteria	Actinobacteria	Actinomycetales	Intrasporangiaceae	Phycoccus

**Venlafaxine**

<b>OTU</b>	<b>Kingdom</b>	<b>Phylum</b>	<b>Class</b>	<b>Order</b>	<b>Family</b>	<b>Genus</b>
Otu011	Bacteria	Proteobacteria	Deltaproteobacteria	Myxococcales	Nannocystaceae	unclassified
Otu014	Bacteria	Proteobacteria	Alphaproteobacteria	unclassified	unclassified	unclassified
Otu026	Bacteria	Actinobacteria	Actinobacteria	Actinomycetales	Mycobacteriaceae	Mycobacterium
Otu037	Bacteria	Proteobacteria	Betaproteobacteria	Rhodocyclales	Rhodocyclaceae	Zoogloea
Otu044	Bacteria	Planctomycetes	Planctomycetia	Planctomycetales	Planctomycetaceae	Zavarzinella
Otu058	Bacteria	Actinobacteria	Actinobacteria	Actinomycetales	Intrasporangiaceae	Tetrasphaera
Otu063	Bacteria	Bacteroidetes	Sphingobacteriia	Sphingobacteriales	Saprospiraceae	Haliscomenobacter
Otu074	Bacteria	Planctomycetes	Planctomycetia	Planctomycetales	Planctomycetaceae	Gemmata
Otu076	Bacteria	Proteobacteria	Gammaproteobacteria	Pseudomonadales	Moraxellaceae	Alkanindiges
Otu080	Bacteria	Bacteroidetes	Sphingobacteriia	Sphingobacteriales	Chitinophagaceae	Ferruginibacter
Otu097	Bacteria	Planctomycetes	Planctomycetia	Planctomycetales	Planctomycetaceae	Pirellula
Otu105	Bacteria	Bacteroidetes	Flavobacteriia	Flavobacteriales	Flavobacteriaceae	Chryseobacterium
Otu108	Bacteria	Nitrospirae	Nitrospira	Nitrospirales	Nitrospiraceae	Nitrospira
Otu131	Bacteria	Gemmatimonadetes	Gemmatimonadetes	Gemmatimonadales	Gemmatimonadaceae	Gemmatimonas
Otu137	Bacteria	Acidobacteria	Acidobacteria_Gp10	Gp10	unclassified	unclassified
Otu152	Bacteria	Proteobacteria	Alphaproteobacteria	Caulobacterales	Hyphomonadaceae	Hyphomonas
Otu153	Bacteria	Proteobacteria	Alphaproteobacteria	Rickettsiales	Rickettsiaceae	Rickettsia
Otu158	Bacteria	Proteobacteria	Gammaproteobacteria	Xanthomonadales	Xanthomonadaceae	Dokdonella
Otu198	Bacteria	Bacteroidetes	Cytophagia	Cytophagales	Cytophagaceae	unclassified
Otu204	Bacteria	candidate_division_WPS-2	unclassified	unclassified	unclassified	unclassified

Otu209	Bacteria	Planctomycetes	Planctomycetia	Candidatus_Brocadiales	Candidatus_Brocadiaceae	unclassified
Otu240	Bacteria	Proteobacteria	Gammaproteobacteria	Alteromonadales	Alteromonadaceae	Haliae
Otu271	Bacteria	Proteobacteria	Betaproteobacteria	Burkholderiales	Alcaligenaceae	Azohydromonas
Otu285	Bacteria	Deinococcus-Thermus	Deinococci	Deinococcales	Deinococcaceae	Deinobacterium
Otu449	Bacteria	Proteobacteria	Betaproteobacteria	Burkholderiales	Oxalobacteraceae	Massilia
Otu492	Bacteria	Proteobacteria	Betaproteobacteria	Burkholderiales	Burkholderiaceae	Chitinimonas

**Trimethoprim**

<b>OTU</b>	<b>Kingdom</b>	<b>Phylum</b>	<b>Class</b>	<b>Order</b>	<b>Family</b>	<b>Genus</b>
Otu016	Bacteria	Proteobacteria	Alphaproteobacteria	Rhodobacterales	Rhodobacteraceae	unclassified
Otu030	Bacteria	Proteobacteria	Gammaproteobacteria	Pseudomonadales	Moraxellaceae	unclassified
Otu109	Bacteria	Firmicutes	Bacilli	Lactobacillales	Streptococcaceae	Lactococcus
Otu185	Bacteria	Proteobacteria	Gammaproteobacteria	Pseudomonadales	Pseudomonadaceae	unclassified
Otu196	Bacteria	Bacteroidetes	Cytophagia	Cytophagales	unclassified	unclassified
Otu205	Bacteria	Actinobacteria	Actinobacteria	Actinomycetales	Intrasporangiaceae	Phycoccus

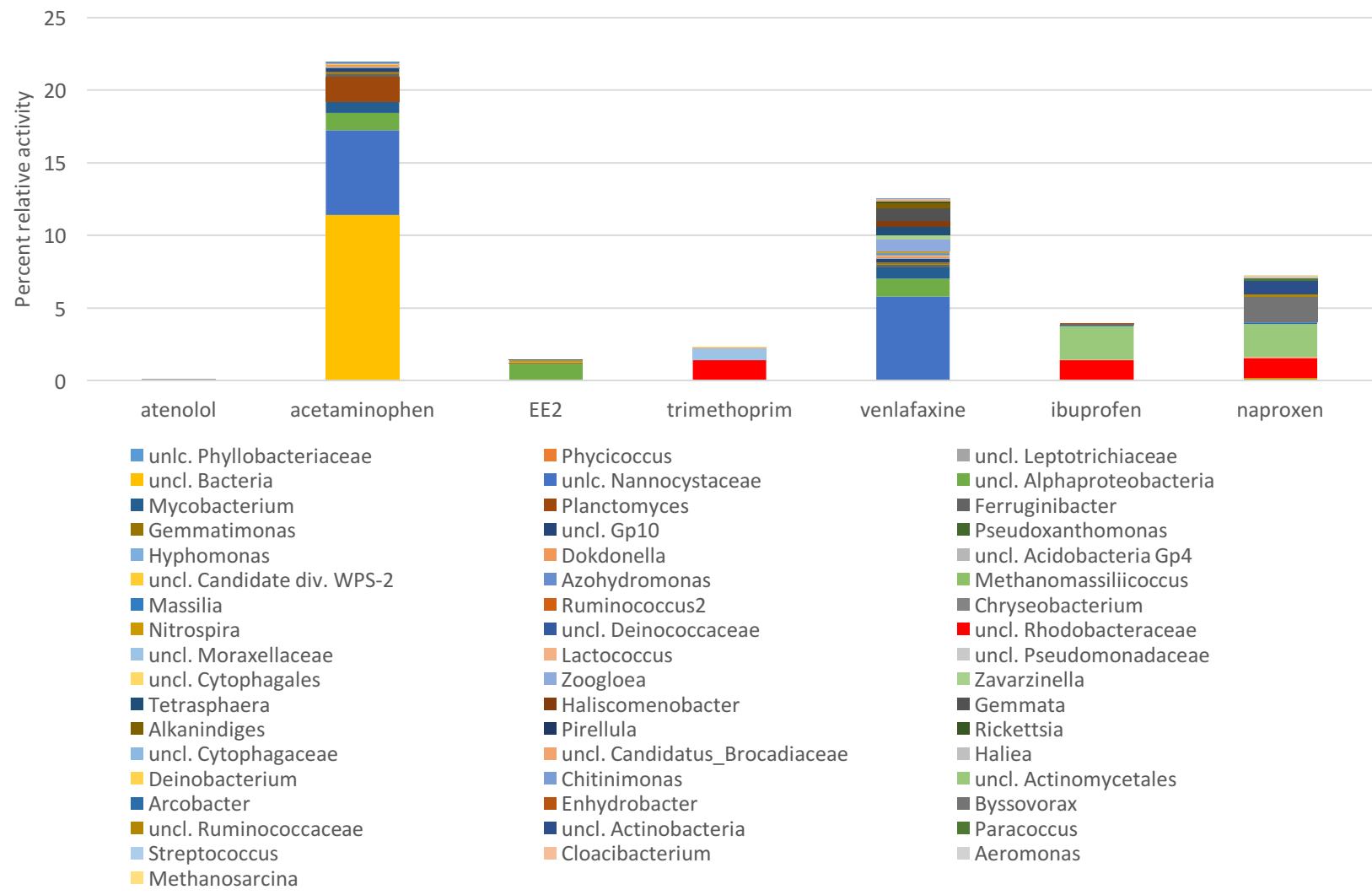


**Figure C4.** Relative activity of significant and positively associated (Spearman,  $p < 0.01$ ) phylotypes for each compound.

## Literature cited

Fayad, P. B.; Prévost, M.; Sauvé, S. On-Line Solid-Phase Extraction Coupled to Liquid Chromatography Tandem Mass Spectrometry Optimized for the Analysis of Steroid Hormones in Urban Wastewaters. *Talanta* **2013**, *115*, 349–360.



## **Appendix D.**

### **Supplementary Information for Chapter 6**

#### **Elucidating the impact of microbial community diversity on pharmaceutical biotransformation during wastewater treatment**

##### **Semi-synthetic sewage media preparation**

1. Freshly collected primary effluent was filtered through glass fiber filters with a pore size of 0.7  $\mu\text{m}$  (Whatman GF/F, Item #0987472, Fisher Scientific, Pittsburgh, Pennsylvania)
2. Primary was then floc-filtered by adding 1 mL per 100 mL of primary of 100 g/L zinc sulfate and adjusting the pH to  $\sim 10.4$  using 10 M sodium hydroxide while mixing vigorously (by placing the primary on a stir plate). After pH adjustment, mixing was halted and the flocs were allowed to settle for 3 minutes
3. The supernatant was pulled off and filtered again through a 0.2  $\mu\text{m}$  filter (Stericup, Millipore, Darmstadt, Germany)
4. The filtered primary was autoclaved for 45 minutes at 121  $^{\circ}\text{C}$ .
5. After cooling, the autoclaved media was supplemented with sterile stock solutions of humic acid, meat extract and peptone, and ammonium-chloride to achieve a final concentration of 2,000 mg-COD/L and 30 mg-N/L as ammonia. Micronutrients were also supplemented assuming a yield of 0.5 g COD/g COD (Grady et al., 2011) to achieve the final concentrations provided in Table D1.
6. The media was pH adjusted to 7.5 using concentrated hydrochloric acid.

**Table D1.** Final concentrations of micronutrients in semi-synthetic sewage media

Nutrient	Concentration (mg/L)
Ca	8.2
Fe	1.65
Co	0.00033
N	71.75
P	14.35
Mg	5.77
Mn	0.08
Mo	0.0033
K	8.25
S	4.95
Zn	0.16
Cu	0.02
Borate	0.01

### **Compound selection approach**

The primary goal of pharmaceutical compound selection was evaluate compounds that would undergo a variety of different biochemical transformation pathways, to accomplish this we used the University of Minnesota’s Pathway Prediction system(Ellis et al., 2006) (UMPPS). Using reactions found in the literature or the University of Minnesota’s Biocatalysis/Biodegradation and Database, UMPPS predicts aerobic biodegradation pathways based on chemical structure and assigns these pathways to rules, these rules are then characterized as “very likely”, “likely,” or “neutral,” by two or more biodegradation experts. We evaluated the biodegradation pathways of 22 compounds using this database accessed in May, 2014. For each compound we accounted for the “very likely”, “likely”, and “neutral” rules for the initial biotransformation step. From these 22 compounds, the list was narrowed to contain compounds which could be measured in our matrix with existing methods but that still encompassed a broad range of unique rules. The final list of compounds along with the rules associated with the compounds is given in Table D2.

**Table D2.** Predicted biotransformation pathways for selected compounds. Unique pathways are indicated in bold.

Compound	Biotransformation pathways	Likelihood	
Atenolol	<b>Primary Amide → Carboxylate</b>	<b>Likely</b>	
	primary Amine → Aldehyde or Ketone	Likely	
	secondary Amine → Amine + Aldehyde or Ketone		
	tertiary Amine → secondary Amine → Aldehyde or Ketone		
	Methylammonium derivative → Trimethylamine + Aldehyde or Ketone	Neutral	
	secondary Alcohol → Ketone		
secondary Alcohol → Ester			
EE2	dialiphatic Ether → Alcohol + Aldehyde	Neutral	
	aromatic-aliphatic Ether → Phenol derivative + Aldehyde		
	<b>1-Hydroxy-2-unsubstituted aromatic → 1,2-Dihydroxyaromatic 4-Hydroxypyridine derivative → 3,4-Dihydroxypyridine derivative</b>	<b>Likely</b>	
Trimethoprim	tertiary Aliphatic → tertiary Alcohol	Neutral	
	secondary Aliphatic → secondary Alcohol	Neutral	
	dialiphatic Ether → Alcohol + Aldehyde	Neutral	
	aromatic-aliphatic Ether → Phenol derivative + Aldehyde		
Venlafaxine	secondary Aliphatic → secondary Alcohol	Neutral	
	primary Amine → Aldehyde or Ketone	Likely	
	secondary Amine → Amine + Aldehyde or Ketone		
	tertiary Amine → secondary Amine → Aldehyde or Ketone		
	Methylammonium derivative → Trimethylamine + Aldehyde or Ketone	Neutral	
dialiphatic Ether → Alcohol + Aldehyde			
Carbamazepine	aromatic-aliphatic Ether → Phenol derivative + Aldehyde	Neutral	
	tertiary Aliphatic → tertiary Alcohol		
	<b>N-substituted Urea derivative → Carbamate + primary Amine</b>	<b>Neutral</b>	
	<b>N,N-disubstituted Urea derivative → N-substituted Carbamate + primary Amine</b>		
	dialiphatic Ether → Alcohol + Aldehyde	Neutral	
	aromatic-aliphatic Ether → Phenol derivative + Aldehyde		
	<b>secondary Amide → Carboxylate + primary Amine</b>	<b>Neutral</b>	
	<b>Lactam → Aminocarboxylate</b>		
	Glyburide	<b>N-substituted Urea derivative → Carbamate + primary Amine</b>	<b>Neutral</b>
		<b>N,N-disubstituted Urea derivative → N-substituted Carbamate + primary Amine</b>	
<b>Sulfamate → Amine</b>		<b>Neutral</b>	
<b>Sulfonamide → Amine + Sulfonate</b>			
N-substituted Amide → Amide + Aldehyde or Ketone		Neutral	
N, N-disubstituted Amide → N-substituted Amide + Aldehyde or Ketone			
N-substituted Urea derivative → Urea derivative + Aldehyde or Ketone			
N,N-disubstituted Urea derivative → N-substituted Urea derivative + Aldehyde or Ketone			
Erythromycin	<b>Ester → Alcohol + Carboxylate</b>	<b>Likely</b>	
	<b>Lactone → Hydroxycarboxylate</b>	Neutral	
	secondary Alcohol → Ketone		
	secondary Alcohol → Ester		

## **Pharmaceutical quantification via liquid chromatography and high resolution mass spectrometry**

Pharmaceuticals were quantified via on-line pre-concentration followed by high performance liquid chromatography (HPLC) and high resolution mass spectrometry (HRMS). Matrix-matched external calibration curves containing a mixture of the target compounds and deuterated analogs were used for quantification. On-line pre-concentration of the compounds of interest was performed using the Equan™ (Thermo Fisher Scientific, Grand Island, New York) system (system details are provided in Fayad et al., 2013). The on-line pre-concentration was performed using a Hypersil Gold aQ trapping column (20 x 2.1 mm, 12 µM particle size; Thermo Fisher Scientific) and chromatographic separation was done with an Accucore aQ column (50 x 2.1 mm, 2.6 µm particle size; Thermo Fisher Scientific). A 500 µL sample was injected onto the trapping column. A mobile phase containing water with 0.1% formic acid and methanol with 0.1% formic acid was applied via gradient flow to elute all compounds with minimal overlap. The mobile phase A was water + 0.1% formic acid and B was methanol + 0.1 % formic acid. The flow rate was 0.175 mL/min and the gradient profile used was as follows: 90% A was held for 3 min, ramped to 90% of B over 8 min, held at 90% B for 1 minutes, flow rate increased to 0.25 mL/min over 0.2 minutes and held at 0.25 ml/min for 1.8 minutes, and finally returned to 90% of A and 0.175 mL/min over 0.2 min. Total run time for one sample was 16 minutes at a flow rate of 1 mL/min on the trapping column and 0.175 – 0.250 mL/min on the analytical column.

Ionization of the compounds was achieved by positive electron spray ionization (ESI). The following source parameters were used: capillary temperature of 250 °C, auxillary gas heater temperature of 275 °C, a spray voltage of 3.5 kV, sheath gas flow rate of 30 arbitrary units,

auxillary gas flow rate of 20 arbitrary units, and sweep gas flow rate of 1 arbitrary unit. A full scan ranging from 150 to 750 m/z was performed at a resolution of 70,000 and target automatic gain control (AGC) of  $1 \times 10^{-6}$ . All data were collected and processed using the Thermo TraceFinder Software Version 3.2 (Thermo Fisher Scientific).

**Table D3.** Target compounds with accurate mass and retention times used for quantification.

Compound	Formula	Accurate mass (m/z)	Retention time (min)	Therapeutic use
Trimethoprim	C <sub>14</sub> H <sub>18</sub> N <sub>4</sub> O <sub>3</sub>	291.14516	6.67	Antibiotic
d9-trimethoprim	C <sub>14</sub> H <sub>9</sub> D <sub>9</sub> N <sub>4</sub> O <sub>3</sub>	300.20165	6.62	
EE2	C <sub>20</sub> H <sub>24</sub> O <sub>2</sub>	279.17434	10.96	Synthetic estrogen
d4-EE2	C <sub>20</sub> H <sub>20</sub> D <sub>4</sub> O <sub>2</sub>	283.19944	10.95	
Atenolol	C <sub>14</sub> H <sub>22</sub> N <sub>2</sub> O <sub>3</sub>	267.17031	4.92	Beta-blocker
d7-atenolol	C <sub>14</sub> H <sub>15</sub> D <sub>7</sub> N <sub>2</sub> O <sub>3</sub>	274.21425	4.88	
Carbamazepine	C <sub>15</sub> H <sub>12</sub> N <sub>2</sub> O	237.10223	9.59	Anticonvulsant
d8-Carbamazepine	C <sub>15</sub> H <sub>4</sub> D <sub>8</sub> N <sub>2</sub> O	245.15245	9.54	
Glyburide	C <sub>23</sub> H <sub>28</sub> CIN <sub>3</sub> O <sub>5</sub> S	494.15109	11.23	Antidiabetic
d11-Glyburide	C <sub>23</sub> H <sub>17</sub> D <sub>11</sub> CIN <sub>3</sub> O <sub>5</sub> S	505.22014	11.20	
Acetaminophen	C <sub>8</sub> H <sub>9</sub> NO <sub>2</sub>	152.07060	5.25	Analgesic and antipyretic
d3-Acetaminophen	C <sub>8</sub> H <sub>6</sub> D <sub>3</sub> NO <sub>2</sub>	155.08943	5.22	

## Dissolved organic carbon oxidation in batch experiments

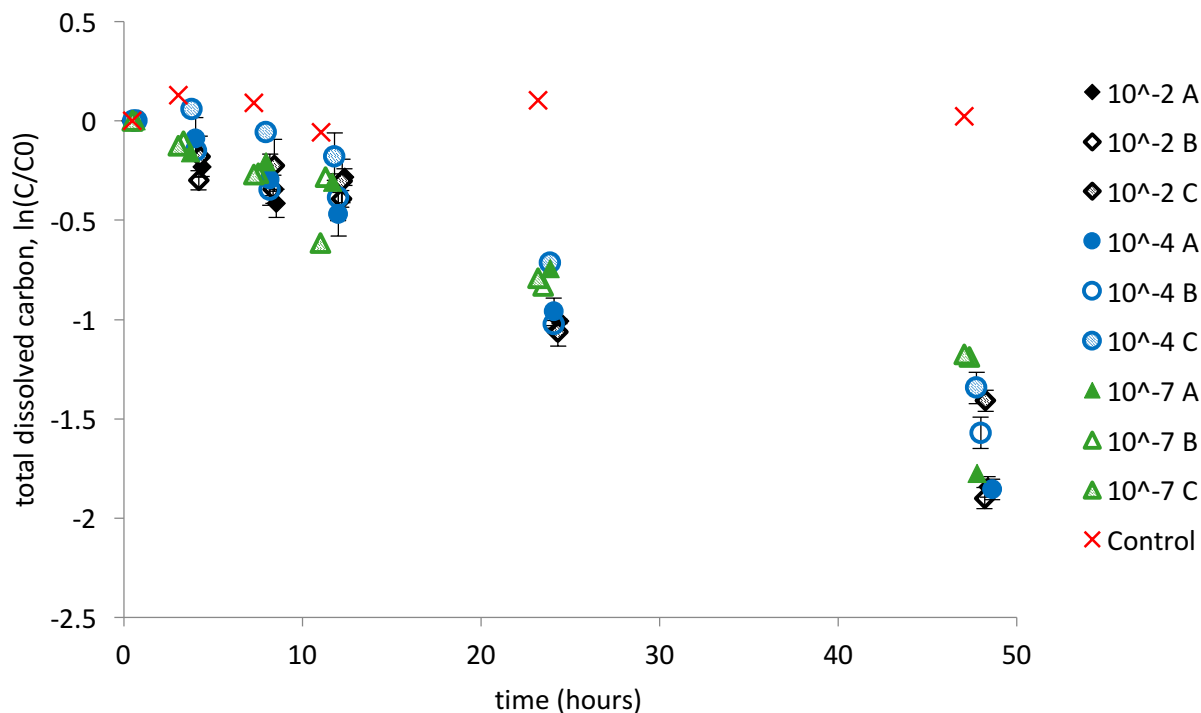


**Figure D1.** Dissolved organic carbon profiles for each batch reactor over the first 2 days of the experiment. Samples from the 10<sup>-2</sup> condition are shown in black, 10<sup>-4</sup> in blue, and 10<sup>-7</sup> in green.

## Pharmaceutical biotransformation data

Initial and final concentrations of the pharmaceuticals, calculated biotransformation rates, and normalized biotransformation rates are shown in Table D4. Biotransformation rates for each compound in each condition were scaled such that the average of the rates were 0 and the standard deviation was equal to 1. The collective biotransformation rate was calculated by averaging the scaled biotransformation rates (Zavaleta et al., 2010; Johnson et al., 2014). Scaled rates were used for testing associations with biodiversity indices using Spearman's rank correlation test.

**Table D4.** Initial and final pharmaceutical concentrations in each batch reactor, biotransformation rates, and rates normalized by volatile suspended solids (VSS) concentration.

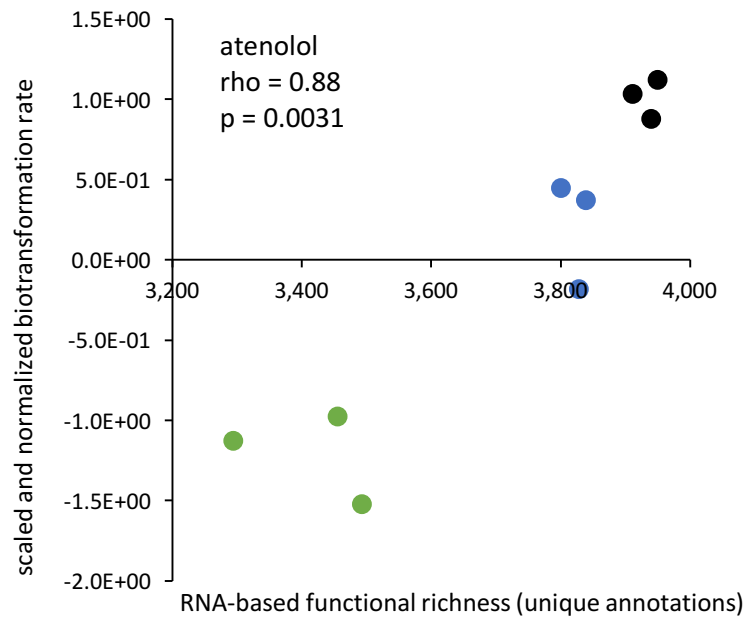
	Concentration ( $\mu\text{g/L}$ )		Rate	rate/VSS
	initial	final	( $\mu\text{g/L/d}$ )	(1/d)
<b>atenolol</b>				
10 <sup>-2</sup> A	9.96	0.00	2.47	1.10E-05
10 <sup>-2</sup> B	9.64	0.00	2.40	1.04E-05
10 <sup>-2</sup> C	9.44	0.00	2.35	1.14E-05
10 <sup>-4</sup> A	9.29	5.39	0.98	6.01E-06
10 <sup>-4</sup> B	9.60	5.23	1.09	8.28E-06
10 <sup>-4</sup> C	9.19	4.07	1.28	8.59E-06
10 <sup>-7</sup> A	9.42	8.04	0.34	2.11E-06
10 <sup>-7</sup> B	9.87	7.53	0.59	2.74E-06
10 <sup>-7</sup> C	9.37	8.92	0.11	5.02E-07
Control	9.80	9.26	0.13	1.09E-06
<b>EE2</b>				
10 <sup>-2</sup> A	8.26	4.08	1.04	4.62E-06
10 <sup>-2</sup> B	8.03	3.65	1.09	4.71E-06
10 <sup>-2</sup> C	8.08	4.32	0.94	4.53E-06
10 <sup>-4</sup> A	7.36	7.02	0.08	5.21E-07
10 <sup>-4</sup> B	7.36	7.20	0.04	2.99E-07
10 <sup>-4</sup> C	7.99	6.92	0.27	1.79E-06
10 <sup>-7</sup> A	8.16	7.28	0.22	1.35E-06
10 <sup>-7</sup> B	8.12	6.87	0.31	1.47E-06
10 <sup>-7</sup> C	7.40	8.15	-0.19	-8.27E-07
Control	8.03	9.62	-0.40	-3.21E-06
<b>trimethoprim</b>				
10 <sup>-2</sup> A	8.66	8.21	0.11	4.97E-07
10 <sup>-2</sup> B	9.28	8.31	0.24	1.04E-06
10 <sup>-2</sup> C	9.37	8.40	0.24	1.17E-06
10 <sup>-4</sup> A	8.84	8.99	-0.04	-2.25E-07
10 <sup>-4</sup> B	9.00	8.87	0.03	2.44E-07
10 <sup>-4</sup> C	8.31	9.05	-0.19	-1.25E-06
10 <sup>-7</sup> A	9.67	9.53	0.03	2.13E-07
10 <sup>-7</sup> B	8.64	9.78	-0.29	-1.34E-06
10 <sup>-7</sup> C	9.64	9.98	-0.08	-3.71E-07
Control	8.80	9.18	-0.10	-7.66E-07
<b>venlafaxine</b>				
10 <sup>-2</sup> A	9.33	8.17	0.29	1.28E-06
10 <sup>-2</sup> B	9.11	8.38	0.18	7.89E-07
10 <sup>-2</sup> C	9.62	8.68	0.23	1.13E-06
10 <sup>-4</sup> A	9.20	8.87	0.08	5.06E-07

10 <sup>-4</sup> B	9.13	8.75	0.09	7.18E-07
10 <sup>-4</sup> C	9.48	9.02	0.12	7.75E-07
10 <sup>-7</sup> A	9.19	8.99	0.05	3.21E-07
10 <sup>-7</sup> B	9.09	8.67	0.11	4.92E-07
10 <sup>-7</sup> C	9.27	9.04	0.06	2.48E-07
Control	9.18	10.13	-0.24	-1.92E-06
<b>carbamazepine</b>				
10 <sup>-2</sup> A	10.11	9.59	0.13	5.67E-07
10 <sup>-2</sup> B	11.22	8.52	0.67	2.90E-06
10 <sup>-2</sup> C	10.49	8.19	0.57	2.76E-06
10 <sup>-4</sup> A	10.32	11.66	-0.33	-2.06E-06
10 <sup>-4</sup> B	11.71	11.83	-0.03	-2.31E-07
10 <sup>-4</sup> C	11.56	14.98	-0.85	-5.74E-06
10 <sup>-7</sup> A	11.70	15.66	-0.99	-6.08E-06
10 <sup>-7</sup> B	12.73	16.22	-0.88	-4.09E-06
10 <sup>-7</sup> C	13.15	18.93	-1.45	-6.36E-06
Control	11.55	13.02	-0.37	-2.98E-06
<b>glyburide</b>				
10 <sup>-2</sup> A	9.51	9.64	-0.03	-1.37E-07
10 <sup>-2</sup> B	8.99	9.36	-0.09	-4.02E-07
10 <sup>-2</sup> C	9.61	9.42	0.05	2.30E-07
10 <sup>-4</sup> A	9.41	9.25	0.04	2.48E-07
10 <sup>-4</sup> B	9.59	9.33	0.07	4.95E-07
10 <sup>-4</sup> C	9.13	9.74	-0.15	-1.03E-06
10 <sup>-7</sup> A	9.60	9.71	-0.03	-1.78E-07
10 <sup>-7</sup> B	9.66	9.77	-0.03	-1.33E-07
10 <sup>-7</sup> C	9.70	10.57	-0.22	-9.64E-07
Control	9.80	9.99	-0.05	-3.83E-07
<b>Erythromycin</b>				
10 <sup>-2</sup> A	9.52	3.97	1.38	6.13E-06
10 <sup>-2</sup> B	9.10	4.34	1.18	5.12E-06
10 <sup>-2</sup> C	9.74	3.97	1.43	6.95E-06
10 <sup>-4</sup> B	9.36	2.43	1.73	1.31E-05
10 <sup>-4</sup> C	9.62	4.19	1.36	9.11E-06
10 <sup>-7</sup> A	10.12	6.18	0.98	6.04E-06
10 <sup>-7</sup> B	9.46	5.05	1.11	5.17E-06
10 <sup>-7</sup> C	9.18	5.17	1.01	4.40E-06
Control	9.83	9.09	0.19	1.51E-06

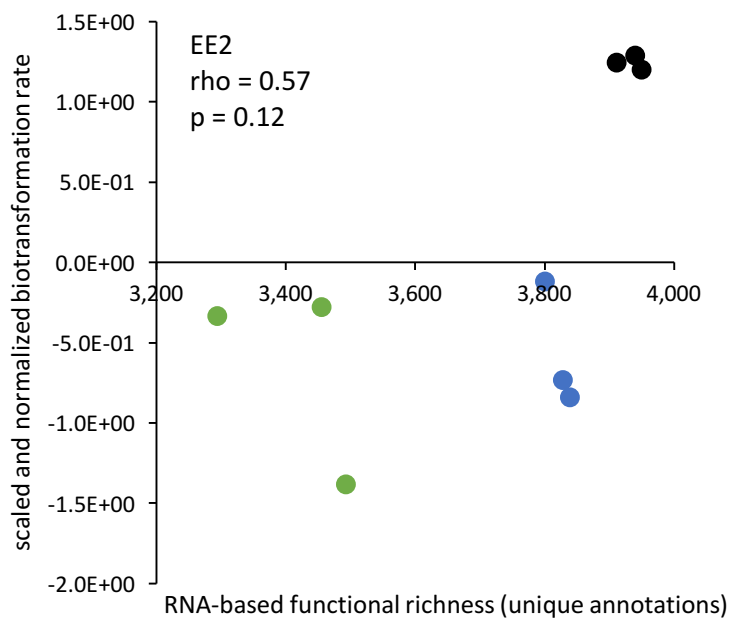


## Pharmaceutical biotransformation rates versus RNA-based functional richness

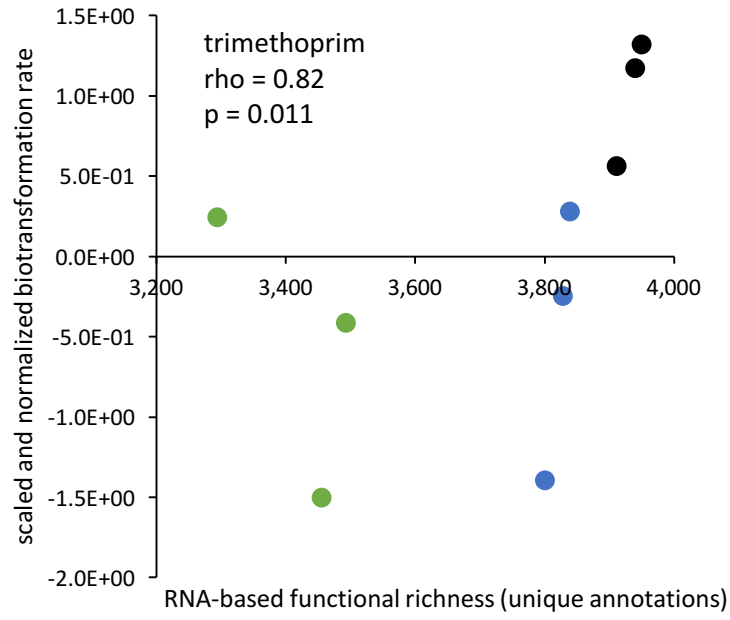
a.



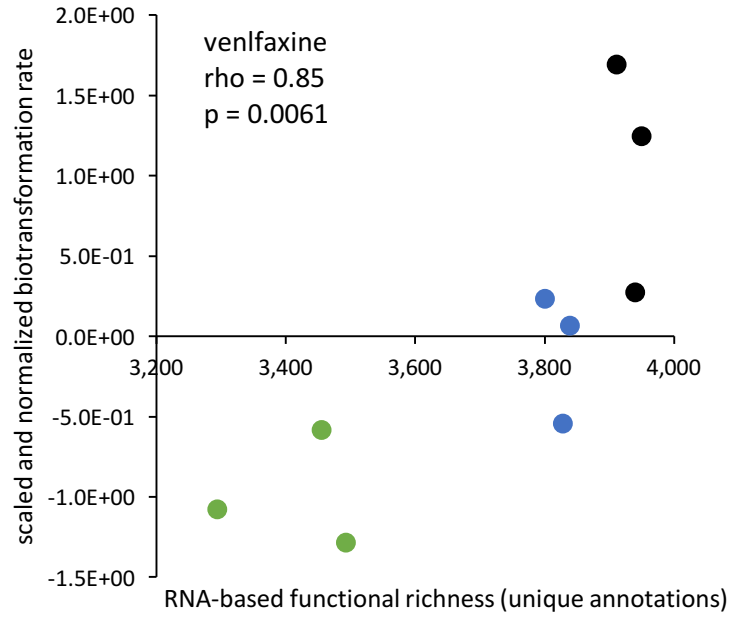
b.



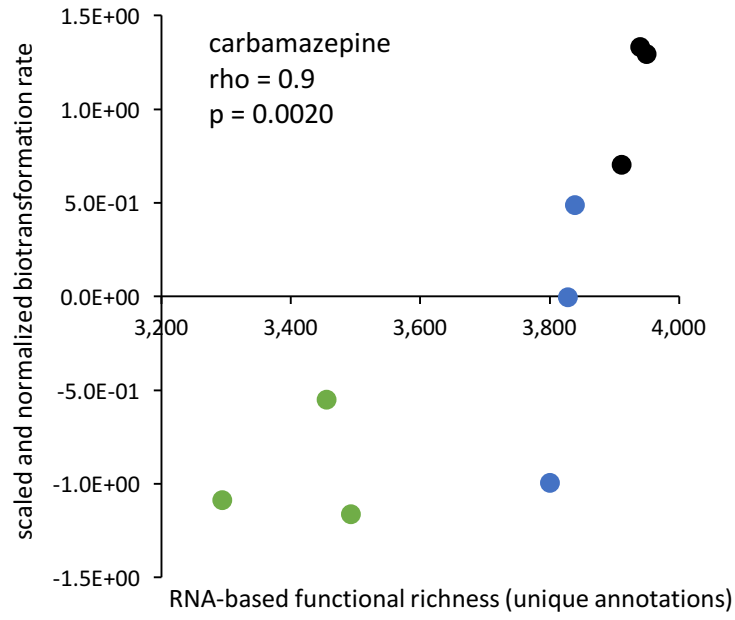
c.



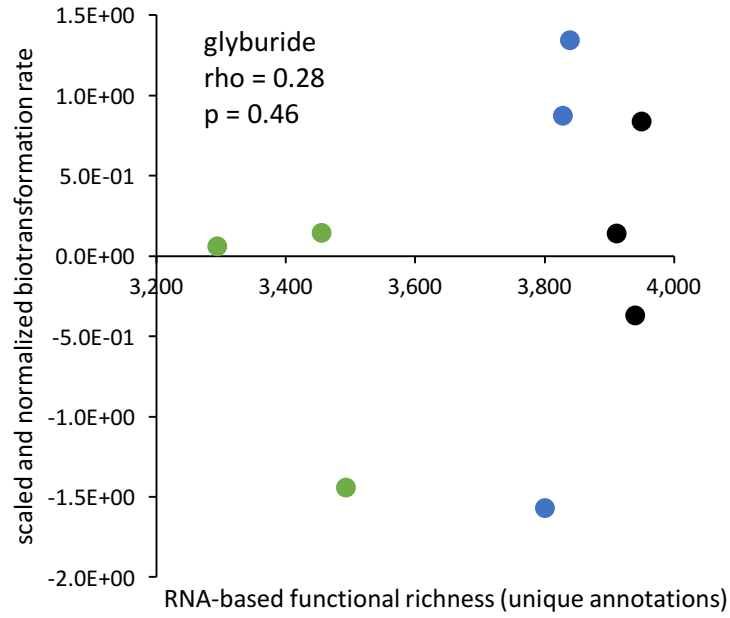
d.



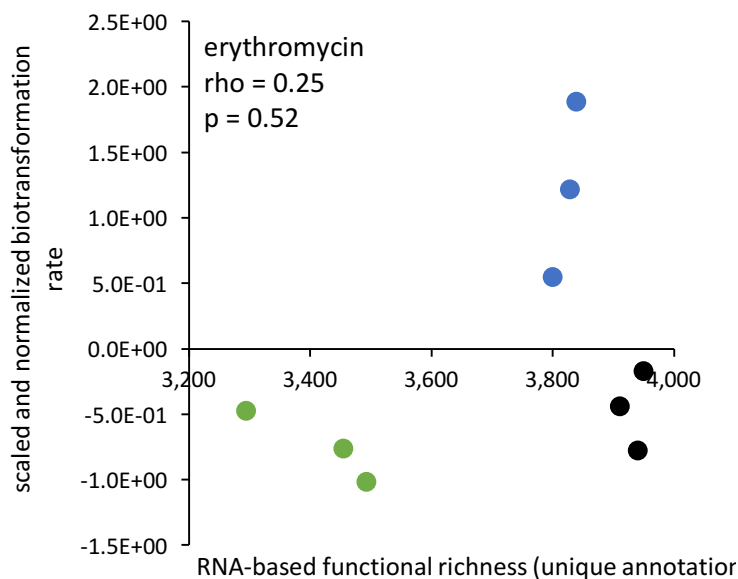
e.



f.



g.



h.

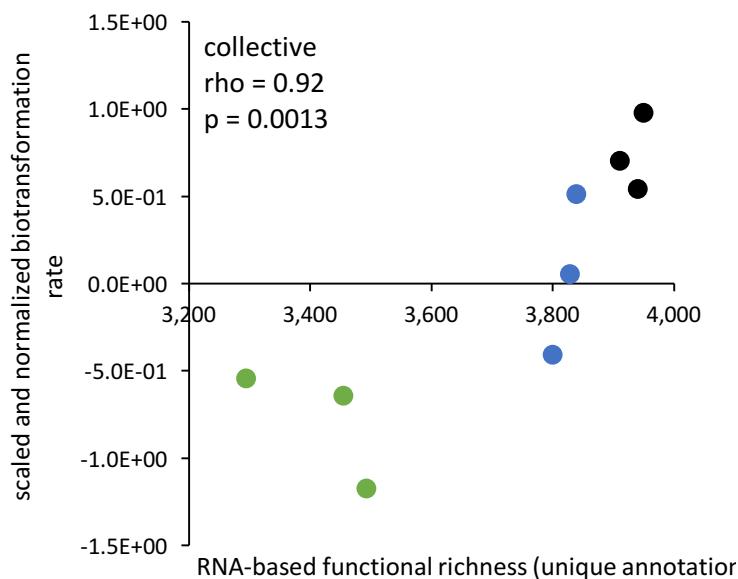


**Figure D2.** RNA-based functional richness versus scaled, normalized biotransformation rates for each compound: atenolol (a), EE2 (b), trimethoprim (c), venlafaxine (d), carbamazepine (e), glyburide (f), erythromycin (g), and collective (h). Samples from the  $10^{-2}$  condition are shown in black,  $10^{-4}$  in blue, and  $10^{-7}$  in green. Spearman's rank correlation test rho and p-values are shown for associations are shown for scale biotransformation rate and RNA-based functional richness.

## Associations between biotransformation rates and richness based on all genes versus only metabolism genes

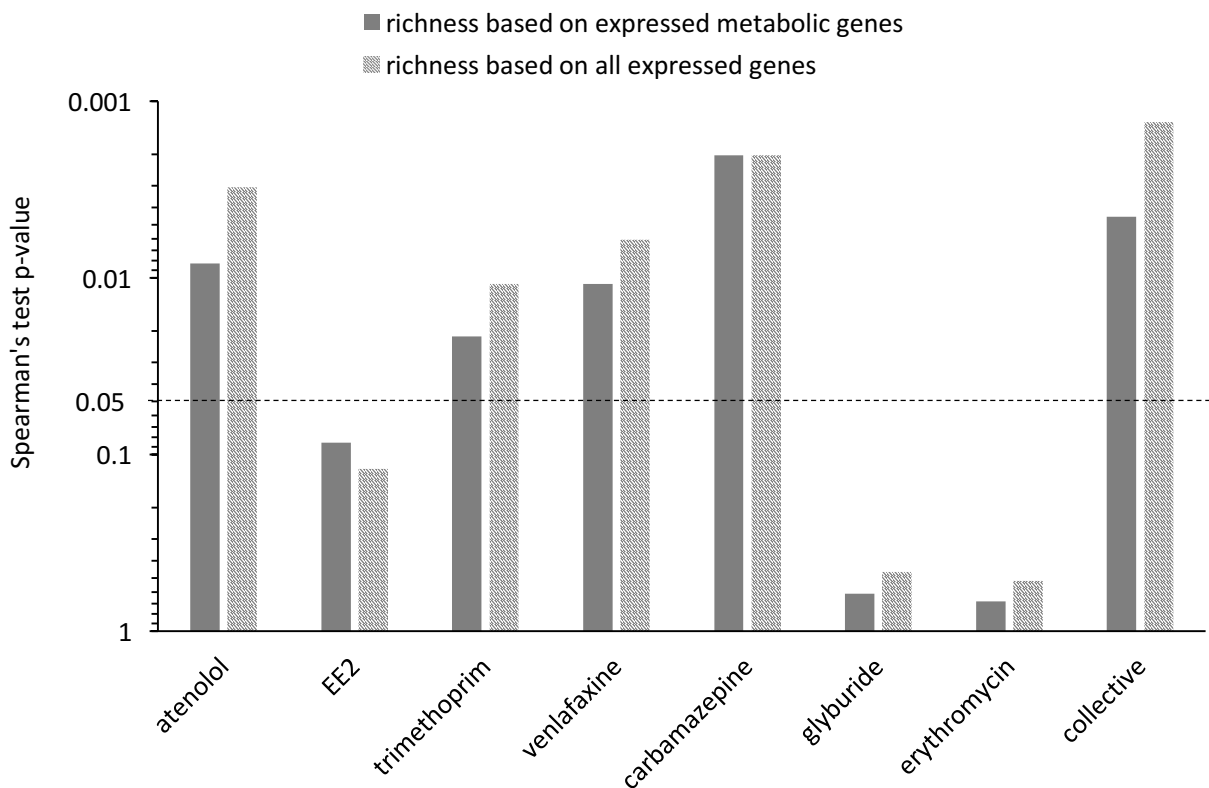


**Figure D3.** Spearman correlation p-values for associations between pharmaceutical biotransformation rates and functional richness based on expressed metabolism genes (solid bar) and all expressed genes (patterned bar). Dashed line signifies  $p = 0.05$ .

### Candidate gene lists and heat maps for each compound

We conducted a two-sided Spearman's rank correlation test between the normalized expression of each gene and each compound's biotransformation rate to identify genes whose expression pattern was significant associated with biotransformation rates. We then narrowed the list of genes by focusing on classes of metabolic genes that were predicted, according to the University of Minnesota's Pathway Prediction System (UM-PPS; Ellis et al., 2006), to be involved in the compounds biotransformation. We focused on the compounds that were transformed to

different extents with increased dilution (atenolol, EE2, trimethoprim, venlafaxine, and carbamazepine) and further narrowed the list of genes relevant to those compounds by selecting genes only if they were lost with increased dilution. Figures D4-6 show the genes that were significantly associated with biotransformation of atenolol, trimethoprim, and venlafaxine, predicted to be involved in transformation of those compounds, and lost between the  $10^{-2}$  and the  $10^{-7}$  conditions. No genes were significantly associated with carbamazepine biotransformation and predicted by UM-PPS to be involved in its transformation. A complete list of candidate genes for each compound is provided in Table D5.

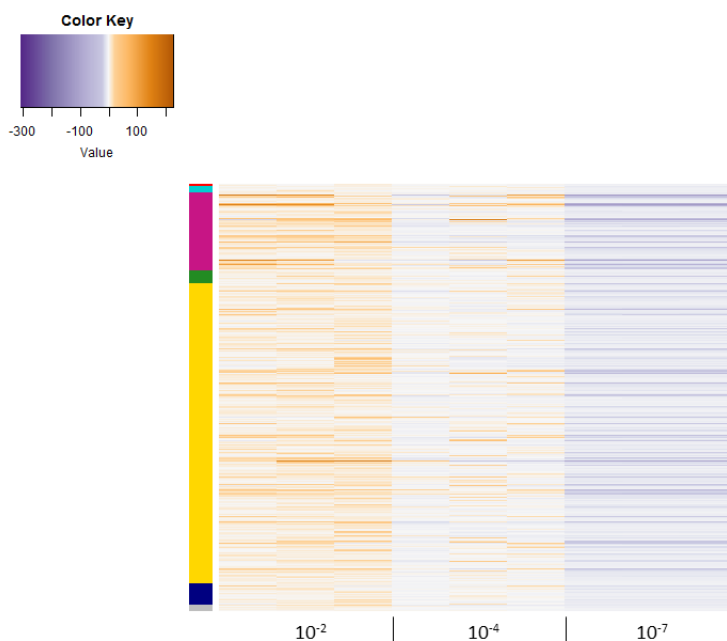


**Figure D4.** Relative expression of significantly differentially expressed genes (likelihood ratio,  $p_{adj} < 0.05$ ) that were also significantly associated with atenolol biotransformation (Spearman,  $p < 0.05$ ). The vertical bar on the left shows amidase genes (red), transaminase genes (turquoise), oxidase genes (purple), hydrolase genes (green), dehydrogenase genes (gold), aminotransferase genes (navy), and monooxygenase genes (grey). Expression value is relative to the average expression of that gene in all conditions.

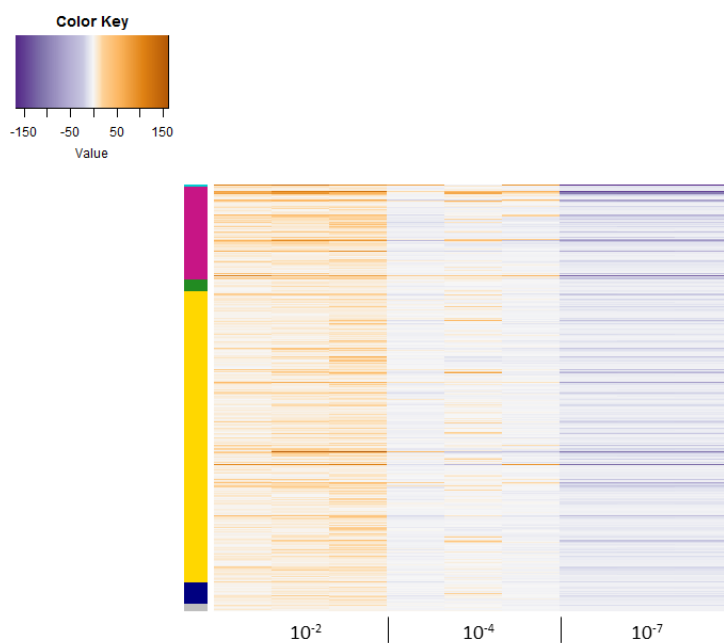


**Figure D5.** Relative expression of significantly differentially expressed genes (likelihood ratio,  $p_{\text{adj}} < 0.05$ ) that were also significantly associated with trimethoprim biotransformation (Spearman,  $p < 0.05$ ). The vertical bar on the left shows transaminase genes (turquoise), oxidase genes (purple), hydrolase genes (green), dehydrogenase genes (gold), aminotransferase genes (navy), and monooxygenase genes (grey). Expression value is relative to the average expression of that gene in all conditions.

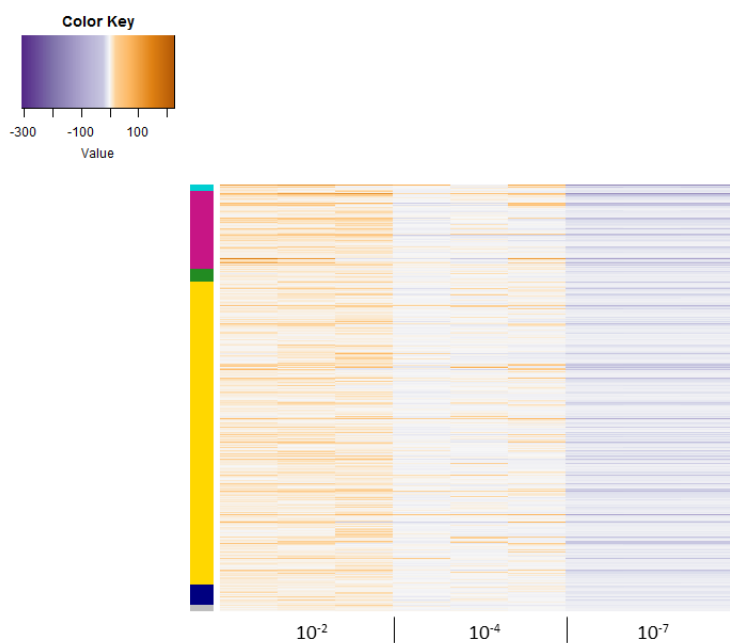


**Figure D6.** Relative expression of significantly differentially expressed genes (likelihood ratio,  $p_{adj} < 0.05$ ) that were also significantly associated with venlafaxine biotransformation (Spearman,  $p < 0.05$ ). The vertical bar on the left shows transaminase genes (turquoise), oxidase genes (purple), hydrolase genes (green), dehydrogenase genes (gold), aminotransferase genes (navy), and monooxygenase genes (grey). Expression value is relative to the average expression of that gene in all conditions.



We also analyzed the genes that were associated with the collective transformation of atenolol, EE2, trimethoprim, venlafaxine, and carbamazepine. The results are shown in Figure D7.

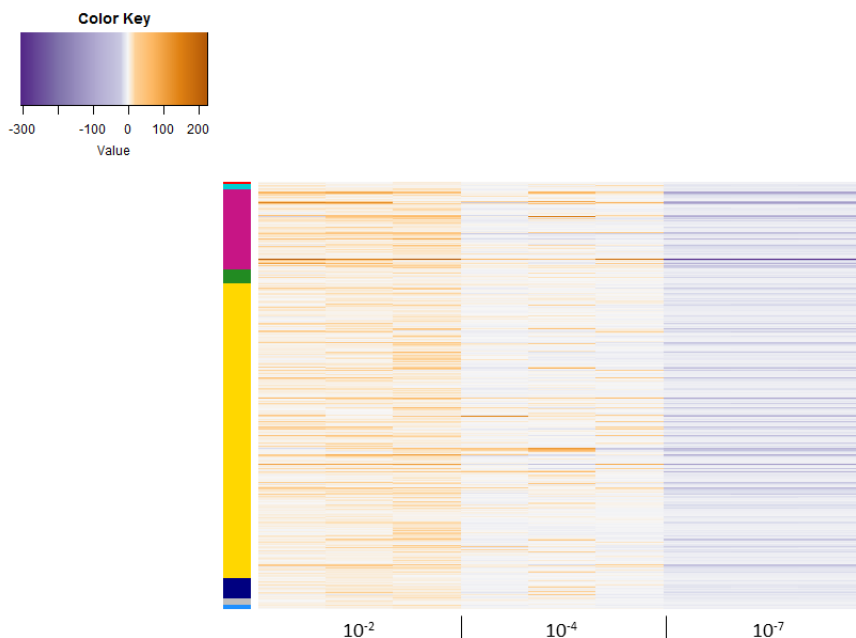


**Figure D7.** Relative expression of significantly differentially expressed genes (likelihood ratio,  $p_{adj} < 0.05$ ) that were also significantly associated with the collective biotransformation of atenolol, EE2, trimethoprim, venlafaxine and carbamazepine (Spearman,  $p < 0.05$ ). The vertical bar on the left shows amidase genes (red), transaminase genes (turquoise), oxidase genes (purple), hydrolase genes (green), dehydrogenase genes (gold), aminotransferase genes (navy), and monooxygenase genes (grey). Expression value is relative to the average expression of that gene in all conditions.

We conducted a two-sided Spearman's rank correlation test between the normalized expression of each gene and erythromycin. Again, we then narrowed the list of genes by focusing on classes of metabolic genes that were predicted, according to the UM-PPS, to be involved in the compounds biotransformation. Because erythromycin did not have increased transformation rates with increased dilution, we did narrow the list of genes to those lost with dilution. The significantly

associated genes are shown in Figure D8. A complete list of candidate genes is provided in Table D5.

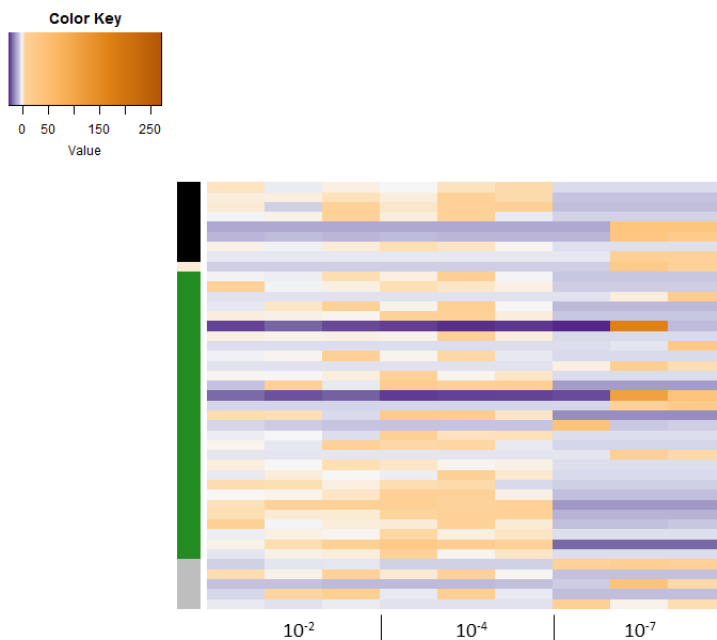


**Figure D8.** Relative expression of significantly differentially expressed genes (likelihood ratio,  $p_{adj} < 0.05$ ) that were also significantly associated with erythromycin biotransformation (Spearman,  $p < 0.05$ ).

The vertical bar on the left shows esterase genes (black), a lactonase gene (white), hydrolase genes (green) and monooxygenase genes (grey). Expression value is relative to the average expression of that gene in all conditions.

**Table D5.** Candidate gene lists for each compound.

<b>EE2</b>	
<b>KEGG Orthology Number</b>	<b>Description</b>
K00500	phenylalanine-4-hydroxylase [EC:1.14.16.1]
K10946	ammonia monooxygenase subunit C [EC:1.13.12.-]
K00459	nitronate monooxygenase [EC:1.13.12.16]
K06134	ubiquinone biosynthesis monooxygenase Coq7 [EC:1.14.13.-]
K00499	choline monooxygenase [EC:1.14.15.7]
<b>Erythromycin</b>	
<b>KEGG Orthology Number</b>	<b>Description</b>
K01126	glycerophosphoryl diester phosphodiesterase [EC:3.1.4.46]
K10804	acyl-CoA thioesterase I [EC:3.1.2.- 3.1.1.5]
K10805	acyl-CoA thioesterase II [EC:3.1.2.-]
K01119	2',3'-cyclic-nucleotide 2'-phosphodiesterase [EC:3.1.4.16]
K01066	esterase / lipase [EC:3.1.1.-]
K07404	6-phosphogluconolactonase [EC:3.1.1.31]
K01491	methylenetetrahydrofolate dehydrogenase (NADP+) / methenyltetrahydrofolate cyclohydrolase [EC:1.5.1.5 3.5.4.9]
K01497	GTP cyclohydrolase II [EC:3.5.4.25]
K01495	GTP cyclohydrolase I [EC:3.5.4.16]
K00602	phosphoribosylaminoimidazolecarboxamide formyltransferase / IMP cyclohydrolase [EC:2.1.2.3 3.5.4.10]
K01070	S-formylglutathione hydrolase [EC:3.1.2.12]
K01442	choloylglycine hydrolase [EC:3.5.1.24]
K03336	3D-(3,5/4)-trihydroxycyclohexane-1,2-dione hydrolase [EC:3.7.1.-]
K01139	guanosine-3',5'-bis(diphosphate) 3'-pyrophosphohydrolase [EC:3.1.7.2]
K11755	phosphoribosyl-ATP pyrophosphohydrolase / phosphoribosyl-AMP cyclohydrolase [EC:3.6.1.31 3.5.4.19]
K10216	2-hydroxymuconate-semialdehyde hydrolase [EC:3.7.1.9]
K07127	5-hydroxyisourate hydrolase [EC:3.5.2.17]
K06193	phosphonoacetate hydrolase [EC:3.11.1.2]
K01069	hydroxyacylglutathione hydrolase [EC:3.1.2.6]
K01451	hippurate hydrolase [EC:3.5.1.32]
K00466	tryptophan 2-monooxygenase [EC:1.13.12.3]
K03379	cyclohexanone monooxygenase [EC:1.14.13.22]
K00459	nitronate monooxygenase [EC:1.13.12.16]
K06134	ubiquinone biosynthesis monooxygenase Coq7 [EC:1.14.13.-]

<b>Venlafaxine</b>	
<b>KEGG Orthology Number</b>	<b>Description</b>
K00836	diaminobutyrate-2-oxoglutarate transaminase [EC:2.6.1.76]
K00832	aromatic-amino-acid transaminase [EC:2.6.1.57]
K14260	alanine-synthesizing transaminase [EC:2.6.1.66 2.6.1.2]
K00822	beta-alanine--pyruvate transaminase [EC:2.6.1.18]
K09471	gamma-glutamylputrescine oxidase [EC:1.4.3.-]
K00425	cytochrome d ubiquinol oxidase subunit I [EC:1.10.3.-];cytochrome bd-I oxidase subunit I [EC:1.10.3.-]
K00426	cytochrome d ubiquinol oxidase subunit II [EC:1.10.3.-];cytochrome bd-I oxidase subunit II [EC:1.10.3.-]
K02495	oxygen-independent coproporphyrinogen III oxidase [EC:1.3.99.22]
K00406	cb-type cytochrome c oxidase subunit III [EC:1.9.3.1];cytochrome c oxidase cb-type subunit III
K00405	cb-type cytochrome c oxidase subunit II [EC:1.9.3.1];cytochrome c oxidase cb-type subunit II
K00404	cb-type cytochrome c oxidase subunit I [EC:1.9.3.1];cytochrome c oxidase cb-type subunit I [EC:1.9.3.1]
K02274	cytochrome c oxidase subunit I [EC:1.9.3.1]
K02275	cytochrome c oxidase subunit II [EC:1.9.3.1]
K13020	UDP-D-GlcNAcA oxidase [EC:1.1.1.-]
K03782	catalase/peroxidase [EC:1.11.1.6 1.11.1.7]
K00274	monoamine oxidase [EC:1.4.3.4]
K00275	pyridoxamine 5'-phosphate oxidase [EC:1.4.3.5]
K02298	cytochrome o ubiquinol oxidase subunit I [EC:1.10.3.-]
K02299	cytochrome o ubiquinol oxidase subunit III [EC:1.10.3.-]
K02297	cytochrome o ubiquinol oxidase subunit II [EC:1.10.3.-]
K02300	cytochrome o ubiquinol oxidase operon protein cyoD
K00432	glutathione peroxidase [EC:1.11.1.9]
K00228	coproporphyrinogen III oxidase [EC:1.3.3.3]
K03153	glycine oxidase [EC:1.4.3.19]
K01491	methylenetetrahydrofolate dehydrogenase (NADP+) / methenyltetrahydrofolate cyclohydrolase [EC:1.5.1.5 3.5.4.9]
K01495	GTP cyclohydrolase I [EC:3.5.4.16]
K00602	phosphoribosylaminoimidazolecarboxamide formyltransferase / IMP cyclohydrolase [EC:2.1.2.3 3.5.4.10]
K01442	choloyl-glycine hydrolase [EC:3.5.1.24]
K03336	3D-(3,5/4)-trihydroxycyclohexane-1,2-dione hydrolase [EC:3.7.1.-]
K01139	guanosine-3',5'-bis(diphosphate) 3'-pyrophosphohydrolase [EC:3.1.7.2]
K01484	succinylarginine dihydrolase [EC:3.5.3.23]
K11755	phosphoribosyl-ATP pyrophosphohydrolase / phosphoribosyl-AMP cyclohydrolase [EC:3.6.1.31 3.5.4.19]
K10216	2-hydroxymuconate-semialdehyde hydrolase [EC:3.7.1.9]
K01069	hydroxyacylglutathione hydrolase [EC:3.1.2.6]
K01067	acetyl-CoA hydrolase [EC:3.1.2.1]
K01436	aminoacylase [EC:3.5.1.14];amidohydrolase [EC:3.5.1.-]

K01825	3-hydroxyacyl-CoA dehydrogenase / enoyl-CoA hydratase / 3-hydroxybutyryl-CoA epimerase / enoyl-CoA isomerase [EC:1.1.1.35 4.2.1.17 5.1.2.3 5.3.3.8]
K00340	NADH-quinone oxidoreductase subunit K [EC:1.6.5.3];NADH dehydrogenase I subunit K [EC:1.6.5.3]
K00341	NADH dehydrogenase I subunit L [EC:1.6.5.3];NADH-quinone oxidoreductase subunit L [EC:1.6.5.3]
K00343	NADH dehydrogenase I subunit N [EC:1.6.5.3];NADH-quinone oxidoreductase subunit N [EC:1.6.5.3]
K00027	malate dehydrogenase (oxaloacetate-decarboxylating) [EC:1.1.1.38]
K02472	UDP-N-acetyl-D-mannosaminuronic acid dehydrogenase [EC:1.1.1.-]
K02474	UDP-N-acetyl-D-galactosamine dehydrogenase [EC:1.1.1.-]
K00121	S-(hydroxymethyl)glutathione dehydrogenase / alcohol dehydrogenase [EC:1.1.1.284 1.1.1.1]
K00658	2-oxoglutarate dehydrogenase E2 component (dihydrolipoamide succinyltransferase) [EC:2.3.1.61]
K09472	gamma-glutamyl-gamma-aminobutyraldehyde dehydrogenase [EC:1.2.1.-]
K00018	glycerate dehydrogenase [EC:1.1.1.29]
K00019	3-hydroxybutyrate dehydrogenase [EC:1.1.1.30]
K00117	quinoprotein glucose dehydrogenase [EC:1.1.5.2]
K00116	malate dehydrogenase (quinone) [EC:1.1.5.4]
K00111	glycerol-3-phosphate dehydrogenase [EC:1.1.5.3]
K13378	NADH dehydrogenase I subunit C/D [EC:1.6.5.3];NADH-quinone oxidoreductase subunit C/D [EC:1.6.5.3]
K04118	pimeloyl-CoA dehydrogenase [EC:1.3.1.62]
K00135	succinate-semialdehyde dehydrogenase (NADP+) [EC:1.2.1.16]
K00134	glyceraldehyde 3-phosphate dehydrogenase [EC:1.2.1.12]
K00133	aspartate-semialdehyde dehydrogenase [EC:1.2.1.11]
K00130	betaine-aldehyde dehydrogenase [EC:1.2.1.8]
K13821	proline dehydrogenase / delta 1-pyrroline-5-carboxylate dehydrogenase [EC:1.5.99.8 1.5.1.12]
K00097	4-hydroxythreonine-4-phosphate dehydrogenase [EC:1.1.1.262]
K00140	malonate-semialdehyde dehydrogenase (acetylating) / methylmalonate-semialdehyde dehydrogenase [EC:1.2.1.18 1.2.1.27];methylmalonate-semialdehyde dehydrogenase [EC:1.2.1.27]
K00147	glutamate-5-semialdehyde dehydrogenase [EC:1.2.1.41]
K00239	succinate dehydrogenase flavoprotein subunit [EC:1.3.99.1]
K00031	isocitrate dehydrogenase [EC:1.1.1.42]
K00259	alanine dehydrogenase [EC:1.4.1.1]
K00252	glutaryl-CoA dehydrogenase [EC:1.3.99.7]
K00253	isovaleryl-CoA dehydrogenase [EC:1.3.99.10]
K00254	dihydroorotate dehydrogenase [EC:1.3.5.2]
K00255	long-chain-acyl-CoA dehydrogenase [EC:1.3.99.13]
K01782	3-hydroxyacyl-CoA dehydrogenase / enoyl-CoA hydratase / 3-hydroxybutyryl-CoA epimerase [EC:1.1.1.35 4.2.1.17 5.1.2.3]
K00342	NADH-quinone oxidoreductase subunit M [EC:1.6.5.3];NADH dehydrogenase I subunit M [EC:1.6.5.3]
K12524	bifunctional aspartokinase/homoserine dehydrogenase 1 [EC:2.7.2.4 1.1.1.3];bifunctional aspartokinase / homoserine dehydrogenase 1 [EC:2.7.2.4 1.1.1.3]
K00010	myo-inositol 2-dehydrogenase [EC:1.1.1.18]
K00012	UDPglucose 6-dehydrogenase [EC:1.1.1.22]
K00013	histidinol dehydrogenase [EC:1.1.1.23]
K00014	shikimate dehydrogenase [EC:1.1.1.25];shikimate 5-dehydrogenase [EC:1.1.1.25]

K00016	L-lactate dehydrogenase [EC:1.1.1.27]
K00156	pyruvate dehydrogenase (quinone) [EC:1.2.5.1];pyruvate dehydrogenase (cytochrome) [EC:1.2.2.2]
K00074	3-hydroxybutyryl-CoA dehydrogenase [EC:1.1.1.157]
K00075	UDP-N-acetylmuramate dehydrogenase [EC:1.1.1.158]
K00294	1-pyrroline-5-carboxylate dehydrogenase [EC:1.5.1.12]
K14519	NADP-dependent aldehyde dehydrogenase [EC:1.2.1.4]
K00058	D-3-phosphoglycerate dehydrogenase [EC:1.1.1.95]
K00055	aryl-alcohol dehydrogenase [EC:1.1.1.90]
K00057	glycerol-3-phosphate dehydrogenase (NAD(P)+) [EC:1.1.1.94]
K02302	uroporphyrin-III C-methyltransferase / precorrin-2 dehydrogenase / sirohydrochlorin ferrochelatase [EC:2.1.1.107 1.3.1.76 4.99.1.4]
K00052	3-isopropylmalate dehydrogenase [EC:1.1.1.85]
K08685	quinohemoprotein amine dehydrogenase [EC:1.4.98.1];amine dehydrogenase [EC:1.4.99.3]
K00331	NADH dehydrogenase I subunit B [EC:1.6.5.3];NADH-quinone oxidoreductase subunit B [EC:1.6.5.3]
K00330	NADH-quinone oxidoreductase subunit A [EC:1.6.5.3];NADH dehydrogenase I subunit A [EC:1.6.5.3]
K00333	NADH dehydrogenase I subunit D [EC:1.6.5.3];NADH-quinone oxidoreductase subunit D [EC:1.6.5.3]
K00332	NADH-quinone oxidoreductase subunit C [EC:1.6.5.3];NADH dehydrogenase I subunit C [EC:1.6.5.3]
K00335	NADH dehydrogenase I subunit F [EC:1.6.5.3];NADH-quinone oxidoreductase subunit F [EC:1.6.5.3]
K00334	NADH-quinone oxidoreductase subunit E [EC:1.6.5.3];NADH dehydrogenase I subunit E [EC:1.6.5.3]
K00337	NADH dehydrogenase I subunit H [EC:1.6.5.3];NADH-quinone oxidoreductase subunit H [EC:1.6.5.3]
K00336	NADH-quinone oxidoreductase subunit G [EC:1.6.5.3];NADH dehydrogenase I subunit G [EC:1.6.5.3]
K00339	NADH dehydrogenase I subunit J [EC:1.6.5.3];NADH-quinone oxidoreductase subunit J [EC:1.6.5.3]
K00338	NADH-quinone oxidoreductase subunit I [EC:1.6.5.3];NADH dehydrogenase I subunit I [EC:1.6.5.3]
K13953	alcohol dehydrogenase, propanol-preferring [EC:1.1.1.1]
K13954	alcohol dehydrogenase [EC:1.1.1.1]
K00318	proline dehydrogenase [EC:1.5.99.8]
K00102	D-lactate dehydrogenase (cytochrome) [EC:1.1.2.4]
K06445	acyl-CoA dehydrogenase [EC:1.3.99.-]
K06447	succinylglutamic semialdehyde dehydrogenase [EC:1.2.1.71]
K00128	aldehyde dehydrogenase (NAD+) [EC:1.2.1.3]
K00123	formate dehydrogenase, alpha subunit [EC:1.2.1.2]
K00124	formate dehydrogenase, beta subunit [EC:1.2.1.2]
K00127	formate dehydrogenase, gamma subunit [EC:1.2.1.2]
K05358	quininate dehydrogenase (quinone) [EC:1.1.5.8];quininate dehydrogenase (pyrroloquinoline-quinone) [EC:1.1.99.25]
K00146	phenylacetaldehyde dehydrogenase [EC:1.2.1.39]
K00627	pyruvate dehydrogenase E2 component (dihydrolipoamide acetyltransferase) [EC:2.3.1.12]
K00088	IMP dehydrogenase [EC:1.1.1.205]
K00164	2-oxoglutarate dehydrogenase E1 component [EC:1.2.4.2]
K00166	2-oxoisovalerate dehydrogenase E1 component, alpha subunit [EC:1.2.4.4]
K00161	pyruvate dehydrogenase E1 component subunit alpha [EC:1.2.4.1]
K00162	pyruvate dehydrogenase E1 component subunit beta [EC:1.2.4.1]

K00163	pyruvate dehydrogenase E1 component [EC:1.2.4.1]
K07516	3-hydroxyacyl-CoA dehydrogenase [EC:1.1.1.35]
K00029	malate dehydrogenase (oxaloacetate-decarboxylating)(NADP+) [EC:1.1.1.40]
K00024	malate dehydrogenase [EC:1.1.1.37]
K00020	3-hydroxyisobutyrate dehydrogenase [EC:1.1.1.31]
K00249	acyl-CoA dehydrogenase [EC:1.3.99.3]
K00241	succinate dehydrogenase cytochrome b556 subunit;succinate dehydrogenase cytochrome b-556 subunit [EC:1.3.99.1];succinate dehydrogenase cytochrome b-556 subunit
K00240	succinate dehydrogenase iron-sulfur protein [EC:1.3.99.1];succinate dehydrogenase iron-sulfur subunit [EC:1.3.99.1]
K00242	succinate dehydrogenase hydrophobic membrane anchor protein [EC:1.3.99.1];succinate dehydrogenase hydrophobic membrane anchor protein;succinate dehydrogenase membrane anchor subunit
K00005	glycerol dehydrogenase [EC:1.1.1.6]
K00003	homoserine dehydrogenase [EC:1.1.1.3]
K00001	alcohol dehydrogenase [EC:1.1.1.1]
K00263	leucine dehydrogenase [EC:1.4.1.9]
K00262	glutamate dehydrogenase (NADP+) [EC:1.4.1.4]
K00261	glutamate dehydrogenase (NAD(P)+) [EC:1.4.1.3]
K00285	D-amino-acid dehydrogenase [EC:1.4.99.1]
K00281	glycine dehydrogenase [EC:1.4.4.2]
K00382	dihydrolipoamide dehydrogenase [EC:1.8.1.4]
K12254	4-guanidinobutyraldehyde dehydrogenase / NAD-dependent aldehyde dehydrogenase [EC:1.2.1.54 1.2.1.-]
K00831	phosphoserine aminotransferase [EC:2.6.1.52]
K00812	aspartate aminotransferase [EC:2.6.1.1]
K00817	histidinol-phosphate aminotransferase [EC:2.6.1.9]
K00818	acetylmethionine aminotransferase [EC:2.6.1.11]
K14267	N-succinylmethionine aminotransferase [EC:2.6.1.17]
K14268	5-aminovalerate aminotransferase [EC:2.6.1.48]
K00826	branched-chain amino acid aminotransferase [EC:2.6.1.42]
K00821	acetylmethionine/N-succinylmethionine aminotransferase [EC:2.6.1.11 2.6.1.17]
K00820	glucosamine--fructose-6-phosphate aminotransferase (isomerizing) [EC:2.6.1.16]
K00823	4-aminobutyrate aminotransferase [EC:2.6.1.19]
K12256	putrescine aminotransferase [EC:2.6.1.-]
K00466	tryptophan 2-monooxygenase [EC:1.13.12.3]
K10946	ammonia monooxygenase subunit C [EC:1.13.12.-]
K03379	cyclohexanone monooxygenase [EC:1.14.13.22]
K03863	vanillate monooxygenase [EC:1.14.13.82]
K00459	nitronate monooxygenase [EC:1.13.12.16]
K06134	ubiquinone biosynthesis monooxygenase Coq7 [EC:1.14.13.-]
K00499	choline monooxygenase [EC:1.14.15.7]
<b>Trimethoprim</b>	

KEGG Orthology Number	Description
K00836	diaminobutyrate-2-oxoglutarate transaminase [EC:2.6.1.76]
K00822	beta-alanine--pyruvate transaminase [EC:2.6.1.18]
K09471	gamma-glutamylputrescine oxidase [EC:1.4.3.-]
K00425	cytochrome d ubiquinol oxidase subunit I [EC:1.10.3.-];cytochrome bd-I oxidase subunit I [EC:1.10.3.-]
K00426	cytochrome d ubiquinol oxidase subunit II [EC:1.10.3.-];cytochrome bd-I oxidase subunit II [EC:1.10.3.-]
K02495	oxygen-independent coproporphyrinogen III oxidase [EC:1.3.99.22]
K00406	cb-type cytochrome c oxidase subunit III [EC:1.9.3.1];cytochrome c oxidase cb-type subunit III
K00405	cb-type cytochrome c oxidase subunit II [EC:1.9.3.1];cytochrome c oxidase cb-type subunit II
K00404	cb-type cytochrome c oxidase subunit I [EC:1.9.3.1];cytochrome c oxidase cb-type subunit I [EC:1.9.3.1]
K02274	cytochrome c oxidase subunit I [EC:1.9.3.1]
K02275	cytochrome c oxidase subunit II [EC:1.9.3.1]
K03782	catalase/peroxidase [EC:1.11.1.6 1.11.1.7]
K02298	cytochrome o ubiquinol oxidase subunit I [EC:1.10.3.-]
K02299	cytochrome o ubiquinol oxidase subunit III [EC:1.10.3.-]
K02297	cytochrome o ubiquinol oxidase subunit II [EC:1.10.3.-]
K02300	cytochrome o ubiquinol oxidase operon protein cyoD
K00432	glutathione peroxidase [EC:1.11.1.9]
K00228	coproporphyrinogen III oxidase [EC:1.3.3.3]
K01491	methylenetetrahydrofolate dehydrogenase (NADP+) / methenyltetrahydrofolate cyclohydrolase [EC:1.5.1.5 3.5.4.9]
K00602	phosphoribosylaminoimidazolecarboxamide formyltransferase / IMP cyclohydrolase [EC:2.1.2.3 3.5.4.10]
K01442	choloylglycine hydrolase [EC:3.5.1.24]
K03336	3D-(3,5/4)-trihydroxycyclohexane-1,2-dione hydrolase [EC:3.7.1.-]
K01139	guanosine-3',5'-bis(diphosphate) 3'-pyrophosphohydrolase [EC:3.1.7.2]
K01484	succinylarginine dihydrolase [EC:3.5.3.23]
K10216	2-hydroxymuconate-semialdehyde hydrolase [EC:3.7.1.9]
K01067	acetyl-CoA hydrolase [EC:3.1.2.1]
K01825	3-hydroxyacyl-CoA dehydrogenase / enoyl-CoA hydratase / 3-hydroxybutyryl-CoA epimerase / enoyl-CoA isomerase [EC:1.1.1.35 4.2.1.17 5.1.2.3 5.3.3.8]
K00340	NADH-quinone oxidoreductase subunit K [EC:1.6.5.3];NADH dehydrogenase I subunit K [EC:1.6.5.3]
K00341	NADH dehydrogenase I subunit L [EC:1.6.5.3];NADH-quinone oxidoreductase subunit L [EC:1.6.5.3]
K00343	NADH dehydrogenase I subunit N [EC:1.6.5.3];NADH-quinone oxidoreductase subunit N [EC:1.6.5.3]
K00027	malate dehydrogenase (oxaloacetate-decarboxylating) [EC:1.1.1.38]
K02474	UDP-N-acetyl-D-galactosamine dehydrogenase [EC:1.1.1.-]
K00121	S-(hydroxymethyl)glutathione dehydrogenase / alcohol dehydrogenase [EC:1.1.1.284 1.1.1.1]
K00658	2-oxoglutarate dehydrogenase E2 component (dihydrolipoamide succinyltransferase) [EC:2.3.1.61]
K09472	gamma-glutamyl-gamma-aminobutyraldehyde dehydrogenase [EC:1.2.1.-]
K00018	glycerate dehydrogenase [EC:1.1.1.29]
K00019	3-hydroxybutyrate dehydrogenase [EC:1.1.1.30]
K00117	quinoprotein glucose dehydrogenase [EC:1.1.5.2]



K00116	malate dehydrogenase (quinone) [EC:1.1.5.4]
K00111	glycerol-3-phosphate dehydrogenase [EC:1.1.5.3]
K13378	NADH dehydrogenase I subunit C/D [EC:1.6.5.3];NADH-quinone oxidoreductase subunit C/D [EC:1.6.5.3]
K04118	pimeloyl-CoA dehydrogenase [EC:1.3.1.62]
K00135	succinate-semialdehyde dehydrogenase (NADP+) [EC:1.2.1.16]
K00134	glyceraldehyde 3-phosphate dehydrogenase [EC:1.2.1.12]
K00133	aspartate-semialdehyde dehydrogenase [EC:1.2.1.11]
K00130	betaine-aldehyde dehydrogenase [EC:1.2.1.8]
K13821	proline dehydrogenase / delta 1-pyrroline-5-carboxylate dehydrogenase [EC:1.5.99.8 1.5.1.12]
K00097	4-hydroxythreonine-4-phosphate dehydrogenase [EC:1.1.1.262]
K00140	malonate-semialdehyde dehydrogenase (acetylating) / methylmalonate-semialdehyde dehydrogenase [EC:1.2.1.18 1.2.1.27];methylmalonate-semialdehyde dehydrogenase [EC:1.2.1.27]
K00147	glutamate-5-semialdehyde dehydrogenase [EC:1.2.1.41]
K00239	succinate dehydrogenase flavoprotein subunit [EC:1.3.99.1]
K00031	isocitrate dehydrogenase [EC:1.1.1.42]
K00259	alanine dehydrogenase [EC:1.4.1.1]
K00252	glutaryl-CoA dehydrogenase [EC:1.3.99.7]
K00253	isovaleryl-CoA dehydrogenase [EC:1.3.99.10]
K00342	NADH-quinone oxidoreductase subunit M [EC:1.6.5.3];NADH dehydrogenase I subunit M [EC:1.6.5.3]
K12524	bifunctional aspartokinase/homoserine dehydrogenase 1 [EC:2.7.2.4 1.1.1.3];bifunctional aspartokinase / homoserine dehydrogenase 1 [EC:2.7.2.4 1.1.1.3]
K00010	myo-inositol 2-dehydrogenase [EC:1.1.1.18]
K00013	histidinol dehydrogenase [EC:1.1.1.23]
K00014	shikimate dehydrogenase [EC:1.1.1.25];shikimate 5-dehydrogenase [EC:1.1.1.25]
K00156	pyruvate dehydrogenase (quinone) [EC:1.2.5.1];pyruvate dehydrogenase (cytochrome) [EC:1.2.2.2]
K00074	3-hydroxybutyryl-CoA dehydrogenase [EC:1.1.1.157]
K00294	1-pyrroline-5-carboxylate dehydrogenase [EC:1.5.1.12]
K14519	NADP-dependent aldehyde dehydrogenase [EC:1.2.1.4]
K00058	D-3-phosphoglycerate dehydrogenase [EC:1.1.1.95]
K00057	glycerol-3-phosphate dehydrogenase (NAD(P)+) [EC:1.1.1.94]
K00052	3-isopropylmalate dehydrogenase [EC:1.1.1.85]
K08685	quinoxinoprotein amine dehydrogenase [EC:1.4.98.1];amine dehydrogenase [EC:1.4.99.3]
K00331	NADH dehydrogenase I subunit B [EC:1.6.5.3];NADH-quinone oxidoreductase subunit B [EC:1.6.5.3]
K00330	NADH-quinone oxidoreductase subunit A [EC:1.6.5.3];NADH dehydrogenase I subunit A [EC:1.6.5.3]
K00333	NADH dehydrogenase I subunit D [EC:1.6.5.3];NADH-quinone oxidoreductase subunit D [EC:1.6.5.3]
K00332	NADH-quinone oxidoreductase subunit C [EC:1.6.5.3];NADH dehydrogenase I subunit C [EC:1.6.5.3]
K00335	NADH dehydrogenase I subunit F [EC:1.6.5.3];NADH-quinone oxidoreductase subunit F [EC:1.6.5.3]
K00334	NADH-quinone oxidoreductase subunit E [EC:1.6.5.3];NADH dehydrogenase I subunit E [EC:1.6.5.3]
K00337	NADH dehydrogenase I subunit H [EC:1.6.5.3];NADH-quinone oxidoreductase subunit H [EC:1.6.5.3]
K00336	NADH-quinone oxidoreductase subunit G [EC:1.6.5.3];NADH dehydrogenase I subunit G [EC:1.6.5.3]
K00339	NADH dehydrogenase I subunit J [EC:1.6.5.3];NADH-quinone oxidoreductase subunit J [EC:1.6.5.3]

K00338	NADH-quinone oxidoreductase subunit I [EC:1.6.5.3];NADH dehydrogenase I subunit I [EC:1.6.5.3]
K13953	alcohol dehydrogenase, propanol-preferring [EC:1.1.1.1]
K13954	alcohol dehydrogenase [EC:1.1.1.1]
K00318	proline dehydrogenase [EC:1.5.99.8]
K06445	acyl-CoA dehydrogenase [EC:1.3.99.-]
K06447	succinylglutamic semialdehyde dehydrogenase [EC:1.2.1.71]
K00128	aldehyde dehydrogenase (NAD+) [EC:1.2.1.3]
K00123	formate dehydrogenase, alpha subunit [EC:1.2.1.2]
K00124	formate dehydrogenase, beta subunit [EC:1.2.1.2]
K00127	formate dehydrogenase, gamma subunit [EC:1.2.1.2]
K05358	quininate dehydrogenase (quinone) [EC:1.1.5.8];quininate dehydrogenase (pyrroloquinoline-quinone) [EC:1.1.99.25]
K00146	phenylacetaldehyde dehydrogenase [EC:1.2.1.39]
K00627	pyruvate dehydrogenase E2 component (dihydrolipoamide acetyltransferase) [EC:2.3.1.12]
K00088	IMP dehydrogenase [EC:1.1.1.205]
K00164	2-oxoglutarate dehydrogenase E1 component [EC:1.2.4.2]
K00166	2-oxoisovalerate dehydrogenase E1 component, alpha subunit [EC:1.2.4.4]
K00161	pyruvate dehydrogenase E1 component subunit alpha [EC:1.2.4.1]
K00163	pyruvate dehydrogenase E1 component [EC:1.2.4.1]
K07516	3-hydroxyacyl-CoA dehydrogenase [EC:1.1.1.35]
K00029	malate dehydrogenase (oxaloacetate-decarboxylating)(NADP+) [EC:1.1.1.40]
K00024	malate dehydrogenase [EC:1.1.1.37]
K00020	3-hydroxyisobutyrate dehydrogenase [EC:1.1.1.31]
K00249	acyl-CoA dehydrogenase [EC:1.3.99.3]
K00241	succinate dehydrogenase cytochrome b556 subunit;succinate dehydrogenase cytochrome b-556 subunit [EC:1.3.99.1];succinate dehydrogenase cytochrome b-556 subunit
K00240	succinate dehydrogenase iron-sulfur protein [EC:1.3.99.1];succinate dehydrogenase iron-sulfur subunit [EC:1.3.99.1]
K00263	leucine dehydrogenase [EC:1.4.1.9]
K00262	glutamate dehydrogenase (NADP+) [EC:1.4.1.4]
K00261	glutamate dehydrogenase (NAD(P)+) [EC:1.4.1.3]
K00285	D-amino-acid dehydrogenase [EC:1.4.99.1]
K00281	glycine dehydrogenase [EC:1.4.4.2]
K00382	dihydrolipoamide dehydrogenase [EC:1.8.1.4]
K12254	4-guanidinobutyraldehyde dehydrogenase / NAD-dependent aldehyde dehydrogenase [EC:1.2.1.54 1.2.1.-]
K00831	phosphoserine aminotransferase [EC:2.6.1.52]
K00817	histidinol-phosphate aminotransferase [EC:2.6.1.9]
K00826	branched-chain amino acid aminotransferase [EC:2.6.1.42]
K00821	acetylornithine/N-succinyldiaminopimelate aminotransferase [EC:2.6.1.11 2.6.1.17]
K00820	glucosamine--fructose-6-phosphate aminotransferase (isomerizing) [EC:2.6.1.16]
K00823	4-aminobutyrate aminotransferase [EC:2.6.1.19]
K12256	putrescine aminotransferase [EC:2.6.1.-]

K00466	tryptophan 2-monooxygenase [EC:1.13.12.3]
K10946	ammonia monooxygenase subunit C [EC:1.13.12.-]
K00459	nitronate monooxygenase [EC:1.13.12.16]
K06134	ubiquinone biosynthesis monooxygenase Coq7 [EC:1.14.13.-]
K00499	choline monooxygenase [EC:1.14.15.7]
<b>Atenolol</b>	
<b>KEGG Orthology Number</b>	<b>Description</b>
K01426	amidase [EC:3.5.1.4]
K01434	penicillin amidase [EC:3.5.1.11]
K12251	N-carbamoylputrescine amidase [EC:3.5.1.53]
K00836	diaminobutyrate-2-oxoglutarate transaminase [EC:2.6.1.76]
K00832	aromatic-amino-acid transaminase [EC:2.6.1.57]
K14260	alanine-synthesizing transaminase [EC:2.6.1.66 2.6.1.2]
K00822	beta-alanine--pyruvate transaminase [EC:2.6.1.18]
K09471	gamma-glutamylputrescine oxidase [EC:1.4.3.-]
K00425	cytochrome d ubiquinol oxidase subunit I [EC:1.10.3.-];cytochrome bd-I oxidase subunit I [EC:1.10.3.-]
K00426	cytochrome d ubiquinol oxidase subunit II [EC:1.10.3.-];cytochrome bd-I oxidase subunit II [EC:1.10.3.-]
K02495	oxygen-independent coproporphyrinogen III oxidase [EC:1.3.99.22]
K00406	cb-type cytochrome c oxidase subunit III [EC:1.9.3.1];cytochrome c oxidase cb-type subunit III
K00405	cb-type cytochrome c oxidase subunit II [EC:1.9.3.1];cytochrome c oxidase cb-type subunit II
K00404	cb-type cytochrome c oxidase subunit I [EC:1.9.3.1];cytochrome c oxidase cb-type subunit I [EC:1.9.3.1]
K02274	cytochrome c oxidase subunit I [EC:1.9.3.1]
K02275	cytochrome c oxidase subunit II [EC:1.9.3.1]
K13020	UDP-D-GlcNAcA oxidase [EC:1.1.1.-]
K03782	catalase/peroxidase [EC:1.11.1.6 1.11.1.7]
K00274	monoamine oxidase [EC:1.4.3.4]
K00275	pyridoxamine 5'-phosphate oxidase [EC:1.4.3.5]
K00276	primary-amine oxidase [EC:1.4.3.21]
K02298	cytochrome o ubiquinol oxidase subunit I [EC:1.10.3.-]
K02299	cytochrome o ubiquinol oxidase subunit III [EC:1.10.3.-]
K02297	cytochrome o ubiquinol oxidase subunit II [EC:1.10.3.-]
K02300	cytochrome o ubiquinol oxidase operon protein cyoD
K00432	glutathione peroxidase [EC:1.11.1.9]
K00228	coproporphyrinogen III oxidase [EC:1.3.3.3]
K01491	methylenetetrahydrofolate dehydrogenase (NADP+) / methenyltetrahydrofolate cyclohydrolase [EC:1.5.1.5 3.5.4.9]
K01495	GTP cyclohydrolase I [EC:3.5.4.16]
K00602	phosphoribosylaminoimidazolecarboxamide formyltransferase / IMP cyclohydrolase [EC:2.1.2.3 3.5.4.10]
K01442	choloylglycine hydrolase [EC:3.5.1.24]

K03336	3D-(3,5/4)-trihydroxycyclohexane-1,2-dione hydrolase [EC:3.7.1.-]
K01139	guanosine-3',5'-bis(diphosphate) 3'-pyrophosphohydrolase [EC:3.1.7.2]
K01484	succinylarginine dihydrolase [EC:3.5.3.23]
K11755	phosphoribosyl-ATP pyrophosphohydrolase / phosphoribosyl-AMP cyclohydrolase [EC:3.6.1.31 3.5.4.19]
K10216	2-hydroxymuconate-semialdehyde hydrolase [EC:3.7.1.9]
K01067	acetyl-CoA hydrolase [EC:3.1.2.1]
K01436	aminoacylase [EC:3.5.1.14];amidohydrolase [EC:3.5.1.-]
K01825	3-hydroxyacyl-CoA dehydrogenase / enoyl-CoA hydratase / 3-hydroxybutyryl-CoA epimerase / enoyl-CoA isomerase [EC:1.1.1.35 4.2.1.17 5.1.2.3 5.3.3.8]
K00340	NADH-quinone oxidoreductase subunit K [EC:1.6.5.3];NADH dehydrogenase I subunit K [EC:1.6.5.3]
K00341	NADH dehydrogenase I subunit L [EC:1.6.5.3];NADH-quinone oxidoreductase subunit L [EC:1.6.5.3]
K00343	NADH dehydrogenase I subunit N [EC:1.6.5.3];NADH-quinone oxidoreductase subunit N [EC:1.6.5.3]
K00027	malate dehydrogenase (oxaloacetate-decarboxylating) [EC:1.1.1.38]
K02472	UDP-N-acetyl-D-mannosaminuronic acid dehydrogenase [EC:1.1.1.-]
K02474	UDP-N-acetyl-D-galactosamine dehydrogenase [EC:1.1.1.-]
K00121	S-(hydroxymethyl)glutathione dehydrogenase / alcohol dehydrogenase [EC:1.1.1.284 1.1.1.1]
K00658	2-oxoglutarate dehydrogenase E2 component (dihydrolipoamide succinyltransferase) [EC:2.3.1.61]
K09472	gamma-glutamyl-gamma-aminobutyraldehyde dehydrogenase [EC:1.2.1.-]
K00018	glycerate dehydrogenase [EC:1.1.1.29]
K00019	3-hydroxybutyrate dehydrogenase [EC:1.1.1.30]
K00117	quinoprotein glucose dehydrogenase [EC:1.1.5.2]
K00116	malate dehydrogenase (quinone) [EC:1.1.5.4]
K00111	glycerol-3-phosphate dehydrogenase [EC:1.1.5.3]
K13378	NADH dehydrogenase I subunit C/D [EC:1.6.5.3];NADH-quinone oxidoreductase subunit C/D [EC:1.6.5.3]
K04118	pimeloyl-CoA dehydrogenase [EC:1.3.1.62]
K00135	succinate-semialdehyde dehydrogenase (NADP+) [EC:1.2.1.16]
K00134	glyceraldehyde 3-phosphate dehydrogenase [EC:1.2.1.12]
K00133	aspartate-semialdehyde dehydrogenase [EC:1.2.1.11]
K00130	betaine-aldehyde dehydrogenase [EC:1.2.1.8]
K13821	proline dehydrogenase / delta 1-pyrroline-5-carboxylate dehydrogenase [EC:1.5.99.8 1.5.1.12]
K00090	gluconate 2-dehydrogenase [EC:1.1.1.215]
K00097	4-hydroxythreonine-4-phosphate dehydrogenase [EC:1.1.1.262]
K03885	NADH dehydrogenase [EC:1.6.99.3]
K00140	malonate-semialdehyde dehydrogenase (acetylating) / methylmalonate-semialdehyde dehydrogenase [EC:1.2.1.18 1.2.1.27];methylmalonate-semialdehyde dehydrogenase [EC:1.2.1.27]
K00147	glutamate-5-semialdehyde dehydrogenase [EC:1.2.1.41]
K00239	succinate dehydrogenase flavoprotein subunit [EC:1.3.99.1]
K00031	isocitrate dehydrogenase [EC:1.1.1.42]
K00259	alanine dehydrogenase [EC:1.4.1.1]
K00252	glutaryl-CoA dehydrogenase [EC:1.3.99.7]
K00253	isovaleryl-CoA dehydrogenase [EC:1.3.99.10]

K00254	dihydroorotate dehydrogenase [EC:1.3.5.2]
K00255	long-chain-acyl-CoA dehydrogenase [EC:1.3.99.13]
K01782	3-hydroxyacyl-CoA dehydrogenase / enoyl-CoA hydratase / 3-hydroxybutyryl-CoA epimerase [EC:1.1.1.35 4.2.1.17 5.1.2.3]
K00342	NADH-quinone oxidoreductase subunit M [EC:1.6.5.3];NADH dehydrogenase I subunit M [EC:1.6.5.3]
K12524	bifunctional aspartokinase/homoserine dehydrogenase 1 [EC:2.7.2.4 1.1.1.3];bifunctional aspartokinase / homoserine dehydrogenase 1 [EC:2.7.2.4 1.1.1.3]
K00010	myo-inositol 2-dehydrogenase [EC:1.1.1.18]
K00012	UDPglucose 6-dehydrogenase [EC:1.1.1.22]
K00013	histidinol dehydrogenase [EC:1.1.1.23]
K00014	shikimate dehydrogenase [EC:1.1.1.25];shikimate 5-dehydrogenase [EC:1.1.1.25]
K00016	L-lactate dehydrogenase [EC:1.1.1.27]
K00156	pyruvate dehydrogenase (quinone) [EC:1.2.5.1];pyruvate dehydrogenase (cytochrome) [EC:1.2.2.2]
K00074	3-hydroxybutyryl-CoA dehydrogenase [EC:1.1.1.157]
K00075	UDP-N-acetylmuramate dehydrogenase [EC:1.1.1.158]
K00294	1-pyrroline-5-carboxylate dehydrogenase [EC:1.5.1.12]
K14519	NADP-dependent aldehyde dehydrogenase [EC:1.2.1.4]
K00058	D-3-phosphoglycerate dehydrogenase [EC:1.1.1.95]
K00055	aryl-alcohol dehydrogenase [EC:1.1.1.90]
K00057	glycerol-3-phosphate dehydrogenase (NAD(P)+) [EC:1.1.1.94]
K02302	uroporphyrin-III C-methyltransferase / precorrin-2 dehydrogenase / sirohydrochlorin ferrochelatase [EC:2.1.1.107 1.3.1.76 4.99.1.4]
K00052	3-isopropylmalate dehydrogenase [EC:1.1.1.85]
K08685	quinohemoprotein amine dehydrogenase [EC:1.4.98.1];amine dehydrogenase [EC:1.4.99.3]
K00331	NADH dehydrogenase I subunit B [EC:1.6.5.3];NADH-quinone oxidoreductase subunit B [EC:1.6.5.3]
K00330	NADH-quinone oxidoreductase subunit A [EC:1.6.5.3];NADH dehydrogenase I subunit A [EC:1.6.5.3]
K00333	NADH dehydrogenase I subunit D [EC:1.6.5.3];NADH-quinone oxidoreductase subunit D [EC:1.6.5.3]
K00332	NADH-quinone oxidoreductase subunit C [EC:1.6.5.3];NADH dehydrogenase I subunit C [EC:1.6.5.3]
K00335	NADH dehydrogenase I subunit F [EC:1.6.5.3];NADH-quinone oxidoreductase subunit F [EC:1.6.5.3]
K00334	NADH-quinone oxidoreductase subunit E [EC:1.6.5.3];NADH dehydrogenase I subunit E [EC:1.6.5.3]
K00337	NADH dehydrogenase I subunit H [EC:1.6.5.3];NADH-quinone oxidoreductase subunit H [EC:1.6.5.3]
K00336	NADH-quinone oxidoreductase subunit G [EC:1.6.5.3];NADH dehydrogenase I subunit G [EC:1.6.5.3]
K00339	NADH dehydrogenase I subunit J [EC:1.6.5.3];NADH-quinone oxidoreductase subunit J [EC:1.6.5.3]
K00338	NADH-quinone oxidoreductase subunit I [EC:1.6.5.3];NADH dehydrogenase I subunit I [EC:1.6.5.3]
K13953	alcohol dehydrogenase, propanol-preferring [EC:1.1.1.1]
K13954	alcohol dehydrogenase [EC:1.1.1.1]
K00318	proline dehydrogenase [EC:1.5.99.8]
K00102	D-lactate dehydrogenase (cytochrome) [EC:1.1.2.4]
K06445	acyl-CoA dehydrogenase [EC:1.3.99.-]
K06447	succinylglutamic semialdehyde dehydrogenase [EC:1.2.1.71]
K00128	aldehyde dehydrogenase (NAD+) [EC:1.2.1.3]
K00123	formate dehydrogenase, alpha subunit [EC:1.2.1.2]

K00124	formate dehydrogenase, beta subunit [EC:1.2.1.2]
K00127	formate dehydrogenase, gamma subunit [EC:1.2.1.2]
K05358	quininate dehydrogenase (quinone) [EC:1.1.5.8];quininate dehydrogenase (pyrroloquinoline-quinone) [EC:1.1.99.25]
K00146	phenylacetaldehyde dehydrogenase [EC:1.2.1.39]
K00627	pyruvate dehydrogenase E2 component (dihydrolipoamide acetyltransferase) [EC:2.3.1.12]
K00088	IMP dehydrogenase [EC:1.1.1.205]
K00164	2-oxoglutarate dehydrogenase E1 component [EC:1.2.4.2]
K00166	2-oxoisovalerate dehydrogenase E1 component, alpha subunit [EC:1.2.4.4]
K00161	pyruvate dehydrogenase E1 component subunit alpha [EC:1.2.4.1]
K00162	pyruvate dehydrogenase E1 component subunit beta [EC:1.2.4.1]
K00163	pyruvate dehydrogenase E1 component [EC:1.2.4.1]
K07516	3-hydroxyacyl-CoA dehydrogenase [EC:1.1.1.35]
K00029	malate dehydrogenase (oxaloacetate-decarboxylating)(NADP+) [EC:1.1.1.40]
K00024	malate dehydrogenase [EC:1.1.1.37]
K00020	3-hydroxyisobutyrate dehydrogenase [EC:1.1.1.31]
K00249	acyl-CoA dehydrogenase [EC:1.3.99.3]
K00241	succinate dehydrogenase cytochrome b556 subunit;succinate dehydrogenase cytochrome b-556 subunit [EC:1.3.99.1];succinate dehydrogenase cytochrome b-556 subunit
K00240	succinate dehydrogenase iron-sulfur protein [EC:1.3.99.1];succinate dehydrogenase iron-sulfur subunit [EC:1.3.99.1]
K00242	succinate dehydrogenase hydrophobic membrane anchor protein [EC:1.3.99.1];succinate dehydrogenase hydrophobic membrane anchor protein;succinate dehydrogenase membrane anchor subunit
K00005	glycerol dehydrogenase [EC:1.1.1.6]
K00003	homoserine dehydrogenase [EC:1.1.1.3]
K00001	alcohol dehydrogenase [EC:1.1.1.1]
K00263	leucine dehydrogenase [EC:1.4.1.9]
K00262	glutamate dehydrogenase (NADP+) [EC:1.4.1.4]
K00261	glutamate dehydrogenase (NAD(P)+) [EC:1.4.1.3]
K00285	D-amino-acid dehydrogenase [EC:1.4.99.1]
K00281	glycine dehydrogenase [EC:1.4.4.2]
K00382	dihydrolipoamide dehydrogenase [EC:1.8.1.4]
K12254	4-guanidinobutyraldehyde dehydrogenase / NAD-dependent aldehyde dehydrogenase [EC:1.2.1.54 1.2.1.-]
K00831	phosphoserine aminotransferase [EC:2.6.1.52]
K00812	aspartate aminotransferase [EC:2.6.1.1]
K00817	histidinol-phosphate aminotransferase [EC:2.6.1.9]
K00818	acetylmethionine aminotransferase [EC:2.6.1.11]
K14268	5-aminovalerate aminotransferase [EC:2.6.1.48]
K00826	branched-chain amino acid aminotransferase [EC:2.6.1.42]
K00821	acetylmethionine/N-succinylmethionine aminotransferase [EC:2.6.1.11 2.6.1.17]
K00820	glucosamine--fructose-6-phosphate aminotransferase (isomerizing) [EC:2.6.1.16]
K00823	4-aminobutyrate aminotransferase [EC:2.6.1.19]
K00840	succinylmethionine aminotransferase [EC:2.6.1.81]

K12256	putrescine aminotransferase [EC:2.6.1.-]
K00466	tryptophan 2-monooxygenase [EC:1.13.12.3]
K10946	ammonia monooxygenase subunit C [EC:1.13.12.-]
K03379	cyclohexanone monooxygenase [EC:1.14.13.22]
K03863	vanillate monooxygenase [EC:1.14.13.82]
K00459	nitronate monooxygenase [EC:1.13.12.16]
K06134	ubiquinone biosynthesis monooxygenase Coq7 [EC:1.14.13.-]
K00499	choline monooxygenase [EC:1.14.15.7]

## Literature cited

Ellis, L. B. M.; Roe, D.; Wackett, L. P. The University of Minnesota Biocatalysis/biodegradation Database: The First Decade. *Nucleic Acids Res.* **2006**, *34* (suppl 1), D517–D521.

Fayad, P. B.; Prévost, M.; Sauvé, S. On-Line Solid-Phase Extraction Coupled to Liquid Chromatography Tandem Mass Spectrometry Optimized for the Analysis of Steroid Hormones in Urban Wastewaters. *Talanta* **2013**, *115*, 349–360.

Grady, C. P. L. Jr.; Daigger, G. T.; Love, N. G.; Filipe, C. D. M. *Biological Wastewater Treatment*, 3rd ed.; CRC Press, **2011**.

Johnson, D. R.; Helbling, D. E.; Lee, T. K.; Park, J.; Fenner, K.; Kohler, H. P. E.; Ackermann, M. Association of Biodiversity with the Rates of Micropollutant Biotransformations among Full-Scale Wastewater Treatment Plant Communities. *Appl. Env. Microbiol.* **2015**, *81* (2), 666-675.

Zavaleta, E. S.; Pasari, J. R.; Hulvey, K. B.; Tilman, G. D. Sustaining Multiple Ecosystem Functions in Grassland Communities Requires Higher Biodiversity. *Proc. Natl. Acad. Sci.* **2010**, *107* (4), 1443–1446.